

Unit 3, Gabalfa Workshops, Excelsior Ind. Est. Cardiff CF14 3AY Tel: (029) 2062 3290 Email: info@abbeybookbinding.co.uk

Bone Morphogenetic Proteins and their co-receptor, Repulsive Guidance molecules, signalling pathways in human cancers

by

Jin Li

Metastasis & Angiogenesis Research Group Cardiff University School of Medicine Cardiff

November 2010

Thesis submitted to Cardiff University for the degree of Doctor of Philosophy

Bone Morphogenetic Proteins and their co-receptor, Repulsive Guidance molecules, signalling pathways in human cancers

by

Jin Li

Metastasis & Angiogenesis Research Group Cardiff University School of Medicine Cardiff

November 2010

Thesis submitted to Cardiff University for the degree of Doctor of Philosophy

UMI Number: U585464

All rights reserved

INFORMATION TO ALL USERS

The quality of this reproduction is dependent upon the quality of the copy submitted.

In the unlikely event that the author did not send a complete manuscript and there are missing pages, these will be noted. Also, if material had to be removed, a note will indicate the deletion.



UMI U585464

Published by ProQuest LLC 2013. Copyright in the Dissertation held by the Author.

Microform Edition © ProQuest LLC.

All rights reserved. This work is protected against

All rights reserved. This work is protected against unauthorized copying under Title 17, United States Code.



ProQuest LLC 789 East Eisenhower Parkway P.O. Box 1346 Ann Arbor, MI 48106-1346

Acknowledgements

This thesis would not have been possible without the help of several individuals who in one way or another contributed and extended their valuable assistance in the preparation and completion of this study. First and foremost, my utmost gratitude to my supervisors Professor Wen G. Jiang, whose encouragement, guidance and support I will never forget and Professor Howard Kynaston for his supervision and support throughout the three years of my Ph.D study. I would like to thank Professor RE Mansel for allowing me to conduct my research in the department.

I am indebted to my many of my colleagues, Dr. Christian Parr, Dr. Andrew J Sanders, Dr. Jane Lane, Dr. Tracey Martin for their helpful suggestions and technical assistance. Especially, I would like to thank Dr. Lin Ye, for his unselfish and unfailing help from the initial to the final level enabled me to develop an understanding of the project and complete this study. It was a great honour and important for me pursuing my degree at this top-class laboratory and having an enjoyable life in this "big family".

I am also very grateful to my parents Qifang Li and Hong Li for their love, concern and support throughout the course of my studies.

This work was kindly supported by Nick Williams and The Fong's Family Foundation.

PUBLICATIONS:

Full papers (published)

Jin Li, Lin Ye, Christian Parr, Anthony Douglas-Jones, Howard G. Kynaston, Robert E. Mansel, Wen G. Jiang (2009). The aberrant expression of bone morphogenetic protein 12 (BMP-12) in human breast cancer and its potential prognostic value. Gene Ther Mol Biol 13A, 186-193

Lin Ye, Bokobza Sivan, Jin Li, Moazzam Muhammad, Chen Jinfeng, Mansel Robert E., Jiang Wen G. (2010). Bone morphogenetic protein-10 (BMP-10) inhibits aggressiveness of breast cancer cells and correlates with poor prognosis in breast cancer. Cancer Sci 101, 2137-2144.

Full papers submitted and in preparation:

Jin Li, Lin Ye, Howard G. Kynaston and Wen G. Jiang. Repulsive guidance molecules (RGMs) and their implication in cancer as co-receptor of BMPs.

Jin Li, Lin Ye, Anthony Douglas-Jones, Howard G. Kynaston, Robert E. Mansel, Wen G. Jiang. RGMs (repulsive guidance molecules) and the potential prognostic value in cancer.

Jin Li, Lin Ye, Howard G. Kynaston and Wen G. Jiang. The role of Repulsive Guidance Molecule-B (RGMB) (DRAGON) in breast cancer via BMP signalling pathways.

Jin Li, Lin Ye, Howard G. Kynaston and Wen G. Jiang. RGMs (repulsive guidance molecules) inhibit prostate cancer proliferation and metastasis and association with BMP signalling pathways.

Jin Li, Lin Ye, Howard G. Kynaston and Wen G. Jiang. The implication of BMP11 in breast cancer as candidate novel regulators.

ABSTRACT & CONFERENCE PRESENTATIONS:

Jin Li, Lin Ye, Sanders Andrew J., Mansel Robert E., Jiang Wen G. (2009). The Role of Dragon (Repulsive Guidance Molecule-B, RGM-B) in Human Breast Cancer. Cancer Res 69, 875S-875S

Jin Li, Christian Parr, Lin Ye, Anthony Douglas-Jones, Robert E Mansel, Wen G Jiang. The aberrant expression of Bone Morphogenetic Protein 12 (BMP12) in human breast cancer and its potential prognostic value. National Cancer Reaserch Institute (NCRI) Cancer Conference, 2008, Birmingham, UK

Summary

RGMs (repulsive guidance molecules) are a group of recently identified GPI (glycosylphosphatidylinositol)-linked cell-membrane-associated proteins, comprising three family members, which have been implicated in BMPs (Bone morphogenetic proteins) signalling. BMPs have been shown to play profound roles in bone metastases from breast cancer and prostate cancer. This study aims to investigate the implication of RGMs in prostate cancer and breast cancer and their role in coordinating signal transduction by BMPs during disease progression of cancer.

The aberrant expression of RGMs was found in breast cancer which was associated with prognosis of breast cancer patients. RGMA, B and C were detected in prostate cancer cell lines and only RGMB was expressed in breast cancer cell lines which allowed for the knockdown study of RGMs in PC-3 and RGMB in MDA-MB-231 using ribozyme transgenes. The knockdown of RGMB in breast cancer cells resulted in an increase of cellular proliferation, adhesion, motility and migration in vitro, which contributed to a tumour's growth and metastasis. Furthermore, an inhibition of caspase-3 was seen in cells after knockdown of RGMB which indicated RGMB as a regulator of cell survival. Up-regulation of FAK and Paxillin were also seen in the cancer cells after loss of RGMB expression, together with an evident induction of EMT (epithelial-mesenchymal transition) which may contribute to the promoted cell-matrix adhesion and cell mobility. The knockdown of RGMs in prostate cancer cells also lead to an increase of cell ability to grow, adhere and move, in which differentiated response of ID-1, a BMPs target gene was seen.

As RGMs were reported to be involved in BMP signalling, knockdown of RGMB was found to induce promotion on Smad-dependent pathways (especially Smad-1/5/8 pathway) and inhibition on BMP Smad-independent pathways (MAPK JNK pathway). It suggests that RGMs are important partners to fine-tune responses of cells to BMPs stimuli, particularly during the progression and dissemination of cancer cells, and are potential targets for developing a novel cancer therapy.

CONTENTS

DECLARATION ACKNOWLEDGMENTS PUBLICATION AND PRESENTATION SUMMARY LIST OF FIGURES LIST OF TABLES ABBREVIATIONS	II III IV VI XI XV XVI
CHAPTER 1 GENERAL INTRODUCTION	1
1.1 Prostate Cancer and Breast Cancer 1.1.1 Epidemiology and risk factors 1.1.2 Diagnosis and Tumour Markers 1.1.3 Metastasis 1.1.3.1 Immune escape of cancer cells 1.1.3.2 Cell adhesion molecules 1.1.3.3 Invasion and motility 1.1.3.4 Urokinases-type plasminogen activator 1.1.3.5 Hepatocyte growth factor/scatter factor (HGF/SF) 1.1.3.6 Tumour metastasis suppressor genes 1.1.4 Management Therapy for prostate cancer	2 2 10 20 21 21 24 24 26 27 28
1.2 Bone metastasis in prostate cancer and breast cancer	34
 1.3 Bone morphogenetic proteins and their signalling pathway in cancer 1.3.1 BMPs 1.3.2 BMP signalling in cancer 1.3.2.1 BMP receptors and their implication in cancer 1.3.2.2 Smad 1.3.2.3 Impact of BMPs on cancer 	36 36 40 43 45
1.4 Repulsive guidance molecules 1.4.1 RGM 1.4.1.1 RGMA 1.4.1.2 RGMB 1.4.1.3 RGMC 1.4.2 Receptor of RGM 1.4.3 The role of RGM in the BMP signalling pathway 1.4.3.1 The regulators of BMP signalling 1.4.3.2 The involvement of RGMs in BMP signalling	49 49 50 57 62 67 74 74
1.5 Hypothesis and aim of this study	80
CHAPTER 2 MATERIALS AND METHODS	83
2.1 General Materials 2.1.1 Animals, cell lines and tissues 2.1.2 Primers 2.1.3 Antibodies	84 84 85 88
	VII

2.1.3.1 Primary antibodies	89
2.1.3.2 Secondary antibodies	90
2.1.3.3 Inhibitors, activators and proteins	90
2.1.4 General reagents and solutions	91
2.2 Cell Culture and storage	98
2.2.1 Preparation of growth medium and maintenance of cells	98
2.2.2 Trypsinisation and counting of cells	98
2.2.3 Storage of cell lines in liquid nitrogen	99
2.2.4 Resuscitation of cell lines	100
2.3 Methods for Detection of mRNA	101
2.3.1 Total RNA isolation	101
2.3.2 Reverse transcription (RT)	102
2.3.3 Polymerase chain reaction (PCR)	103
2.3.4 Agarose gel DNA electrophoresis	105
2.3.5 Real time quantitative PCR	105
2.4 Methods for Detection of Proteins	106
2.4.1 Sodium dodecyl sulphate polyacrylamide gel electrophosis (SDS-PAGE) and	106
western blot analysis	
2.4.1.1 Cellular lysis and protein extraction	106
2.4.1.2 Protein quantification	107
2.4.1.3 Sodium Dodecyl Sulphate PolyAcrilamide Gel Electrophoresis (SDS-PAGE)	108
2.4.1.4 Western blotting	110
2.4.2 Immunoprecipitation of phosphorylated proteins	112
2.4.3 Immunohistochemical (IHC) and Immunocytochemical (ICC) staining	113
2.4.4 Immunofluorescent staining	115
2.5 TOPO Cloning	117
2.5.1 Knockdown of gene transcripts using ribozyme transgenes	117
2.5.2 TOPO TA cloning reaction	123
2.5.3 Transformation	124
2.5.4 Selection and analysis of colonies	126
2.5.4 Selection and analysis of colonies	126
2.5.5 Purification and quantification of plasmid DNA	128
2.5.6 Transfection via electroporation into mammalian cells	129
2.5.7 Establishing a RGM knockdown mutant and Selection of plasmid positive cells	130
2.6 In vitro Cell function Assays	131
2.6.1 Cell growth assay	131
2.6.2 Invasion assay	132
2.6.3 Cell-matrix adhesion assay	133
2.6.4 Motility assay (Cytodex beads)	134
2.6.5 Wounding (Migration) assay	135
2.6.6 ECIS assay	136
2.6.7 Flow cytometric analysis of apoptosis	137
2.6.8 Cell cycle analysis	138
2.7 Statistical Analysis	139
y -	

CHAPTER 3 ABERRANT EXPRESSION OF RGMS IN CANCER CELLS AND TISSUES	140
3.1 Introduction	141
3.2 Materials and methods	143
3.3 Results	145
3.4 Discussion	155
CHAPTER 4 EXPRESSION OF RGMS IN BREAST CANCER AND THEIR ASSOCIATION WITH CHARACTERISTICS OF THE DISEASE	158
4.1 Introduction	159
4.2 Materials and methods	160
4.3 Results	161
4.4 Discussion	177
CHAPTER 5 KNOCKDOWN OF RGMS IN PROSTATE CANCER CELLS AND THE INFLUENCE ON CELLULAR FUNCTIONS	179
5.1Introduction	180
5.2 Materials and methods	181
5.3 Results	185
5.4 Discussion	198
CHAPTER 6 THE KNOCKDOWN OF RGMB IN BREAST CANCER AND INFLUENCES ON CELLULAR BEHAVIOURS	200
6.1 Introduction	201
6.2 Materials and methods	202
6.3 Results	204
6.4 Discussion	217
CHAPTER 7 THE MECHANISMS UNDERLYING THE IMPACT OF RGMB ON CELLULAR ADHESION AND MOTILITY IN BREAST CAN	219 ICER
7.1 Introduction	220
7.2 Materials and Methods	223
7.3 Results	224
7.4 Discussion	233
CHAPTER 8 MECHANISMS UNDERLYING THE FUNCTIONS OF RGMS IN BREAST CANCER PROLIFERATION	236
3.1 Introduction	237
3.2 Materials and Methods	239
3.3 Results	241
3.4 Discussion	253

CHAPTER 9 THE SIGNALLING PATHWAY OF RGMS KNOCKDOWN 256 IN PROSTATE CANCER AND ASSOCIATION WITH REGULATION ON TARGET GENES

9.1 Introduction:	257
9.2 Materials and Methods:	259
9.3 Results:	261
9.4 Discussion:	274
CHAPTER 10 GENERAL DISCUSSION	274
BIBLIOGRAPHY	283

List of Figures

Chapter1

Figure 1.1 Annual Age-adjusted Cancer Incidence Rates among Males and	3
Females for Selected Cancers	
Figure 1.2. Distribution and five-year Relative Survival Rates among patients	9
and diagnosed with breast prostate cancer by race and stage at diagnosis	
Figure 1.3 Classification of Prostate cancer (7 th edition)	16
Figure 1.4 Schematic view of the prostate, bladder and lymph nodes	30
Figure 1.5 Breast cancer surgeries	32
Figure 1.6. BMP signalling pathway through Smads and non-Smads	42
Figure 1.7 Comparison of human RGMs genomic loci and gene structures	52
Figure 1.8 Main domain model of RGM protein	55
Figure 1.9 Predicted interactions of RGM and other proteins	61
Figure 1.10 Structure of RGM and Neogenin	69
Chapter 2	
Figure 2.1 Secondary structures and sequences of the minimal (A) and	118
full-length (B) hammerhead ribozymes.	
Figure 2.1A The predicted secondary structure of human RGMA mRNA,	118
from which the anti-RGMA ribozymes were designed.	
Figure 2.1B The predicted secondary structure of human RGMB mRNA,	118
from which the anti-RGMB ribozymes were designed.	
Figure 2.1C The predicted secondary structure of human RGMC mRNA,	118
from which the anti-RGMC ribozymes were designed.	
Figure 2.2 The figure summarizes the features of the pEF6/V5-His-TOPO vector.	125
Chapter 3	
Figure 3.3.1 A Expression of RGM transcripts in cell lines of human	147
origin and human tissues.	_ ,,
Figure 3.3.1 B Expression of RGM transcripts in human tissues.	148
J 1 1 1 1 1 1 1 1 1 1 1 1 1 1 1 1 1 1 1	

Figure 3.3.2 A IHC staining of RGMA in prostate specimens.	152
Figure 3.3.2 B IHC staining of RGMB in prostate specimens.	153
Figure 3.3.2 C IHC staining of RGMC in prostate specimens.	154
Chapter 4	
Figure 4.3.1 A IHC staining of RGMA in breast specimens.	163
Figure 4.3.1 B IHC staining of RGMB in breast specimens.	164
Figure 4.3.1 C IHC staining of RGMC in breast specimens.	165
Figure 4.3.2.1 The transcript level of RGMs in breast cohort analyzed against	
clinical data.	166
Figure 4.3.2.2 The transcript level of RGM in breast cohort analyzed against NPI.	167
Figure 4.3.2.3 The transcript level of RGMs in breast cohort analyzed against	168
tumour grade.	
Figure 4.3.2.4 The transcript level of RGMs in breast cohort analyzed against TNM.	169
Figure 4.3.2.5 The transcript level of RGMB in breast cohort analyzed against	170
clinical outcome.	
Chapter 5	
Figure 5.3.1.1 The generation of ribozyme transgenes specific to RGM.	186
Figure 5.3.1.2 The expression of RGMs in genetic manipulation of PC-3.	187
Figure 5.3.1.3 The expression of RGMs in genetic manipulation of PC-3.	188
Figure 5.3.2 Effects of RGMs knockdown on the capacity of adhesion (A),	
proliferation (B), invasiveness (C), motility (D), and migration (E) in vitro in PC-3.	
A1: Matrix adhesion of PC-3 RGM knockdown cells	192
A2: Effects of RGM knockdown on cell-matrix adhereion.	193
B. RGM knockdown on cell growth.	194
C. RGM knockdown on motility.	195
D. RGM knockdown and cell migration determined using the ECIS model.	196
E RGMs and the in vitro invasiveness of cancer cells.	197

Chapter 6

	Figure 6.3.1.1 The mRNA level of RGMB in wild type MDA231 and	206
	the cells transfected with pEF empty plasmid and RGMB ribozyme.	
	Figure 6.3.1.2 The RGMB expression was reduced in RGMB knockdown	207
	cells from protein level compared to the control cells, proved by western blot.	
	Figure 6.3.1.3 ICC staining of RGMB proteins in RGMB knockdown cells	208
	and pEF control cells.	
	Figure 6.3.2 A RGMB knockdown on cell growth in breast cancer.	212
	Figure 6.3.2 B RGMB knockdown on invation of breast cancer cell.	213
	Figure 6.3.2 C RGMB knockdown on matrix adhesion of breast cancer cells.	214
	Figure 6.3.2 D ECIS-based attachment assay.	215
	Figure 6.3.2 E Migration of RGMB knockdown cells.	216
C	Chapter 7	
	Figure 7.3.1.1A The protein level of FAK and Paxillin in MDA231 cells	226
	transfected with empty plasmid and RGMB ribozyme.	
	Figure 7.3.1.1 B mRNA level of FAK and Paxillin in control and RGMB	227
	knockdown cells.	
	Figure 7.3.1.2 The pattern of activated Smad-dependent pathway molecules in control	228
	and RGMB knockdown cells and the association with FAK and Paxillin expression.	
	Figure 7.3.1.3 Activated Smad-1 levels in the transfected cells with treatment.	229
	Figure 7.3.2.1 The expression of EMT regulators altered by RGMB knockdown	231
	in MDA-MB-231.	
	Figure 7.3.2.2 mRNA level of Snail in the transfected cells with treatment.	232
C	hapter 8	
	Figure 8.3.1.1A RGMB knockdown protected MDA-MB-231 cells survival from	243
	apoptosis.	
	Figure 8.3.1.1B Analysis of apoptotic cells in MDA-MB-231 cells using Hoechst	244
	staining.	
	Figure 8.3.1.2 Cell cycle analysis of RGMB knockdown cells.	245
	Figure 8.3.2 The protein level of caspase-3 in MDA-MB-231 pEF and RGMB	247
	knockdown cells.	

Figure 8.5.5 A The expression of C-Myc is promoted in Robbis knockdown cens.	249
Figure 8.3.3 B ICC staining of c-Myc in RGMB knockdown cells.	250
Figure 8.3.4 The MAPK pathway regulated by RGMB.	252
Chapter 9	
Figure 9.3.1 ID-1 transcripts level in the transfected cells.	262
Figure 9.3.2 ID-1 transcripts levels in the transfected cells under no or	263
BMP7 treatment.	
Figure 9.3.3 Smad1 and Smad3 activation in the transfected cells under	266
BMP7 treatement.	
Figure 9.3.4 Quantification of P-Smad-3 level showed in the western.	267
Figure 9.3.5 IFC staining of activated Smad-3.	268
Figure 9.3.6 IFC staining of ID-1.	269
Figure 9.3.7 BMPRI A and BMPRII levels in transfected PC-3 cells.	271
Chapter 10	
Figure 10.1 RGMs signalling pathway	282

List of Tables

Chapter 1	
Table 1.1 Association of breast and prostate cancer with human races	4
Table 1.2 Breast cancer stage 1-3	14
Table 1.3 RGMs and their interacting molecules	79
Chapter 2	
Table 2.1.2 Primers used in this study	86
Table 2.1.3.1 Antibodies used in study	89
Table 2.1.3.2 Secondary antibodies used in this study	90
Table 2.1.3.3 Inhibitors and recombinant proteins	90
Table 2.4.1.3A Components for resolving gels	108
Table 2.4.1.3B Components for stacking gels	109
Chapter 3	
Table 3.3.1.1 RGMs expression detected in different tissues	150
Table 3.3.1.2 The expression of RGMs in breast and prostate tissue and cell lines	150
Chapter 4	
Table 4.3.1 Clinical and pathologic information	175
Table 4.3.2 The transcript level of RGMs in breast cancer	176

Abbreviations

amino acid aa antibody Ab

activin receptor-1 ActR-I activin receptor IIA **ACTRIIA** activin A receptor, type I ACVR1 activin A receptor, type IIA ACVR2A activin A receptor, type IIB ACVR2B

antigen Ag

activated leukocyte cell adhesion molecule **ALCAM**

Activin receptor-like kinase **ALK** ALP Alkaline phosphatase Ankyrin repeat domain 34 Ankrd34 Ammonium Persulfate APS

American Type Culture Collection **ATCC**

BMP and activin membrane bound inhibitor **BAMBI**

Bone Morphogenetic Protein receptor, type BMPR-IA/Brk1

IA

BMPR-IB BMP type IB receptors Type II receptor for BMP **BMPRII** Bone Morphogenic Proteins **BMPs**

base pair bp

BPH Benign Prostatic Hyperplasia

BRCa breast cancer tissues **BSA** Bovine Serum Albumin **Bovine Saline Soultion BSS**

CA Cancer antigen

CaP prostate cancer tissues Carcinoembryonic antigen **CEA**

carcinoembryonic antigen-related cell CEACAM1

adhesion molecule

cerebellar granule neurons **CGNs**

chromodomain helicase DNA binding

protein 1 and 2 Cytokeratin-19

CK19 **CNS** central nerve system Corl colorectal tissues

Co-Smads common-mediator Smads

cysteine rich transmembrane BMP

CRIM1 regulator 1

Chd1 and 2

c-Src cellular sarcoma
CST corticospinal tract

DCC deleted in colorectal cancer

DCIS Ductal Carcinoma in Situ

DEPC Diethyl pyroncarbonate

DMEM Dulbecco's modified eagles medium

DMSO dimethyl sulphoxide
DNA deoxyribonucleic acid

DRAGON DRG11-responsive axonal guidance and

outgrowth of neurite (RGMB)

DRAGON.Fc purified soluble RGMB fused to the Fc

portion of human IgG l digital rectal examination dorsal root ganglion

DRG dorsal root ganglion

ECACC European Collection of Animal Cell Cultures
electric cell—substrate impedance sensing

ECM extracellular matrix EDTA disodium edetate

DRE

EDTA ethylene diaminetetraacetic acid
EGFR epidermal growth factor receptor
EMT epithelial-to-mesenchymal transition

ER oestrogen receptor

ErbB2 v-erb-b2 erythroblastic leukemia viral oncogene

homolog 2

FAK Focal Adhesion Kinase
Fas Fatty acid synthase

FasL Fas ligand

FGF Fibroblast growth factors
FGFs fibroblast growth factors
FITC fluorescein isothiocyanate
FNIII fibronectin type III

GAPDH glyceraldehyde-3-phosphate dehydrogenase

GDF Growth/differentiation Factor GPI glycosylphosphatidylinositol

HAI-1 hepatocyte growth factor activator inhibitor

HAMP hepcidin antimicrobial peptide

HCL hydrogen acid

HepaCAM hepatocyte cell adhesion molecule
N-hydroxyethylpiperazine-N'-2-

HEPES ethansulphoxide

HER2 Human epidermal growth factor receptor 2

HFE2 Hemochromatosis type 2 protein

HGF/SF Hepatocyte growth factor/scatter factor HIFU High-intensity focused ultrasound

HJV Hemojuvelin

HLA Human leukocyte antigen

HLH helix-loop-helix

high molecular weight uPA HMW-uPA hereditary prostate cancer 1 HPC1 **HRP** horseradish peroxidise inflammatory breast cancer **IBC** intercellular adhesion molecule **ICAM** inhibitor of differentiation factor ID-1 Insulin-like growth factor 1 receptor IGF-1R **IGFs** insulin-like growth factors (IGFs)

I-Smads inhibitory Smads

JH juvenile hemochromatosis
JNKs Jun Nterminal kinases (JNKs)

LARG Rho guanine nucleotide exchange factor

LIMK LIM kinase

Lix1 Limb expression 1

Lix11 limb expression 1 homolog-like protein

LMW-uPA low molecular weight uPA
Lnpep leucy1/cystiny1 aminopeptidase

LPS lipopolysaccharide

MAD mothers against decapentaplegic homolog

MAPK mitogen-activated protein kinase

Mctp2 multiple C2 domains, transmembrane 2

MDCK Mink Kidney Epithelial

Mel-CAM melanoma cell adhesion molecule MH1 and MH2 Mad-homology domains 1 and 2

MLC myosin light chain

MMPs matrix metalloproteinases

NB normal breast

NCAM neural cell adhesion molecule

NF-kB NF-kappaB NLK Nemo-like kinase

NPI Nottingham Prognostic Index

Omgp oligodendrocyte myelin glycoprotein

OPG osteoprotegrin
OV ovary tissues

PAK1 p21 protein (Cdc42/Rac)-activated kinase 1

PBS Phosphate Buffered Saline

PCR polymerase chain reaction

PDGF platelet- derived growth factor

PECAM platelet/endothelial cell adhesion molecule

PI Propidium Iodide

Polr3gl DNA-directed RNA polymerase III subunit

RPC7-like

PPC pro-protein convertase
PR progesterone receptor
PS phosphatidylserine
PSA prostate-specific antigen

PTH-rP parathyroid-hormone-related peptide

PTK2 protein tyrosine kinase 2

RANKL receptor activator of NF-kappa-B ligand

RET receptor tyrosine kinase
RGD arginie-glycine-aspartic acid
RGM repulsive guidance molecule

RhoC ras homolog gene family, member C Riok2 right open reading frame kinase 2

RNA ribonucleic acid

R-Smads receptor-activated Smads

RT reverse transcription

RTK receptor tyrosine kinase

SBE Smad-binding element

SDS-PAGE Sodium dodecyl sulphate polyacrylamide gel

electrophosis

SIP1 Survival of motor neuron protein-interacting

protein 1

Slco3a1 solute carrier organic anion transporter

family member 3A1
Slug Zinc finger protein

Smad Sma and MAD Snail snail homolog 1

Slug

SPARC secreted acidic cysteine rich glycoprotein

SSXS Ser-Ser-X-Ser

STRING Search Tool for the Retrieval of Interacting

Genes/Proteins

TAK1 TGF-B activated tyrosine kinase 1

TER transendothelial

TGF-β Transforming growth factor beta

TIMPs Tissue inhibitor of metalloproteases

TMZ Temozolomide

TNM Tumour Node Metastasis staging
TRIR Total RNA Isolation Reagent

Tris Tris-(hydoxymethyl)-aminomethane
TRITC Tetra-Rhodamine Isothiocyanate

TRUS Transrectal ultrasound

Txnip thioredoxin interacting protein

UKCCCR United Kingdom Coordinating Committee on

Cancer Research

Unc unco-ordinated

UNC5H UNCoordinated family member 5 homolog

uPA Urokinases-type plasminogen activator

UVITEC UVIband software package VCAM-1 vascular cell adhesion molecule 1

vWF von Willebrand factor

WT wild type

XIAP X-linked inhibitor of apoptosis protein

Chapter 1 General Introduction

1.1 Prostate Cancer and Breast Cancer

1.1.1 Epidemiology and risk factors

Prostate cancer and breast cancer have been the most common forms of malignant disease in the Western world since 1975, now accounting for one third of cancers in males and females.

Incidence

The recorded incidence of breast cancer has been sharply increased since the 1980s, reaching a peak in 1987 and remaining at a high level until now, as in some countries the number of cases is gradually diminishing. (Fig. 1.1 source: cancer statistics 2009). In North America, breast cancer is the most common malignancy among women, accounting for 27 percent of all female cancers. Fifteen percent of all cancer deaths are currently due to cancer of the breast, although since the mid-1980s the mortality from lung cancer has equalled and subsequently exceeded that of breast cancer as a cause of death in women. In the United States of America, 192,370 new cases of breast cancer were diagnosed in 2009 and there were about 40,170 deaths from the disease. The equivalent figures for prostate cancer are 192,280 and 27,360, respectively. (Jemal et al., 2009) The incidence of prostate cancer appeared to peak in 1992, approximately 5 years after introduction of prostate-specific antigen (PSA) as a screening test. It fell precipitously until 1995 which is attributed to the "cull effect" of identifying previously unknown cancers in the population by the use of PSA. The slow rise since then has been at a gradient similar to that observed before the PSA era.

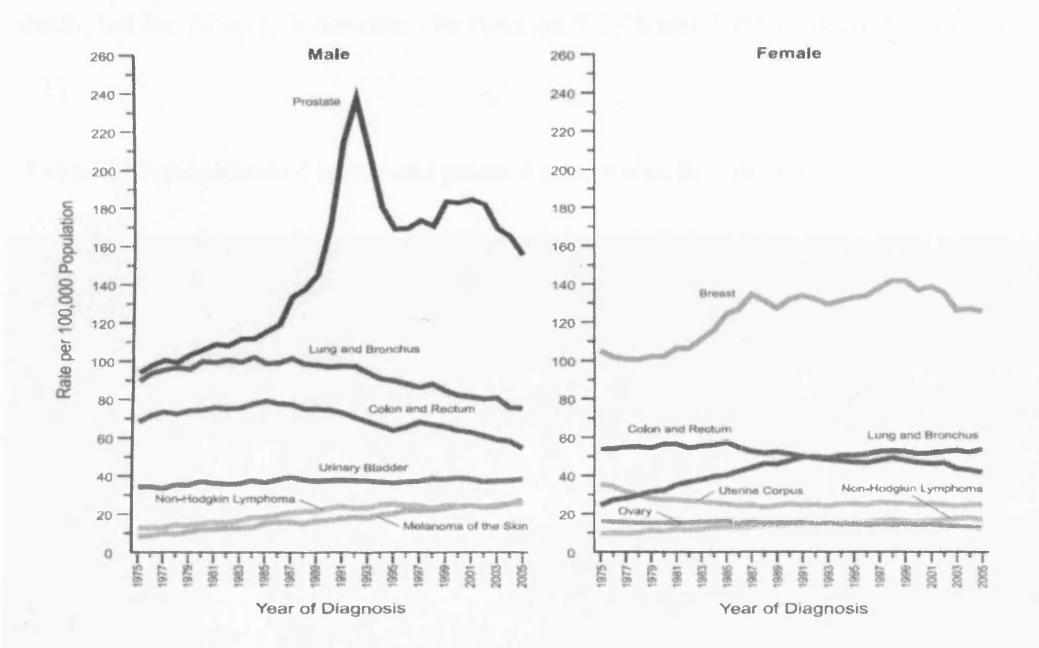


Figure 1.1 Annual Age-adjusted Cancer Incidence Rates among Males and Females for Selected Cancers, United States, 1975-2005. Source: Cancer Statistics, 2009

The estimated lifetime risk of prostate cancer in the US is 15.39% for Caucasians and 18.32% for African Americans, with a lifetime risk of death being 2.63% and 4.42%, respectively.

The Caucasians have 7.21% lifetime risk of breast cancer and 2.82% risk of death, but for African Americans, the risks are 9.29% and 3.2% respectively. (Table 1.1)

Table 1.1 Association of breast and prostate cancer with human races

	Caucasians	African	All	Type of
	Caucasians	Americans	races	Cancer
	130.6	117.5	502.8	Breast cacner
Incidence*	156.7	248.5	710.3	Prostate cancer
Mortality*	24.4	33.5	20.9%	Breast cancer
	24.6	59.4	14.2%	Prostate cancer
Lifetime risk of disease	7.21%	9.29%	9.36%	Breast cancer
(2004-2006)	15.39%	18.32%	15.9%	Prostate cancer
Lifetime risk of death	2.82%	3.2%	2.84%	Breast cancer
(2004-2006)	2.63%	4.42%	2.8%	Prostate cancer

^{*} Per 100,000 population, age adjusted to the 2000 US standard population.

Source: Cancer stat 2009 and DevCan: Probability of Developing or Dying of Cancer Software, Version 6.4.0. Statistical Research and Applications Branch, National Cancer Institute, 2009. www.srab.cancer.gov/devcan

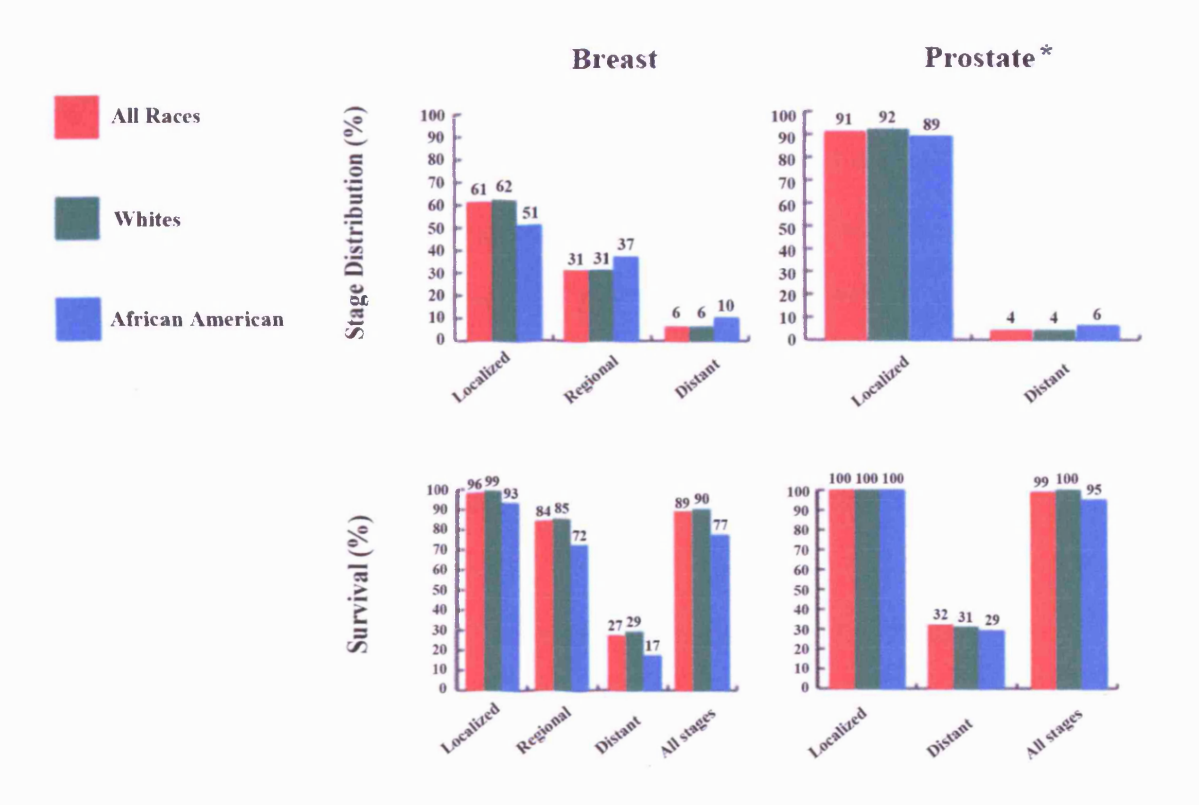


Figure 1.2. Distribution and five-year Relative Survival Rates among patients diagnosed with breast and prostate cancer by race and stage at diagnosis, US, 1996-2004.

^{*} The rate for localized stage represents localized and regional stages combined. Staging is according to surveillance, epidemiology, and end results historic stage categories rather than according to the American Joint Committee on Cancer staging system. Source: Ries LAG, Melbert D, and Krapcho M, et al.

Compared with whites, African American men and women have poorer survival once cancer is diagnosed. Five-year relative survival among patients diagnosed with both breast cancer and prostate cancer is lower in African Americans than in whites within every stratum of stage (localized, regional and distant). (Fig 1.2)

Gender plays a doubtless role in the aepidemiological analysis and is particularly important in breast cancer and prostate cancer. Overall, the lifetime probability of being diagnosed with an invasive cancer is higher for men (44%) than for women (37%). Doubtlessly, female gender is a major risk factor for breast cancer, although it is often forgotten, as breast cancer is 100 times more common in women than in men.

In the UK in 2007 almost 277 men and 45,700 women were diagnosed with breast cancer, that's around 125 women a day (CancerStats, Cancer Reasearch UK 2009). Female breast cancer incidence rates have increased by around 50% over the last twenty-five years and have increased by 5% in the last ten years. However, Breast cancer survival rates have been consistently improving for the past forty years. More women are surviving breast cancer than ever before. Now more than 8 out of 10 women with breast cancer will survive the disease beyond five years, compared to around 5 out of 10 in the 1970s. In 2008 around 12,000 women and around 70 men died from breast cancer. Death rates for breast cancer have fallen by almost a fifth in the last ten years, but it is still the second most common cause of death from cancer in women after lung in the UK.

In 2007 in the UK about 36,100 men were diagnosed with prostate cancer and around 338,000 men were diagnosed in Europe in 2008 (CancerStats, Cancer

Reasearch UK 2009). More than three-quarters of men diagnosed with prostate cancer now survive their disease beyond five years; compared to less than a third in the 1970s. Whereas prostate cancer is still the second most common cause of cancer death in UK men, after lung cancer. In 2008 in the UK about 10,170 men died from prostate cancer.

Risk factors

Risk factors for breast cancer

The incidence of breast cancer increases with age, as other epithelial cancers. It is only occasionally seen in the late teens. The age-specific rate increases sharply up to the age of 40 years. The increase thereafter slows down dramatically, although the overall breast cancer rate keeps rising until old age. However, the cumulative risk of developing breast cancer shows the majority of patients with breast cancer are over the age of 50 years.

A family history of breast cancer can be associated with an increased risk of the disease and susceptibility to breast cancer can be inherited. Up to 20 percent of women diagnosed with breast cancer have at least one affected family member and about 5 per cent of breast cancers appear attributable to inherited gene mutations that are dominant and highly penetrative.

Some other factors such as dietary fat or cholesterol intake, alcohol consumption, endocrine factors, nulliparity may also need to be factored in.

The cause of breast cancer remains unknown. However, epidemiological data normally suggests risk factors that show an increased possibility of developing the

disease. Such factors for breast cancer are divided into three main groups: genetic, endocrine, and environmental; each may be of major, intermediate, or minor importance. Although many minor factors have become the source of continued debate, some of these factors were thought to play a more important role in the aetiology of breast cancer, as evidence accumulates. Recently, this has been particularly proved by links with oral contraceptive and hormone replacement therapie (Benshushan and Brzezinski, 2002; Buchholz et al., 2008)

Risk factors for prostate cancer

The particular causes of prostate cancer initiation and progression are not yet known, but substantial evidence indicates that both genetics and environment play a role in this disease. A number of potential risk factors have been identified by classic epidemiology and molecular epidemiology associated with the development of prostate cancer.

Sporadic cancers account for about 85% of all prostate cancers, and about 15% are familial or hereditary. Hereditary prostate cancer accounts for 43% of early-onset disease (55 years old or younger) but only 9% of all cancers occurring by the age of 85 years (Carter *et al.*, 1992). At least eight candidate prostate cancer susceptibility genes have been reported which accounts for only a small fraction of the observed genetic predisposition to prostate cancer. HPC1 is the best characterized among the known susceptibility genes. (Cooney *et al.*, 1997; Eeles *et al.*, 1998; Smith *et al.*, 1996)

An accumulation of aepidemiological, histological and genetic evidence suggest that chronic inflammation leading to cellular hype-proliferation to replace damaged tissue contributes to the development of prostate cancer (Coussens and Werb, 2002; De Marzo *et al.*, 2004).

An analysis of the known prostate cancer susceptibility genes and other genetic defects in prostate cancer suggests that inherited and acquired defects in cellular defence mechanisms against inflammatory oxidants may initiate and perpetuate prostatic carcinogenesis (Coussens and Werb, 2002; De Marzo *et al.*, 2004).

Androgens have effects on the development, maturation and maintenance of the prostate, particularly by regulating both proliferation and differentiation of the luminal epithelium. Doubtlessly, a lifetime of variable exposure of the prostate to androgens plays an important role in prostate carcinogenesis. Oestrogens have been postulated to protect against prostate cancer by inhibiting growth of prostate epithelial cell but alternatively they have also been shown to increase risk by eliciting inflammation in concert with androgens (Naslund *et al.*, 1988) or by the production of mutagenic metabolites (Yager, 2000). Insulin-like Growth Factor Axis, Leptin, Vitamin D, Vitamin D Receptor, and Calcium might also be involved in tumourigenesis and subsequent disease progression

1.1.2 Diagnosis and Tumour Markers

Diagnosis of breast cancer and prostate cancer

There are many different types of breast cancer according to their histological types, at different stages, with different aggressiveness, and genetic makeups; survival varies greatly depending on these factors. The two most common types are; ductal carcinomas which present at ducts of mammary gland, lobular carcinomas occurring at lobules.

Women who are diagnosed with early stage breast carcinomas almost always appear to have no breast problems. Mammography is recommended for screening women at higher risks. Screening mammograms usually take 2 views (x-ray pictures taken from different angles) of each breast. For some patients, such as women with breast implants, more pictures may be needed to include as much breast tissue as possible. Women who are breast-feeding can still have mammograms, although these are probably not quite as accurate because the breast tissue tends to be dense. For diagnosing a breast cancer, "triple test" is routinely performed, including a breast examination by a trained medical practitioner, mammography and fine needle aspiration cytology.

The first noticeable symptom of breast cancer is typically a lump that feels different from the rest of the breast tissue. However, by the time a breast lump is noticeable, it has probably been growing for years. Lumps found in lymph nodes located in the armpits can also indicate breast cancer. Pain is not the main symptom, as other symptoms accompanying a lump may include changes in breast size or shape,

skin dimpling, nipple inversion, or spontaneous single-nipple discharge. Some patients would present with breast pain, swelling, warmth and redness throughout the breast, as well as an orange-peel texture to the skin referred to as *peau d'orange*. This is termed inflammatory breast cancer (IBC) which is caused by breast cancer cells invading the dermal small lymph vessels resulting in symptoms similar to inflammation. Paget's disease of the breast is used to describe another symptom complex of breast cancer with symbolic eczematoid skin changes. Patients diagnosed with Paget's experience tingling, itching, increased sensitivity, burning, pain, and probably a lump as well. Some metastatic breast cancers may cause severe symptoms due to the impact that the metastatic lesions have on tissues and organs being involved.

Similar to breast cancer, prostate cancer rarely causes symptoms in the early phase because the majority of adenocarcinomas arise in the periphery of the gland distant from the urethra. The presence of systemic symptoms (like bone pain, renal failure, anaemia) caused by prostate cancer suggests an advanced disease with local invasion or distant metastases. Growth of prostate cancer into the urethra or bladder neck can result in obstructive (e.g., hesitancy, decreased force of stream, intermittency) and irritative (e.g., frequency, nocturia, urgency, urge incontinence) symptoms.

If local invasion of prostate cancer affects the trigone of the bladder, it will lead to ureteral obstruction and can cause renal failure if the obstructions are bilateral. Local progression of disease and obstruction of the ejaculatory ducts will result in hemaetospermia and the presence of decreased ejaculate volume. Although rare in

the PSA era, impotence can be a sign of prostate cancer that has spread outside the prostatic capsule to involve the branches of the pelvic plexus (neurovascular bundle) responsible for innervation of the corpora cavernosa.

Axial or appendicular skeleton affected by metastatic disease can cause bone pain or microfractures or anaemia from replacement of the bone marrow. Cancerous involvement of the pelvic lymph nodes and compression of the iliac veins or lymphatics can result in lower extremity oedema. The early detection by PSA testing has reduced the proportion of patients with prostate cancer diagnosed by symptoms suggestive of advanced disease. Although the patients with prostate cancer might have voiding symptoms which suggest prostate disease, the majority (over 80%) of men diagnosed today with prostate cancer are initially suspected of disease on the basis of DRE (digital rectal examination) abnormalities or serum PSA (prostate-specific antigen) elevations. The combination of DRE and serum PSA is the most important first-line test for assessing the risk of prostate cancer being present in an individual. Associated with DRE and PSA findings, Transrectal ultrasound (TRUS)-guided, systematic needle biopsy is the most reliable method, at present, to ensure accurate sampling of prostatic tissue in men considered at high risk of harboring prostatic cancer.

PSA

PSA, which is located on chromosome 19, is a member of the human kallikrein gene family of serine proteases. It is the most important biological marker to date for the diagnosis, staging, and monitoring of prostate cancer (Polascik *et al.*, 1999). Serum PSA has been shown to associate directly with pathologic stage and tumour

volume (Noldus et al., 1998; Stamey and Kabalin, 1989; Stamey et al., 1989a; Stamey et al., 1989b; Stamey et al., 1989c). However, because PSA is not specific to prostate cancer cells and can be influenced by BPH and tumour grade and PSA levels overlap between stages, it cannot be used alone to predict accurately the extent of disease for an individual patient. Men with more advanced prostate cancer have higher grade and higher volume tumours that produce less PSA per gram of tumour (Partin et al., 1990).

Staging of breast cancer and prostate cancer

The goals of cancer staging are to allow the assessment of prognosis and facilitate educated decision-making regarding available treatment options. The TNM classification for breast cancer is based on the size of the tumour (T), whether or not the tumour has spread to the lymph nodes (N) in the armpits, and whether the tumour has metastasised (M) or spread to a more distant part of the body. Larger size, nodal spread, and metastasis have a higher stage number and a worse prognosis.

The main stages are:

Stage 0 is a pre-malignant disease or marker. For example, DCIS (Ductal Carcinoma in Situ) is one type of Stage 0 tumours seen in breast cancer.

Stages 1–3 are defined as 'early' cancer and potentially curable (Table 1.2).

Table 1.2 Breast cancer stage 1-3

Stage IA	TI	N0	M0
Store ID	T0	N1mi	M0
Stage IB	Tl	N1mi	M0
	T0	N1	M0
Stage IIA	T1	N1	M0
	T2	N0	M0
Stage IIB	T2	N1	M0
Stage IIB	T3	N0	M0
	T0	N2	M0
	T1	N2	M0
Stage IIIA	T2	N2	M0
	T3	N1	M0
	T3	N2	M0
	T4 ,	N0	M0
Stage IIIB	T4	N1	M0
	T4	N2	M0
Stage IIIC	Any T	N3	M0

T0 No evidence of primary tumour; **T1** Tumour \leq 20 mm in greatest dimension; **T2** Tumour > 20 mm but \leq 50 mm in greatest dimension; **T3** Tumour > 50 mm in greatest dimension; **T4** Tumour of any size with direct extension to the chest wall and/or to the skin (ulceration or skin nodules)

No regional lymph node metastases; N1 Metastases to movable ipsilateral level I, II axillary lymph node(s) (mi: Micrometastases (greater than 0.2 mm and/or more than 200 cells, but none greater than 2.0 mm)); N2 Metastases in ipsilateral level I, II axillary lymph nodes that are clinically fixed or matted; or in clinically detected* ipsilateral internal mammary nodes in the absence of clinically evident axillary lymph node metastases; N3 Metastases in ipsilateral infraclavicular (level III axillary) lymph node(s) with or without level I, II axillary lymph node involvement; or in clinically detected* ipsilateral internal mammary lymph node(s) with clinically evident level I, II axillary lymph node metastases; or metastases in ipsilateral supraclavicular lymph node(s) with or without axillary or internal mammary lymph node involvement

M0 No clinical or radiographic evidence of distant metastases

Stage 4 is defined as 'advanced' and/or 'metastatic' cancer and incurable (any T or any N with distant detectable metastasis).

Clinical staging of prostate cancer usually employs a variety of parameters such as DRE, PSA, needle biopsy findings, and radiologic imaging, to predict the true extent of disease. There are two main classification systems for prostate cancer clinical staging: the Whitmore-Jewett and the tumour, node, metastases (TNM) classification systems. The Whitmore-Jewett system was created in 1956 and was used until 1975 when the TNM system was adopted by the American Joint Committee for Cancer Staging and End Results Reporting (AJCC) (Wallace *et al.*, 1975). The disease can be staged in accordance with extent of tumours, lymph node involvement and distant metastasis. According to the UICC (Union for International Cancer Control) 6th edition (2002) and UICC 7th edition (2010), the tumour, lymph node, metastasis can be combined into four stages of worsening severity. As **Fig.1.3** shown, Stage I has been expanded from T1a to T1 and T2a this year and Stage II has been revised from including T1 1a, 1b, 1c and T2 to including T2b~T2c.

T1 Not palpable or visible STAGE GROUPING (ANATOMIC) T1a ≤5% or less (UICC) T1b >5% T1c Detected by needle biopsy Stage I T1, T2a No Stage II T2b-2c **T2 Confined within prostate** Stage III T3 N0 T2a ≤ half of one lobe Stage IV T4 N0 T2b > half of one lobe Any T N1 T2c **Both lobes** Any T Any N M1 T3 Through prostate capsule T3a Extracapsular T3b Seminal vesicle(s) T4 Fixed or invades adjacent structures No change from 6th

Figure 1.3 Classification of Prostate cancer

UICC TNM Classification of Malignant Tumours, 2010, (7th edition)

Source: (http://www.uicc.org/node/7735)

N0: there has been no spread to the regional lymph nodes; N1: there has been spread to the regional lymph nodes

M0: there is no distant metastasis; M1: there is distant metastasis

The Whitmore-Jewett system is similar to the TNM system, with approximately equivalent stages.

A: tumour is present, but not detectable clinically; found incidentally

A1: tissue resembles normal cells; found in a few chips from one lobe

A2: more extensive involvement

B: tumour can be felt on physical examination but has not spread outside the prostatic capsule

BIN: tumour can be felt, it does not occupy a whole lobe, and is surrounded by normal tissue

B1: tumour can be felt and it does not occupy a whole lobe

B2: tumour can be felt and it occupies a whole lobe or both lobes

C: tumour has extended through capsule

C1: tumour has extended through the capsule but does not involve seminal vesicles

C2: tumour involves seminal vesicles

D: tumour has spread to other organs

The Gleason grading system is used to help evaluate the prognosis of men with prostate cancer from a biopsy of prostate tissue or from the prostate removed

after surgery. Cancers with a higher Gleason score are more aggressive and have a worse prognosis. The Gleason score ranges from 2 to 10, with 10 having the worst prognosis, based on the 5 Gleason patterns. The score is the sum of the first majority tumour pattern and the second majority pattern. Increasingly, pathologists provide details of the "tertiary" component. This is why there is a small component of a third (generally more aggressive) pattern. So there could be a Gleason 3+4 with a tertiary component of pattern 5.

The patterns are classified by the features:

- Pattern 1 The cancerous prostate closely resembles normal prostate tissue. The glands are small, well-formed, and closely packed.
- Pattern 2 The tissue still has well-formed glands, but they are larger and have more tissue between them.
- Pattern 3 The tissue still has recognizable glands, but the cells are darker. At high magnification, some of these cells have left the glands and are beginning to invade the surrounding tissue.
- Pattern 4 The tissue has few recognizable glands. Many cells are invading the surrounding tissue
- Pattern 5 The tissue does not have recognizable glands. There are often just sheets of cells throughout the surrounding tissue.

Pathological stage of prostate cancer is determined after prostate removal and involves careful histological analysis of the prostate, seminal vesicles, and pelvic lymph nodes if a lymphadenectomy has been performed. The pathological staging for

breast cancer depends on the cancer cells' original derivation and the differentiation ability: well differentiated (low grade), moderately differentiated (intermediate grade), and poorly differentiated (high grade).

With the exception of prostate-specific antigen (PSA), tumour markers do not have sufficient sensitivity or specificity for screening. Cancer antigen 15-3 (CA 15-3) is perhaps the most thoroughly investigated serum tumour markers in breast cancer. Being a normal product of breast cells, CA 15-3 does not cause cancer rather it reflects the increase of breast cancer cells. Ovarian, lung and prostate cancers may also produce CA 15-3. CA 15-3 may be requested along with other tests, such as oestrogen and progesterone receptors, Her2/neu, and BRCA-1 and BRCA-2 genetic testing, when advanced breast cancer is first diagnosed to help determine cancer characteristics and treatment options.

Breast cancer cells with oestrogen receptor (ER) and/or progesterone receptor (PR) depend on oestrogen and/or progesterone to grow. Testing for ER and PR is done to find out if a cancer is likely to be successfully treated with hormone therapy, such as tamoxifen (Nolvadex). Human epidermal growth factor receptor 2 (HER2) is present in 20% to 25% of breast cancers. Anti-HER2 treatments block HER2 to stop the growth of cancer cells induced by EGF. Testing for HER2 helps doctors to assess if a cancer can be treated with anti-HER2 treatments, such as Trastuzumab (Herceptin), and in some cases, may suggest whether additional treatment with chemotherapy may be helpful. Cancer antigen (CA) 27.29 is used most frequently to follow response to therapy in patients with metastatic breast cancer. (Chan et al.,

1997; Gion *et al.*, 1999). The CA 27.29 level is elevated in approximately one third of women with early-stage breast cancer (stage I or II) and in two thirds of women with late-stage disease (stage III or IV). Because of superior sensitivity and specificity, CA 27.29 has supplanted CA 15-3 as the preferred tumour marker in breast cancer. The metastatic breast cancer patients will have elevated levels of associated tumour markers because of the metastasis site. Carcinoembryonic antigen (CEA), an oncofetal glycoprotein, is expressed in normal mucosal cells and overexpressed in adenocarcinoma, especially colorectal cancer. Cancer antigen 15-3 (CA 15-3), cancer antigen 27.29 (CA 27.29), and carcinoembryonic antigen (CEA) are found in 50% to 90% of patients with metastatic breast cancer. However, these tumour markers are not sensitive in the early stage of cancer and are not specific to breast cancer. They can only be used as indicators of metastasis, prognosis and treatment.

1.1.3 Metastasis

Metastasis is a key-defining feature of malignancy and most problematic to cure. Up to 90% of deaths from cancer are due to metastasis (Hanahan and Weinberg, 2000). It is difficult to identify the aggressive tumour definitively during the early stage so it is still controversial as to whether patients should undergo conservative treatment at this stage. All the uncertainty and questions finally attribute to the understanding of the mechanism of metastasis. Cancer derives from a collection of multiple genetic aberrations and the same can be said regarding the development of metastasis. A number of metastasis-related genes have been revealed. Therein some

key genes have been shown to be responsible for the steps and biologic mechanisms leading to metastasis.

1.1.3.1 Immune escape of cancer cells

Tumour cells wisely employ some mechanisms to escape from the attack of immune cells, thus disrupt and suppress the host immune system. These mechanisms include loss of tumour antigen, alteration of HLA class I antigen, defective death receptor signalling, lack of co-stimulation, immunosuppressive cytokines and T cells. Fas and FasL might be involved in this (Gutierrez et al., 1999). The FasL expression by breast tumours may induce the apoptosis of activated infiltrating Fas-lymphocytes. The expression of FasL is upregulated by oestrogen in breast cancer cells and the upregulation can be blocked by tamoxifen, thus allowing the killing of cancer cells by activated lymphocytes (Mor et al., 2000). Fas exists in transmembrane and soluble forms. The circulating soluble form of Fas presents at higher levels in breast cancer patients (Ueno et al., 1999), induces host lymphocyte apoptosis and impairs expression of NKG2D and T-cell activation (Bewick et al., 2001). Therefore, the soluble form of Fas is considered to have potential value in clinical prognosis.

1.1.3.2 Cell adhesion molecules:

Metastasis occurs through a series of sequential steps, all of which a metastatic cell must successfully complete in order to establish growth at the secondary site. During the tumour progression, the profile of the cell surface adhesion molecules changes and the metastatic cells acquire the profile allowing them to detach from the

primary site and attach at the secondary site. The main morphological change of the tumour transition from benign to malignant and metastatic is that tumour cells change from a highly differentiated, epithelial morphology to a migratory and invasive mesenchymal phenotype, a biological process referred to as epithelial-mesenchymal transition (EMT). During the process of epithelial-mesenchymal transition (EMT), cells progressively redistribute or down-regulate their apical and basolateral epithelial-specific tight and adherens junction proteins (such as E-cadherin and cytokeratins) and re-express mesenchymal molecules (including vimentin and N-cadherin).

Selectins, integrins, immunoglobulin-cell adhesion molecules and cadherins are four major groups of adhesion molecules that are possibly correlated with metastasis. Cadherins are located in adherens junctions and desmosomes. Of the three major types of cadherins, type-I and desmosomal cadherein have been shown to inversely correlate with the metastatic properties of cancer cells. Intercellular adhesion mediated by cadherins depends on the interaction of the cadherins with the cytoskeleton. Distruption of the cadherin-cadherin interactions and cadherin-cytoskeleton linkages have a strong biological impact on the aggressiveness of cancer cells. Apart from the functional influence of cadherins on the aggressiveness of cancer cells, the transcription regulation of the cadherins also plays a key part in cancer spreading. The specific transcriptional repressors (including Snail, Slug, SIP1, Twist, and E12/E47), RTKs (EGFR, c-Met, IGF-1R, FGF receptors), non-RTK c-Src, secreted proteases as MMPs (matrix metalloproteinases), even the oestrogen receptor

status and growth factors (ErbB2 and TGF-β) can lead to the loss of E-cadherin. Loss of E-cadherin disrupts adhesion junctions between neighbouring cells and thereby supports detachment of malignant cells from the epithelial cell layer. This has direct effects on signalling pathways which promote tumour cell migration and proliferation. The loss of E-cadherin is frequently associated with the gain of N-cadherin, which has been shown to replace E-cadherin at cell-cell contacts during invasion, migration and metastatic dissemination of cancer cells. The loss of E-cadherin and gain of N-cadherin is an important and interesting biological pattern during the EMT process.

The immunoglobulin super family of cell adhesion molecules (ALCAM, VCAM-1, ICAM, CEACAM1, NCAM, Mel-CAM, HepaCAM, PECAM) have 1-7 extracellular immunoglobulin-like domains. They are attached to the plasma membrane by a single, hydrophobic transmembrane sequence and have a cytoplasmic tail. They are shown to be involved in both homotypic and heterotypic adhesion (Epstein, 2003).

The Selectins consist of three family members: E-selectin, L-selectin and P-selectin, which are expressed by both platelets and vascular endothelium. They are a group of cell surface lectins that mediate the adhesion between leukocytes, platelets and endothelial cells. Selectin mediated adhesion to ensure the recruitment of leukocytes roll to the area of injury and inflammation. Selectins have also been implicated as one of the key mechanisms during the 'docking' process of the circulating tumours cells, in which tumour cells use selectin mediated adhesion,

which occurs fast, to quickly lodge over the endothelial layer, before the subsequent 'docking' process to take place.

Integrins are transmembrane glycoproteins expressed as heterodimeric cellsurface receptors that consist of α and β subunits. Intergrins are pivotal in controlling cell attachment, cell migration, cell cycle progression and apoptosis.

1.1.3.3 Invasion and motility:

The ability of invasion and motility is important for dissemination of cancer cells and is required in the process of cancer metastasis. Metastasis consists of distinct steps: (a) migration of tumour cells from the primary tumour. A key event happened prior to or during the dissociation from primary tumour is epithelial-mesenchymal transition (EMT) which confers cancer cells the crucial phenotype and capacities for detaching and migrating away from the primary tumour; (b) invading to neighboring tissue and penetrating through the basement membrane and entering blood or lymphatic vessels, the latter of which is referred to as intravasation. After the progressive growth of primary tumour cells and extensive vascularisation, some key genes are involved in the initial local invasion of the host stroma, detachment and embolization of small tumour cell in circulation and the survival tumour cells arrested in the capillary beds of organs and extravasation by invasion again.

1.1.3.4 Urokinases-type plasminogen activator:

Several gene families of extracellular proteinases have a role in the control of the invasion ability of breast cancer cells through the degradation of the extracellular

matrix. The serine proteinases such as urokinases-type plasminogen activator (uPA) are essential for tumour cell invasion, metastasis and proliferation. The uPA protein converts plasminogen to plasmin by specific cleavage of an Arg-Val bond in plasminogen. Plasmin in turn cleaves this protein at a Lys-Ile bond to form a twochain derivative in which a single disulfide bond connects the amino-terminal Achain to the catalytically active, carboxy-terminal B-chain. This two-chain derivative is also called HMW-uPA (high molecular weight uPA). HMW-uPA can be further processed into LMW-uPA (low molecular weight uPA) by cleavage of chain A into a short chain A (A1) and an amino-terminal fragment. LMW-uPA is proteolytically active but does not bind to the uPA receptor. Alternatively spliced transcript variants encoding different isoforms have been found for this gene. MDA-MB-231 cells are highly invasive and express high levels of uPA. The silence of uPA in MDA-MB-231 cells suppressed their invasion and proliferation (Arens et al., 2005). A similar observation was made with prostate cancer cells (Pulukuri and Rao, 2007). The uPA expression correlates with the progression of prostate cancer, and the level of uPA was proposed as a useful biochemical predictor of recurrence in patients undergoing radical prostatectomy (Kumano et al., 2009). Bikunin, a Kunitz-type protease inhibitor, markedly suppresses the cell motility possibly through a coordinated downregulation of uPA which is likely to contribute to the cell invasion processes (Kobayashi, 2001) while the p38 MAPK pathway participates in endothelial cell migration by regulating uPA expression.(Yu et al., 2004)

The zinc-dependent matrix metalloproteinases (MMPs) is another important protease family whose primary function is degradation of proteins in the extracellular

matrix. There are overwhelming amount of experimental data to suggest that MMPs (19 family members) are involved in primary and metastatic tumour initiation, invasion and metastasis (Chambers and Matrisian, 1997; Duffy and McCarthy, 1998). Activation of MMP-9 directly mediated by uPA promotes cell invasion (Zhao *et al.*, 2008). High levels of at least two MMPs (MMP-2 and stromelysin-3) have been found to correlate with poor prognosis in patients with breast cancer (Duffy *et al.*, 2000).

The leukocyte elastases and the cysteine proteinases such as cathepsin D and L are reported to be involved in this step of cancer metastasis.

1.1.3.5 Hepatocyte growth factor/scatter factor (HGF/SF)

Hepatocyte growth factor/scatter factor (HGF/SF) is a paracrine cellular growth, motility and morphogenic factor. Hepatocyte growth factor is mostly secreted by stromal cells in the body and acts as a multi-functional cytokine on cells of mainly epithelial origin. Its ability to stimulate mitogenesis, cell motility, and matrix invasion makes it a key player in angiogenesis, tumourigenesis and tissue regeneration. Hepatocyte growth factor regulates cell growth, cell motility and morphogenesis by activating a tyrosine kinase signalling cascade after binding to the proto-oncogenic c-Met receptor. PAK proteins, a family of serine/threonine p21-activating kinases, link RhoGTPases to cytoskeleton reorganization and nuclear signaling. Knockdown of PAK1 inhibits HGF-stimulated migration and loss of cell-cell junctions in DU145 prostate carcinoma cells. This can be seen in PC-3 prostate carcinoma cells with knockdown of both PAK1 or PAK2, which lack cell-cell

junctions (Bright et al., 2009). In breast cancer, HGF stimulates tumour growth and angiogenesis in vivo (Lamszus et al., 1996) and invasiveness in vitro (Matteucci et al., 2005; Meiners et al., 1998). HGF was found to disrupt tight junctions in breast cancer cells (Martin et al., 2004) and enhance its adhesion to endothelial cells through upregulation of CD44, a well characterised homing receptor for cancer cells (Mine et al., 2003). HGF activator inhibitors (HAI-1 and HAI-2) (Parr and Jiang, 2006) and c-MET silencing (Jiang et al., 2001) reduce migration and invasiveness of breast cancer cells induced by HGF. NK-4 is a specific antagonist to HGF and suppresses in vivo tumour growth and angiogenesis (Martin et al., 2003b), cell motility and invasion in vitro (Hiscox et al., 2000). This antagonist also affects changes in the transendothelial (TER) and paracellular permeability of human vascular endothelial cells induced by HGF (Martin et al., 2002).

HGF also can be used as predictor of recurrence and survival. Breast cancer patients with more advanced TNM staging (Sheen-Chen *et al.*, 2005) and 82.9% with recurrence (Taniguchi *et al.*, 1995) were shown to have higher serum soluble HGF.

1.1.3.6 Tumour metastasis suppressor genes

There are at least 13 genes characterized as metastasis suppressors to date, including: Nm23, KAI-1, KISS-1, TXNIP (VDUP1), CRSP3, MKK4, Src-suppressed C kinase substrate (SSeCKS), RhoGDI2, E-cadherin, Drg-1, Tissue inhibitor of metalloproteases (TIMPs), RKIP, and BRMS1. Tumour suppressor genes function by loss-of-function mutations. The mutation or deletion of these genes might disrupt signal transduction pathways to induce cancer.

Traditionally, it is regarded that tumour cells acquire the metastatic genotype and phenotype late during tumour development. Recently, it has been shown that tumour cells acquire the genetic changes relevant to their metastatic capacity early in tumourigenesis by analysing the disseminating breast cancer cells during primary and early stages (Demou and Hendrix, 2008; Kong et al., 2001; Smith et al., 1993).

1.1.4 Management Therapy for prostate cancer

Treatment for prostate cancer may involve active surveillance (monitoring for tumour progress or symptoms), surgery (i.e. radical prostatectomy), radiation therapy including brachytherapy (prostate brachytherapy) and external beam radiation therapy, High-intensity focused ultrasound (HIFU), chemotherapy, oral chemotherapeutic drugs (Docetaxel), cryosurgery, hormonal therapy, or some combination.

Traditionally, conservative management (active monitoring) has been reserved for older patients with a life expectancy of less than 10 years and a low-grade (Gleason score 2 to 5) prostate cancer. Deferred therapy for patients with prostate cancer is usually based on close observation with semiannual PSA tests and DRE and annual biopsies (Carter et al., 2002; Choo et al., 2002; el-Geneidy et al., 2004; Klotz et al., 2004; Patel et al., 2004; Zietman et al., 2001). However, active monitoring is now being studied in younger patients with low-volume, low- or intermediate-grade tumours to avoid or to delay treatment that might not be immediately necessary.

A report of a randomized clinical trial from Scandinavia showed that patients with clinically localized prostate cancer managed with watchful waiting have significantly higher rates of local cancer progression, metastases, and death from prostate cancer and a shorter cancer-specific overall survival than those treated initially with radical prostatectomy (Bill-Axelson *et al.*, 2005).

Hormone therapy and chemotherapy are never curative, and not all cancer cells can be eradicated consistently by radiation or other physical forms of energy, even if the tumour is contained within the prostate gland. Preoperative clinical and pathological parameters are often recruited to predict the pathologic stage and as additional information for operation. The operation can be performed by a number of methods including through perineal, retropubic, laparoscopic, and even robotic approach (Figure 1.4). The post-operation serum PSA level test has be used to monitor the tumour recurrence. The most common late complications of radical prostatectomy are erectile dysfunction, urinary incontinence, inguinal hernia, and urethral stricture but always associated with the patient's age. The patients with high risk (clinical stage: T2b and upwards; PSA level: ≥10; Gleason score: ≥7) whose life expectancy is at least 10 years are recommended to have the operation in conjunction with radiation therapy. Radiation therapy is another important treatment approach but with the main adverse side effects of injury to the microvasculature of the bladder, rectum, striated sphincter muscle, and urethra.

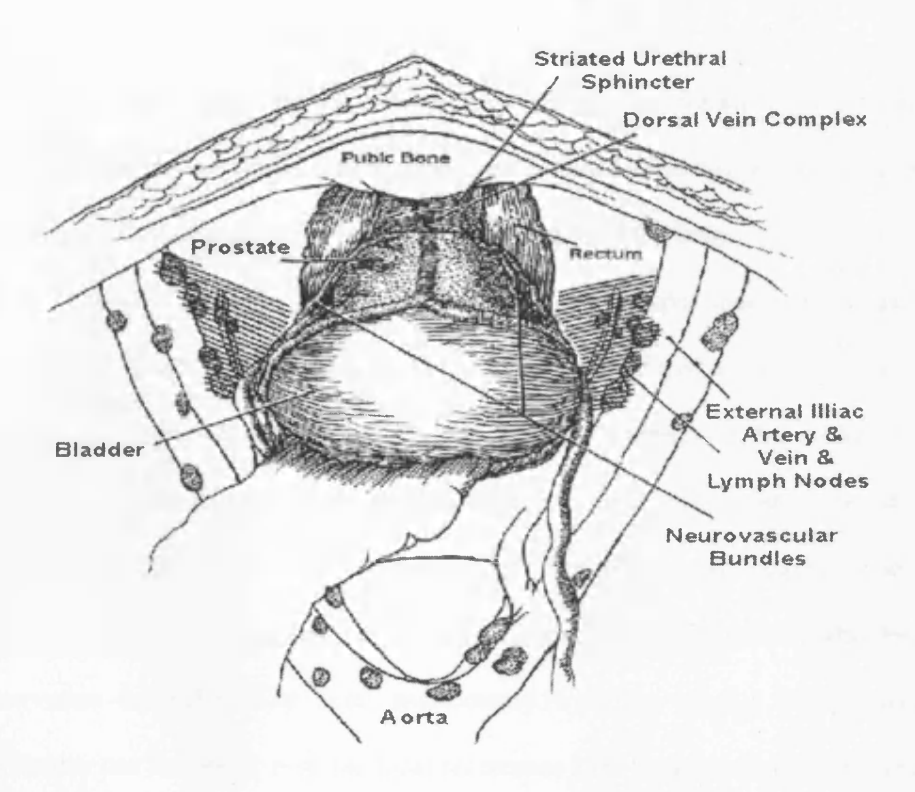


Figure 1.4 Schematic view of the prostate, bladder and lymph nodes.

It's the view the surgeon has after the abdominal incision has been made. Inside the shaded area are the lymph nodes removed during a staging lymphadenectomy. Source from *Dr. Patrick Walsh's Guide to Surviving Prostate Cancer* by Patrick C. Walsh, M.D., and Janet Farrar Worthington http://www.phoenix5.org/books/Walsh2/WalshRRP01.html

Treatment for breast cancer

For the local breast tumour, the traditional surgical treatment involves total removal of the breast (mastectomy). The most commonly performed operation was the Halsted radical mastectomy (including the removal of the breast, underlying chest muscle (pectoralis major and pectoralis minor), and lymph nodes of the axilla) (Figure 1.5). Breast conservation treatment can be considered according to patient choice, tumour size, the position of the cancer in the breast, and the nature of the breast cancers themselves. Most authorities recommend total mastectomy if the tumour is more than 3 or 4 cm in diameter, multicentricity, mulifocality, centrally located or poorly differentiated. The overall incidence of local recurrence after breast conservation is higher than total mastectomy. (Newman et al., 1999) Salvage mastectomy can be used to treat the local recurrence after breast conservation therapy. Systemic treatment with tamoxifen or chemotherapy may alleviate symptoms but responses are often quite short lived when recurrence is widespread (Biglia et al., 2003).

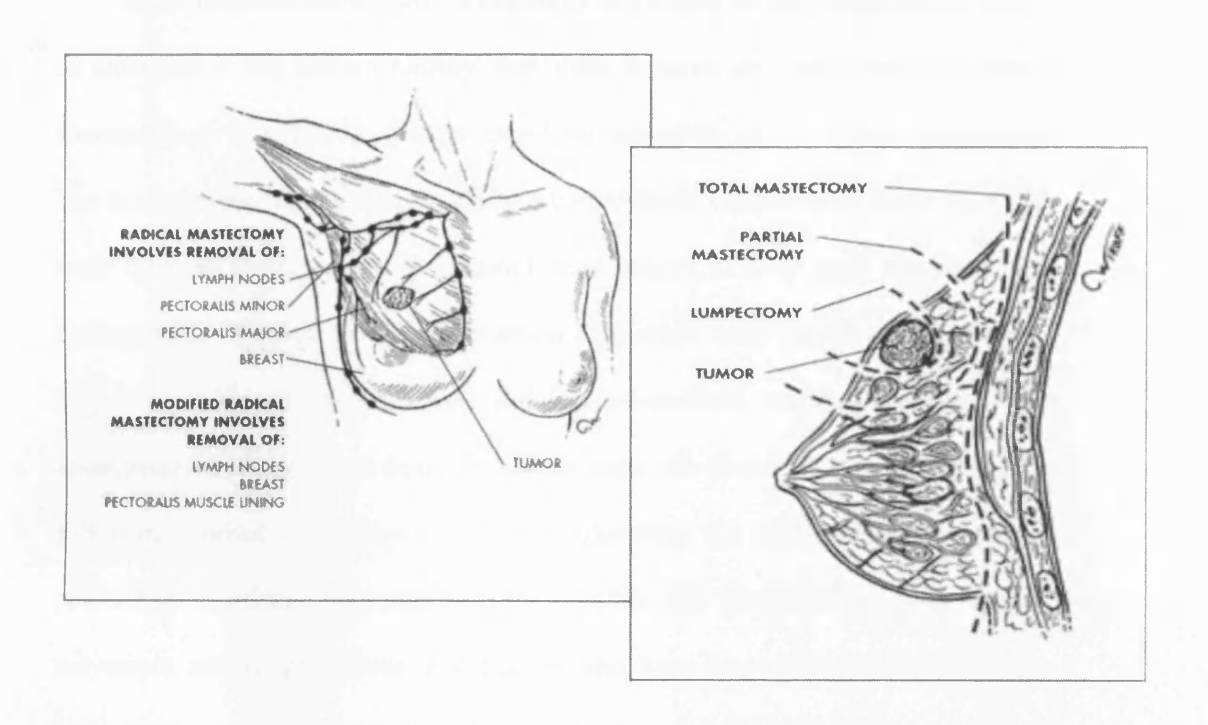


Figure 1.5 Breast cancer surgeries

Radical mastectomy of breast cancer (left). Methods of different kinds of breast cancer surge ries (right). Source from healthsquare.com.

Local recurrence after total mastectomy is difficult to treat. Radiotherapy may be attempted if this has not already been used; adjuvant drug treatment with either chemotherapy or endocrine therapy may help reduce the risk of further recurrence. The management of the axillary nodes is a controversial topic to date. There are three main types of axillary surgery: sentinel node biopsy, axillary node sampling and axillary node clearance. Recent instruction of sentinel node biopsy has, to a great degree, transformed the procedure and has substantially reduced the scale and unnecessary axillary dissections. If cancer cells are found in the lymph nodes following sentinel node biopsy or axillary sampling, the patient should normally proceed to an axillary clearance with the possible side effect of pain, limit of arm movement and lymphoedema. For people who have large breast tumours where mastectomy would be necessary, chemotherapy or hormone therapy is sometimes prescribed before surgery to shrink the tumour to improve the surgery successful rate, which called neoadjuvant therapies. Women who have a mastectomy may also have breast reconstruction, either at the same time (immediate reconstruction) or at some time in the future (delayed reconstruction). Adjuvant treatment given after surgery includes one or more of radiotherapy, chemotherapy, hormone therapy, and targeted (biological) therapy and depends on the risk of the cancer recurring or spreading.

Generally speaking, the management once metastasis has occurred must be delicate. Radio- and chemotherapy could be an option. Endocrine therapy has been an important pillar in the treatment of breast cancer metastasis recently. The use of biphosphonates and radiotherapy could be the emphasis in the management of prostate cancer bone metastasis.

1.2 Bone metastasis in prostate cancer and breast cancer

Bone is the most common site of metastasis for certain tumour types. Breast cancer and prostate cancer are the two tumour types that most commonly metastasise to bone (Mundy, 2002).

Most circulating tumour cells pass through the bone marrow, as a consequence of its vascularity. This may be the reason why cancers have such high avidity for bone. The bone environment also provides a particularly fertile ground for the growth and aggressive behaviour of the tumour cells that reach it. There are different patterns of bone effects in patients with cancer, ranging from mostly destructive or osteolytic (breast cancer, myeloma), to mostly bone-forming or osteoblastic (prostate cancer). In breast cancer, osteolysis is caused by osteoclast stimulation – not by the direct effects of cancer cells on bone (Boyde *et al.*, 1985), while the predominant osteolysis effect is coupled with local bone formation response (Stewart *et al.*, 1982). In prostate cancer, there is a profound local stimulation of osteoblasts adjacent to the metastatic tumour cells. However, some patients also have osteolytic lesions which are similar to those with metastatic breast cancer. These two processes (bone resorption and bone formation) seem to be linked and both activated in bone metastases.

Parathyroid-hormone-related peptide (PTH-rP) is one of the main and specific mediators of osteolysis in metastastic breast cancer and the mediator of bone destruction in most other osteolytic cancers (Bryden *et al.*, 2002; Miki *et al.*, 2000). When breast cancer cells are present in the bone microenvironment, PTHrP is

overproduced (Guise and Mundy, 1996; Guise et al., 1996), an increase in production far greater than that seen in other metastatic sites (Powell et al., 1991; Southby et al., 1990). Production of the PTHrP by tumour cells activates osteoblasts to produce RANKL (receptor activator of nuclear factor-κB ligand) and downregulate osteoprotegrin (OPG). This activates osteoclast precursor cells, leading to osteolysis. Resorbed bone releases bone-derived growth factors, including TGF-β and IGF1 (insulin-like growth factor1) and raises extracellular calcium (Ca²+) concentrations. The growth factors bind to receptors on the tumour cell surface and activate phosphorylation and signalling through pathways that involve Smad and MAPK (mitogen activated protein kinase). Extracellular Ca²+ binds and activates a Ca²+ pump. These growth factors promote breast cancer cell proliferation and further release of PTHrP, to cause more bone resorption, thus forms a cycle of regulations (Guise et al., 1996; Rasmussen and Cullen, 1998; Yin et al., 1999; Yu and Rohan, 2000).

The mechanisms by which osteoblastic lesion is regulated are far from clear. There are several mechanisms of osteoblastic bone metastasis caused by prostate cancer. TGF-β2, which is expressed at high levels by prostate cancer cell line PC-3, promotes the proliferation of osteoblasts *in vitro*, as well as bone formation *in vivo* (Marquardt *et al.*, 1987). Overexpression of uPA (serine protease urokinase) by rat prostate cancer cells has been shown to induce bone metastasis *in vivo* (Achbarou *et al.*, 1994), and an amino-terminal fragment of uPA has been shown to have mitogenic activity for osteoblasts (Rabbani *et al.*, 1992). uPA is also activated by

PSA (prostate-specific antigen), a serine protease which can activate other growth factors, such as IGF1 (insulin-like growth factor 1) and TGF- β and cleave PTHrP into inactive fragments.

1.3 Bone morphogenetic proteins and their signalling pathway in cancer

1.3.1 BMPs

The Transforming Growth Factor-β (TGF-β) superfamily is one of the biggest and important families of proteins, which participates in the development and homeostasis of diverse tissues and organs through regulating cellular differentiation, proliferation, apoptosis and motility. Up to date, more than 30 structurally related growth factors have been identified in the TGF-β superfamily including TGF-βs, Activins, Inhibins, Bone Morphogenic Proteins (BMPs), Growth and Differentiation Factors (GDFs), and Mullerian Inhibiting Substance (MIS) (Heldin *et al.*, 1997). BMPs may also be alternatively named as GDFs.

The TGF- β family members play crucial roles in bone metastases. The bone formation involves a cascade of events, which triggers cellular events including osteoblast proliferation and differentiation as well as osteoclast apoptosis. Osteoblast proliferation is induced by mitogenic factors, such as transforming growth factor- β (TGF- β), insulin-like growth factors (IGFs), fibroblast growth factors (FGFs) and platelet- derived growth factor (PDGF). TGF- β might be released as a consequence of resorption to induce osteoclast apoptosis and impair continued resorption. The osteoblast differentiation involves expression of the structural proteins of the bone

matrix. BMPs are predominantly responsible for osteoblast differentiation and bone matrix production and mineralization

BMPs are highly related molecules which compose a subgroup of the transforming growth factor- β (TGF- β) super family. So far, more than 20 molecules have been discovered to be BMP family members, of which the first was identified by Urist *et al.* in 1965.

Bone Morphogenic Proteins (BMPs) are osteogenic factors abundant in bone matrix and have been indicated to be crucial to bone metastasis of cancer. BMP2, BMP4 and BMP7 are expressed in a spatially and temporally dynamic pattern, prior to the formation of cartilage elements (Francis-West et al., 1995; Francis et al., 1994) and expressed in the perichondrium within the developing limb cartilage elements (Jones et al., 1991; Lyons et al., 1990; Macias et al., 1997; Tabas et al., 1993). BMP6 is expressed in prehypertrophic and hypertrophic chondrocytes (Zou et al., 1997). BMP8B is found in mice but not in humans. Another BMP family member, GDF5(Growth/differentiation factor 5) is isolated as cartilage-derived morphogenetic protein-1 (CDMP-1) (Chang et al., 1994; Storm et al., 1994) and expressed in the developing joints and perichondrium (Chang et al., 1994; Storm et al., 1994), while GDF9 was found only abundantly in oocytes in ovaries (Dong et al., 1996).

The BMP family proteins comprise an amino-terminal pro-region and a carboxy-terminal ligand of 110-140 amino acids in length. BMPs are first synthesised as large precursor proteins, processed into mature proteins, and secreted as homo- or heterodimers (Ozkaynak *et al.*, 1990; Wozney *et al.*, 1990; Wozney *et al.*, 1988). Once they have been processed and activated, BMP proteins are biologically

active both as homodimer, and as heterodimer molecules connected by disulfide bonds. The active domain of BMPs contains a conserved motif of seven cysteines and six of them form a cysteine knot, which is involved in dimerisation (Massague *et al.*, 1994). However, the heterodimers of BMP4/7, BMP2/6, BMP2/7 and BMP7/GDF7 are more effective than their homodimers (Aono *et al.*, 1995; Butler and Dodd, 2003; Israel *et al.*, 1996; Suzuki *et al.*, 1997).

After activation, BMPs regulate transcription of their target genes mainly by signalling through specific serine-threonine receptors and intracellular Smad proteins (Itoh *et al.*, 2000). Six of the seven Type-I receptors (ALK1, ALK2/ACTR-I, ALK3/BMPR-IA, ALK4/ACTR-IB, ALK5/TβR-I, ALK6/BMPR-IB, ALK7) and three of the five Type-II receptors (TβR-II, ACTRIIA, ACTRIIB, BMPRII, AMHRII) have been implicated in BMP signalling, of which BMPR-IA, BMPR-IB (Type-I) and BMPR-II (Type-II) are specific for BMPs (Shi and Massague, 2003).

BMP and bone metastasis

Osteoblast differentiation induced by BMPs is mediated mainly via the Smadsignalling pathway, whereas chondrogenic differentiation may be transmitted by Smad-dependent and independent pathways (Fujii et al., 1999). Active forms of bone morphogenetic protein (BMP) type I receptors and those of activin receptor-like kinase (ALK)-1 and ALK-2 (ALK-1 group), R-Smads (Smad1, 5) induced alkaline phosphatase activity in C2C12 cells. BMP6 dramatically enhanced alkaline phosphatase activity induced by Smad1 or Smad5 which can be repressed by Smad6 and Smad7. More interestingly, ALK-2 and ALK-3 (or ALK-6) were found to

synergistically induce higher transcriptional activity and osteoblast differentiation of C2C12 cells than any receptor alone (Aoki *et al.*, 2001).

The investigation of BMPs into their role in bone formation and bone metastasis are becoming increasingly interesting. It is embodied in that, apart from bone development and bone metastasis, BMPs also participate in various physiological and pathophysiological processes, such as embryonic development, organogenesis, and adult tissue homeostasis. BMP2 and BMP4 have potent bone and cartilage-inducing activity in vivo (Winnier et al., 1995; Zhang and Bradley, 1996). Osteogenic protein-1 (OP-1; also named BMP7), OP-2 (BMP8), OP-3 (BMP8B), BMP5 and BMP6 (also named Vgr-1) form another subfamily. OP-1 (BMP7) potentially has bone- and cartilage inducing activity in vivo and the null mice appear to be associated with defects in eye, kidney and skeletal morphogenesis (Dudley et al., 1995; Luo et al., 1995). BMP8B null mice were shown to have defects in spermatogenesis (Zhao et al., 1996). GDF5 acts in a relatively specific fashion for chondrogenesis when assayed using rat limb bud cells (Hotten et al., 1996). This, together with GDF6 and GDF7 were shown to induce tendon and ligament formation when implanted at ectopic sites in vivo (Wolfman et al., 1997). The members in the GDF5 subgroup act specifically in the morphogenesis of the limb skeleton. GDF8 (also termed myostatin) and GDF9 are structurally distantly related to the other BMPs. GDF8 (myostatin) negatively regulates the growth of skeletal muscle cells in vivo (McPherron et al., 1997). GDF9 is important to ovarian folliculogenesis (Dong et al., 1996).

1.3.2 BMP signalling in cancer

There are two signalling pathways via which BMPs act to activate intracellular signalling molecules: the Smad dependent or Smad independent pathways.

The two different types of serine-threonine kinase transmembrane BMP receptors, Type I and type II are recruited by both pathways upon activation by BMPs. If the dimeric ligand of BMPs bound to the two receptors simultaneously, the Type-II receptors would transphosphorylate the GS domain of the Type-I receptors (Moustakas and Heldin, 2002). The type I receptor then transduces the signal by phosphorylating intracellular targets, including members of the Smad family (Hoodless *et al.*, 1996; Liu *et al.*, 1996). This is known as the Smad dependent pathway.

Intracellular signals are transduced by Smad proteins. After phosphorylation, the R-Smads (Smad1, 5 and 8) are released from the receptor and recruit the Co-Smad (Smad4) to form heteromeric complexes, and translocate into the nucleus where they may activate transcription of various genes (Figure 1.6). BMP4 and growth/differentiation factor 5 (GDF5) induce osteoblast differentiation through the activation of three receptor-regulated Smads (i.e. Smad1, Smad5 and Smad8). In contrast, BMP6 and BMP7 induce alkaline phosphatase activity through Smad1 and Smad5, but not through Smad8 (Aoki *et al.*, 2001). Another report also determined BMP7 binds predominantly to Smad1, Smad5, and Smad8, but not Smad2 and Smad3 and stably interacts with BMPR-IB (BMP type IB receptors) which is phosphorylated by BMPR-II (Type II receptor for BMPs) in the rat osteoprogenitor-like cell line, ROB- C26 (Tamaki *et al.*, 1998). Consistent with these findings, BMP4

has been shown to induce phosphorylation and nuclear translocation of Smad1, Smad5 and Smad8, but BMP-6 activated only Smad1 and Smad5. BMP4 and GDF5 are known to bind to activin receptor-like kinase 3 (ALK-3) and/or ALK-6 (also termed BMP type IA and type IB receptors, respectively), whereas BMP6 and BMP7 preferentially bind to ALK-2 (Aoki *et al.*, 2001). Smad6 and Smad7 are inhibitory Smads, and inhibit TGF-β family signalling by preventing the activation of R-Smads and Co-Smads (Itoh *et al.*, 2001).

If BMP ligands bound to ALK3 or ALK6 first, and then recruited BMPRII into a hetero-oligomeric complex (BMP-induced signalling complexes, BISC), this would lead to the activation of the Smad independent pathway (Nohe et al., 2004). During intracellular signal transduction, the X-linked inhibitor of apoptosis protein (XIAP) functions as an adaptor protein bridging between the Type I receptor and TGF-\(\beta\) activated binding protein (TAB1/2/3), which is an activator of the MAPKKK TGF-\(\beta\) activated tyrosine kinase 1 (TAK1) (Shibuya et al., 1996; Yamaguchi, 1995; Yamaguchi et al., 1999). The activation of TAK1 can lead to activation of p38, a mitogen-activated protein kinase (MAPK) (Kimura et al., 2000; Moriguchi et al., 1996a; Nohe et al., 2002). TAK1 can also activate Jun N-terminal kinases (JNKs), NF-kappaB (NF-kB) and Nemo-like kinase (NLK) (Ishitani et al., 1999; Lee et al., 2002; Shirakabe et al., 1997).

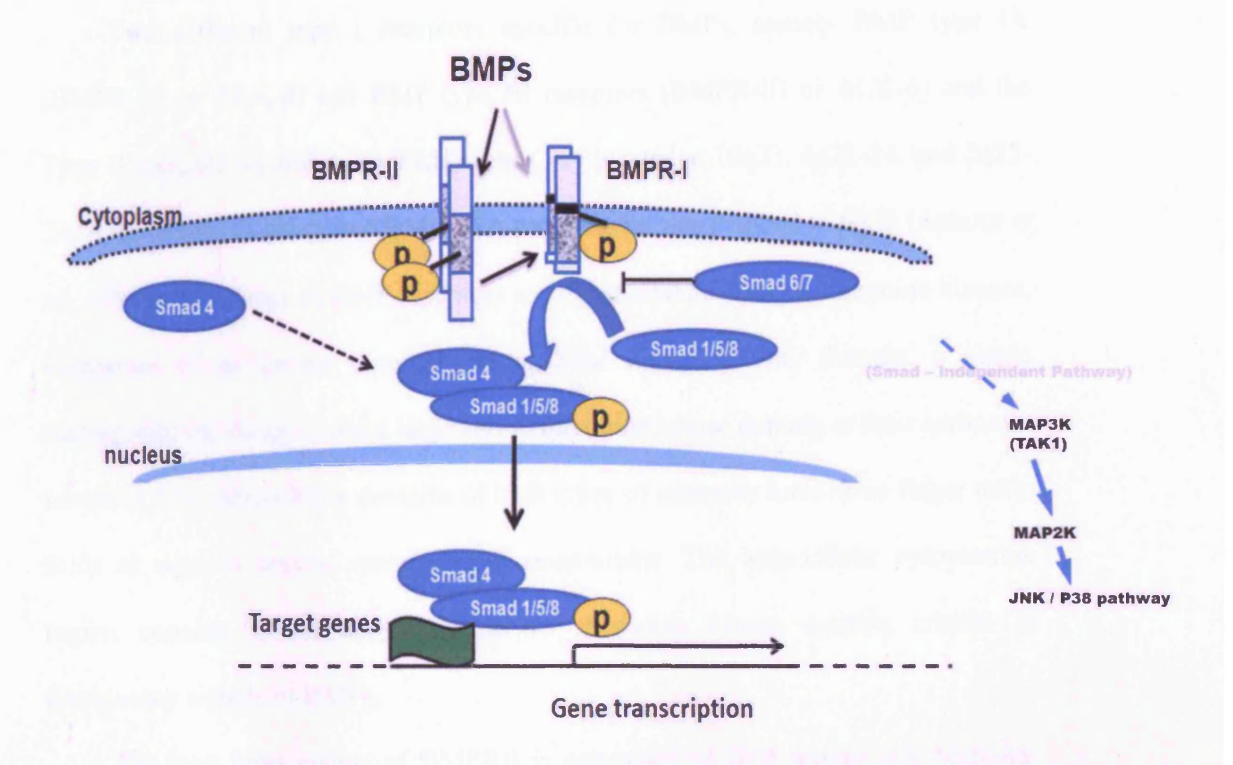


Figure 1.6. BMP signalling pathway through Smads and non-Smads

When BMP ligands bind to BMPR-I and BMPR-II simultaneously, the Smad1/5/8 pathway was activated. Upon phosphorylation by type I receptors, ligand-specific Smads formed complex with Smad 4 and translocated into nucleus to activate the transcription of target genes. On the other hand, when BMPs bind to BMPR-I first and then recruit BMPR-II, intracellular signal transduction will be relayed by Smad-independent pathways.

1.3.2.1 BMP receptors and their implication in cancer

Two different type I receptors specific for BMPs, namely BMP type IA (BMPR-IA or ALK-3) and BMP type IB receptors (BMPR-IB or ALK-6) and the Type II receptor for BMP (BMPRII) genes, are located at 10q23, 4q22-24, and 2q33-34, respectively. A processed BMPR-IA pseudogene was mapped to 6q23 (Astrom et al., 1999). Both types of BMP receptors are transmembrane serine/threonine kinases, composed of an amino terminal extracellular ligand binding domain, a single transmembrane domain, and a large serine/threonine kinase domain at their carboxylterminal. The extracellular domains of both types of receptors have three finger toxin folds as seen in several snake venom neurotoxins. The intracellular cytoplasmic region consists of an enzymatic serine/ threonine kinase domain critical in transducing signals of BMPs.

The long form variant of BMPRII is composed of 1038 amino acid residues, which has a long C-terminal tail and occurs by alternative splicing of mRNA (Beppu et al., 1997). The short form is rarely seen in most cell types and its function is identical with the long form when assayed in Xenopus embryos (Ishikawa et al., 1995). The two type I BMP receptors share 85% amino acids sequence identity and have very similar protein structures. Upon binding to ligands, BMPR-II may interact with multiple type I receptors, including BMPR-IA/Brk1, BMPR-IB, and ActR-I, which is also an activin type I receptor. The co-operation of BMPRII and ActR-I required by BMPs signalling reveals the crosstalk with the activin receptor system (Liu et al., 1995). Up to date, functional differences between the intracellular domains of the two type I BMP receptors are not fully characterised.

Aberrant expression and functions of BMP receptors have been implicated in the tumourigenesis and disease progression of malignant tumours. BMPR-IB and BMPRII have been indicated in the prostate cancer, in which they mediate inhibitory effect on both in vitro and in vivo growth of prostate cancer cells (Miyazaki et al., 2004; Ye et al., 2008). For example, over-expression of BMPR-IB (ALK-6) in PC-3 cells resulted in an inhibition of both in vitro proliferation and in vivo tumour growth (Miyazaki et al., 2004). Similarly, loss of BMP signalling molecules (including BMPR-IA, BMPR-IB, BMPRII, Smad4, and phosphorylated Smad1,5,8) have been shown to be correlated tightly with progression of human colon adenomas to colorectal cancer and occurs relatively early during cancer progression (Kodach et al., 2008). In addition, decreased expression of BMPR-IB correlates with poor prognosis in breast cancer patients and leads to increased cell proliferation of breast cancer cells in vitro (Bokobza et al., 2009). BMPR-IB was also demonstrated to be a major hallmark of the progression and dedifferentiation of oestrogen receptor-positive breast cancer (Helms et al., 2005). The impact of BMPR-IB on tumour progression, proliferation, and cytogenetic instability was mainly mediated via phosphorylation of Smad1. The pro-proliferative effect was indicated by XIAP and IAP-2 expression in BMPR-IB-positive carcinomas. The aberrant expression of BMP receptors in cancer may be due to regulation by hormones, growth factors and methylation status of the particular genes. In oestrogen-treated MCF-7 cells, estradiol decreased the expression levels of BMPR-IA, BMPR-IB, ACVR2A, and ACVR2B but did not affect ACVR1 and BMPRII (Takahashi et al., 2008).

1.3.2.2 Smad

Smad proteins can be divided into three distinct classes: the receptor-activated Smads (R-Smads), the common-mediator Smads (Co-Smads) and the inhibitory Smads (I-Smads). R- and Co-Smads have two highly conserved domains, Madhomology domains 1 and 2 (MH1 and MH2) at N- and C-terminal parts of the proteins, respectively. The MH1 domain of R- and Co-Smad can bind to specific DNA sequences (Dennler et al., 2002; Dennler et al., 1999; Jonk et al., 1998; Shi et al., 1998; Yagi et al., 2002; Yingling et al., 1997; Zawel et al., 1998). The MH2 domains are used in homo- and hetero-meric complex formation (Lagna et al., 1996; Wu et al., 1997). R-Smads are the only Smads that have an SSXS (Ser-Ser-X-Ser) motif in their C-terminal region which can be phosphorylated by type I serine/threonine receptors during signal transduction (Macias-Silva et al., 1998; Zhang et al., 1996). Among the R-Smads, Smads2/3 are described as TGF-β/activin activated Smads, whereas Smad1/5/8 are activated by BMPs (Miyazawa et al., 2002). However, some recent studies have shown that Smad2/3 can also be mediated by BMPs (Buijs et al., 2007b; Izumi et al., 2006). Co-Smad (Smad4) forms a heteromeric complex with R-Smads and translocates to the nucleus with them.

I-Smads interfere with the phosphorylation of R-Smads by Type-I receptors through interacting with activated Type-I receptors. Smad6 has been reported to occur in two forms, a short form mainly consisting of the MH2 domain and a long form containing an N-terminal sequence with weak similarity to the MH1 domains of R- and Co-Smads. The shorter form is a stronger inhibitor of BMP signalling than the

long form of Smad6. Smad7 is responsible for inhibiting TGF-β/activin and BMP signalling, whereas Smad6 is specific for BMP signalling (Ishida *et al.*, 2000; Nagarajan *et al.*, 1999).

Smad4 and Smad7 were observed in the majority of colorectal cancer specimens. Autocrine activation of Smad signalling may affect tumour environment via suppression of tumour-infiltrating immune cells and probably contributes to tumour cell aggressiveness (Gulubova et al., 2010). The changes in inhibitory Smads also contribute to disease progression as demonstrated in non-small cell lung cancer (Jeon and Jen, 2010). A hyperactive R-Smad2 signalling pathway is critical for EMT and consequent disease progression of breast cancer. Disrupting Smad signalling in mesenchymal breast cancer cells resulted in DNA demethylation and re-expression of the genes, which was accompanied by an acquisition of epithelial morphology and a suppression of invasive properties (Papageorgis et al., 2010).

Smad target genes include Id1-3, type-I collagen, Jun B and Mix.2. Id-1 (Inhibitor of differentiation-1) is an important regulator covering a variety of functions. Id-1 negatively regulates cell differentiation and promotes proliferation, survival and invasion of both cancer cells and vascular endothelial cells, particularly during angiogenesis and metastasis in various cancers (Ling *et al.*, 2006).

1.3.2.3 Impact of BMPs on cancer

BMP proteins have diverse effects on cancer cells. The diversity of the biological influence can be seen by: 1. the difference in the signalling pathways that they utilised namely Smad dependent vs Smad independent pathways, 2. different BMPs have contrast effect on the same cells, and 3. the same BMP may have an opposite effect on different cancer cells. Autocrine bone morphogenetic protein-9 signals through activin receptor-like kinase-2/Smad1/Smad4 to promote ovarian cancer cell proliferation (Herrera et al., 2009). However, BMP9 inhibits the growth of prostate cancer cells due to induced apoptosis, which is related to an up-regulation of prostate apoptosis response-4 through BMPRII and Smad1 (Ye et al., 2008). BMP7 induces ageing and death of breast cancer cells, by a mechanism involving inhibition of telomerase activity and telomere maintenance via BMPRII receptor- and Smad3-mediated repression of the hTERT gene (Cassar et al., 2009). Meanwhile, BMP7 inhibits the proliferation of androgen-insensitive PC-3 and DU-145 prostate cancer cells in a medium containing 1% fetal bovine serum through CDK1, observed as decreased incorporation of [(3)H] thymidine and decreased cell number (Miyazaki et al., 2004). BMP6 regulates the proliferation and gene expression profile of macrophages, in which BMPRII, ALK-2 and ALK-3 function as its receptors (Hong et al., 2009). BMP2 acts as a tumour suppressor promoting apoptosis in mature colonic epithelial cells and BMPR-IA, BMPRII and Smad1, Smad4 might be involved in this (Hardwick et al., 2004).

In the Smad-independent pathway, TAK1 is a Map kinase kinase activated by BMP4 and BMP2 stimulation, through which BMP4 or BMP2 subsequently activates the p38 pathway (Kimura et al., 2000; Moriguchi et al., 1996b; Shibuya et al., 1998). BMP2 and BMP4 are known to play a role in the regulation of apoptosis (Fujita et al., 1999; Macias et al., 1997; Omi et al., 2000; Piscione et al., 2001). BMP2, in the presence of IL6, mediates apoptosis in MH60 cells through the TAK1 p38 pathway. The apoptosis induced by BMP2 can be prevented completely by the expression of a kinase negactive form of TAK1. The activation of TAK1 can be blocked by Smad6 and Smad7. BMP6 and BMP7 inhibit oestrogen-induced proliferation of breast cancer cells by suppressing p38 mitogen-activated protein kinase activation through the Smad-independent pathway (Takahashi et al., 2008). However, TAK1 pathway is known to be able to induce or suppress apoptosis. TAK1-MKK4-JNK pathway has been reported to induce apoptosis in 293T cells (Yang et al., 2004). JNK plays an essential role through its ability to interact and modulate the activities of diverse proand antiapoptotic proteins (induce BAX, inhibit Bcl2 and so on) (Dhanasekaran and Reddy, 2008).

Taken together, BMPs and their signalling pathways have been implicated in development and progression of cancer, particularly in the bone metastasis. BMP signalling has been extensively involved in the regulation of proliferation, apoptosis, motility and invasion of both cancer cells and vascular endothelial cells, conferring favourable phenotypic features and environment during the disease progression and dissemination.

1.4 Repulsive guidance molecules (RGMs)

Apart from BMP receptors which are transmembrane kinase receptors, on the surface of cells, there exist other molecules which have influence on the action of BMPs. RGMs are the first identified BMP co-receptors on cell surface which are assumed to enhance the BMP signal pathway and will be the emphasis of the present study. This is in addition to BMP-binding proteins, Noggin and Chordin that extracellularly regulate BMP functions by acting as their antagonists.

1.4.1 **RGM**

In 2001, Wiemann et al. isolated a cDNA corresponding to human RGM (GenBank AL136826). RGMA was first cloned from mRNA of chick embryonic optic tectum (Monnier et al., 2002). RGMA, RGMB and RGMC were subsequently identified in mouse in 2004 (Niederkofler et al., 2004; Oldekamp et al., 2004; Schmidtmer and Engelkamp, 2004). RGMA was initially found to mediate repulsive axonal guidance and neural tube closure, while RGMB (Dragon) contributes to neuronal cell adhesion through homophilic interactions. The RGMC gene may play role in the inherited condiction juvenile hemochromatosis a disorder of iron overload in which RGMC gene is muated.

1.4.1.1 RGMA

RGMA has been found highly conserved in vertebrates including humans (accession number: AK074910), mice (BC059072), chickens (AY128507), frog (BC061329), zebrafish (BC091800), and salmon (BT045779) etc.

RGMA Gene characteristic:

The human *RGMA* gene was located at Chromosome 15q26.1. In human, mouse and chicken, RGMA is positioned in the opposite transcriptional orientation from the other nearby genes. Mctp2 (multiple C2 domains, transmembrane 2) is found near the 5' end to RGMA, and Chd2 (chromodomain helicase DNA-binding protein 2), St8sia2 (ST8α-N-acetyl-neuraminide α-2,8-sialytransferase), and Slco3a1 (solute carrier organic anion transporter family member 3A1) are located near the 3' end. The RGM genes are located on the same chromosome that encodes transducers of regulated cAMP response element-binding protein, bloom syndrome protein, Furin precursor, Isocitrate dehydrogenase, Mesoderm Posterior protein, Neurite outgrowth associated protein, Mesenchymal stem cell protein, Synaptic vesicle glycoprotein, Tubulin polyglutamylase.

Human RGMA gene is ~46 kb and composed of four exons, which is similar to mouse (~44 kb). After transcription, human RGMA is assembled as an mRNA of 3.2 kb (Figure. 1.6). The 5' end exon is non-coding, which mostly comprises the 5' untranslated region (UTR) of RGMA mRNA. The remaining 5' UTR is included in part

of the second exon. The second exon encodes 26 condons of the RGMA protein, while 72 amino acids (aa) encoded by the 3rd exon and 328 aa by the 4th exon, respectively. The 4th exon contains another ~1800 nucleotides and a single polyadenylation signal of 3' end. The 3 introns in human RGMA are of similar lengths as in mouse, but are not as conserved as the exons (up to 99%). Slight differences in the 5' UTR bring about six gene variants. These gene variants consequently derived 3 protein isoforms with different lengths and N-terminals.

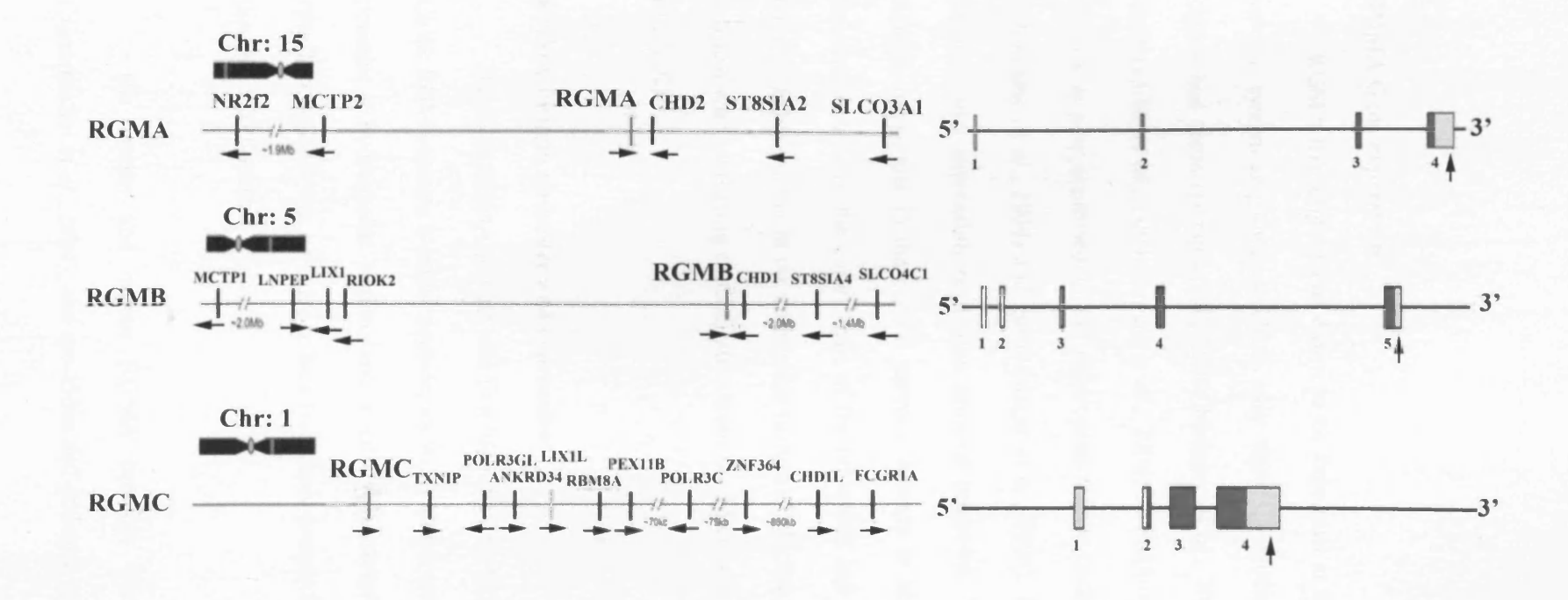


Figure 1.7 Comparison of human RGMs genomic loci and gene structures.

The relative position of the RGM genes (red line) is indicated on each chromosome (left). Neighbouring genes in the chromosome are presented with their transcriptional direction (arrow). Lix1-like (grey) is a putative pseudo-gene (Lix11). Right is the anatomy of human RGMs gene. Exons are indicated by boxes, with coding regions in blue and non-coding regions in yellow. The polyadenylation site is represented by a vertical arrow. Modified from Severyn *et al.*, 2009.

RGMA Gene expression

RGMA transcripts were shown to be expressed at higher levels in the central nervous system and lower levels in other tissues, including heart, liver, lung, skin, kidney and testis (Babitt et al., 2005; Metzger et al., 2005; Monnier et al., 2002; Niederkofler et al., 2004; Samad et al., 2004; Schmidtmer and Engelkamp, 2004). RGMA is also expressed in the developing mouse cochlea, lung, limb primordia (Oldekamp et al., 2004) and gut (Metzger et al., 2005). To date, the mechanism of RGMA gene expression regulation remains unknown. The expression pattern of RGMA transcripts in the central nervous extends to hippocampus, midbrain, the ventricular zone of the cortex, part of the brainstem and the spinal cord during the embryo development. In the embryonic tectum of chicken, its mRNA distributes in a gradient with increasing concentration from the anterior to posterior pole (Monnier et al., 2002).

RGMA Protein structure and expression

The chick RGMA protein was first identified by Monnier, Sierra *et al.* in 2002. Chick RGM contains a signal peptide, an RGD site, a von Willebrand factor (vWF) domain, a hydrophobic region, and a GPI (glycosylphosphatidylinositol) anchor (Fig.1.8). RGMA was revealed to be a two-chain protein bound to the cell membrane through a GPI-anchor.

The human and mouse RGMA proteins were subsequently identified (Niederkofler et al., 2004), and are 450aa and 454aa in size, respectively. At present,

it is estimated that human RGMA (accession number: B2RTW1) has two isoforms, one with the length of 450aa and the other 485aa. The human and mouse RGMA protein also share very high homology with chick RGMA protein. Although the first amino acid of mature protein has not been characterised experimentally, the RGMA precursor was estimated to contain a ~ 30 residue signal peptide at the N-terminus and a conserved GPI attachment signal peptide at the C-terminus, around 45 amino acids. Two more interesting elements, namely an RGD motif and a partial vWD domain have been found in the remaining protein sequence. RGD motif (arginieglycine-aspartic acid) is a tripeptide characterized as an integrin-binding site (Ruoslahti and Obrink, 1996). Von Willebrand factor is a glycoprotein composed of five distinct structural domains (vWA, B, C, D and CK). This was reported to help mediate platelet adhesion at damaged blood vessels through interactions with blood clotting Factor VIII. (Jorieux et al., 2000; Sadler, 1998). The type D domain (partial vWD region) has been conserved in all RGMs, which contains a site of intramolecular proteolytic cleavage. The mature RGMA is a disulfide-bonded twochain protein composed of an N-terminal fragment of ~123 residues and a Cterminal segment of ~238, which is linked to the outside of the plasma membrane through its GPI anchor. It appears that mature RGMA protein is generated by intramolecular cleavage during the biosynthesis, although the mechanism has not been confirmed by experiments (Hata et al., 2006; Matsunaga and Chedotal, 2004; Monnier et al., 2002; Stahl et al., 1990).

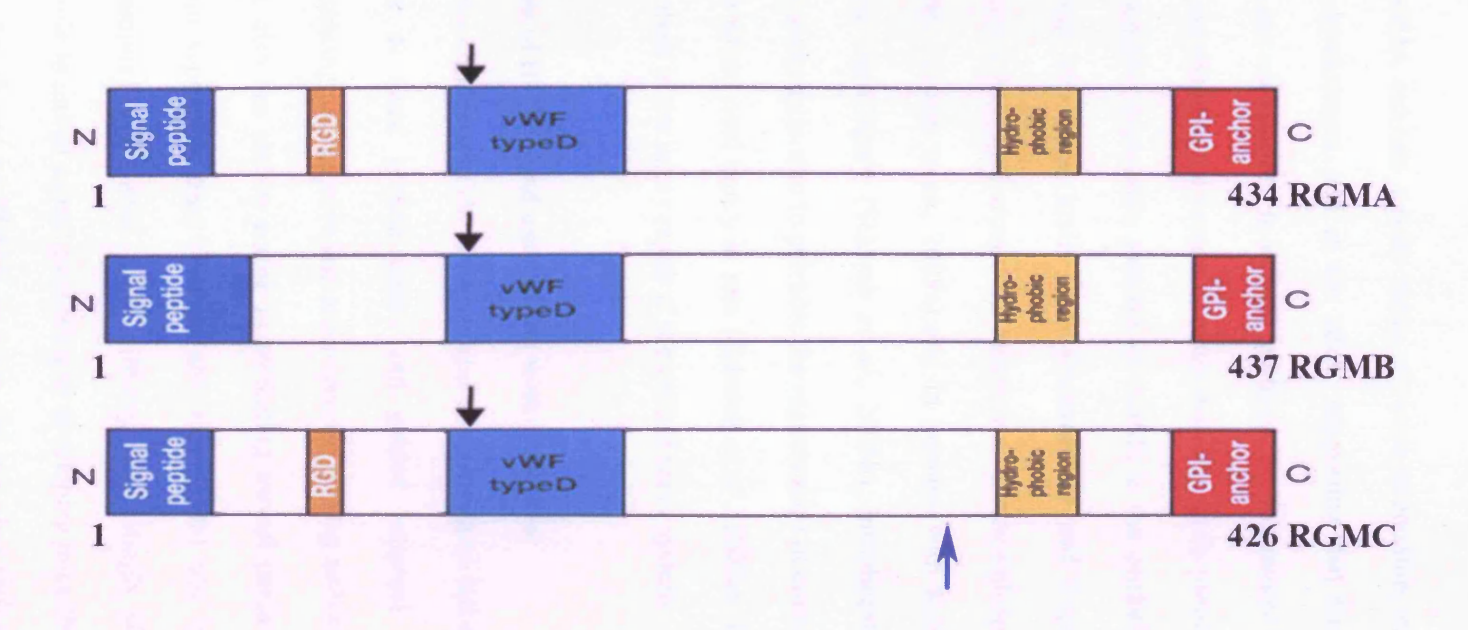


Figure 1.8 Main domain model of RGM protein.

RGMs are composed of a N-terminal signal peptide, an RGD site (except for RGMB), von Willebrand factor (vWF) domain, a hydrophobic region, and a C-terminal GPI (glycosylphosphatidylinositol) anchor. The arrow marks the proteolytic cleavage site. The arrow (purple) indicates the PPC cleaving site (RGMC only). RGMA, RGMB and RGMC proteins are 434, 437 and 426 aas respectively.

RGMA exhibits a wide range of tissue expression, in different species, both during development and in the adult, suggesting that the potential functions of RGMA are not confined to axonal guidance. During mouse development, RGMA is widely expressed in the central nervous system, mostly non-overlapping with RGMB. These separate expression patterns of RGMs in the central nervous system persist after birth in several brain areas (Schmidtmer and Engelkamp, 2004). RGMA expression is increased around the lesion sites in rats with spinal cord injury (Hata *et al.*, 2006; Schwab *et al.*, 2005a) and in humans with focal cerebral ischaemia or traumatic brain injury (Schwab *et al.*, 2005b). Intrathecal administration of anti-RGMA antibody is able to promote the regeneration of corticospinal tract axons after thoracic spinal cord injury in rats (Schwab *et al.*, 2005a). This suggests that RGMs are involved in the injury repair at the central nerve system.

The role of RGMA and association with Neogenin

Recombinant RGM at nanomolar concentrations induced collapse of temporal but not of nasal growth cones and guided temporal retinal axons *in vitro*, demonstrating its repulsive and axon-specific guiding activity (Monnier *et al.*, 2002). RGMA also has shown a role in mediating axonal guidance in Xenopus embryo forebrain supraoptic tract (Wilson and Key, 2006) and in the developing mouse hippocampus (Brinks *et al.*, 2004), although interestingly RGMA does not appear to play a role in retinal axonal patterning in developing mice (Niederkofler *et al.*, 2004). Genetic knock out of RGMA in mice did not alter retinal axonal patterning, but caused defects in neural tube closure (Niederkofler *et al.*, 2004).

RGMA functiones to suppress cell proliferation and induce neuronal apoptosis signalling through its receptor, Neogenin, in early vertebrate development (Shin and Wilson 2008) and CRC cells (Li, Yuen et al. 2009). However, Matsunaga et al. 2004 and Matsunaga et al. 2006 showed RGMA acts as a cell survival factor which inhibits the pro-apoptotic activity of Neogenin (Matsunaga et al., 2004).

RGMA also functions as a myelin-derived neurite outgrowth inhibitor *in vitro* and *in vivo*, and inhibits axon regeneration and functional recovery in the injured central nerve system (CNS) (Hata *et al.*, 2006). The study by Hata was the first report to demonstrate that RGMA as an axon growth inhibitor in adult mammals. The authors used a function-blocking antibody to inhibit the RGMA signal. Rats that undergo spinal cord hemisection show better locomotor recovery and axon growth of the CST (corticospinal tract) after treatment with the function-blocking antibody than after treatment with the control antibody.

1.4.1.2 **RGMB**

RGMB, also known as Dragon, is a myelin-derived inhibitor of axon growth in the CNS.

RGMB Gene sequence and expression

RGMB is a single-copy gene identified in eight mammalian species. Similar to RGMA, RGMB was located in a conserved chromosomal locus (5q15), and was one of the five linked genes which were found according to the same orientation in human, mouse and chicken genomes. Upstream of RGMB are Riok2 (right open

reading frame kinase 2), Lix1 (Limb expression 1) and Lnpep (leucy1/cystiny1 aminopeptidase). Downstream is Chd1, but with a tail to tail transcriptional orientation to RGMB.

The RGMB gene is ~25 kb in length, and contains 5 exons (Figure 1.7). The two 5' non-coding exons include ~406 nucleotides of a ~524 nucleotides 5' UTR of RGMB mRNA. The 5' end of exon 1 has not been mapped. There are 45 codons being located in the third exon, 170 codons in the forth, and 222 codons in the fifth plus a 3' end UTR of 308 nucleotides.

The gene encoding RGMB/DRAGON was identified by using a genomic DNA-binding strategy to identify genes regulated by DRG11, a homeobox transcription factor expressed in embryonic dorsal root ganglion (DRG) and dorsal horn neurons (Samad *et al.*, 2004). The gene was named RGMB (DRG-'ON' or Dragon), reflecting that it was turned "on" in the "DRG". It was regulated by and colocalized with DRG11 in dorsal root ganglia and spinal cord. As well as these two regions, RGMB mRNA was also found to be expressed in the retina, optic nerve, and in brain regions including the developing mouse midbrain, hindbrain and forebrain shown by the results of *in situ* hybridization experiments. (Niederkofler *et al.*, 2004; Oldekamp *et al.*, 2004; Samad *et al.*, 2004; Schnichels *et al.*, 2007)

RGMB Protein and its association with neogenin

The human RGMB protein is predicted to comprise 437 amino acids. The primary RGMB translation product contains an N-terminal signal peptide of ~50 residues (this has not been verified experimentally) and a C-terminal glycosylphosphatidylinositol (GPI) attachment signal of ~35 amino acids (supplied

by OMIM). The vWD element was included in the identifiable motifs in RGMB. (Samad et al., 2005; Samad et al., 2004) RGMB contains a putative internal proteolytic cleavage site similar to that in RGMA, but only a single-chain RGMB form being attached to the outer face of the cell membrane. The mature RGMB contains 14 cysteines but the structure is unclear.

RGMB is expressed by oligodendrocytes and neurons in the adult rat CNS, and the expression of RGMB is up-regulated especially around the site of spinal cord injury (Liu et al., 2009). It has also been found in myelin isolated from an adult rat brain (Liu et al., 2009). RGMB is co-expressed with neogenin in CGNs (cerebellar granule neurons) and entorhinal cortex neurons (Liu et al., 2009) and upregulated in the retinas of glaucoma-affected mice, together with RGMA and neogenin (Schnichels et al., 2007).

Moreover, DRG axons do not express endogenous neogenin and are unresponsive to RGMA. DRG axons become responsive to RGMA after neogenin expression (Rajagopalan *et al.*, 2004). Neogenin-RGMB interaction might be involved in neuronal migration in the dentate gyrus (Conrad *et al.*). The evidence showed that Neogenin and RGMB were expressed in non-overlapping compartments of the developing dentate gyrus.

The binding with neogenin may be a common property of all the RGMs, as both RGMA and RGMC have shown the direct binding to neogenin. Some of the known and predicted functions of RGMB are manifected in the context of RGMB-neogenin association. *In vitro* and *in vivo* migration of dentate neuroepithelial cells was abolished by RGMB, and cell adhesion was reduced when cells expressing

neogenin came into contact with cells expressing RGMB. RGMB was shown to suppress BMP signalling in C2C12 myoblasts and over-expression of neogenin did not alter the inhibitory capacity of RGMB (Kanomata et al., 2009a).

However, the function of RGMB may be independent upon the association with neogenin. RGMB is a myelin-derived inhibitor of axon growth in the CNS and inhibits neurite outgrowth *in vitro* (Liu *et al.*, 2009). RGMB might be involved in cell-cell adhesion due to homophilic interactions (Samad *et al.*, 2004). Elevated expression in the retinas of glaucoma-affected mice and around the lesion site of spinal cord injury in rats suggest that RGMB may have a role in the response to injury of the nervous system.

Although no other biological functions of RGMB have been reported except for its possible role as a BMP co-receptor, as other RGMs, the molecules related to RGMs could be predicted by the gene location, gene fusion, co-occurrence, co-expression, homology and so on based on RGM sequences. Fig. 1.9 shows the potential interactions of RGMs with other molecules searched by STRING, including the information already proved by experiments. Besides sharing high identity with RGMA and C, RGMB might bind to BMPR-IA, BMPR-IB, BMPRII, BMP2, BMP4, and interact with Smad-1, Smad-9, Noggin with more than 90% score. Additionally, neogenin might also interact with RGMA and RGMC as a putative receptor, and RGMC may also interact with Hepcidin and transferring receptor protein.

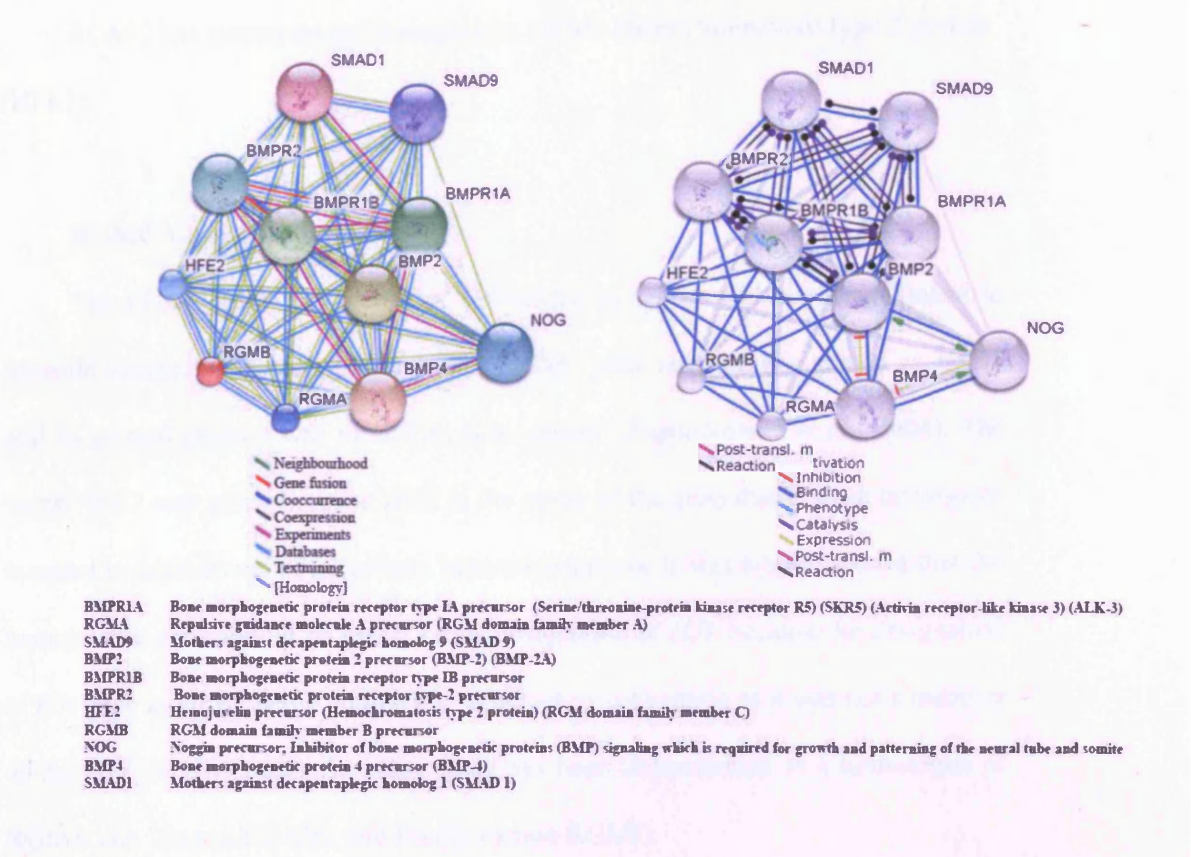


Figure 1.9 Predicted interactions of RGM and other proteins.

Human RGMB was searched and modified from STRING 8.3 as representation. RGMB might bind to BMPRIA, BMPRIB, BMPRII, BMP2, BMP4, and interact with Smad1, Smad9, Noggin with more than 90% score. RGMA, B and C share more than 90% identity. RGMA and RGMC might additionally have interaction with neogenin and RGMC have interaction with hepcidin and transferrin receptor protein, compared to RGMB. Left displayed all the potential interactions of RGMB. Right shows the modes of actions. (Sources from: http://string-db.org/)

1.4.1.3 RGMC

RGMC has synonyms as Hemojuvelin (HJV), Hemochromatosis type 2 protein (HFE2).

RGMC Gene characteristic

The *RGMC* gene was identified in humans as a gene within a locus linked to juvenile haemochromatosis in 2003. The *RGMC gene* and was designated as *HFE2* and its protein product was named as hemojuvelin (Papanikolaou *et al.*, 2004). The name *HFE2* was given because *HFE* is the name of the gene that is most commonly mutated in adult forms of hereditary hemochromatosis. It was later proposed that the hemojuvelin gene should be given a new designation of *HJV* because the designation of this gene as HFE2 being contrary to established convention as it was not a member of the HFE family. Later, the same gene has been characterized as a homologue of RGMA and Dragon/RGMB, and finally named RGMC.

Human *RGMC* gene was located chromosome 1q21.2. *RGMC* is one of 10 linked genes in a syntenic locus that includes, Txnip (thioredoxin interacting protein) (1q11), Polr3gl (DNA-directed RNA polymerase III subunit RPC7-like) (1q21.1), Ankrd34 (ankyrin repeat domain 34) (1q21.1), Lix11 (related to Lix1, which maps near RGMB) (1q21.1), and Chd11 (related to Chd1 and Chd2, which are located near RGMB and RGMA respectively).

Moreover, the transcriptional orientation of RGMC and Chd11 is tail to head, which is different from that of RGMA-Chd2 and RGMB-Chd1 (tail to tail). The

RGMC chromosome environment is similar in mouse and human but differs from zebrafish. There is no Chd homologue present at the zebrafish RGMC locus.

Human and mouse *RGMC* genes are around 4.3 kb and 4.0 kb respectively and composed of four exons separated by three introns. The exon at the 5' end contains most of the 5' UTR of RGMC mRNA, which is approximately 160 nucleotides. The second exon contains the remaining 90 nucleotides of 5' UTR and the first 31 codons of the RGMC protein. The following 173 codons are found in the third exon and the remaining 222 condons in the forth exon plus a 3' UTR of around1150 nucleotides with a single polyadenylation signal. The four RGMC exons are well-conserved between human and mouse. The nucleotide sequence identities in the exons range from 73% to 83%, but the three introns are less conserved, although of similar length (Fowler, 2008).

However, as RGMA differs from RGMB, RGMC has 4 variants due to the differences in the 5' UTR and 5' coding region, resulting in 3 protein isoforms (isoform a, b and c).

RGMC gene expression

RGMC is detected in the heart and liver (Kuninger et al., 2004; Niederkofler et al., 2004; Oldekamp et al., 2004) and is also highly expressed during skeletal muscle differentiation (Kuninger et al., 2004; Niederkofler et al., 2004; Oldekamp et al., 2004). During embryonic development of mouse, RGMC is detected at E11.5 in the precursors of skeletal muscle, which is similar to Zebrafish, and at E13.5 in the heart and liver (Kuninger et al., 2004; Niederkofler et al., 2005; Samad et al., 2004;

Sprague *et al.*, 2006). As with RGMA and RGMB, the knowledge of RGMC gene regulation remains largely unknown. RGMC has been shown to be down-regulated by LPS (lipopolysaccharide) through tumour necrosis factor-alpha (Constante *et al.*, 2007). However, mechanisms of gene transcription have not been reported, nor the structure and the function of RGMC gene reporter.

RGMC Protein structure

The initial cloning of cDNA indicated the mouse and human RGMC protein are 426 aa and 420 aa respectively. Human RGMC has three isoforms, with the length of 426aa (isoform a), 313aa (isoform b) and 200aa (isoform c). Similar to its paralogues RGMA and RGMB, RGMC is composed of a predicted N-terminal signal peptide of approximately 31 residues and a C-terminal GPI-attachment signal of approximately 45 aas. RGMC also contains up to three asparagine-linked glycosylation sites and several motifs including an RGD sequence and a partial vWD domain with a conserved proteolytic cleavage site. Furthermore, RGMC encodes a sequence near the C-terminus for recognition and cleavage by a furin-like PPC (pro-protein convertase) (Kuninger et al., 2008; Lin et al., 2008; Silvestri et al., 2008a). As a result, RGMC is processed to be the three distinct isoforms in skeletal muscle after a series of biosynthetic steps. According to their reports, the myoblast has two forms of RGMC associated with the cell membrane through GPI-links. One is a disulfidelinked heterodimer of N- and C- terminal fragments (20/35 kDa) from the intracellular proteolytic processing of endogenous RGMC. The cleavage of RGMC occurs within a Gly-Asp-Pro-His sequence that is conserved in RGMA and RGMB.

The other is full-length RGMC (50 kDa), which can be released from the cell surface and accumulates in the extracellular fluid of cultured cells as two isoforms, each containing an intact N-terminus, and potentially varying in the number of asparagine-linked glycosylation sites, 50 and 40 kDa respectively. It is interesting to note that RGMB and RGMA do not have the similar isoforms and structures to RGMC.

Functions of RGMC

A role played by RGMC in systemic iron metabolism was first reported by (Papanikolaou *et al.*, 2004). The defects in RGMC (HFE2) are the cause of hemochromatosis type 2A (HFE2A) [MIM:602390]; also known as juvenile hemochromatosis (JH), whereas Type 2B HH is caused by mutations in the secreted hepatic peptide hepcidin. HFE2A is an early-onset autosomal recessive disorder due to severe iron overload resulting in hypogonadotrophic hypogonadism, hepatic fibrosis or cirrhosis and cardiomyopathy, occurring typically before the age of 30. It is the consequence of intestinal iron hyperabsorption associated with macrophages that do not load iron. Deleterious mutations of HFE2 reduced HAMP (hepcidin) levels despite iron overload, which normally induces HAMP expression (Barton *et al.*, 2008; Barton *et al.*, 2007; Murugan *et al.*, 2008).

RGMC induces expression of hepcidin, which is a negative regulator of both the uptake of dietary iron from the duodenum and the release of stored iron from macrophages. The most possible mechanism for the action of RGMC in iron metabolism is that cell-membrane associated RGMC facilitates signalling via a selective subset of BMP ligands and receptors, independent of neogenin, to promote

hepcidin gene expression (Andriopoulos et al., 2009; Babitt et al., 2006; Babitt et al., 2007; Xia et al., 2008). However, a soluble form of hemojuvelin (s-hemojuvelin) exists in blood and acts as an antagonist of GPI-hemojuvelin to downregulate hepcidin expression, sequestering BMPs away from cell-surface receptors. Iron overload has been shown to reduce soluble HJV production in vitro (Silvestri et al., 2007), while iron deficiency increases soluble HJV levels both in vitro and in vivo (Zhang et al., 2007). These data indicated that s-hemojuvelin could be one of the mediators of hepcidin regulation by iron (Lin et al., 2005; Lin et al., 2008). Hypoxia may also upregulate production of the soluble HJV in vitro (Kuninger et al., 2008).

RGMC expression was not suppressed by interleukin-6 but by tumour necrosis factor-alpha, whereas hepcidin levels are directly regulated by interleukin-6 but not by tumour necrosis factor-alpha (Constante *et al.*, 2007). Regulation of iron-related genes by different cytokines may allow for time-dependent control of iron metabolism in accordance with iron load and different circumstances.

Matriptase-2 can interact with HJV by cleaving hemojuvelin (HJV) at the plasma membrane. Through HJV, deficiency of TMPRSS-6 (also known as matriptase-2) was found to cause a decrease in BMP6 mRNA and an increase in hepcidin levels and Id1 thereby contribute to iron deficiency anaemia (Finberg et al., 2010). This suggests that Matriptase-2 is a suppressor of the HJV-hepcidin pathway by cleaving HJV. Matriptase, is a type II membrane serine protease widely expressed in normal epithelial cells and human carcinoma cells, being involved in cancer progression (Jin *et al.*, 2006). Matriptase-2 itself was found to inhibit breast tumour growth and invasion which correlates with favourable prognosis for breast cancer

patients (Parr et al., 2007) and reduces the aggressiveness of prostate cancer cells in vitro and in vivo (Sanders et al., 2008).

Although the direct impact on cancer of RGMC has not been elucidated, the interactions between RGMC and other molecules such as BMPs, matriptase-2 and neogenin suggest a potential implication of this molecule in cancer.

RGMC and its association with neogenin

Similar to RGMA, RGMC binds to the extracellular part of neogenin (Kuns-Hashimoto *et al.*, 2008; Zhang *et al.*, 2005). Recently, it was shown that HJV-induced BMP signalling and hepcidin expression were not altered by neogenin overexpression or by inhibition of endogenous neogenin expression, indicating that HJV is able to mediate the BMP signalling independently of nogenin (Xia *et al.*, 2008). However, a contradictory report suggests that neogenin is required for HJV enhanced BMP-4 signalling (Zhang *et al.*, 2009).

1.4.2 Receptor of RGM

Neogenin is a multifunctional transmembrane receptor belonging to the immunoglobulin superfamily, which was originally isolated from embryonic chicken cerebellum (Vielmetter *et al.*, 1994). Its secondary structure is identifical to DCC deleted in colorectal cancer, a netrin receptor that is involved in axon guidance and cell survival. As DCC, Neogenin transduces signals induced by netrin. The

neogenin-netrin interaction has been implicated in tissue morphogenesis, angiogenesis, myoblast differentiation and most recently in axon guidance.

As already discussed in early sections, Neogenin is also a receptor for repulsive guidance molecules (RGM). Rajagopalan *et al.* 2004 presented evidence that neogenin functions as a receptor for RGM (Rajagopalan *et al.*, 2004). Like RGM, neogenin was expressed in a gradient across the embryonic chicken retina. The avoidance (a kind of guidance) of RGM by chicken temporal retinal axons was blocked by anti-neogenin antibody and the soluble neogenin ectodomain (Wilson and Key, 2006). Dorsal root ganglion axons were unresponsive to RGM, but were converted to a responsive state by neogenin expression (Rajagopalan *et al.*, 2004).

The extracellular domain of human neogenin protein contains four V-shaped immunoglobulin-like domains and six fibronectin type III (FNIII)-like domains. RGM interacts with the fibronectin domain of neogenin (Rajagopalan *et al.*, 2004) (Figure 1.10). Netrin-1 also binds to the FNIII-like domain, but the binding affinity of RGM for neogenin (Kd = 230 pM) is much higher than that of netrin-1 (Kd = 2nM) (Geisbrecht *et al.*, 2003).

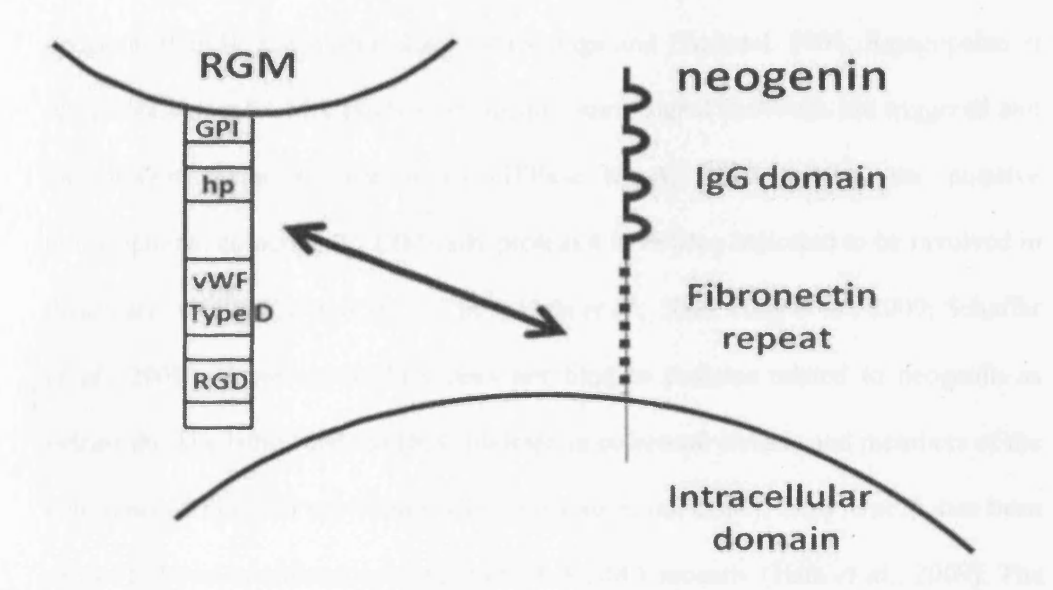


Figure 1.10 Structure of RGM and Neogenin.

RGMs attached to the cytoplasmic membrane through GPI-anchor. The specific domain of RGM which interacts with the extracellular fibronectin domain of neogenin remains unknown.

The interaction with RGMA and involvement in tumour proliferation

RGMA regulates repulsive guidance of retinal axons through binding to neogenin (Cirulli and Yebra, 2007; Matsunaga and Chedotal, 2004; Rajagopalan et al., 2004). After RGMA binds to neogenin, some signal pathways are triggered and the protein kinase C, the small GTPase RhoA, RhoA kinase, the putative transcriptional co-activator, LIM-only protein 4 have been indicated to be involved in these early events (Conrad et al., 2007; Hata et al., 2006; Hata et al., 2009; Schaffar et al., 2008). However, RGMA does not bind to proteins related to neogenin as netrins do. The latter binds to DCC (deleted in colorectal cancer) and members of the Unc (unco-ordinated) sub-family (Rajagopalan et al., 2004). Only Unc5b has been shown to have an indirect association with RGMA recently (Hata et al., 2009). The mechanism of how neogenin regulates the biological effects of RGMA has not been fully determined, only Matsunaga et.al (Matsunaga et al., 2004) have reported that the interaction between RGMA and neogenin promoted neuronal survival, except for the regulation on retinal axonal guidance.

The mechanisms for the regulation of cell death are diverse. There is a type of cell death involving the absence of ligand induced self-activation of the receptor, by a mechanism still unknown, and the subsequent proteolytic processing of the receptor triggers apoptotic cell death. Ligand binding blocks the proteolytic processing and the pro-apoptotic activity of the receptor. The apoptosis might be caused by the proteolytic cleavage of the receptor by activated caspase-3 or other proteases, to expose a pro-apoptotic region in the cytoplasmic domains of the receptor (DCC, Ptc, etc.) or to create cytoplasmic fragments inducing apoptotic signals (RET, UNC5H,

etc.) (Porter and Dhakshinamoorthy, 2004). Consistent with this suggestion, Neogenin overexpression or down regulation of RGMA by short interfering RNA at E1.5 in the area of the developing dorsal metencephalon, mesencephalon and caudal diencephalons in chick embryos results in an decrease in the number of cells positive for TdT-mediated dUTP nick end labeling (TUNEL) (Matsunaga *et al.*, 2004).

Apoptosis is caused by the proteolytic cleavage of the receptor by activated caspase-3, although knowledge regarding the underlying signal transduction mechanisms is limited. A subsequent study has indicated that RGMA might play a positive role in chick embryo development, in addition to rescuing cells by suppressing neogenin-mediated cell death. Overexpression of RGMA in the neural tube promotes neuronal differentiation, whereas suppression of RGMA represses this (Matsunaga *et al.*, 2006). Thus, RGMA not only suppresses neogenin-induced cell death but also enhances neuronal differentiation. The final cell fate decisions might be made on the basis of the relative expression levels of RGMA and neogenin. No alterations in cellular proliferation or neuronal differentiation have been reported in RGMA mutant mice suggesting redundant mechanisms exist in rodents.

However, RGMA was also reported to suppress cell proliferation and induce neuronal apoptosis signalling through its receptor, Neogenin, in early vertebrate development (Shin and Wilson, 2008) and CRC cells (Li et al., 2009b).

Hata et al. 2006 reported that RGMA inhibits axon regeneration and functional recovery in the injured CNS (Hata et al., 2006). Neogenin is expressed widely in the adult CNS and spinal cord, and is distributed predominantly in the grey matter

(Manitt et al., 2004). Netrin-1 stimulates neurite growth through neogenin (Barallobre et al., 2005), preventing the binding of RGMA to neogenin might allow the axons to be navigated by netrin-1.

The interaction with RGMC and involvement in iron metabolism

The RGMC-neogenin complex is necessary for iron accumulation within cells and responsible for the RGMC-induced changes in iron homeostasis (Zhang *et al.*, 2005). Neogenin is indicated to regulate iron homeostasis via inhibiting secretion of RGMC (soluble HJV, an inhibitor of BMP signalling) to enhance BMP signalling and hepcidin expression (Lee *et al.*, 2010). HJV is believed to be a coreceptor of BMPs in the regulation of hepcidin expression, whereas extracellular/soluble HJV (sHJV) may act as an antagonist in BMP2-induced Smad1/5/8 phosphorylation, a major BMP activated signalling pathway that induces hepcidin expression.

The mechanisms of RGM and neogenin interaction

The signal transduction mechanisms underlying other aspects of the RGM-neogenin interaction are mostly unknown. However, during axon inhibition, RGMA activates the Rho/Rho kinase pathway in neurons through neogenin. Myelin-derived neurite outgrowth inhibitors — namely MAG, Nogo and oligodendrocyte myelin glycoprotein (OMgp) — in oligodendrocytes also induce inhibitory signalling in neurons by activating the Rho/Rho kinase pathway through the Nogo receptor complex comprising p75/Troy, NgR and Lingo-1. Downstream molecules of Rho kinase, such as myosin light chain (MLC), LIM kinase (LIMK) and CRMP-2, might

also have roles in axon growth inhibition. However, the mechanism underlying the activation of the RhoA/ Rho kinase pathway after RGMA binds to neogenin remains unknown. Both neogenin and DCC bind to focal adhesion kinase (FAK) through their highly homologous intracellular domain, and subsequently regulate the netrin-1-stimulated outgrowth of cortical axons (Liu et al., 2004; Ren et al., 2004). Some RhoGEFs (full name) might associate with neogenin to induce the activation of RhoA specifically in response to RGM, such as PDZ-RhoGEF and LARG, which are phosphorylated by FAK (Chikumi et al., 2002; Swiercz et al., 2002).

Neogenin-netrin interactions have been implicated in tissue morphogenesis, angiogenesis, myoblast differentiation and most recently in axon guidance (Wilson and Key, 2007). Netrin-1 is a secreted neural guidance cue with the unique ability to attract both blood vessels and axons, stimulates angiogenesis *in vivo* and augments the response to vascular endothelial growth factor (Park *et al.*, 2004). Netrin-4 acts as an antiangiogenic factor through binding to neogenin and recruitment of Unc5B (Lejmi *et al.*, 2008). However, neogenin is also a receptor for repulsive guidance molecule. Although evidence is yet forthcoming, RGMs may have direct effects on tumour angiogenesis, and this effect may be the results of the RGM-neogenin interaction and the involvement of BMPs in angiongenesis.

1.4.3 The role of RGM in the BMP signalling pathway

1.4.3.1 The regulators of BMP signalling

In the extracelluar region, several secreted proteins have been described to bind and sequester BMPs and thus prevent their interaction with BMP receptors: Noggin, twisted gastrulation, Chordin family (Cordin and Crim1), Follistatin, DAN family (Gremlin, Cerberus, dan, Usag1, Sclerostin, Coco, PRDC), Tsg, and CCN family (Balemans and Van Hul, 2002; Canalis *et al.*, 2003; Ebara and Nakayama, 2002; Gazzerro and Canalis, 2006; Reddi, 2001). Many of the antagonists themselves are target genes of BMP signalling, thus appropriate coordination of extracellular BMP is ensured by the feedback loop.

Inside the cell, a number of molecules are able to finely alter BMP signals. Firstly, R-Smad/Co-Smad transcriptional co-activators and co-repressors (as Smurfl and Inhibitory SMADs) can regulate transcription by inducing acetylation and deacetylation of histones respectively. I-Smads are also BMP target genes, as with extracellular antagonists, creating another feedback mechanism for BMP signals. Some Smad-partner proteins (as Shn2) can bind directly or indirectly to Smads, and they can be either ubiquitous or cell specific, ensuring cell-dependent transcriptional responses. The BMP signalling pathway is also modulated by cross-talk between the canonical Smad signalling pathway and other pathways such as the Mitogen Activated Protein Kinase (MAPK), PI3K/Akt, Notch, and STAT pathways, which have either synergistic or antagonistic effects, depend on their cellular context.

CRIM1 (cysteine rich transmembrane BMP regulator 1 (chordin-like)), BAMBI (BMP and activin membrane-bound inhibitor) and RGMs are described as some of the membrane modulation mechanisms of BMP signalling. The antagonist-like function of the transmembrane protein CRIM1 prevents the actions of BMP7 and BMP4 in the Golgi compartment by affecting ligand processing (Wilkinson *et al.*, 2003). BAMBI is a pseudoreceptor which interacts with type I receptors and interferes with the proper formation of the hetero-tetrameric receptor complex, thus inhibiting the signal transduction to R-Smads (Onichtchouk *et al.*, 1999). On the other hand, RGMs act as co-receptors to facilitate and enhance BMP signalling transduction.

1.4.3.2 The involvement of RGMs in BMP signalling

In 2005, DRAGON was the first member of the RGM family to be identified as a BMP co-receptor (Samad *et al.*, 2005). Transfection of DRAGON cDNA into cells enhances transcription of a BMP-responsive luciferase reporter (BRE-Luc), but not a TGF-β responsive luciferase reporter (CAGA-Luc). DRAGON sensitizes cells to respond more robustly to low levels of BMP2 ligand (Samad *et al.*, 2004; Xia *et al.*, 2005). DRAGON expression by siRNA inhibits BMP2 signalling as measured by both BRE-Luc and alkaline phosphatase activity assays in C2C12 murine myoblast cells (Halbrooks *et al.*, 2007). The enhancement of BMP signalling by the transfection of DRAGON cDNA could be blocked by administration of Noggin, which sequestered the endogenously expressed BMP ligands (Samad *et al.*, 2005).

However, RGMB can also be described as an inhibitor of BMP signalling in C2C12 myoblasts and this inhibition was dependent on the secretary form of the von Willbrand factor type D domain (Kanomata et al., 2009b). In C2C12 cells, only DRAGON suppressed ALP and Id1 promoter activities induced by BMP4 or by constitutively activated BMP type I receptors, or even by constitutively activated Smad1. DRAGON.Fc (purified soluble RGMB fused to the Fc portion of human IgG1) significantly inhibited BMP2 or BMP4 but was less effective in inhibiting BMP5, BMP6 or BMP7 and did not inhibit BMP9 (Andriopoulos *et al.*, 2009). It suggests that the soluble DRAGON.Fc inhibits BMP signalling, presumably by binding to BMP ligands and preventing their access to cell surface type I and type II receptors in the same way as those BMP antagonists, while cell surface GPI-anchored RGMB enhances BMP signalling.

RGMB directly interacts and forms a complex with BMP type I (ALK-2, ALK-3, and ALK-6) and type II receptors (ACTRIIA, BMPRII, and ACTRIIB), and enhances signal transduction through the canonical intracellular SMAD1/5/8 pathway in transfected HEK293 cells (Samad *et al.*, 2005).

A role for RGMA in the BMP signalling pathway was investigated after the homologous DRAGON/RGMB was shown to function as a BMP co-receptor *in vitro* (Samad *et al.*, 2005). Transfection of RGMA cDNA into BMP-responsive cells enhances signalling by endogenous BMP ligands *in vitro* as measured by BMP-responsive promoter luciferase reporter assays (Babitt *et al.*, 2005). TGF-β signalling was unaffected by RGMA (Xia *et al.*, 2007). However, compared to RGMA and C,

RGMB seems to have the least significant effect on the involvement of BMP signalling (Halbrooks *et al.*, 2007). In a cell-free system, purified human RGMA.Fc (the extracellular domain of RGMA fused to the Fc portion of human lgG) binds directly to 125 I-BMP-2 and 125 I-BMP-4 with a K_D of 2.4 and 1.4 nM respectively, and this binding is not competed by excess cold BMP7 or TGF- β 1. The regulation of RGMA on BMP signalling is via an interaction with type I receptors (ALK-3 and ALK-6) and type II receptors (ACTRIIA and BMPRII) thereby activating the canonical intracellular SMAD1/5/8 cascade, which can be inhibited by the silence of ALK-3, ALK-6, ACTRIIA or BMPRII or Smad1(Babitt *et al.*, 2005; Xia *et al.*, 2007). The interaction is in the manner that RGMA.Fc forms a complex with ALK-6 in the absence or presence of BMP2 in solution.

The underlying cause of iron overload in juvenile hemochromatosis due to *HJV* mutations is hepcidin deficiency and that HJV acts upstream of hepcidin, positively modulating its levels (Huang *et al.*, 2005; Niederkofler *et al.*, 2005; Papanikolaou *et al.*, 2004). This is due to the fact that BMP signalling can positively regulate hepcidin transcription *in vitro*, while HJV/RGMC acts as a BMP co-receptor and enhancer (Babitt *et al.*, 2006). As with other RGM family members, transfection of HJV was demonstrated to enhance BMP in hepatoma-derived cells, but not TGF-β signalling as measured by BRE-Luc and CAGA-Luc assays (Babitt *et al.*, 2006; Halbrooks *et al.*, 2007; Xia *et al.*, 2008). Furthermore, siRNA-mediated inhibition of endogenous HJV inhibits BMP2 signalling as measured by both BRE-Luc and alkaline phosphatase activity assays in C2C12 murine myoblast cells (Halbrooks *et al.*, 2007).

RGMC ligand can dependently bind to BMP2, BMP4, and BMP6 in hepatomaderived cells *in vitro*, but not BMP7 and TGF-β1 (Andriopoulos *et al.*, 2009; Babitt *et al.*, 2006; Xia *et al.*, 2008).

The binding affinity of HJV.Fc for BMP2 was found to be similar to RGMA.Fc and DRAGON.Fc by BIAcore assay (Yang et al., 2008). However, HJV seems have a different ligand selectivity compared to other RGM family members based on the bioinhibition properties of soluble HJV.Fc protein for inhibiting signalling by various BMP ligands in a reporter assay. DRAGON.Fc is a strong inhibitor of BMP2 and BMP4, only weakly inhibits BMP5, BMP6, and BMP7, but does not inhibit BMP9 (as discussed above); HJV.Fc is the most potent inhibitor of BMP6 ligands, has a relatively weak inhibition on signalling by BMP2, BMP4, and BMP5, and little or no inhibition on BMP7 or BMP9 signalling (Andriopoulos et al., 2009; Babitt et al., 2007).

Different from other RGMs, RGMC can be cleaved from the plasma membrane by matriptase-2 which will weaken the BMP signalling and thereby suppress hepcidin expression levels to inhibit iron-deficient anaemia ((Finberg et al.; Finberg et al., 2010; Silvestri et al., 2008b). However, the cleavage has nothing to do with the soluble HJV, which is secreted by an intracellular mechanism (Silvestri et al., 2008b).

As other RGM family members do, HJV affects signalling via both types of BMP receptors and the Smad intracellular signalling pathway (**Table 1.3**). It can interact with ALK-2, ALK-3 and ALK-6 (Xia *et al.*, 2008) and form a complex with ALK-6 in the presence of BMP2 (Babitt *et al.*, 2006). In hepatoma-derived cells,

HJV was found to not only signal through BMPRII and ACTRIIA, but also alter the preference of BMP2 and BMP4 to signal via BMPRII alone or additionally via ACTRIIA (Xia et al., 2008). This might be a property shared by all RGM family members, however, RGMC might act more frequently through ACTRIIA as a BMP co-receptor, which is predominantly expressed in liver. RGMC has been shown to interact with neogenin as discussed above (Kuns-Hashimoto et al., 2008; Zhang et al., 2005). Neogenin can regulate iron homeostasis via inhibiting secretion of HJV, to enhance BMP signalling and hepcidin expression (Lee et al., 2010).

Table 1.3 RGMs and their interacting molecules

RGMs	Receptor	BMPs	BMP receptor	Downstream molecule
RGMA	Neogenin	BMP2/4	ALK-3, ALK-6 ACTRIIA,BMPRII	Smad1/5/8
RGMB	Neogenin?	BMP2/4	ALK-2, ALK-3, ALK-6, ACTRIIA, BMPRII, ACTRIIB	Smad1/5/8
RGMC	Neogenin	BMP2/4/6	ALK-2, ALK-3, ALK-6 BMPRII, ACTRIIA	Smad1/5/8

This table shows receptor for RGMs and their interaction with BMP signalling. (Xia et al., 2008)

However, to date, the exact mechanism of how RGM enhances the BMP signalling and the structure of RGM-BMPRs-BMP remains unknown, and its implication in cancer through this pathway needs to be revealed. It is highly probable that two combined distinct RGM co-receptors (complex) are required for more efficient signalling than one individually. To enhance the recruitment of BMP ligands to BMP receptors complex, RGMA and RGMC form the most potent co-receptor pair, but it is unclear whether they exist as a heterodimer or two distinct proteins (Halbrooks *et al.*, 2007).

1.5 Hypothesis and aim of this study

RGMs play a profound role in axonal guidance, neuronal development and iron metabolism. However their implication in cancer remains unknown.

As mentioned above, The BMPs and their signalling pathways are crucial to bone metastasis of cancer as BMPs played an important part in bone development by their effects on osteoblast differentiation and bone matrix production. BMPs have distint and diverse effects on tumour cells depending on the cancer type. In some circumstances, BMPs played a contrast role in same cancer type during different studies.

Given the diverse role of BMPs played in cancer, the effects of RGMs on cancer are somewhat mysterious. However, the RGMs might at least enhance the effects of BMPs on cancer. As the BMP-Smad dependent pathway has an effect on the regulation of osteoblast differentiation where RGMs also participate, the RGM family might also have effects on bony metastasis. RGMs may have their own

regulation on cancer through BMP signalling pathway. However, whether RGMs are involved in the development and progression of cancer remains unknown.

Secondly, if the RGMs do have correlation with cancer progression, how they participate in the regulation of cancer cells' behaviours and what's the mechanism underlying it need to be revealed. Furthermore, it will be interesting to know if there is any difference or common place for the three RGM members in the regulation of caner cells.

Thirdly, as a co-receptor of BMPs, how RGMs participate in BMP signalling pathway and utilise these pathways to execute their regulation on tumour cells and the mechanisms responsible for this need to be revealed further. Notably, different RGMs might have diverse effects on cancer, due to the distinct role of each molecule involved in this pathway.

Together, the expression pattern of RGMs in cancer, the regulation on tumour cells behaviour, the target genes responsible for these regulations, the mediation on the target genes through BMP signalling pathway and the potential therapeutic value associated with the clinical prognosis could form a network and provide us a glimpse on RGMs function in cancer.

Based on the questions above, the study had the following aims:

 To determine the expression profile of RGMs in diverse cancer cell lines and and tissues and to deduce a possible clinical and prognostic value for the RGMs;

- 2. To investigate the role of RGMs in prostate cancer and breast cancer cells.
- 3. To investigate the mechanisms responsible for RGMs regulation in prostate cancer and breast cancer cell. This choice of tumour types was based on the clinical observations that breast and prostate cancer are the two leading solid tumours that develop bone metastasis.
- 4. To reveal the involvement of RGMs in BMP signalling which is associated with the regulation on target genes that might be the mechanism of tumour cellular behaviour changes.

Chapter 2

Materials and methods

2.1 General Materials

2.1.1 Animals, cell lines and tissues

Cell lines used are listed below:

Breast cancer (MDA MB 157, MDA MB 231, MDA MB 436, MDA MB 453, BT474, BT482, BT549, ZR751, MCF 7)

Breast fibrocytic disease (MCF 10A)

Fibroblast (MRC5)

Liver (PLC-PRF-5)

Prostate cancer (DU145, PC-3, CA HPV 10, LNCAP)

Prostate epithelial (PNT1A, PZ-HPV-7)

Bladder cancer (EJ138, RT112)

Colorectal cancer (HRT18, HT115,)

Pancreatic cancer (Mia PaCa, PANC1)

Lung (SKMES1, A549, CorL677, CorL88, CorL23, CorL47)

Cervical cancer (Hela)

The cervical squamous cell carcinoma (A431)

Melanoma (G361)

Monocytic myeloma (U937)

Leukaemic cell (WBC, HL60)

Endothelial (HUVEC, HECV)

Mink Kidney Epithelial cell (MDCK)

Keratinocyte (HaCaT)

Leukocyte (PMN)

All the cell lines, except those primary culture cells, were purchased from the European Collection of Animal Cell Cultures (ECACC, Salisbury, England).

The following tissues are used:

Human placenta, ovary, prostate, normal mammary tissues, breast cancer tissues, skin, omentum, colon, normal mucosa colon (NM), bone, liver, and mesentery tissues (MS) were all collected in the department over the past years and stored in deep freezer (-80 °C), under ethic approval.

A human breast tumour cohort with a 10 year follow-up was collected in the department and was used in the investigation of the the clinical and prognostic link. The presence of tumour cells in the collected tissues was verified by a consultant pathologist, Dr Anthony Douglas-Jones of Department of Pathology of Cardiff University School of Medicicne using H&E staining of frozen sections. All protocols were reviewed and approved by the local ethical committee and all patients gave written informed consent.

2.1.2 Primers

All the primers used in this study were designed using the Beacon Design programme (Palo Alto, California, USA) and synthesised by Invitrogen (Paisley, UK). The forward and reverse primers used for conventional RT-PCR and Real time Quantitative PCR (Q-PCR) are listed in Table 2.1.2. Table 2.1.2 also shows the primers used for ribozyme generation.

Table 2.1.2 Primers used in this study

Gene	Primer name Primer sequence (5'~3')		Annealing temperature(°C)
RGMA	RGMA F1	TCGACAATAATTACCTGAACG	55
	RGMA Zr1	ACTGAACCTGACCGTACACCTG GAAGTTCTTGAAGATG	
	RGMA F9	AGAACTTCCAGGAGTGTGTG	55
	RGMA R9	GAGTGGAGCATCTTGACATC	
RGMB	RGMB F8	GGATCCAGTGCTACTGCTAC	55
	RGMB R8	GTAAAGTTGGCATCACCAGT	
	RGMB F	TTCAGGTTCAAGTGACAAACG	55
	RGMB Zr	ACTGAACCTGACCGTACATCAT CTGTCACAGCTTGGTA	
RGMC	RGMC F	AATGACTTCCTCTTTGTCCA	55
	RGMC Zr	ACTGAACCTGACCGTACACATT CCTGCATGTTCTTAAA	
	RGMC F9	GGACCCTTGTGACTATGAAG	55
	RGMC R9	GTCTGGCAGTATCAATGGTT	
GAPDH	GAPDH F8	GGCTGCTTTTAACTCTGGTA	55
	GAPDH R8	GACTGTGGTCATGAGTCCTT	
	GAPDH F	AAGGTCATCCATGACAACTT	55
	GAPDH Zr	ACTGAACCTGACCGTACAGCCA TCCACAGTCTTCTG	
Snai1	SNAF	ACTATGCCGCGCTCTTTCC	55
	SNAR	TCAGCGGGGACATCCTGAGC	
RhoC	RhoC F8	GAGAAGTGGACCCCAGAG	55
	RhoC Zr	ACTGAACCTGACCGTACACTTC	
		ATCTTGGCCACGCTC	
Slug	Slug ZF	CTCCAAAAAGCCAAACTACA	55
	Slug Zr	ACTGAACCTGACCGTACAGAG GATCTCTGGTTGTGGTA	

Twist	Twist ZF	AAGCTGAGCAAGATTCAGAC	55
	Twist ZR	ACTGAACCTGACCGTACAGAG	
		GACCTGGTAGACCGAAGT	
Neogenin	Neo F1	ATCCATGTCCCTTTCAGAC	55
	Neo Zrl	ACTGAACCTGACCGTACAAG	
		CATGTTTTGAGACGAAGAG	
	Neo F8	CAAAAATGGGGATATGGTTA	55
	Neo R8	TTGTGTTTCTACTCGCAGTG	
FAK	FAK F1	AACAGGTGAAGAGCGATTAT	55
	FAK Zr	ACTGAACCTGACCGTACACAGT ATGATCCC	
Paxillin	Paxil F1	CAATCCTTGACCCCTTAGA	55
	Paxil Zr	ACTGAACCTGACCGTACATTGG	
		AGACACTGGAAGTTTT	
Cytokeratin	CK19 F	CAGGTCCGAGGTTACTGAC	
-19	CK19 Zr	ACTGAACCTGACCGTACACACT	
		TTCTGCCAGTGTGTCTTC	
ID-1	ID-1 F1	TCAACGCCGAGATCAG	
	ID-1 Zr1	ACTGAACCTGACCGTACAGATC	
		GTCCGCAGGAA	
c-Myc	Myc F1	TGCTCCATGAGGAGACAC	
	Myc Zrl	ACTGAACCTGACCGTACATGAT CCAGACTCTGACCTTT	

Gene	Primer name	Primer sequence (5' ~ 3')
RGMA	RGMA rib3F	CTGCAGGCGCACCACGATGGTG
KUMA	KUMA 1103F	GTGCCCTGATGAGTCCGTGAGGA
	RGMA rib3R	ACTAGTGGAGATCCAGGCCAA
	KGMA HUSK	GTACATTTCGTCCTCACGGACT
RGMB	RGMB rib1F	CTGCAGGTCATCTGTCACAGC
KUMB	KOMB filler	TTGGTACTGATGAGTCCGTGAGGA
	RGMB rib1R	ACTAGTGTACAGATCAGAAA
	KOMB HUIK	GTTTCGTCCTCACGGACT
RGMC	RGMC rib3F	CTGCAGATCCCCCAGGTCGGT
KUWIC	ROME 1103F	CACCTCCATTCTGATGAGTCCGTGAGGA
	RGMC rib3R	ACTAGTCCTGTAGCCTTTGAAG
	ROME 1103R	ATGGTTCTATTTCGTCCTCACGGACT
	T7F	TAATACGACTCACTATAGGG
	BGHR	TAGAAGGCAGTCGAGG
	RbBMR	TTCGTCCTCACGGACTCATCAG

2.1.3 Antibodies

2.1.3.1 Primary antibodies

The primary antibodies used are fully detailed in the table 2.1.3.1.

Table 2.1.3.1 Antibodies used in study

Antibody name	Source	Molecular weight (kDa)	Supplier	Product code
Anti-RGMA	Goat	33	SANTA CRUZ BIOTECHNOLOGY, INC.	Sc-46482
Anti-RGMB	Goat	47.5	SANTA CRUZ BIOTECHNOLOGY, INC.	Sc-46487
Anti-RGMC	Goat	45	SANTA CRUZ BIOTECHNOLOGY, INC.	Sc-46491
Anti-FAK	Mouse	125	BD Biosciences	BD 610088
Anti-Paxillin	Mouse	68	BD Biosciences	BD 610051
Anti-Caspase3	Rabbit	32/11/17/20	SANTA CRUZ BIOTECHNOLOGY, INC.	Sc-7148
Anti-C-Myc	Mouse	67	SANTA CRUZ BIOTECHNOLOGY, INC.	Sc-70465
Anti-GAPDH	Mouse	37	SANTA CRUZ BIOTECHNOLOGY, INC.	Sc-47724
TAK1	Rabbit	70	SANTA CRUZ BIOTECHNOLOGY, INC.	Sc-7162
P38	Mouse	38	SANTA CRUZ BIOTECHNOLOGY, INC.	7972
JNK1	Rabbit	46	SANTA CRUZ BIOTECHNOLOGY, INC.	571
ERK1/2	Rabbit	41/42	SANTA CRUZ BIOTECHNOLOGY, INC.	93
XIAP(ILP)	Rabbit	47	SANTA CRUZ BIOTECHNOLOGY, INC.	11426
Pho-Smad-1	Goat	52/56	SANTA CRUZ BIOTECHNOLOGY, INC.	12353
Pho-Smad-3	Rabbit	48	SANTA CRUZ BIOTECHNOLOGY, INC.	130218
BMPRIA	Mouse	66	SANTA CRUZ BIOTECHNOLOGY, INC.	134285
BMPRIB	Goat	50	SANTA CRUZ BIOTECHNOLOGY, INC.	5679
BMPRII	Goat	115.2	SANTA CRUZ BIOTECHNOLOGY, INC.	5683
Pho- Serine/threonine	Rabbit		Abcam plc.	ab17464

2.1.3.2 Secondary antibodies

The secondary antibodies used for western blotting, immunohistochemistry and immunocytochemistrywere horseradish peroxidise (HRP) conjugated which are shown in table 2.1.3.2

Table 2.1.3.2 Secondary antibodies used in this study

Antibody name	Source	Molecular weight (kDa)	Supplier	Product code
Anti-rabbit (whole molecule) IgG peroxidise conjugate	Goat polyclonal antibody	Dependent on primary	Sigma-Aldrich	A-9169
Anti-goat (whole molecule) IgG peroxidise conjugate	Rabbit polyclonal antibody	Dependent on primary	Sigma-Aldrich	A-5420
Anti-mouse (whole molecule) IgG peroxidise conjugate	Rabbit polyclonal antibody	Dependent on primary	Sigma-Aldrich	A-9044

2.1.3.3 Inhibitors, activators and proteins

Inhibitors and recombinant proteins used in this study are listed in table 2.1.3.3

Table 2.1.3.3 Inhibitors and recombinant proteins

Product	Concentration used	Supplier	Catalogue number
Specific Inhibitor of Smad3 (SIS3)	3µmol/ml	Merck Chemicals Ltd.	566405
Recombinant human protein BMP7 (rh- BMP7)	40ng/ml	R&D Systems	354-BP

SIS3: A cell-permeable pyrrolopyridine compound that selectively inhibits TGF- β 1-dependent Smad3 phosphorylation and Smad3-mediated cellular signaling with no effect on Smad2, p38 MAPK, ERK, or PI 3-K signalling.

2.1.4 General reagents and solutions

Antibiotics

Penicillin (120mg/ml)

Six hundred milligrams of Crystapen Injection Benzylpenicillin sodium (Britannia Pharmaceuticals limited, Surrey, UK) was dissolved into 5ml Sterile Injection water (B.Braun, Germany).

Streptomycin Sulphate (250mg/ml)

Five grams of Streptomycin Sulphate was dissolved into 20ml sterile injection water, filtered through 0.2μm Minisart filter and store at -20°C until required.

Solutions for cell maintenance and detachment

0.05M EDTA

Distilled water was used to dissolve 1g KCL (Fisons Scientific Equipment, Loughborough, UK), 5.72g Na₂HPO₄, 1g KH₂PO₄, 40g NaCl and 1.4g EDTA (Duchefa Biochemie, Haarlem, The Netherlands) to make a final volume of 5L. The PH was adjusted to 7.4 and the solution autoclaved and prior to use.

Trypsin (25mg/ml)

Five hundred milligrams of Trypsin was dissolved into 20ml 0.05M EDTA, mixed and filtered through a 0.2µm Minisart filter (Sartorius, Epsom, UK), aliquoted to

250µl samples and stored at -20°C for until required. For use in cell culture one 250µl aliquot was diluted in a further 10ml of 0.05M EDTA solution and used for cell detachment.

Tissue culture medium for general use:

DMEM / Ham's F12 with L-Glutamine medium purchased from PAA Laboratories, Somerset, UK.

Serum:

Heat inactivated foetal calf serum was also purchased from PAA Laboratories, Somerset, UK.

Other solutions for Cell culture:

Balanced salt solution (BSS)

NaCl 79.5g, KCl 2.2g, KH₂PO₄2.1g, and Na₂HPO₄1.1g was dissolve in distilled water to make a final volume of 10L. Adjust pH to 7.2.

Solutions for RT

DEPC water

Diethyl pyroncarbonate (DEPC) was added 250µl to 4750µl distilled water. Autoclaved before use.

Solutions for DNA detection

5X Tris, Boric acid, EDTA (TBE)

Distilled water were used to dissolve 540g of Tris-Cl (Melford Laboratories Ltd., Suffolk, UK), 275g Boric acid (Duchefa Biochemie, Haarlem, The Netherlands) and 46.5g of disodium EDTA and make up to a final volume of 10L. Stored at room temperature and diluted to 1X concentrate prior to use in agarose gel electrophoresis.

Ethidum bromide

Ten milliliter distilled water was used to dissolve 0.1g of Ethidium Bromide powder. Container was wrapped in aluminium foil to protect solution from sunlight and stored safely before use.

Solutions for protein extraction

Lysis Buffer

Two millimoles CaCl₂, 0.5% Triton X-100, 1 mg/ml Leupeptin, 1 mg/ml Aprotinin and 10 mM sodium orthovanadate were dissolved into distilled water, stored at 4°C until required.

Solutions for western blot

10% Ammonium Persulfate (APS)

One gram of ammonium persulfate were dissolve in 10ml of distilled water, separated into 2.5ml aliquotes and stored at 4°C until required.

10X Running buffer

Tris 303g, 1.44Kg Glycine and 100g SDS were dissolve into distilled water to a final volume of 10L. The 10X stock solution was diluted to 1X strength in distilled water before use.

Transfer buffer

Tris 15.15g, 72g Glycine (Fisher Scientific, Leicestershire, UK) were dissolved in distilled water before adding and 1L Methanol. This was made up to a 5L final volume.

10X TBS

Tris 121.1g and 400.3g NaCl were dissolve in distilled water, made up to a final volume of 5L and adjust pH to 7.4.

Ponceau S stain

Supplied directly by Sigma.

Amido black stain

Amido black (Edward Gurr Ltd., London, UK) 2.5g were dissolved in 50ml Acetic acid (Fisher Scientific, Leicestershire, UK) and 125ml Ethanol (Fisher Scientific, Leicestershire, UK), added 325ml distilled water and mixed well.

Amido black destain

Acetic acid 100ml were mixed with 250ml Ethanol and 650ml distilled water.

Coomasie blue stain

One gram of Coomassie blue was dissolved in 400ml of Methanol and 100ml of Acetic acid, made up to a final volume of 1L using distilled water.

Coomasie blue destain

Five hundred millilitres of Methanol were mixed with 100ml of Acetic acid, made up to a final volume of 1L.

Solutions for cell and tissue staining

Wash buffer: 20X Optimax wash buffer (Biogenex, California, USA) was diluted

1:20 to form a working solution.

DAB chromagen

The DAB chromagen was prepared by mixing the following reagents in order, 2

drops of wash buffer, 4 drops DAB (Vector Laboratories Inc., Burlingame, USA) and

2 drops of H₂O₂ to 5ml of distilled water. The mixture was shaken well after the

addition of each reagent.

ABC Complex

The ABC complex was prepared using a kit obtained from Vector Laboratories Inc.,

Burlingame, USA. 4 drops of reagent A were added to 20ml of wash buffer, followed

by the addition of 4 drops of reagent B and thorough mixing. The ABC complex was

then left to stand for approximately 30 minutes before use.

Solutions for cloning work

LB agar

96

Ten grams of tryptone, 5g yeast extract, 10g NaCl and 15g agar were dissolved in distilled water to a final volume of 1L and adjusted to pH 7.0. Autoclaved and cooled slightly before adding selective antibiotic (if required) and pouring into 10cm petri dish plates (Bibby Sterilin Ltd., Staffs, UK) and allowing to cool and harden, inverted and stored at -4°C.

LB broth

Ten grams of tryptone (Duchefa Biochemie, Haarlem, The Netherlands), 5g yeast extract (Duchefa Biochemie, Haarlem, The Netherlands) and 10g NaCl were dissolve in distilled water to a final volume of 1L and adjust to pH 7.0. The medium was autoclave and allowed to cool before adding selective antibiotic (if required), stored at room temperature.

2.2 Cell Culture and storage

2.2.1 Preparation of growth medium and maintenance of cells

Cells were routinely maintained in DMEM / Ham's F12 medium base supplemented with streptomycin, penicillin and 10% (v/v) foetal calf serum. Transfected cell lines, containing the pEF6 plasmid, were cultured initially in selection medium containing 5 μ g/ml blasticidin S and then later were routinely cultured in a maintenance medium containing 0.5 μ g/ml blasticidin S.

Cells were maintained and grown in either 25cm^2 or 75cm^2 tissue culture flasks (Greiner Bio-One Ltd, Gloucestershire, UK) in an incubator at 37.0°C , 5% CO₂ and 95% humidity. All tissue culture techniques were carried out following aseptic techniques inside of a class II laminar flow cabinet. Cells were routinely sub cultured when reaching 80-90% confluency as described below.

2.2.2 Trypsinisation and counting of cells

When cells reached approximately 80 – 90% confluency, medium was removed and the cells rinsed briefly with EDTA. Following this, adherent cells were detached from the tissue culture flask by incubating with trypsin/EDTA for several minutes. Once detached the cell suspension was placed in 20ml universal container (Greiner Bio-One Ltd, Gloucestershire, UK) and a cell pellet was collected by centrifuging at 1600 RCF for 5 minutes. The cell pellet was resuspended in an appropriate volume

of fresh medium before either determining cell numbers per millilitre (for use in cellular assays) or transferring a small volume of cell suspension into new tissue culture flask.

A haemocytometer counting chamber allows the number of cells in a previously determined volume of suspension fluid to be calculated. Cells were counted on a Neubauer haemocytometer counting chamber using an inverted microscope (Reichet, Austria) under 10 x magnification. The dimensions of each 16 square area, containing cells to be counted, is 1mm x 1mm x 0.2mm which allowed the number of cells per milliliter to be determined using the following equation:

Cell number / ml = (number of cells counted in 16 squares \div 2) x (1 x 10⁴)

This allowed the number of cells per millilitre to be determined and accurate numbers of cells to be seeded in the *in vitro* and *in vivo* cellular functional assays.

2.2.3 Storage of cell lines in liquid nitrogen

Low passage cells were first trypsinised from a large 75cm² flask using EDTA/Trypsin and pelleted by centrifuge. These cells were then resuspended in the required volume (dependent on the number of samples to be frozen) of a protective medium consisting of 10% dimethyl sulphoxide (DMSO) in normal growth medium. Following resuspension, cells were alliquoted into pre-labeled 1.8ml cryotubes (Nunc,

Fisher Scientific, Leicestershire, UK) in 1 ml volumes and stored overnight at -81°C in a deep freezer. Cells were later transferred to liquid nitrogen tanks for long term storage.

2.2.4 Resuscitation of cell lines

Cells were placed in a water bath at 37°C immediately after their removal from liquid nitrogen. The outside of the cryotube was cleaned thoroughly with a sterile swab and placed in a universal container containing 10ml of pre-warmed medium to immediately dilute the DMSO present. The universal containers were then centrifuged at 1600 RCF for 5 minutes to pellet the cells. The medium was then aspirated to remove any traces of DMSO and the cell pellet was resuspended in 5ml of pre-warmed medium and placed into a fresh 25cm³ tissue culture flask and incubated for 4 - 5 hours. Following incubation, the flask was examined under the microscope to obtain an estimation of the number of healthy adherent cells, the medium was then changed to remove any dead cells which did not survive the freezing/resuscitation process. The flask was then returned to the incubator and standard sub-culture techniques carried out when further necessary.

Cell viability was tested using Trypan blue exclusion test as necessary. 20ul of cell suspension was mixed with 100ul of 1% Trypan Blue (1gram of Trypan blue dissolved in 100ml of BSS. Spin the solution before use). The percentage of non-viable cells (blue under the microscope) was calculated.

2.3 Methods for Detection of mRNA

2.3.1 Total RNA isolation

Total RNA was extracted using ABgene Total RNA Isolation Reagent (TRIR) Kit and protocol (ABgene, Surrey, UK). Desired cells were previously cultured in 25cm² flasks until 85-90% confluent, the medium was then removed and 1ml of TRIR was added to the cell monolayer. A plastic cell scraper was used to completely detach the cells and collect the lysate. The cell lysate was then passed through a transfer pipette several times before being transferred into a 1.8ml eppendorf. The mixture was kept at 4°C for 5 minutes before adding 0.2ml chloroform and vigorously shaking the samples for 15 seconds. Samples were then centrifuged in a refrigerated centrifuge (Boeco, Wolf laboratories, York, UK) at 4°C and 12,000g for 15 minutes. The upper aqueous phase, containing RNA, was carefully removed and added to a pre-labelled eppendorf containing an equal volume of isopropanol, the samples were then stored at 4°C for 10 minutes before centrifuging at 12,000g and 4°C for 10 minutes. At this stage RNA will be precipitated out of solution as a pellet in the bottom of the eppendorf. The RNA pellet was washed twice after the supernatant was discarded in 75% ethanol (prepared in a 3:1 ratio of absolute ethanol: DEPC water). Each wash consisted of the addition of 1ml of 75% ethanol, vortexing and subsequent centrifugation at 4°C and 7,500g for 5 minutes. Ethanol was removed from the eppendorf after the final wash. The pellet was placed in a Techne, Hybridiser HB-1D drying oven (Wolf laboratories, York, UK) at 50°C to briefly dry and remove any remaining ethanol. Finally, the pellet was dissolved in 50 - 100µl (depending on pellet size) of DEPC water before proceeding to quantify the RNA

present in the sample. DEPC is a histidine specific alkylating agent and inhibits the action of RNases which rely on histidine active sites for their activity. DEPC water was used in RNA isolation to reduce the effects of any RNases that may be present.

2.3.2 Reverse transcription (RT)

After isolation, UV1101 Biotech Photometer (WPA, Cambridge, UK) was used to detect ssRNA ($\mu g/\mu l$) and to quantify RNA in a 1 in 10 dilution, based on the difference in absorbance at 260nm wavelength compared to a DEPC blank. All samples were measured in a Starna glass curvette (Optiglass limited, Essex, UK).

Following RNA isolation and quantification, 0.5µg of RNA was converted into complementary DNA (cDNA) using an iScript cDNA Synthesis Kit (Bio-Rad laboratories Inc, UK), following their one-Step RT-PCR protocol.

For each reaction, a sufficient volume of RNA (0.5µg) suspended in DEPC water (isolated previously) was added to nuclease-free water to make up a total volume of 15µl in a thin-walled 200µl PCR tube. The following were then added into each tube (per reaction):

- 5X iscript reaction mix 4 μl
- iScript reverse transcriptase 1 μl

After mixing gently and centrifuging, the samples were placed in a T-Cy Thermocycler (Creacon Technologies Ltd, The Netherlands) and underwent the following procedures:

- 5 minutes at 25°C
- 30 minutes at 42 °C
- 5 minutes at 85 °C
- Hold samples at 4 °C

Samples were stored at -20°C after being diluted 1:3 with PCR water, ready for further use. The cDNA generated was tested using conventional PCR probing for β -actin expression to confirm successful reverse transcription.

2.3.3 Polymerase chain reaction (PCR)

PCR was carried out using a REDTaq ReadyMix PCR Reaction mix (Sigma, Dorset, UK). Primers were designed using the Beacon Designer programme (Palo Alto, California, USA) and were synthesised by Invitrogen (Paisley, UK), based on the full sequence of the gene of interest. Primers were diluted to a concentration of 10pM before use in the PCR reaction. Twenty microlitre reactions were set up for each sample to be tested as follows:

- 2X REDTaq ReadyMix PCR Reaction mix 10μl
- Specific Forward primer (10pM) 1µl

• Specific Reverse primer (10pM)

PCR water 6μl

• cDNA 2μl

When the above reaction had been set up in a 200µl PCR tube (ABgene, Surrey, UK), they were mixed briefly and centrifuged before being placed in a T-Cy Thermocycler (Creacon Technologies Ltd, The Netherlands) and subjected to the following temperature shifts:

 1μ l

- Stage 1: Initial denaturing period 94°C for 5 minutes
- Stage 2: Denaturing step 94°C for 1 minute

Annealing step – reaction specific temperature for 2 minutes

Extension step – 72°C for 3 minutes

• Stage 3: Final extension period – 72°C for 10 minutes

Stage 2 was repeated over 38 cycles. Specific reaction annealing temperatures together with primer sequence data is detailed in table of section 2.1.2.

2.3.4 Agarose gel DNA electrophoresis

Once the DNA had been amplified through the sufficient number of cycles in the thermocycler, the sample was separated according to size using agarose gel electrophoresis. Agarose gels were made by adding the required amount (0.8% or 2%) of agarose (Melford Chemicals, Suffolk, UK) to TBE solution. The mixture was heated to fully dissolve, poured into the electrophoresis cassette and allowed to set around a plastic comb creating loading wells. Once set, the gel was submerged in TBE running buffer, 8µl of a 1Kb ladder (Invitrogen, Paisley, Scotland) or 10µl of sample was then added to the wells. The samples were loaded into either 0.8% (samples greater than approximately 500bp) or 2% (samples less than 500bp) agarose gels, dependent on the predicted size of the DNA products. The samples were then separated electrophoretically at 95V for a period of time to allow sufficient separation of the samples.

2.3.5 Real time quantitative PCR

The real time quantitative PCR was carried out to determine the levels of RGM transcripts in the breast cancer cohort and cell lines. The assay was based on the Amplifuor technology and primers were designed using Beacon Designer software which included complementary sequence to universal Z probe (Intergen Inc., Oxford, United Kingdom), as previously reported (Jiang et al., 2005a; Parr et al., 2004). Primers used for RGMs quantitation and housekeeping GAPDH are listed in section

2.1.2. Each 10μl reaction contains 5μl of Hot-start Q-master mix (Abgene), 10 pmol of specific forward primer, 1 pmol reverse primer which has the Z sequence, 10 pmol of FAM-tagged universal Z probe (Intergen Inc., Oxford, United Kingdom), and 50ng cDNA. The Q-PCR was carried out using IcyclerIQTM (Bio-Rad, Hemel Hemstead, England, UK), which is equipped with an optic unit that allows real time detection of 96 reactions. The following condition was used in the reaction: 94°C for 12 minutes, 60 cycles of 94°C for 15 seconds, 55°C for 40 seconds (the data capture step) and 72°C for 20 seconds. The levels of the transcripts were generated from an internal standard that was simultaneously amplified with the samples. Cytokeratin-19 (CK19) or GAPDH was used to normalise cellularity during the analysis of the RGM expression related to clinical data. Data are shown in Chapter 3 as either the number of transcripts (mean number of RGM transcript per 50ng total RNA) or as RGM: CK19 ratio.

2.4 Methods for Detection of Proteins

2.4.1 Sodium dodecyl sulphate polyacrylamide gel electrophosis (SDS-PAGE) and western blot analysis

2.4.1.1 Cellular lysis and protein extraction

Upon reaching sufficient confluency, the medium was removed and changed into cold BSS buffer (leaving in ice). The cell monolayer was detached from the flask using a sterile cell scraper. Both the detached cells and buffer were then transferred to a universal container using a sterile transfer pipette. The cell suspension was then

centrifuged for 5 minutes at 1800 RCF to pellet cells and protein at the bottom of the universal container. Following centrifugation, the medium was aspirated off and the cells were lysed in 120 – 250µl (depending on pellet size) of lysis buffer before being transferred to a 1.8ml eppendorf (Alpha Laboratories, Hampshire, UK) and placed on a Labinco rotating wheel (Wolf laboratories, York, UK) for 1 hour. The lysis solution was then spun at 13,000 rpm in a microcentrifuge for 15 minutes, and the supernatant was transfer to a fresh eppendorf to await for quantification.

2.4.1.2 Protein quantification

Protein concentration was quantified using Bio-Rad DC Protein Assay kit (Bio-Rad laboratories, Hammelhempstead, UK) following the microplate method as described below. Firstly, a range of standard samples of known concentrations were set up using a serial dilution of a 100mg/ml Bovine Serum Albumin (BSA) standard (Sigma, Dorset, UK), standards were serially diluted from 100µg/ml to 0.05µg/ml in lysis buffer.

Five microlitre of either the sample or standard was added to a fresh well with 25µl of 'Reagent A+S' and 200µl of reagent B. 'Reagent A+S' was prepared by mixing each millilitre of reagent A with 20µl of reagent S and was used as samples contained detergent. Following addition of all the reagents, samples were mixed briefly and then left for approximately 45 minutes to allow the colorimetric reaction to fully occur.

Absorbance of samples and standards at 620nm was then read using an ELx800 plate reading spectro photometer (Bio-Tek, Wolf laboratories, York, UK). Sample final concentrations were determined by a standard curve based on the absorbances of the BSA standards. All samples were then diluted to the desired final concentration of between 1 –2mg/ml with appropriate amount of lysis buffer and further dilution in a 1:1 ratio with 2x Lamelli sample buffer concentrate. Samples were then boiled and stored at -20°C prior to use.

2.4.1.3 Sodium Dodecyl Sulphate PolyAcrilamide Gel Electrophoresis (SDS-PAGE)

OmniPAGE VS10 vertical electrophoresis system (OminPAGE, Wolf Laboratories, York, UK) were used in this procedure. Resolving gels were made up in a universal container and transferred to glass plates held in place in a loading cassette. The percentage of the gel is depending on the predicted size of the protein of interest. Once the resolving gel had set, the stacking gel was prepared and added onto the top of the resolving gel. A plastic comb was placed in the unset stacking gel and the mixture was left to harden and form a gel.

The amount of each ingredient required to make up 15ml (enough for two gels) for 8%, 10% and 15% resolving gels is indicated below:

Table 2.4.1.3A Components for resolving gels

Component	8% gel	10% gel	15% gel

Distilled water	6.9ml	5.9ml	3.4 ml
30% acrylamide mix	4.0ml	5.0ml	7.5 ml
1.5M Tris (pH 8.8)	3.8ml	3.8ml	3.8 ml
10% SDS	0.15ml	0.15ml	0.15ml
10% ammonia	0.15ml	0.15ml	0.15 ml
persulphate	0.009ml	0.006ml	0.006 ml
TEMED			

The components and quantities required to prepare 5ml of stacking gel solution (enough for two gels) are shown below:

Table 2.4.1.3B Components for stacking gels

Component	Stacking gel
Distilled water	3.4ml
30% acrylamide mix	0.83ml
1.0M Tris (pH 6.8)	0.63ml
10% SDS	0.05ml
10% ammonia persulphate	0.05ml
TEMED	0.005ml

Once both resolving and stacking gels had set, the loading cassette was placed into an electrophoresis tank. The combs were then carefully removed after rinsed in 1X running buffer. 8-10µl of molecular weight marker or 18µl of protein samples was added to the wells in order. The proteins were then separated according to

molecular weight using electrophoresis at 125V, 40mA and 50W for a varying length of time (dependent on protein size and gel percentage).

8% gels were used to detect proteins with a molecular weight ranging between 50 - 100kDa and 10% gels were used when protein sizes were predicted to be between 20 - 80kDa.

2.4.1.4 Western blotting

Following PAGE of the protein samples, they were transferred to Hybond nitrocellulose membrane (Amersham Biosciences UK Ltd, Bucks, UK) using Western blotting. Gels were removed from the electrophoresis tank and unclipped from the loading cassette. The stacking gel was cut away and the resolving gel placed on top of a nitrocellulose membrane (face up) in a SD10 SemiDry Maxi System blotting unit (SemiDRY, Wolf Laboratories, York, UK). The gel to membrane transfer sandwich was finished with 3X filter papers underneath and above respectively. The setting up for protein transfer was:

Negative Electrode → 3X Filter Papers → Membrane → Gel → 3X Filter Papers →
Positive Electrode

3mm chromatography paper (Whatman International Ltd., Maidstone, UK) was used as filter paper. Electro-blotting was undertaken at 15V, 500mA, 8W over a 40mins - 1 hour period (depending on the molecular weight). Once complete membranes were removed and stored in 5% skimmed milk, 0.05% polyoxyethylene (20) sorbitan monolaurate (Tween 20) in TBS at 4°C until required for specific antibody probing.

Optional:

Membranes were placed in Ponceau S solution for several minutes to allow visualisation of protein bands on the membrane, the membrane was then cut into the required number of sections before washing off the stain several times in the 10% milk solution used for blocking.

Membranes were transferred to 50ml falcon tubes (Nunc, Fisher Scientific, Leicestershire, UK), placed in a 1:250 specific primary antibody made up in 3% milk solution (3% milk powder, 0.1% Tween 20 in TBS) and rotated on a roller mixer (Stuart, Wolf laboratories, York, UK) after blocking at room temperature 1 hour or 4°C overnight (specific details on antibodies used are outlined in table 2.1.3.1). After the 1 hour incubation period, the primary antibody solution was removed and the membrane subjected to three 15 minute washes with 3% milk to ensure complete removal of the primary antibody. Following these washes, the secondary antibody of the appropriate species tagged with HRP (horse raddish peroxidate) was added in fresh 3% milk solution to the membrane at a concentration of 1:1000 and left for 1 hour. The membrane was then subjected to two 10 minute washes with T-TBS (TBS containing 0.05% tween 20) followed by two 10 minute washes with TBS. After

these washes chemiluminescent detection of the antibody-antigen complex was undertaken using Supersignal West Dura system reagents (Pierce Biotechnology, Rockford, Illinois, USA) and UVITech imager (UVITech, Inc., Cambridge, UK). The membranes were subjected to a number of exposure times and images captured. These images were then further analyzed using the UVIband software package (UVITEC, Cambridge, UK) which allows the protein bands detected on the screen to be quantified and also allow the standardisation of samples, when run in conjunction with housekeeping proteins such as GAPDH, the expression of which should be similar within the same cell types. Western blotting was repeated at least twice and bands from both repeats quantified and standardised separately. Quantification and standardisation was repeated three times and mean values calculated.

Membranes were also stained in Amido black stain following completion of antibody probing and kept as a record. Again membranes were placed into the Amido black solution for several minutes before being removed and placed in Amido Black destain solution to remove background staining. The membranes were then left overnight to dry completely and stored as a record.

2.4.2 Immunoprecipitation of phosphorylated proteins

Duplicate sets of 3×10^6 cells were grown in large 75cm^3 flasks overnight. Serum hunger was then induced by replacing the normal supplemented medium with 5ml of serum free medium and incubating the cells at 37°C for 2 hours. Each of the duplicate flasks was then subjected to a separate treatment for 1 hour or maintained as control. The cells were collected and lysed in 300µl SDS-free lysis buffer followed by rotation on wheel for 1 hour. One hundred microliters of this cell lysate solution was taken to run GAPDH and probe total protein. Two hundred microliters was left for immunoprecipitation.

50μl of phospho-S/T antibody was added (previously diluted 1:5 in SDS-free lysis buffer) to the standardised protein solution (100ul) and the samples were placed on a rotating wheel for 1 hour. 50μl of conjugated A/G protein agarose bead solution (20% Protein A agarose beads, 20% Protein G agarose beads, 60% SDS-free lysis buffer, Both A and G agarose beads were obtained from Santa cruz biotechnology Inc., California, USA) was then added and the samples returned to the rotating wheel for another hour. The samples were then centrifuged at 8,000rpm for 5 minutes and the supernatant discarded, the beads were then washed three times through the addition of 1ml of SDS-free lysis buffer, centrifuged at 8,000rpm for 5 minutes and subsequently the supernatant was removed. 1X sample buffer 50μl was then added to the samples before boiling for 5 minutes. The samples were then stored at -20°C prior to use in SDS-PAGE and as western blot mentioned above.

2.4.3 Immunohistochemical (IHC) and Immunocytochemical (ICC) staining

Frozen sectioning of breast and prostate tissues was kindly undertaken by Mr Gareth Watkins who also contributed to the staining of prostate sections. Frozen tissues were

cut into 5µm sections using a cryostat (Leica Microsystems (UK) Ltd., Bucks, UK) and were left at room temperature for 30 minutes to dry. Once dried the sections were fixed in a 1:1 mixture of acetone and methanol for 20 minutes before staining or storing at -20°C until use.

For ICC, Cells were seeded at a density of 20,000 cells per well in 200µl of normal medium, in a 16 well chamber slide (Lab-Tek, Nagle Nunc Int., Illinois, USA). After cell seeding, the cells were incubated for 24 hours before fixing the cells in 4% formaldehyde in BSS for at least 20 minutes. The slides were ready to use or stored at -20°C for future use.

The tissue sections and cells were allowed to reach room temperature and rehydrate before staining was carried out. When reaching RT, the sections were then placed in Phosphate Buffered Saline (PBS) for 5 minutes and a reservoir was created around the individual sections (to contain the various staining solutions) using a Dako water proof marker pen; cells were rehydrated in BSS for 20 minutes before permeablising the cells in 0.1% triton X100 for 5 minutes.

Non-specific binding was blocked through the addition of Optimax wash buffer containing horse serum (1 drop of horse serum per 5ml of wash buffer) to the samples for 20 minutes. The samples were then washed in wash buffer 3 times before the addition of the primary antibody at an appropriate concentration (made up in wash buffer containing serum and tested before use) for 1 hour at room temperature. Unbound primary antibody was then removed by washing the sections 3 times in wash buffer before adding a universal secondary antibody (Vectorstain ABC Kit,

Vector Laboratories Inc., Burlingame, USA) for 30 minutes at room temperature (4 drops of universal secondary per 5ml wash buffer). Again unbound secondary antibody was removed by washing the sections in wash buffer 3 times. The sections were then incubated with the ABC complex for 30 minutes at room temperature, washed 3 times in wash buffer and incubated with the DAB chromogen for 5 minutes in the dark. The DAB was removed by placing the samples in running tap water for 2 minutes before finally counterstaining the sections with Mayer's Haemotoxylin for 1 minute and placing the sections in running water for 5 minutes.

2.4.4 Immunofluorescent staining

Cells were seeded at a density of 8,000 cells per well in 200µl of normal medium, in a 16 well chamber slide (Lab-Tek, Nagle Nunc Int., Illinois, USA). After cell seeding, the cells were incubated for 24 hours and subjected to treatment before fixing the cells in ice-cold pure ethanol at -20°C for 20 minutes. Cells were then rehydrated in BSS for 20 minutes at room temperature before permeablising the cells in 0.1% triton X100 (in a BSS buffer) for 5 minutes. Non-specific binding was then blocked for 20 minutes by placing MenaPath Autowash buffer (A. Menarini Diagnostics, Berkshire, UK) solution (diluted 1:20 in distilled water) containing horse serum (2 drops per 5 ml diluted wash buffer) over the cells. Following the blocking stage the cells were washed twice with diluted wash buffer solution. Specific staining was then undertaken through the addition of a specific primary antibody (made up in wash buffer containing serum) for 1 hour on an orbital shaker

platform (Biddy Sterilin Ltd., Staffordshire, UK) (1:100). From this step, the chamber slide was either placed in a dark box or wrapped using a Aluminium foil in order to keep the slide in dark. The primary antibody was then removed and the cells washed three times in diluted wash buffer. The appropriate FITC conjugated secondary antibody was then added to the cells (1:150) and the slides were incubated on a rotating platform in the dark for 1 hour before removing the secondary and washing the cells three times with diluted wash buffer. After this protocol had been completed the well compartments were broken from the chamber slide, the cells were covered with Fluoro-save (Merck Chemicals Ltd., Nottingham, UK), a fluorescent saving buffer, and cover slips added over the top. These slides were then placed at -4°C overnight in the fridge to allow the fluoro-save to harden before visualizing any staining under a fluorescent microscope (Olympus, Japan) using a GFP filter. Representative pictures were then taken at x100 objective magnification using the Optimas 6 software package. The experiment was repeated three times and representative data was presented (See Chapter 9).

2.5 TOPO Cloning

2.5.1 Knockdown of gene transcripts using ribozyme transgenes

The expression of RGM was down-regulated at the messenger RNA level using ribozyme transgenes that specifically targeted and cleaved the RGM mRNA transcript. Hammerhead RNAs are frequently used structure. The hammerhead ribozyme functions as a enzyme, carries out a very simple chemical reaction that results in the breakage of the substrate strand of RNA, the cleavage-site nucleotide. Much of the experimental work carried out on hammerhead ribozymes has used a minimal construct. The minimal hammerhead ribozyme is composed of three base paired helices, separated by short linkers of conserved sequence. The cleavage reaction occurs between helix III and I (Figure 2.1 secondary structure of hammerhead). The best target sites of high efficiency for cleavage were found to be ATC, GTC and TTC.

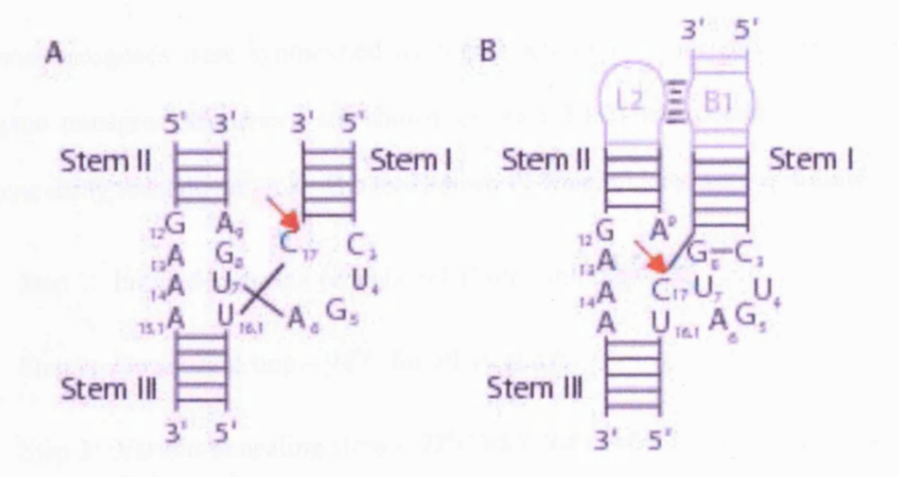


Figure 2.1 Secondary structures and sequences of the minimal (A) and full-length (B) hammerhead ribozymes.

Conserved and invariant nucleotides are shown explicitly. Watson-Crick base-paired helical stems are represented as ladder-like drawings. The red arrow depicts the cleavage site, 3' to C17, on each construct. (Source from: http://upload.wikimedia.org/wikipedia/en/8/89/Minimal_and_full_length_hammerhead_sequences.png)

The secondary structure of the transcript of interest was predicted using Zuker's RNA mFold software (Zuker, 2003). The second structures of human RGMA, RGMB and RGMC generated for the present study were shown in Figures 2.1a, 2.1b, and 2.1c respectively. A suitable GUC or AUC ribozyme target site was then selected from within the secondary structure and the ribozyme designed to specifically bind the sequence surrounding this target codon. This allowed the hammerhead catalytic region of the ribozyme to interact and accurately cleave a specific GUC or AUC sequence within the target mRNA transcript. Once designed the oligos for the

ribozyme transgenes were synthesised by SigmaGenesis as sense/antisense strands (ribozyme transgene sequences are shown in table 2.1.2) and combined into the transgene using touchdown PCR. The touchdown PCR conditions were as follows:

- Step 1: Initial denaturing period 94°C for 2 minutes
- Step 2: Denaturing step 94°C for 30 seconds
- Step 3: Various annealing steps 72°C/68°C/64°C/60°C/55°C for 30 seconds.
- Step 4: Extension step 72°C for 30 seconds
- Step 5: Final extension period 72°C for 7 minutes

Step 2-4 was repeated over 65 cycles, composed of 10, 10, 10, 10, 25 cycles respectively depending on annealing temperature.

On completion of the generation, the ribozyme PCR products were separated on a 2% agarose gel, in order to visualise the success of the amplification. These PCR products were later inserted into the pEF6 plasmid using the TOPO cloning reaction described later.

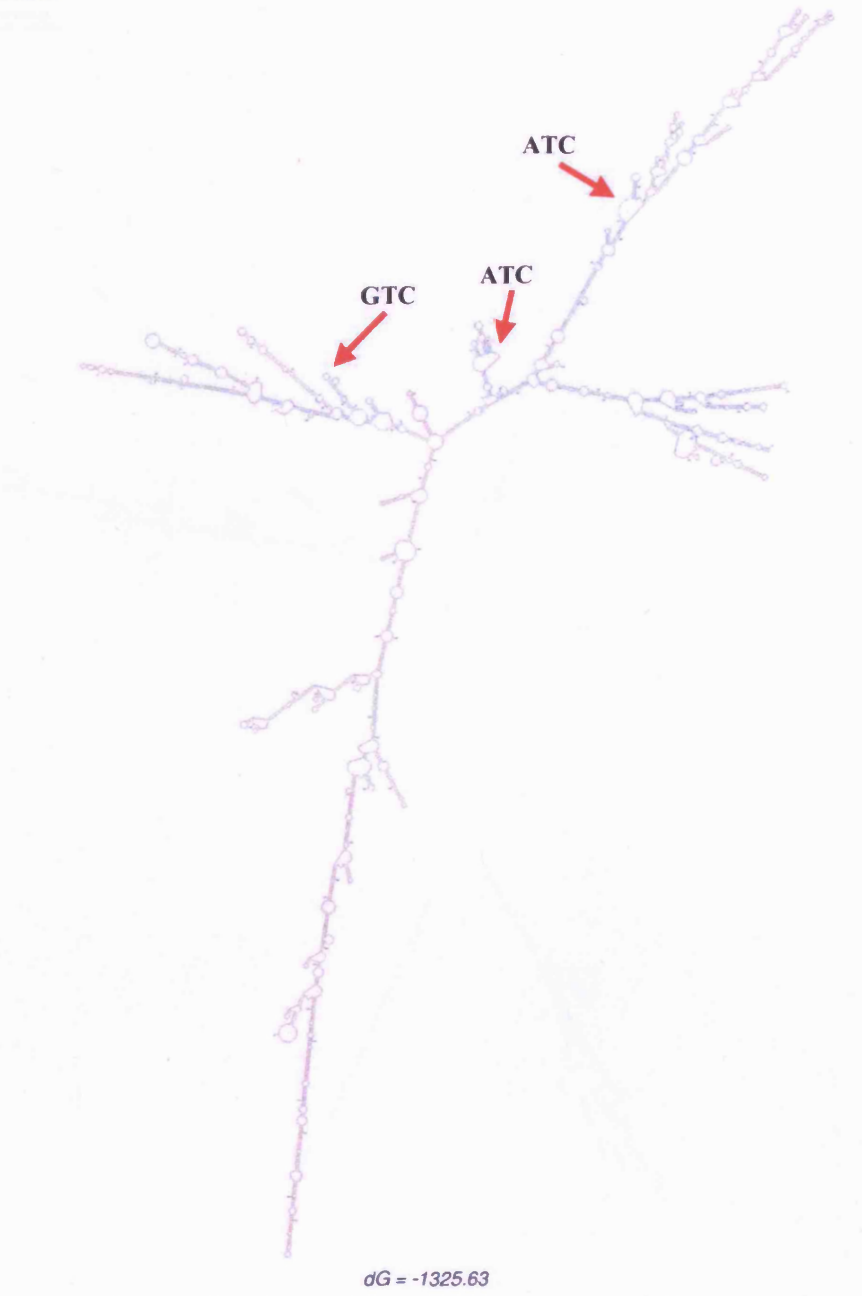


Figure 2.1A The predicted secondary structure of human RGMA mRNA, from which the anti-RGMA ribozymes were designed.

The secondary structure of human RGMA mRNA was predicted using Zuker's mfold programme. The arrows (red) indicate potential target sites chosen for the ribozyme transgenes.



dG = -785.44

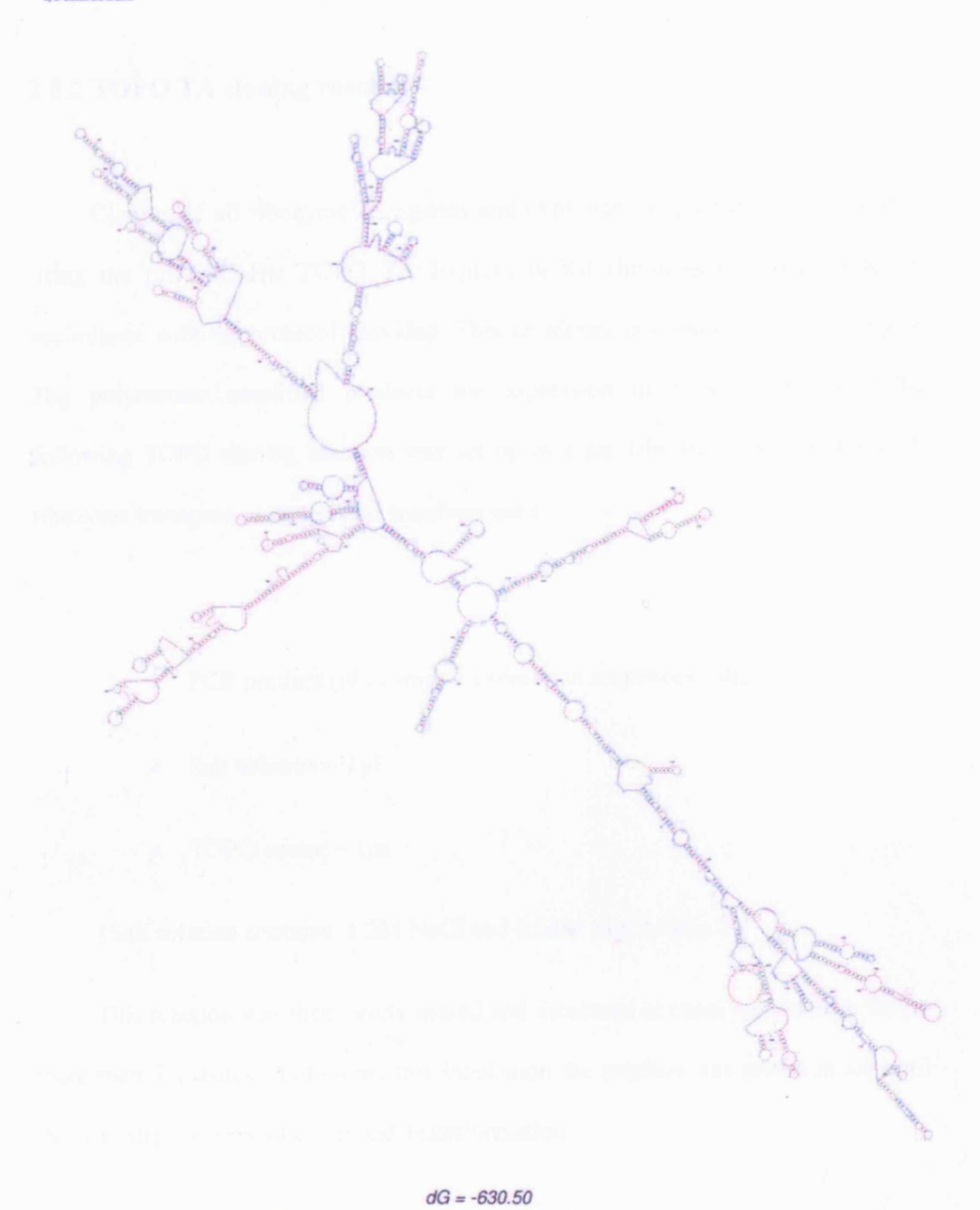


Figure 2.1C The predicted secondary structure of human RGMC mRNA, from which the anti-RGMC ribozymes were designed.

2.5.2 TOPO TA cloning reaction

Cloning of all ribozyme transgenes and expression sequences was completed

using the pEF6/V5-His TOPO TA Expression Kit (Invitrogen, Paisley, UK) in

accordance with the protocol provided. This kit allows fast and effective cloning of

Tag polymerase amplified products for expression in mammalian cells. The

following TOPO cloning reaction was set up in a pre labelled PCR tube for each

ribozyme transgene or expression sequence used:

• PCR product (ribozyme or expression sequence) – 4μl

Salt solution - 1µl

TOPO vector - 1µl

(Salt solution contains: 1.2M NaCl and 0.06M MgCl₂/50 µl)

This reaction was then gently mixed and incubated at room temperature for no

more than 5 minutes. Following this incubation the reaction was stored in ice until

the next step-- One Shot Chemical Transformation.

123

2.5.3 Transformation

Five microlitre of completed TOPO cloning reaction was added to a vial of One Shot TOP10 Chemically Competent *E. coli* and gently mixed. The mixture can be stirred using the pipette tip but pipetting up and down will damage the bacteria. The vial was then incubated for 30 minutes on ice, before being heat-shocked at 42°C for 30 seconds and immediately placed back into ice. Two hundred and fifty microlitre of room temperature SOC medium was next added to each tube; the tubes were then capped and shake horizontally at 37°C and 200rpm on a horizontal orbital shaker (Bibby Stuart Scientific, UK) for 1 hour. Following this incubation period the bacteria of the tube was spread onto two selective agar plates (containing 100μg/ml ampicillin) at both a high and low seeding density and allowed to grow overnight at 37°C in an incubator. The pEF6 plasmid contains two antibiotic resistance genes that allow only cells containing the plasmid to grow under ampicillin and blasticidin S selection, a schematic of the plasmid is shown below (Figure 2.2).

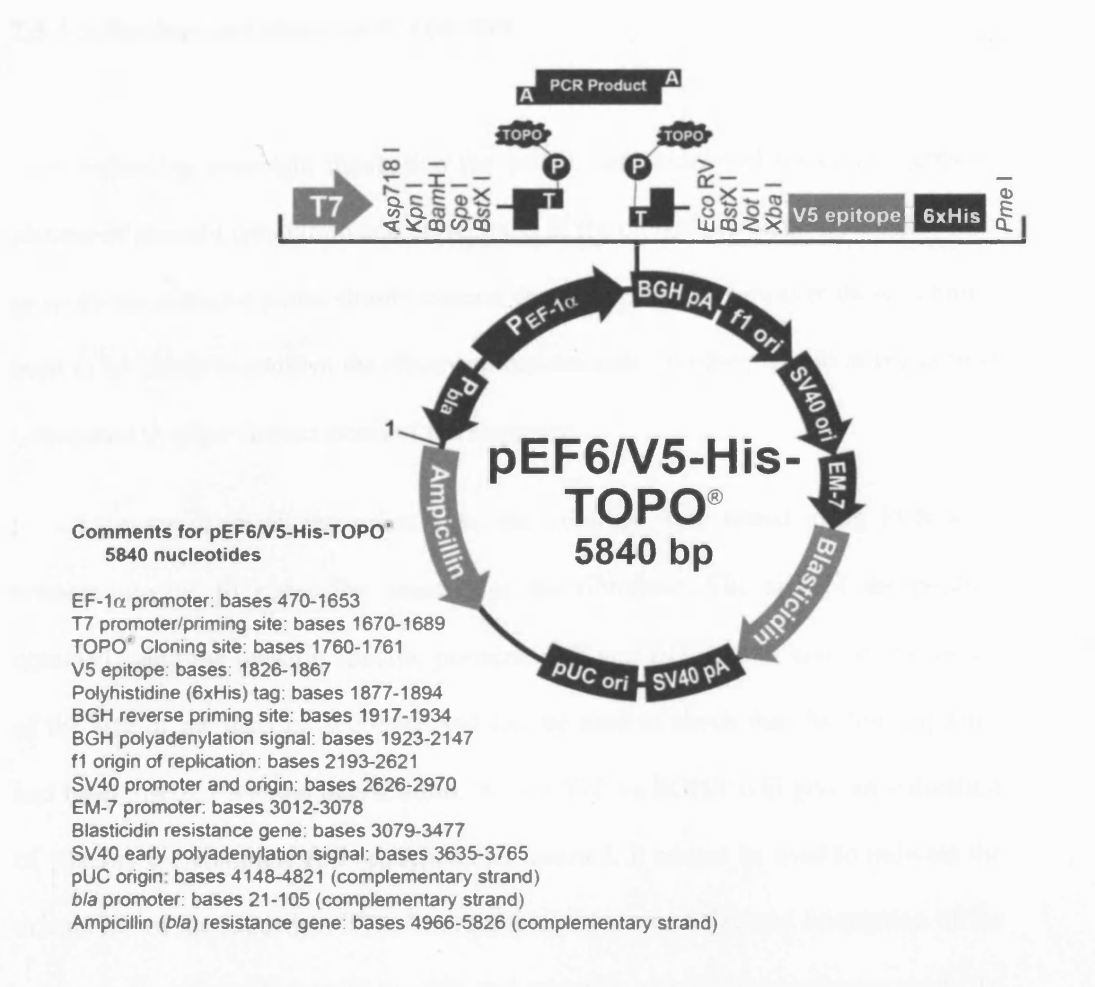


Figure 2.2 The figure summarizes the features of the pEF6/V5-His-TOPO vector.

The vector is supplied linearized between base pairs 1,760 and 1,761. This is the TOPO Cloning site. Unique restriction sites flanking the TOPO Cloning site are shown.

2.5.4 Selection and analysis of colonies

Following overnight incubation the plates were examined for colony growth, success of plasmid generation and correctness of the cloned products. Colonies which grow on the selective plates should contain the pEF6 plasmid, however these colonies need to be tested to confirm the ribozyme has inserted into the plasmid in the correct orientation to allow transcription of the sequence.

In order to check the orientation, the colonies were tested using PCR with primers specific to either the plasmid or the ribozyme. The size of the product obtained using the plasmid specific primers; T7F and BGHR will give an indication of the size of the inserted sequence and can be used to check that the full sequence had been inserted without degradation. Whilst T7F vs BGHR will give an indication of whether the complete full sequence had inserted, it cannot be used to indicate the orientation of the sequence. Thus in order to check correct size and orientation of the sequence a mixture of plasmid specific and sequence specific primers were used. To check the ribozyme sequences, a combination of T7F vs RbBMR (the forward ribozyme sequence) and BGHR vs RbBMR (the reverse ribozyme sequence) were used. There are approximately 90bp between the T7F promoter and the beginning of the insert, thus correct orientation and ribozyme size (based on approximate ribozyme size of 50bp) would be confirmed by a band of approximately 140bp in the T7F vs RbBMR reaction. Likewise a band of approximately 140bp in the BGHR vs RbBMR would indicate incorrect orientation of the sequence.

Ten discrete colonies were randomly selected for orientation analysis and marked and labelled on the plates. For each colony, two PCR reactions were carried out as follows:

Ribozyme orientation reaction 1

- 8µl 2X REDTaq ReadyMix PCR Reaction mix
- 1µl BGHR plasmid specific reverse primer
- 1µl Ribozyme specific reverse primer (RbBMR)
- 6µl PCR water

Ribozyme orientation reaction 2

- 8µl 2X REDTaq ReadyMix PCR Reaction mix
- 1µl T7F plasmid specific forward primer
- 1µl Ribozyme specific reverse primer (RbBMR)
- 6µl PCR water

A sample of selected colonies was picked from the plate using a sterile pipette tip and dipped into both set of mixes before the addition of the specific primers. Each

reaction mix was then placed in a thermal-cycler and subjected to the following conditions:

- Step 1: Initial denaturing period 95°C for 10 minutes
- Step 2: Denaturing step 94°C for 1 minute
- Step 3: Annealing step 55°C for 1 minute
- Step 4: Extension step 72°C for 1 minutes
- Step 5: Final extension period 72°C for 10 minutes

The mixture was then run on a 2% agarose gel and visualized under ultra violet light. Colonies showing correct orientation of the insert were picked off the plate and used to inoculate 10ml of ampicilin selective LB broth and incubated overnight whilst being horizontally shaken at 225 RPM.

2.5.5 Purification and quantification of plasmid DNA

Plasmid extraction was carried out using the Sigma GenElute Plasmid MiniPrep Kit and following the provided protocol. LB broth 5ml with the correct colony cultured overnight (described above), was spun at 3,000 RCF in at 4°C to obtain a pellet of bacteria and the supernatant was discarded. The bacterial pellet was then resuspended

in 200μl of resuspension solution (containing RNase A) and mixed through pipetting. Lysis solution 200μl was then added and the container was inverted 5 - 6 times. This stage was finished within 5 minutes before adding 350μl of the neutralisation solution, inverting 4 - 6 times and centrifuging at 12,000 x g in a microcentrifuge. Plasmid DNA was next bound to the column by transferring the cleared lysate to a Mini Spin Column placed inside a collection tube, spinning at 12,000 x g for 30 seconds - 1 minute and discarding the flow through. Next 750μl of wash solution (containing ethanol) was added to the column before spinning at 12,000 x g for 30 seconds - 1 minute and again discarding flow through. An additional spin at 12,000 x g for 30 seconds - 1 minute was then undertaken to remove any remaining flow through before transferring the Mini Spin Column to a fresh collection tube and eluting the plasmid DNA through the addition of 80μl of elution solution and spinning at 12,000 x g for 1 minute. (The empty column was eluted again with 100ul PCR water and collected as back up.) The eluted plasmid solution was then run on a 0.8% agarose gel to confirm presence and correct size of the plasmid.

2.5.6 Transfection via electroporation into mammalian cells

Following plasmid purification and quantification, the extracted plasmid was used to transform the prostate cancer PC-3 and breast cancer MDA-MB-231 cell lines. Confluent PC-3 or MDA-MB-231 wild type cells were detached from tissue culture flasks using trypsin/EDTA, pelleted and counted following resuspension as previously described. One million cells in 800µl were then added in an

electroporation curvette (Eurgenetech, Southampton, UK) together with 1-3µg of the purified plasmid. This was mixed briefly before being subjected to an electrical pulse of 310V and 1500 capacitance from an electroporator (Easyjet, Flowgene, Surrey, UK). Following this pulse the cell and plasmid suspension was quickly transferred into 10ml of pre-warmed medium in a flask and placed in an incubator to allow any surviving cells to fully recover from the electroporation process.

2.5.7 Establishing a RGM knockdown mutant and Selection of plasmid positive cells

As previously described, the pEF6 plasmid used to transform the cells encodes two antibiotic resistance genes. The ampicillin resistance gene allows initial selection of prokaryotic bacterial cells containing the plasmid. The plasmid also contains a blasticidin S resistance gene. Blasticidin S is a potent microbial antibiotic that inhibits protein synthesis in both prokaryotes and eukaryotes and is used to specifically select for mammalian cells containing the pEF6 plasmid. The use of two antibiotic resistance genes allows more accurate selection of the plasmid positive cells throughout the cloning.

Following overnight incubation, the cells were subjected to an initial 5 day period of intense selection. During this 5 day period, the cells were incubated in medium that had been supplemented with $5\mu g/ml$ of the blasticidin S antibiotic to kill off all cells that did not contain the pEF6 plasmid. After this initial intense selection finished the cells were maintained in maintenance medium containing $0.5\mu g/ml$ of

blasticidin S, this places a selection pressure on the cells to maintain the plasmid and results in long term transformation of the cells.

All cells were tested initially, and estimated the efficiency and stability of both the transformation and the ribozyme transgene using RT-PCR and Western blot analysis for long periods of use.

2.6 In vitro Cell function Assays

2.6.1 Cell growth assay

Cells were detached from the culture flask and cell density (per milliliter) was determined as mentioned previously. Cells were then seeded into a 96 well plate (Nunc, Fisher Scientific, Leicestershire, UK) at a density of 3,000 cells per well in 200µl of normal medium. Triplicate plates were set up to obtain a cell density reading following 1, 3 and 5 day incubation periods. Following the appropriate incubation period, the medium was removed and cells were fixed in 4% formaldehyde in BSS for at least 5 minutes before staining in 0.5% (w/v) crystal violet in distilled water, for 5 minutes. The excessive staining was washed off with water and the plate was left to air dry. The stain was then extracted from the cells using 10% acetic acid and cell density determined by measuring the absorbance on a plate reading spectrophotometer (ELx800, Bio-Tek, Wolf laboratories, York, UK) at 540nm. Cell growth was presented as percentage increase and calculated by

comparing the absorbances obtained for each incubation period using the following equation:

Increased Percentage = [(day 3 or 5) - day 0] absorbance / day 0 absorbance X

100

Within each experiment at least 6 duplicate wells were set up and the entire experiment protocol was repeated three times.

2.6.2 Invasion assay

The invasive ability of the cells used in this study was determined using an *in vitro* Matrigel invasion assay. This assay measures the cells capacity to degrade and invade through an artificial basement membrane and migrate through the polycarbonate membrane of the insert with an 8µm pore in diameter. The experimental protocol used for these experiments was modified from that described in (Albini *et al.*, 1987; Parish *et al.*, 1992). 24 well cell culture plate inserts (BD Biosciences, Oxford, UK) containing 8µm pores were coated with 50µg of an extracellular matrix protein solution, Matrigel (BD Biosciences, Oxford, UK). The working Matrigel solution was made up in serum free medium to a concentration of 50µg per 100µl, added to the inserts and allowed to set in a drying oven. Once dried,

these inserts were placed into sterile 24 well plates and the artificial membrane was rehydrated in 100µl of serum free medium for 40 minutes before use. Once rehydrated the serum free medium was removed and 1ml of normal medium was added to the well outside the insert in order to sustain any cells that may have invaded through the insert. Fifteen thousand cells in 200µl of normal medium were then added to the insert over the top of the artificial basement membrane. The plate was then incubated for 72 hours at 37°C, 5% CO₂ and 95% humidity.

After 72 hours, the inserts were removed from the plate and the inside of the insert (which was initially seeded with cells) was cleaned thoroughly with tissue paper. Any cells which had invaded through the membrane and passed to the underside of the insert were fixed in 4% formaldehyde (v/v) in BSS for 5 minutes before being stained in 0.5% crystal violet solution (w/v) in distilled water. These cells were allowed to air dry and could then be counted under the microscope under x40 objective magnification. Several random fields were counted per insert before being photographed. Duplicate inserts were set up for each test sample. The experimental procedure was repeated three times.

2.6.3 Cell-matrix adhesion assay

This assay was modified from the technique described previously (Jiang *et al.*, 1995a). The capacity of tumour cells to adhere to an artificial Matrigel basement membrane was examined using an *in vitro* Matrigel adhesion assay.

One hundred microlitre of serum free medium contained 5µg of Matrigel was added to each well of a 96 well plate and dried in an oven to form an artificial basement membrane. This membrane was then rehydrated with 100µl of serum free medium for 40 minutes before use. 45,000 cells were seeded onto the Matrigel basement membrane in 200µl of normal medium or treatment and incubated for 40 minutes. The medium was then removed and the membrane was washed five times with 150µl of BSS solution to remove only loosely attached cells. Adherent cells were then fixed in 4% formaldehyde (v/v) in BSS for at least 5 minutes before being stained in 0.5% crystal violet solution (w/v) in distilled water. Adherent cells were then counted under the microscope under x40 objective magnification at random fields. At least three duplicate wells were set up per sample, the entire experiment was repeated three times.

2.6.4 Motility assay (Cytodex beads)

Cellular motility was assessed using a cytodex-2 bead motility assay as described before (Jiang et al., 1995b). Half million cells for each cell line were incubated in 10ml of growth medium containing 100µl of cytodex-2 beads (GE Healthcare, Cardiff, UK) for 3.5 hours to allow the cells to adhere to the beads. The beads were then washed twice in 5ml of normal growth medium to remove non-adherent or dead cells. Following the second wash the beads carrying the cells were resuspended in 1ml of growth medium. 200µl of this solution was then transfered

into a 24 well plate containing a further 800µl of normal medium and incubated overnight. Following incubation any cells that had migrated from the cytodex-2 beads to the surface of the plate were fixed in 4% formaldehyde (v/v) for 5 minutes, stained with 0.5% crystal violet (w/v) and visualised under x40 objective magnification following removal of cytodex-2 beads through several extensive washes with BSS. Several random fields were counted per well and duplicate wells were set up per sample. The entire experimental procedure was repeated three times.

2.6.5 Wounding (Migration) assay

A wounding/migration assay was also used to assess the migratory properties of the prostate cancer cells. This technique has been modified from a previously described method (Jiang et al., 1999).

Cells were grown in a 24 well plate and upon reaching confluence the monolayer of cells was scraped with a 21G needle. The floating cells were washed off gently and 2ml pre-warmed medium contains HEPES buffer was added. After wounding the cells were given 15 minutes to recover before the closure of the wound via the migration of cells was measured. The 24 well plate was placed on a heated plate (Lecia GmbH, Bristol, UK) to maintain a constant temperature of 37°C. The wound was tracked and recorded using a CCD camera attached to a Lecia DM IRB microscope (Lecia GmbH, Bristol, UK) through taking pictures every 15mins over a 90 minute period. The images saved at 0, 15, 30, 45, 60, 75 and 90 minute time

points. Cell migration was then measured using Optimus 6 motion analysis software: the distance between the two wound fronts at 10 random points per incubation time was calculated. The arbitrary values obtained were then converted into μm by multiplying the value by 22.4. The distance that the wound fronts had migrated into the wound at each time point could then be determined by subtracting the distance between the two fronts at any given time point from that at the initial 0 minute experimental start point. The experimental procedure was repeated in triplicate.

2.6.6 ECIS assay

We used the electric cell-substrate impedance sensing (ECIS) system (Applied Biophysics, Inc., Troy, NY) to conduct the attachment and wounding assay. Cells were cultured in 8W1E ECIS arrays (Applied Biophysics), in which each well for cell culture contains a small gold film circular electrode (5 × 10⁻⁴ cm²) and a larger (0.15 cm²) counter electrode. We seeded cells at a density of 70,000 cells *per* well in the arrays (rehydrated using HEPES medium for half an hour before use) in medium with HEPES buffer. The cells were incubated for more than 4 hours to allow attaching. The increased resistance was measured every 5 seconds to show the attachment of cells to the electrode surface. Once the cells fully attached, the monolayer was electrically wounded by applying an elevated voltage pulse with a frequency of 30 kHz, amplitude of 4 V for 10 s.Ddead and detached cells floated off from the small active electrode. Cells surrounding the small active electrode that had not been submitted to the elevated voltage pulse then migrated inward to replace the

cells killed. The impedance showed the attachment of cell to cell. Cell migration was assessed by continuous resistance measurements for upto 30 hours.

2.6.7 Flow cytometric analysis of apoptosis

Prior to undertaking any flow cytometry analysis, the calibration of the flow cytometry was verified using Partec Calibration Beads 3µm (Partec GmbH, Germany). A small sample of beads (1-2 drops) was diluted in 2ml of BSS and run on the machine under standard calibration settings pre-stored on the machine. Correct calibration of the flow cytometer resulted in a main peak at 100 (log 3) for FSC and SSC and a main peak at 100 (log 4) in FL1 – FL3. Once the calibration of the machine had been verified experimental analysis of test samples was conducted.

Apoptosis was assessed in various cell lines using the Vybrant Apoptosis Assay Kit following the provided experimental protocol. The medium was removed from the cells and stored on ice. Cells were washed in EDTA, trypsinised, harvested and placed in a universal container together with the previously removed cellular medium. This suspension was then centrifuged at 1600 RCF to pellet viable as well as dead cells, before counting the cells and resuspending 1 x 10⁶ cells/ml in 1X annexin binding buffer (made through the dilution of the provided 5X annexin binding buffer by distilled water). To each 100μl aliquote of cells, 5μl of the provided FITC annexin V and 1μl of a previously prepared 100μl/ml Propidium Iodide (PI) solution was added. The PI working solution was prepared by diluting the 1mg/ml PI stock

solution provided in 45µl of 1X annexin binding buffer. Annexin V (a 35-36 KD C_a²⁺-dependent phospholipid-binding protein which has high affinity for phosphatidylserine) labelled with a fluorophore can identify apoptotic cells by binding to PS (phosphatidylserine), which is translocated to plasma membrane outer leaflet when apoptosis happens. PI is a red-fluorescent nucleic acid binding dye which permeates through integral membrane to stain dead cell nucleic acids but not the live cells and the apoptotic cells.

Following the addition of FITC annexin V and the PI working solution cells were incubated for 15 minutes at room temperature in the dark. Next 400µl of annexin-binding buffer was then added to the 100µl cell aliquots, mixed gently and stored on ice. The samples were then analysed as soon as possible using flow cytometry, measuring the emission at 530nm (FL-1) and >575nm (FL-3). The cell population will separate into three groups, low fluorescence or live cells, green fluorescence or apoptotic cells and red and green fluorescence of dead cells. Prior to analysis of test samples using flow cytometry, the flow cytometry instrument was configured using unaltered wild type cells to assess background fluorescence and normal, representative cell populations.

2.6.8 Cell cycle analysis

Cells from the culture flasks were collected by trypsinisation and pooled with the cells floating in the medium which contained detached mitotic, apoptotic and dead cells. The cells were then centrifuged and washed twice with cold PBS and resuspended $1x 10^6$ to $1x10^7$ in 0.5ml of PBS. This was followed by the addition of

4.5ml of 70% ethanol at 4°C for more than 2 hours, t he cells were fixed and permeabilized to make them accessible to propidium iodide (PI). After fixation, the cells were then washed with PBS and stained with PI (for DNA staining) by resuspending in a 1ml PI solution containing Triton x 100 (for additionally permeabilization) and RNase A (to inhibit the interference of double-stranded RNA sections).

After 30 mins at room temperature in the dark, the fluorenscence of PI was detected using the flow cytometer and the cell cycle analysis was performed using the FlowMax software package.

2.7 Statistical Analysis

For statistical analysis experiments were repeated three separate times and at least duplicate each time. Results data were then analyzed using the Minitab 14 statistical software package. The statistical comparisons between the test and control cell lines were made using either a Students two tailed t-test if the data were found be normalised and have equal variances or a non-parametric Mann-Whitney test if the data were not normalised.

In all cases, each test cell line was compared to the pEF6 control cell line (cells containing a closed pEF6 plasmid only) as this also confirmed that it was the ribozyme/expression sequence that was responsible for any changes seen and not the pEF6 plasmid itself.

Chapter 3

Aberrant expression of RGMs in cancer cells and tissues

3.1 Introduction

As discussed in Chapter 1, the RGMs (repulsive guidance molecules) are a group of GPI (glycosylphosphatidylinositol)-linked cell-membrane-associated proteins that have recently been described. RGMs has been shown to be two-chain protein bound to the cell membrane through a GPI-anchor and contains other domains as: a signal peptide, an RGD site, a von Willebrand factor (vWF) domain and a hydrophobic region (Monnier *et al.*, 2002; Samad *et al.*, 2005; Samad *et al.*, 2004). RGMs have been shown to be expressed at the central nervous system and peripheral tissues, including heart, liver, lung, skin, kidney and testis, at least in the adult rat. (Babitt *et al.*, 2005; Metzger *et al.*, 2005; Monnier *et al.*, 2002; Niederkofler *et al.*, 2004; Samad *et al.*, 2004; Schmidtmer and Engelkamp, 2004)

RGMA is initially found to mediate repulsive axonal guidance and neural tube closure, while DRAGON (RGMB) contributes to neuronal cell adhesion through homophilic interactions. The *HJV* (*RGMC*) gene is mutated in juvenile hemochromatosis, a disorder of iron overload. Lately, a role of RGMs as co-receptors for bone morphogenetic proteins (BMPs) has been revealed (Samad et al., 2005).

Bone Morphogenic Proteins (BMPs) are oestrogenic factors abundant in bone matrix which play an important role in bone metastasis of cancer. BMPs are predominantly responsible for osteoblast differentiation and bone matrix production and mineralization (Jikko *et al.*, 1999; Li *et al.*, 1996; Sampath *et al.*, 1992). The BMPs are also reported to be related to in vitro growth, apoptosis, adhesion and

migration in breast cancer and prostate cancer (Alarmo and Kallioniemi; Kwon et al.; Ye et al.).

During the bone metastasis, osteoblast differentiation induced by BMPs is mediated mainly via the Smad-signalling pathway, whereas chondrogenic differentiation may be transmitted by Smad-dependent and independent pathways (Fujii *et al.*, 1999). Regulations of cancer cells by BMPs and BMP signalling molecules are also mainly through Smad-dependent pathway, including proliferation, apoptosis and cell aggressiveness. RGMs work as BMP co-receptors which participate in BMP signalling pathway therefore should also be involved in cancer development and progression.

However, the expression of RGMs in cancer remains unclear. To get the first hand data to evaluate the role of RGMs in cancer, the work presented in this chapter examined the expression profile of RGM in tissues and cell lines. The RNA transcript levels were assessed associated with clinical breast cancer patient prognostic indicators.

3.2 Materials and methods

3.2.1 Cell lines

Cell lines were employed for this study as outlined in section 2.1.1. Cells were routinely cultured in DMEM / Ham's F12 with I-Glutamine (PAA Laboratories, Somerset, UK) supplemented with streptomycin, penicillin and 10% foetal bovine serum (PAA Laboratories, Somerset, UK) and incubated at 37.0°C, 5% CO2 and 95% humidity.

3.2.2 Tissues and patients

All the cancer tissues and normal background tissues were collected during the operative procedure and snap-frozen in liquid nitrogen immediately before storage at -80°C until used. The presence of tumour cells in the tissues was verified by a consultant pathologist (ADJ) using H&E staining of frozen sections. All protocols were reviewed and approved by the local ethical committee and all patients gave written informed consent.

3.2.3 Tissue processing and preparation of RNA and cDNA

Tissue samples were homogenized in RNA extraction reagent (TRI reagent, Sigma-Aldrich Ltd, Poole, England, UK) to extract total RNA. The concentration of RNA was determined using a spectrophotometer. 0.5µg RNA was used in a 20µl reverse transcription reaction to generate cDNA using a RT kit (AbGene Laboratories, Essex, England).

3.2.4 Screening of RGM transcripts expression in cancer cell lines using RT-PCR

Primers were designed using the Beacon Designer software (version 2, Biosoft International, Palo Alto, California, USA), to amplify regions of human RGMs that have no significant overlap with other known sequences, with the amplified products spanning over at least one intron, based on sequence accession numbers. PCR products were separated on agarose gel and photographed using a digital camera mounted over a UV transluminator. GAPDH was used as a housekeeping gene. All the primers used were detailed in 2.1.2

3.2.5 Immunohistochemical Staining of RGM in Prostate Specimen

Briefly, frozen prostate tissues were cut into 5µm sections using a cryostat (Leica Microsystems (UK) Ltd., Bucks, UK). Immunohistochemical staining was performed by using specific primary antibodies against RGMA, RGMB and RGMC. This was

based on the method previous described (Martin et al., 2003b). Positive controls were not available as we were unable to obtain tissue sections that had been confirmed to express RGMs. Negative controls were performed.

Statistical analysis

Normally distributed data was analyzed using the two sample T-test while nonnormally distributed data was analyzed using the Mann-Whitney and Kruskal-Wallis tests.

3.3 Results

3.3.1 The expression of RGMs in human tissues and cell lines

To examine the expression of RGMs in both prostate and breast cancer, conventional RT-PCR was employed to screen a variety of human breast cancer and prostate cancer cell lines together with some samples of other cell types and tissues. I found that transcripts of RGMA, B and C were expressed in prostate cancer cell lines (PC-3, DU-145, PZ-HPV-7, PNT1A, PNT2-C2), whereas only RGMB was detectable in some breast cancer cell lines, such as MDA-MB-231, MDA-MB-436, BT-474, BT-482, BT-549 (Fig.3.3.1A). RGMB levels were higher in the breast cancer tissues compared to the normal mammary tissues, whilst RGMA and RGMC showed similar levels in both. (Fig.3.3.1B)

RGMA was widely expressed in prostate cell lines (CAHPV10 and LNCAP plus the five mentioned above) and a range of human cell lines of various origins

including cervical cancer (A431, Hela), Keratinocyte (HaCaT), Colorectal cancer (HT-115), Fibroblast (MRC5), Endothelial (HECV), MDA-MB-435s and normal human polymorphonuclear cells (OMN) from healthy volunteers. The transcript level of RGMA was barely detected in the breast cancer cell lines but was detected in both the normal breast and breast cancer tissues (Fig. 3.3.1B). Additionally, ovary, liver, skin and colorectal tissues showed weak expression of RGMA and none in prostate tissues (Table 3.3.1.1).

In addition to its expression in most prostate cancer cell lines (except for CAHPV10) and most breast cancer cell lines, RGMB was expressed in cervical cancer (Hela, A431), bladder cancer (RT-112, EJ-138), colorectal cancer (HRT18, HT-115), fibroblast (MRC5), and pancreatic cancer cells (PANC1). In lung cancer cell lines (SKMES1, A549) and endothelial cells (HUVEC), RGMB transcript levels were detected but slightly weaker (Fig. 3.3.1A).

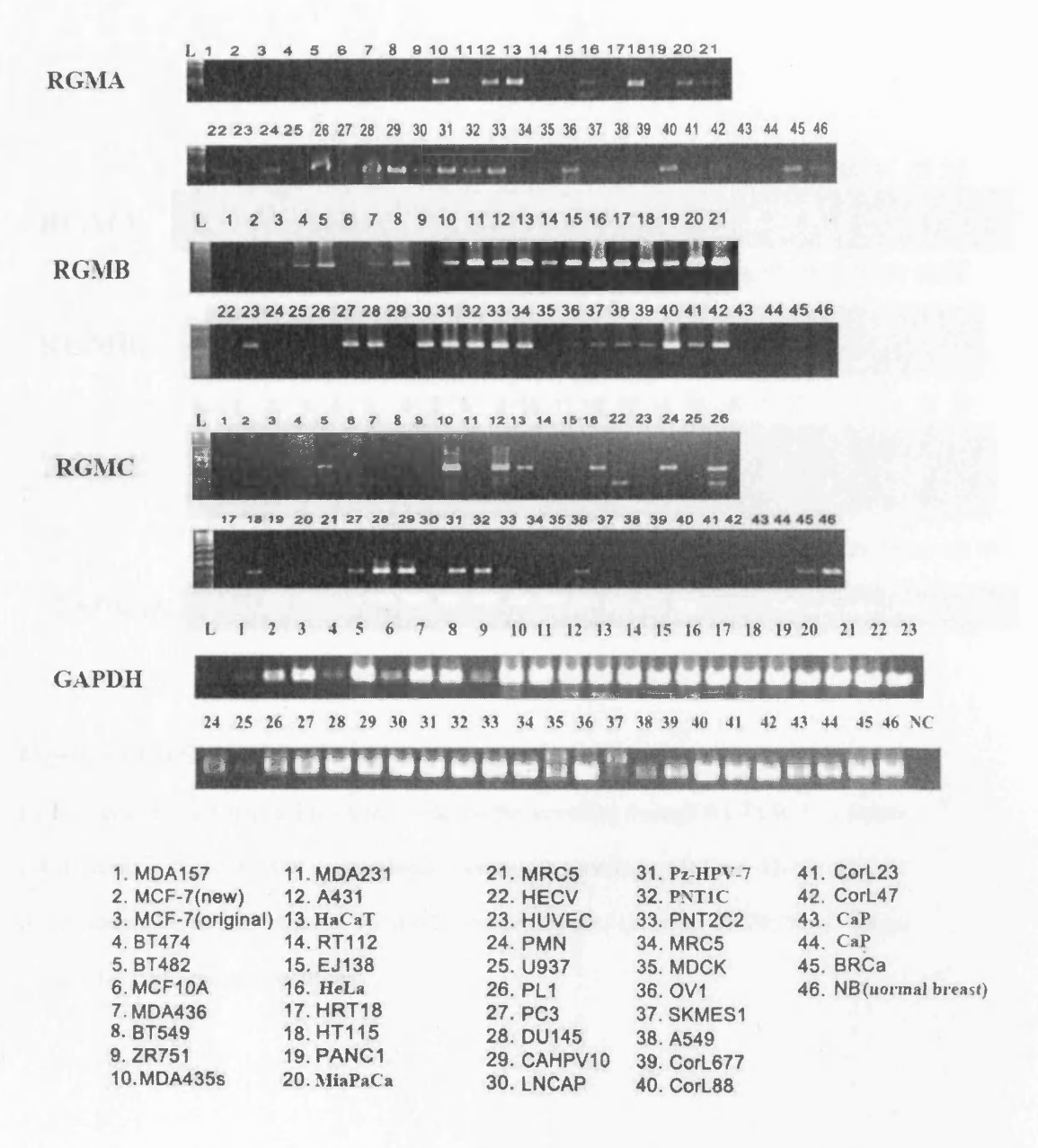


Figure 3.3.1 A Expression of RGM transcripts in cell lines of human origin and human tissues.

RGMA, B and C were found in many cell lines and tissues through RT-PCR.

1-35 and 38 are cell lines and the others are tissues (OV: ovary tissues, Corl: colorectal tissues, CaP: prostate cancer tissues, BRCa: breast cancer tissues, NB: normal breast). The numbers after tissue abbreviation are patients' code.

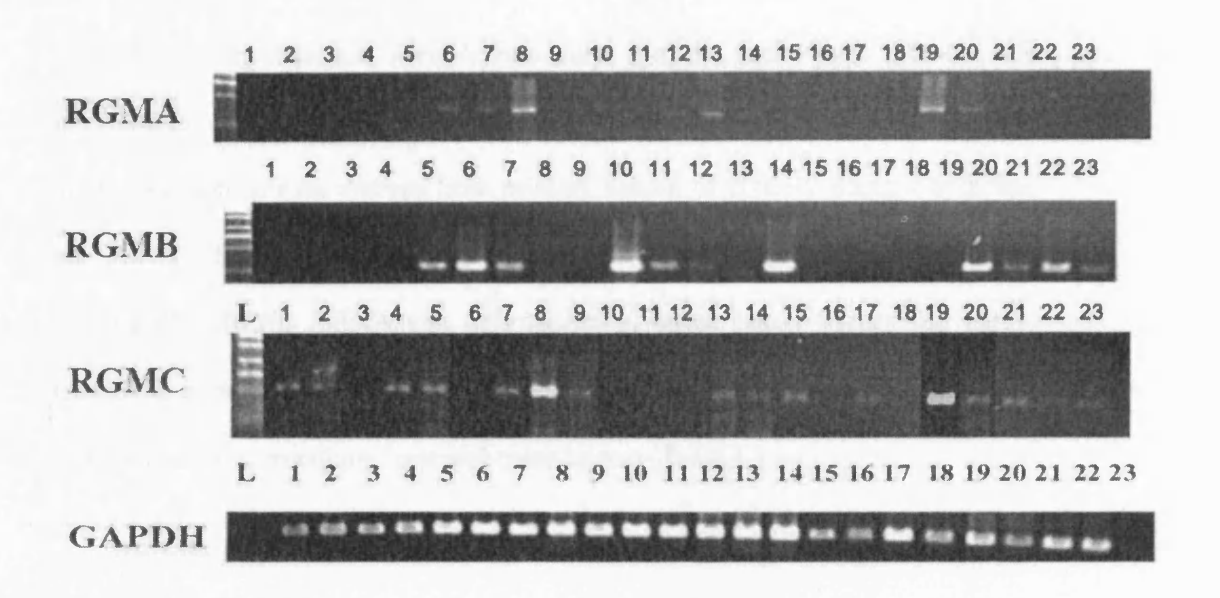


Figure 3.3.1 B Expression of RGM transcripts in human tissues

RGMA, B and C are detected in many tissues in the screening through RT-PCR. L is ladder. 1-4: placenta, 5-7: ovary, 8-9: normal breast tissues, 10: omentum, 11: liver, 12-13: skin, 14: colon cancer, 15: normal mucosa, 16 and 17: miscellaneous, 18: bone, 19-20: breast cancer tissue, 21-23: prostate cancer tissues.

Interestingly, only RGMB was detected in the breast cancer cell lines. Furthermore, I found that RGMB was not detectable in a breast epithelial cell line, MCF10A an immortalised normal mammary epithelial cell lines. RGMB was otherwise found to be expressed by the breast cancer cell lines, including MDA436 and BT-474 which were derived from primary tumour of invasive ductal carcinoma, and MDA-MB-231 isolated from metastasis of invasive ductal carcinoma. Additionally, RGMB mRNA was only shown in breast cancer tissues and hardly detected in normal/background breast tissues. RGMB transcript levels were observed in prostate, ovary, omentum, liver and colon tissues (Table 3.3.1.1).

As with RGMA, RGMC was weakly expressed in breast cancer cell lines. RGMC was detected in most prostate cancer cell lines (extremely weak in PZ-HPV-10 and LNCAP) and other cell lines including MDA-MB-435s, cervical cancer (A431, Hela), leukocyte (PMN), keratinocyte (HaCaT) and colorectal cancer (HT-115). RGMC mRNA was detected in both normal breast and cancer tissues, with no obvious difference in expression levels. In other tissues, there was a visible RGMC level in prostate as well as placenta, ovary and skin (Table 3.3.1.1).

Notably, the RGMA, B and C all have expression in cell line MDA435s. However, whether the MDA435s is a cell line of breast cancer or melanoma remains controversial.

Table 3.3.1.1 RGMs expression detected in different tissues

RGMs	Tissue types with RGM transcript detected	
RGMA	breast, ovary, liver, skin, colon	
RGMB	breast, prostate, ovary, omentum, liver, colon	
RGMC	breast, prostate, placenta, ovary, skin	

In summary, in the human tissues tested in this study, RGMA was found in both breast cancer and normal/background tissues but not in breast cancer cell lines; whilst RGMA was detected in prostate cancer cell line but not prostate tissues in the screening (Table 3.3.1.2). RGMB was shown in both breast (cancer) and prostate tissues and cell lines. Similar to the pattern of RGMA, RGMC was not detected in breast cancer cell lines but in breast tissues, however, it was found in both prostate tissues and prostate cancer cell lines.

Table 3.3.1.2 The expression of RGMs in breast and prostate tissue and cell lines

RGMs\Tissue	Normal breast	Breast cancer	Prostate
RGMA	+	+	
RGMB		+	+
RGMC	+	+	+

Cell line	Breast cancer	Prostate cancer
RGMA		+
RGMB	+	+
RGMC		+

3.3.2 The expression of RGMs in prostate tissues

To further investigate the expression of RGMs in prostate tissues, we examined the protein levels of all three RGMs using immunohistochemistry. Nineteen prostate tissue samples were used in this study. The left panel displays the representative sample with less aggressiveness which had a Gleason score of 6 (Fig 3.3.2). The right panel shows a more aggressive sample of Gleason score 8 (≥7). The immunochemical staining of RGMC protein revealed stronger staining in prostate cancer cells compared to prostate epithelial cells (Fig 3.3.2 C). As shown in Fig 3.3.2 C, the RGM protein was mainly confined to the cytoplasm of cancer cells and some of the mesenchymal cells on the periphery of the tumour area.

The similar pattern was shown in the IHC staining of RGMB. The RGMB proteins were subtly stained in the prostate cancer cells compared to the normal cells. However, RGMA showed little staining in both the normal prostate and the prostate cancer cells.

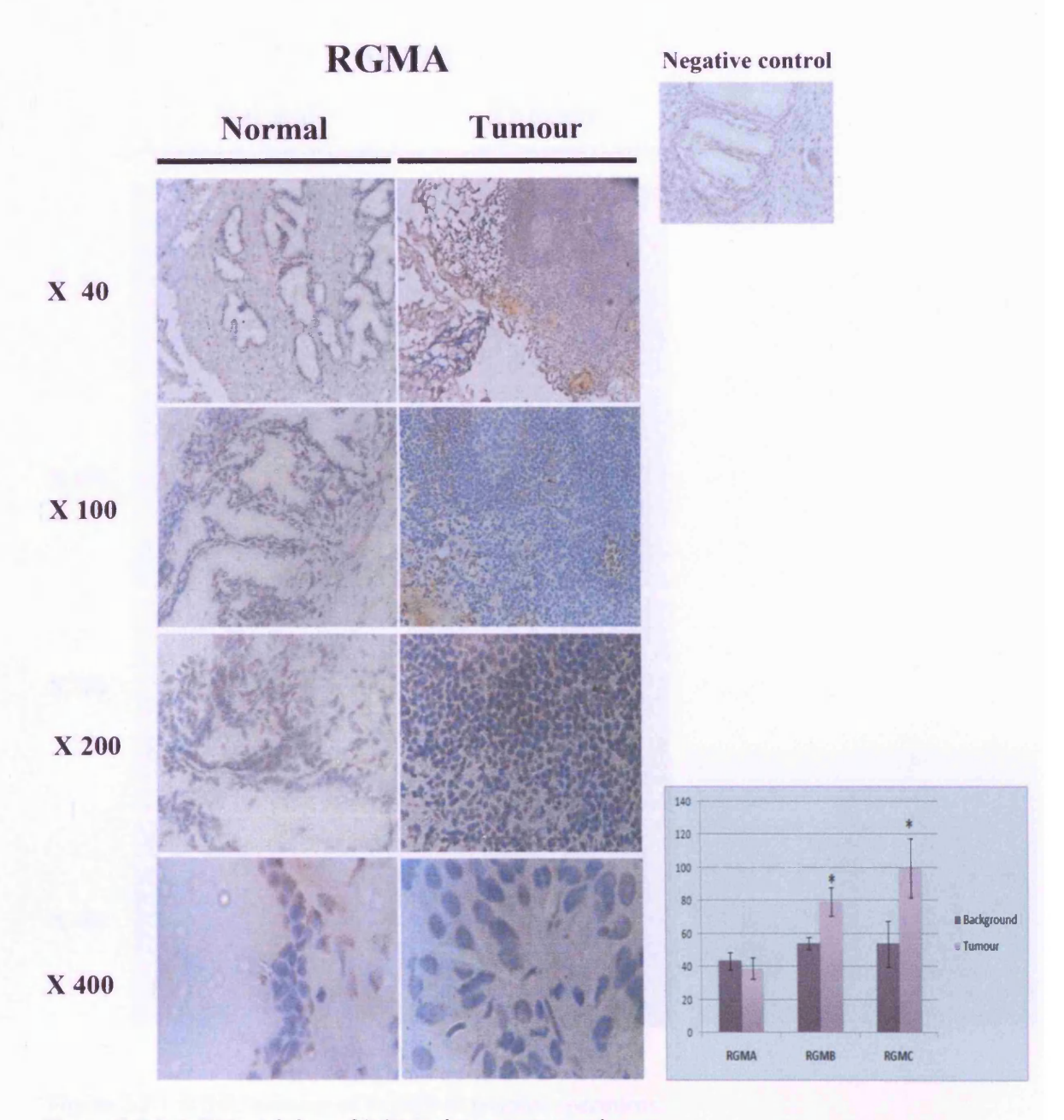


Figure 3.3.2 A IHC staining of RGMA in prostate specimens.

There was no significant staining of RGMA protein by IHC in the normal (left panel) and tumour (right panel) prostate specimens. The graph on the right shows the semi-quantification of IHC staining of RGMA, RGMB (Figure 3.3.2B) and RGMC (Figure 3.3.2C).

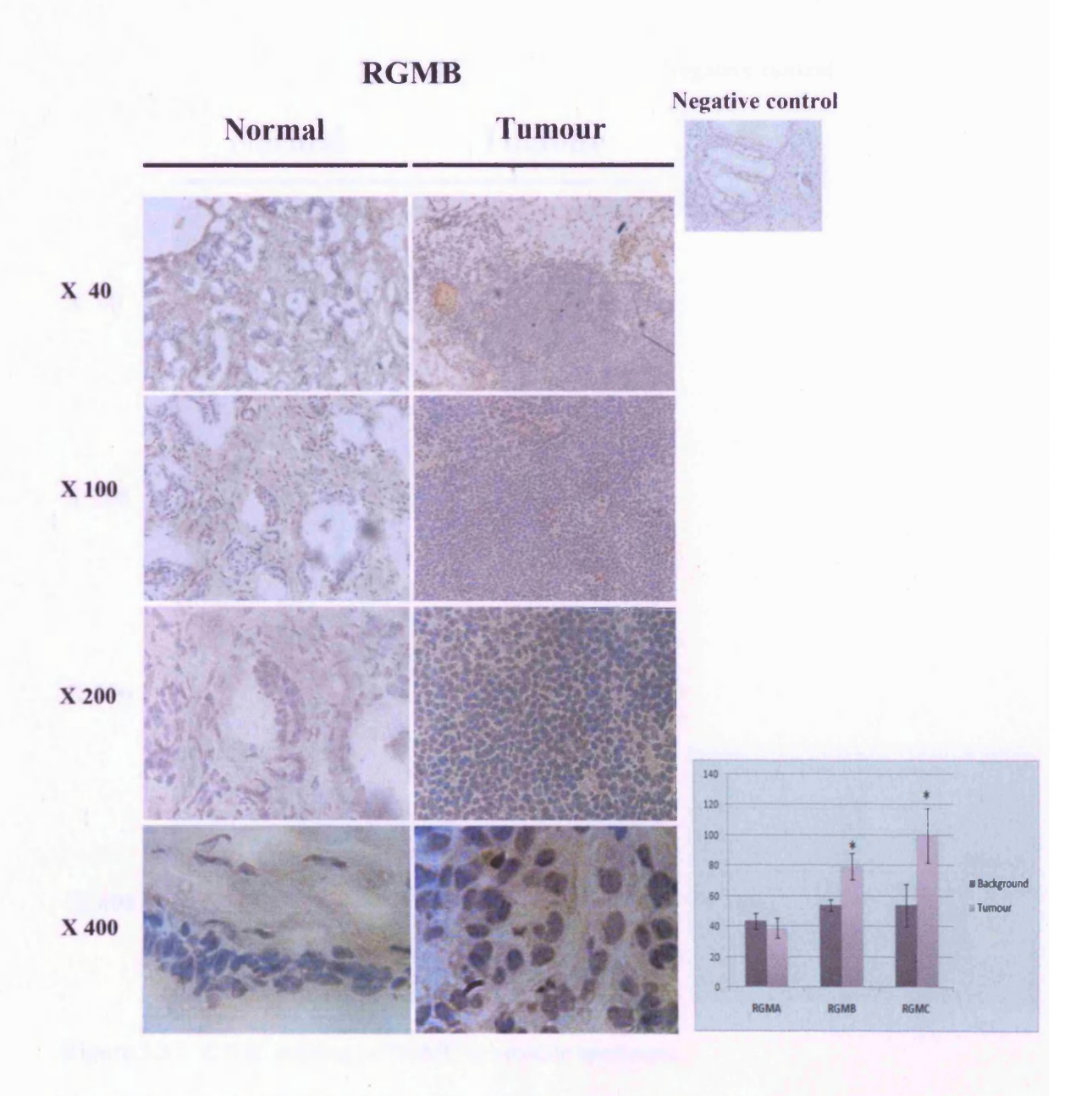


Figure 3.3.2 B IHC staining of RGMB in prostate specimens.

RGMB showed subtle staining in the prostate tumour tissues (right) compared to no staining in the background tissues (left). The staining of RGMB is significantly higher in tumour tissues shown by the semi-quantification of IHC (shown on the right bottom).

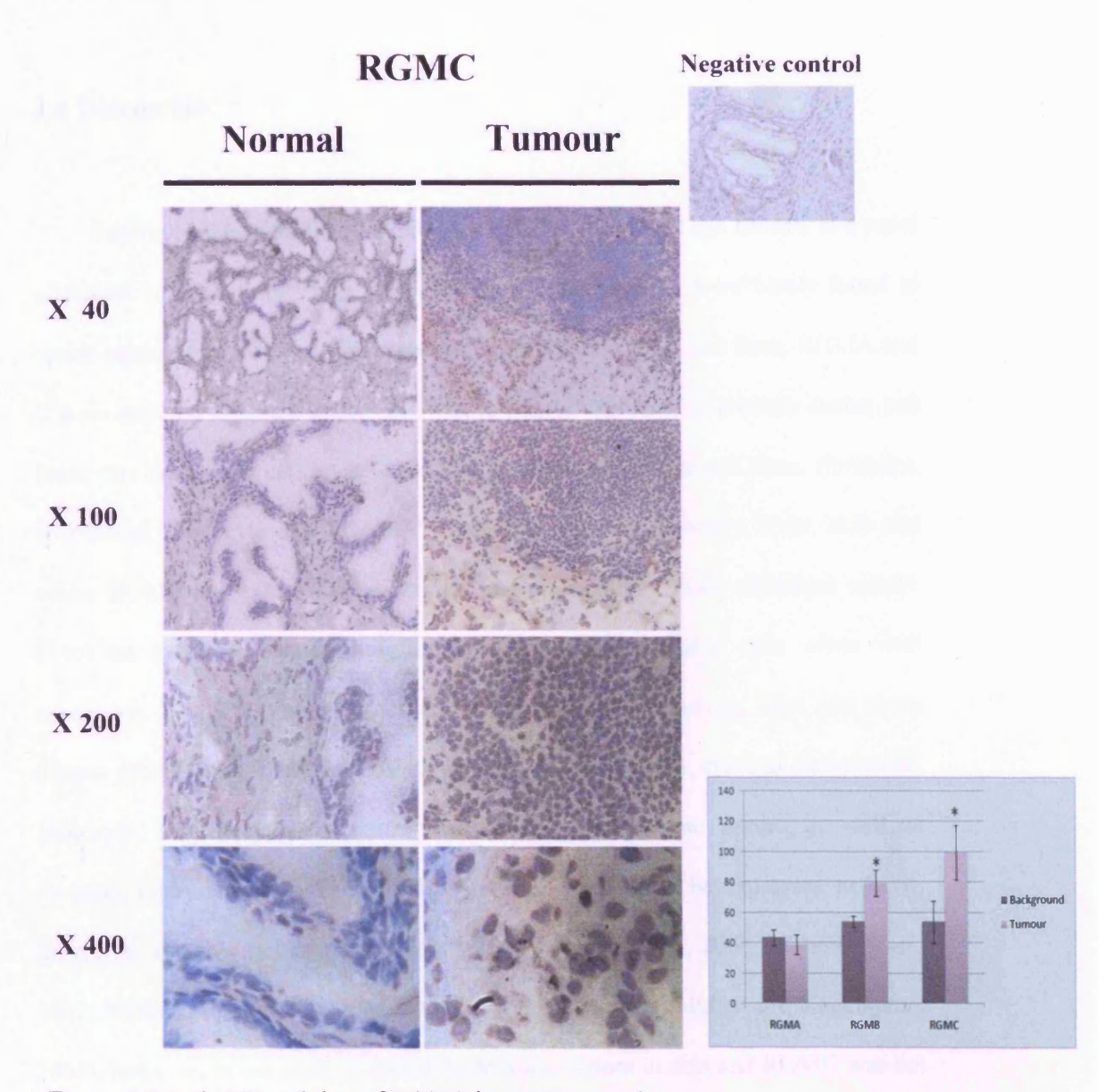


Figure 3.3.2 C IHC staining of RGMC in prostate specimens.

The staining of RGMC protein is slightly higher in the prostate tumour tissues (right) compared to the normal tissues (left) shown by the pictures. The staining of RGMC was mainly confined in the cytoplasm and the marginal ground (X 400 magnification). The staining of RGMC is significantly higher in tumour tissues shown by the semi-quantification of IHC (shown on the right bottom).

3.4 Discussion:

Initially, I screened for the expression of RGMA, RGMB and RGMC in a panel of tissues and cell lines using RT-PCR. RGMA and RGMC were barely found in breast cancer cells. Although no detection in the breast cancer cell lines, RGMA and C were detected in breast tissues. RGMA is widely expressed in prostate cancer cell lines, cervical cancer cell lines, keratinocyte, colorectal cancer cell lines, fibroblast, endothelial, leukocyte and MDA435s and tissues including ovary, liver, skin and colon. RGMB has expression in cervical cancer, bladder cancer, colorectal cancer, fibroblast, pancreas cancer, lung cancer cells and endothelial cells while with expression in breast cancer tissues and prostate, ovary, omentum, liver and colon tissues. RGMC was found in prostate cancer cells, MDA435s, cervical cancer cells, leukocyte, keratinocyte, colorectal cancer cells and prostate tissues as well as placenta, ovary and skin. The RGMs have been reported to be expressed in heart, lung, liver and skin before (Babitt et al., 2005; Metzger et al., 2005; Monnier et al., 2002; Niederkofler et al., 2004; Samad et al., 2004; Schmidtmer and Engelkamp, 2004), however, in our study, I found RGMB was absent in skin and RGMC was not detected in liver in contrast to all the three members: RGMA, RGMB and RGMC.

RGMA was expressed in all seven prostate cell lines (CAHPV10, Hz-HPV-7, PC-3, DU-145, Pz-HPV-7, PNT1A and PNT2-C2). The seven prostate cell lines used in this study represent different clinical characteristics of prostate cancer according to their origin. Pz-HPV-7, PNT1A and PNT2-C2 are immortalised prostate epithelial cell lines. PC-3, DU-145, LNCAP and CAHPV10 are prostate carcinomas amongst

which CAHPV10 is derived from a primary tumour and the other three from various metastatic sites. PC-3, DU-145 and LNCAP have been widely regarded as more aggressive in phenotype than CAHPV10 cells. Among these three aggressive prostate cancer cell lines, LNCAP is androgen sensitive, whilst PC-3 and DU-145 are androgen insensitive. These cell lines have been used as different models for *in vitro* prostate cancer research for decades and as such are well characterised. RGMA has higher levels of expression in the less aggressive cell line CAHPV10, compared to the more aggressive PC-3, DU145 and LNCAP cell lines. This is contrast to the expression of RGMB which is absent in CAPHV10 cells. RGMC was expressed in PC-3, DU-145 and CAHPV10 cells, and absent in LNCAP cells.

In prostate tissues, RGMB and RGMC transcript levels were detected during tissue screening and showed subtle staining of protein in prostate cancer tissue sections, compared with normal prostate specimens (using IHC staining). Although RGMA mRNA was seen in prostate cancer cell lines, it was difficult to detect in tissues and the protein level of RGMA is also weaker in the prostate specimens than the other RGMs. The expression pattern of RGMs thus remains inclusive and the role of RGMs played in prostate cancer warrants further investigation.

Compared to the epithelial cell line (MCF10A), MDA436, BT-474 and MDA-MB-231 are more aggressive cell lines derived from breast carcinoma, with the MDA-MB-231 being most aggressive which is isolated from metastasis. In breast cancer, RGMB mRNA level was unique in breast cancer cell lines. Moreover, the mRNA level of RGMB observed from tissue screening was higher in breast cancer tissue, compared to normal/background tissues. However, RGMA and RGMC were

detected in breast cancer tissues but not in cell lines. This probably reflects the nature of diversity and aberration of RGM expression in cancer cells. To further investigate the association of RGMs with breast cancer, the expression of RGMs in breast cancer will be further elucidated in the following chapter.

Chapter 4

Expression of RGMs in breast cancer and their association with characteristics of the disease

4.1 Introduction

As described in the previous chapter, RGMA, B and C were found to be widely expressed in many cancer cell lines and tissues. To reveal the role of RGMs in breast cancer, we have already examined the mRNA expression of RGMs in breast cancer cell lines and tissues (Chapter 3). RGMA and RGMC were not detected in breast cancer cells during screening. Although no detection in the cell lines, RGMA and C were shown in breast tissues. Only the RGMB mRNA level was detected in breast cancer cell lines, and higher in more aggressive cell lines. Moreover, the mRNA level of RGMB observed from tissue screening was higher in breast cancer tissue, compared to normal/background tissues. In order to further investigate the RGMs expression in breast cancer, the protein levels of RGMs were examined in breast tissues using immunohistochemical staining.

Furthermore, the transcript level of RGMs was also assessed with clinical prognosis of breast cancer. A panel of breast tissues from a cohort of patients with a median followup of 120 months was determined in this study. The transcript levels of RGMA, B and C were determined in breast cancer and normal/background tissues and analyzed against predicted prognosis of the patients, using the Nottingham Prognostic Index (NPI), Tumour Nodal Metastasis (TNM) staging, tumour grade and survival status (clinical outcome). The RGMs have shown their interesting roles in breast cancer according to these analyses related to clinical data.

4.2 Materials and methods

4.2.1 Tissues and patients

All the cancer tissues and normal background tissues were collected during the operative procedure and snap-frozen in liquid nitrogen immediately before storage at -80°C until used. Patients were followed routinely in the clinic and the median followup period for the study cohort was 120 months (last followup June 2004). The presence of tumour cells in the tissues was verified by a consultant pathologist (ADJ) using H&E staining of frozen sections. All protocols were reviewed and approved by the local ethical committee and all patients gave written informed consent.

4.2.2 Determination of RGM transcripts in breast tissues using quantitative PCR

Tissue samples were homogenized in RNA extraction reagent to extract total RNA and 0.5μg RNA was used to generate cDNA using a RT kit. Real time quantitative PCR (RT-QPCR) was carried out to determine the levels of RGMs' transcripts in the breast cancer cohort. The transcript level was subsequently analyzed against clinical data. The assay was based on the Amplifuor technology and primers were designed by Beacon Designer software as we previous reported (Jiang et al., 2005a; Parr et al., 2004). Cytokeratin-19 (CK19) was used as internal control. The protocol and primers used for RGMs quantification were listed in section 2.1.2 and 2.3.5.

4.2.3 Immunohistochemical Staining of RGM in Breast Specimen

Immunohistochemical staining was performed by using specific primary antibodies against RGMA, RGMB and RGMC on frozen breast tissues. This was described in chapter 3 and based on the method previous reported (Martin et al., 2003b). Positive controls were not available as we were unable to obtain tissue sections that had been confirmed to express RGMs. Negative controls were performed.

Statistical analysis

Normally distributed data was analyzed using the two sample T-test while non-normally distributed data was analyzed using the Mann-Whitney and Kruskal-Wallis tests.

4.3 Results

4.3.1 The expression levels of RGMs examined in breast tissues and normal tissues

Protein expression of RGMA, RGMB and RGMC was examined in normal/background and cancer tissues using immunohistochemical staining.

Although RGMB was detected in breast cancer tissues but not in normal breast tissues, the staining of RGMA, B and C protein in the breast cancer tissues did not

differ from that of normal tissues (Fig.4.3.1 A, B and C). Only RGMC are shown some staining in the cytoplasmic region of breast cancer cells, however the staining was weak. Twenty three breast specimens were examined in this study, whilst two of them were normal breast tissues. The representative images were shown in figure-4.3.1. The transcript expression level of RGMs was also determined using a panel of breast tissues. Quantified using Q-PCR, with a median patient followed up of 120 months.

The details of the patients used in this experiment were listed in the tables below (Table 4.3.1). Where insufficient sample quantities were available for the reaction or the sample was invalid, the data was eliminated before analysis took place. Consistent with the protein level shown in tissue screening, the transcript levels of RGMB was significantly higher in patients with breast cancer (p=0.038), as compared to normal/background tissues (Fig.4.3.2.1 B1). A similar trend was also seen in the examination of RGMA level in normal (Mean±SEM 12729±7850) and tumour (Mean±SEM 18223±5504) tissues (Fig.4.3.2.1 A1). However, RGMA and RGMC didn't show significant differences (p value is 0.57 and 0.22 respectively), in the comparison between normal and cancer tissues (Fig.4.3.2.1 A1 and C1).

RGMA

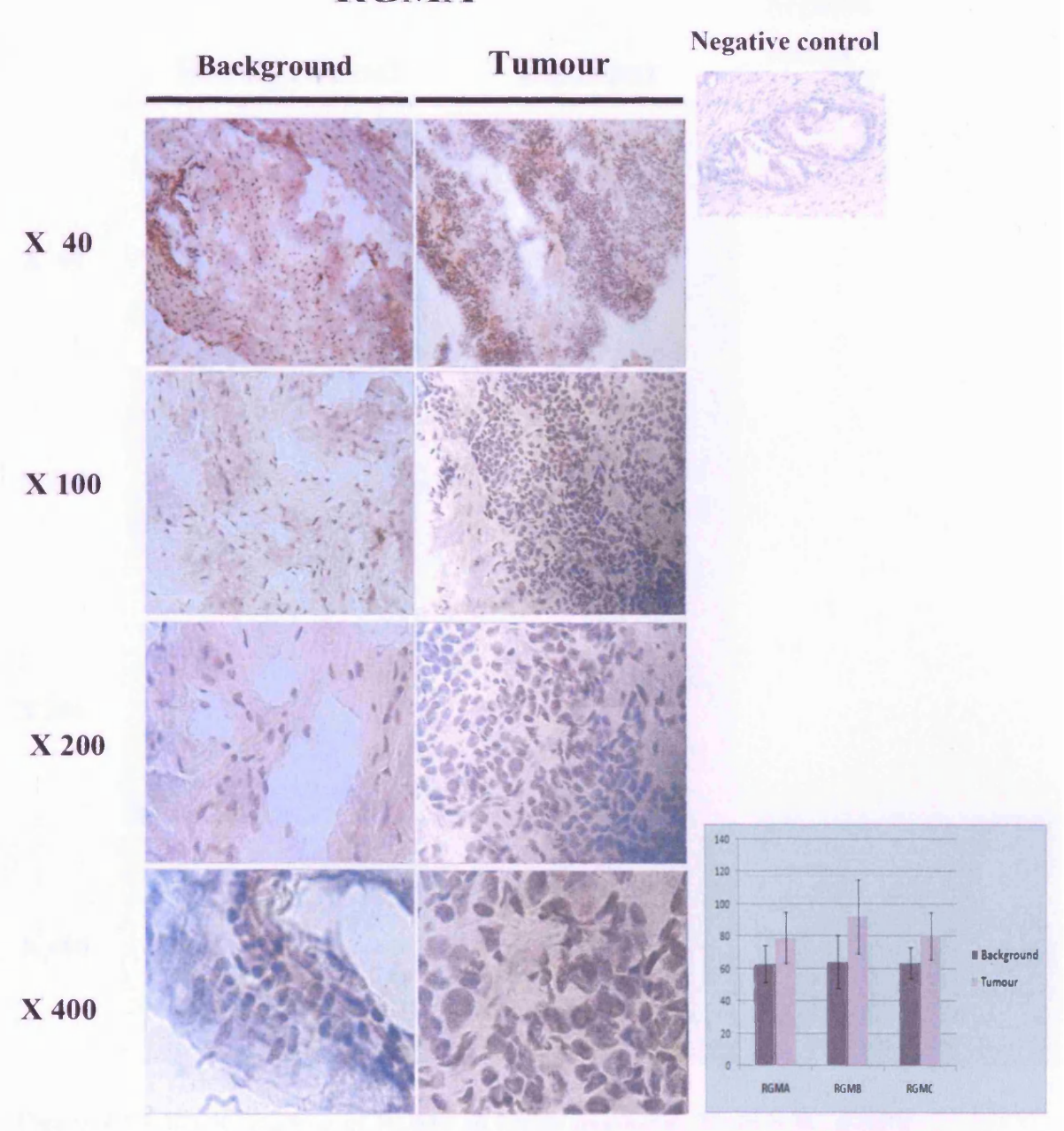


Figure 4.3.1 A IHC staining of RGMA in breast specimens. The left panel shows the breast tissues with a low aggressive nature and the right panel shows breast cancer tissues with high malignity. There is no significant difference in the staining of RGMA proteins between the breast cancer tissues and background tissues as the graph shown on the right displayed the semi-quantification of IHC staining.

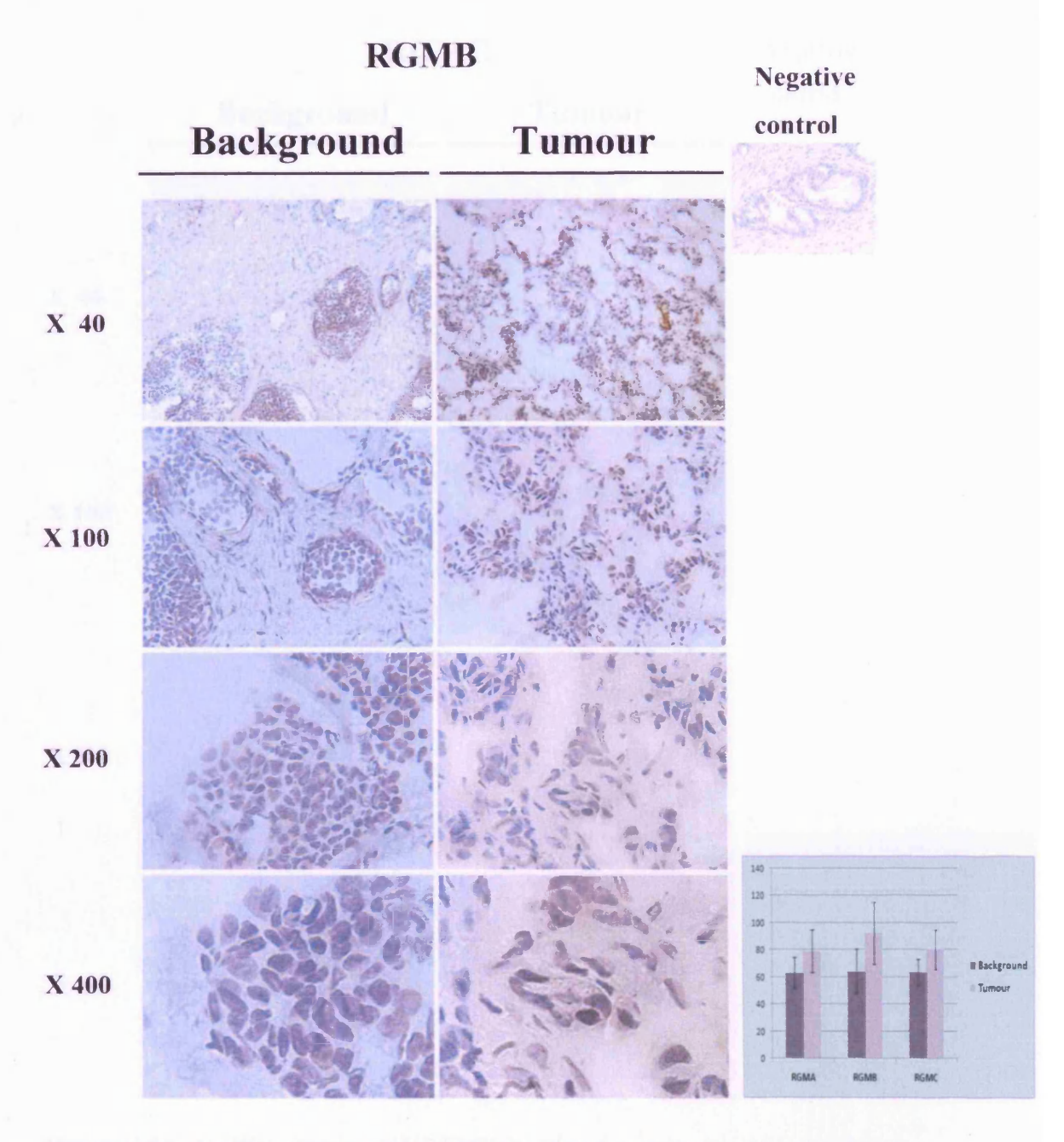


Figure 4.3.1 B IHC staining of RGMB in breast specimens. There is no specific staining of RGMB proteins shown in the breast cancer tissues or background tissues. The graph on the right shows the semi-quantification of IHC which also indicated non-significant differences.

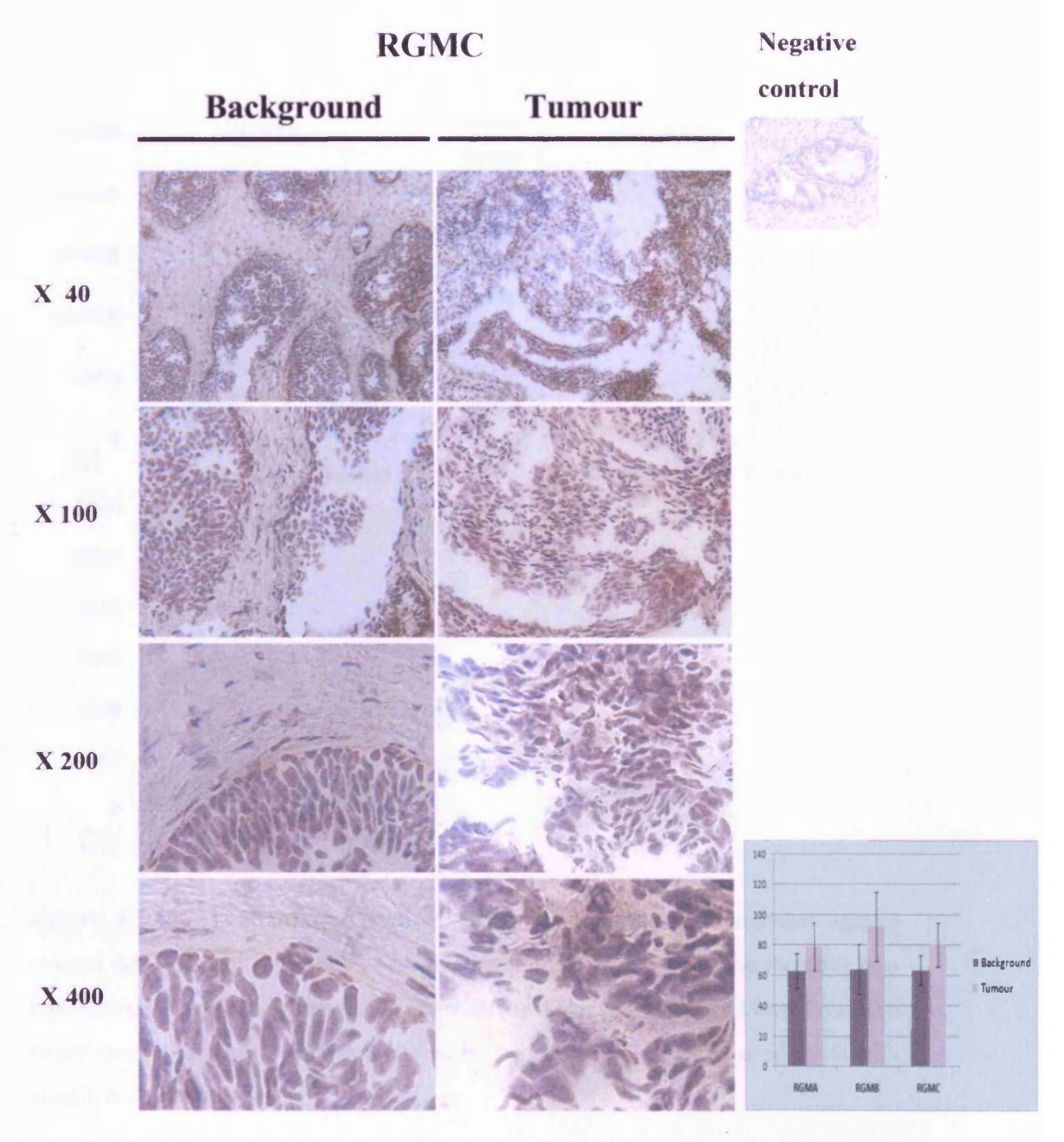


Figure 4.3.1 C IHC staining of RGMC in breast specimens. No significant differences in RGMC staining were seen between breast cancer tissues and background tissues. The graph on the right shows the semi-quantification of IHC staining and also indicates non-significant differences.

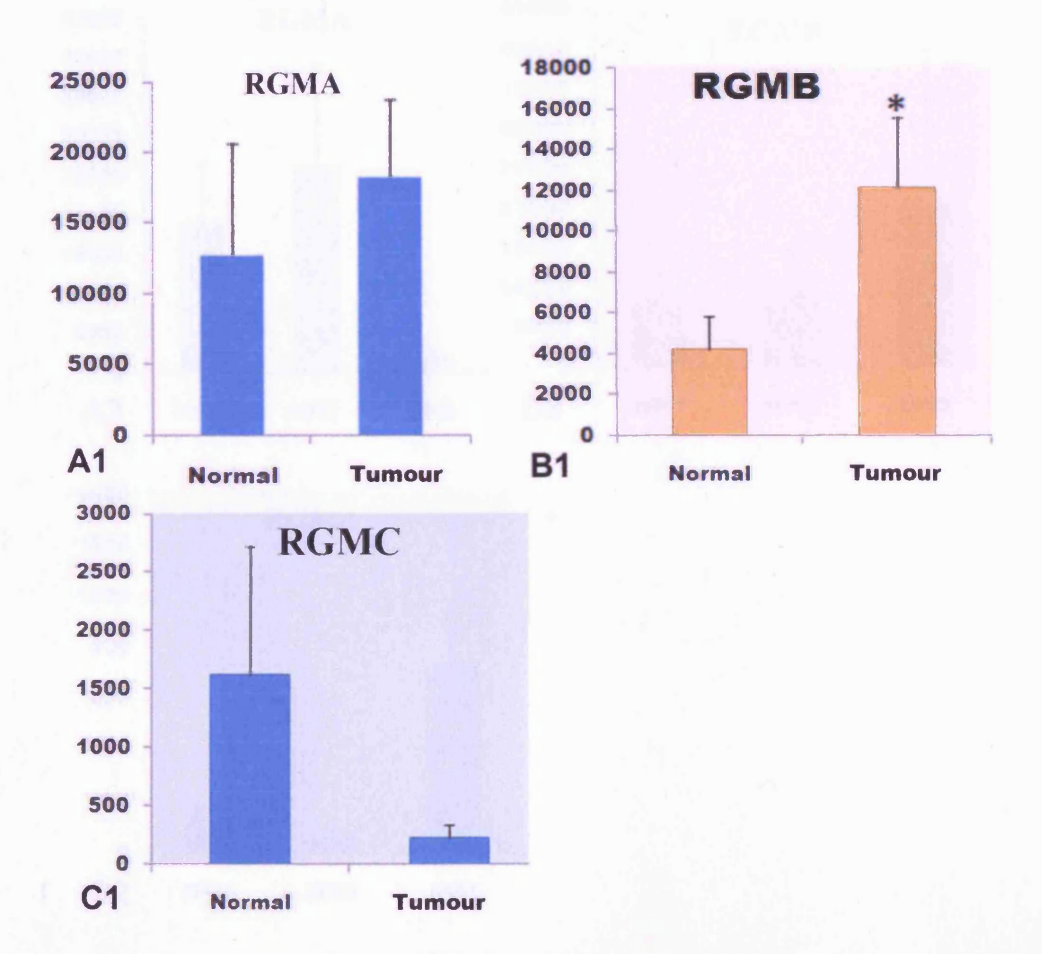


Figure 4.3.2.1 The transcript level of RGMs in breast cohort analyzed against clinical data. The graphs show the mean copy number of the genes and the error bars represent the SE Mean of individual experiments. Data was calculated based on three experiments performed independently and a two sample T-test was used to identify significance levels.

A1: There is a decreased trend of transcript level of RGMA in normal breast tissues (Mean copy number±SE 12729±7850) compared to breast cancer tissues (18223±5504), although it's not significant (p=0.57).

B1: The transcript level of RGMB was significantly higher in patients with breast cancer (n=94), compared to the normal ones (n=29). $(5381\pm2321 \text{ vs } 20660\pm7055, P=0.043)$

C1: RGMC transcript level was higher in normal breast tissues (1616±1110) compared to cancer tissues (220±111), though P is not significant (0.22).

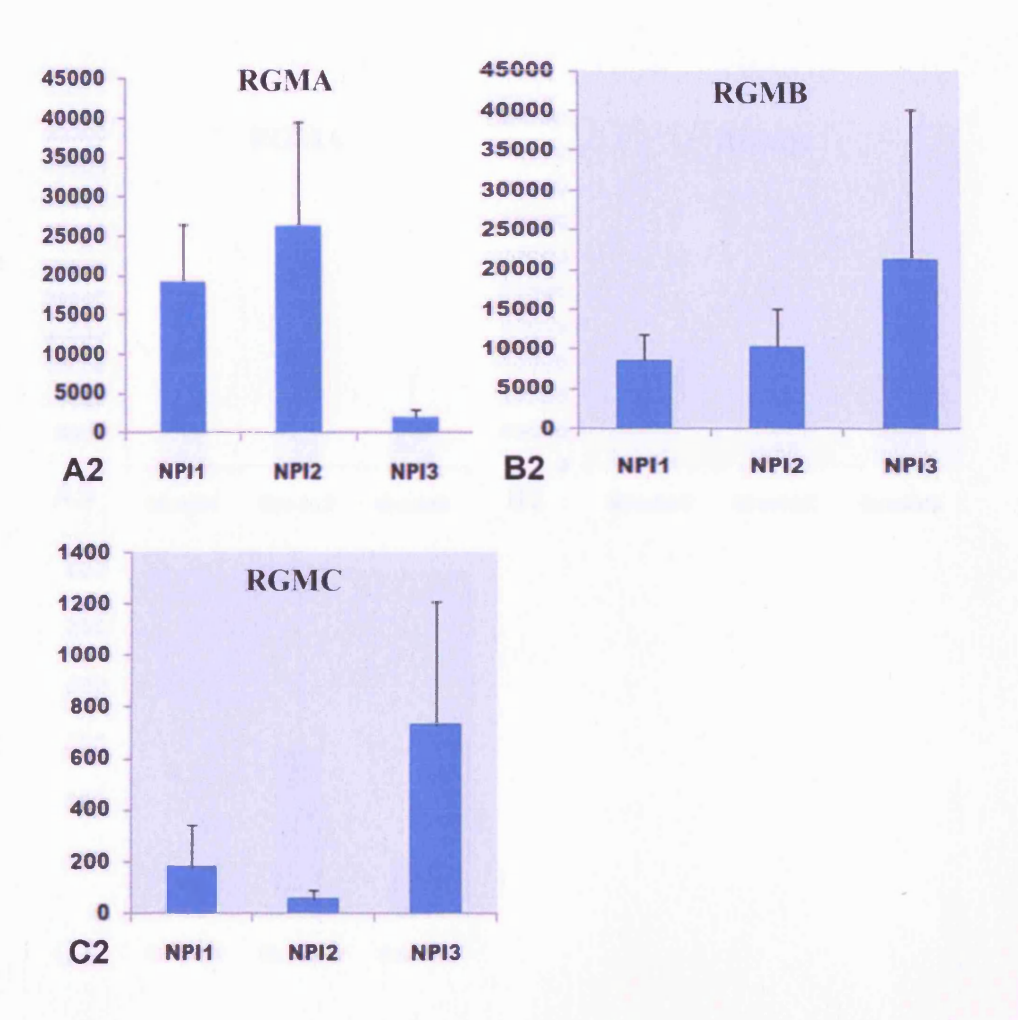


Figure 4.3.2.2 The transcript level of RGM in breast cohort analyzed against NPI

The graphs show the mean copy number of the genes and the error bars represent the SE Mean of individual experiments. Data was calculated based on three experiments performed independently and a two sample T-test was used to identify significance levels.

A2: The expression pattern of RGMA in data related to NPI was not definitive.

B2: The patients with good prognosis group had a trend of lower levels of RGMB (Mean \pm SEM 8602 \pm 3179 for NPI1), compared to that with moderate (10325 \pm 4678, p=0.76) and poor (21245 \pm 18926, p=0.52) prognosis, however, this is not significant.

C2: There was no defenitive pattern shown in the NPI data associated with RGMC transcript level.

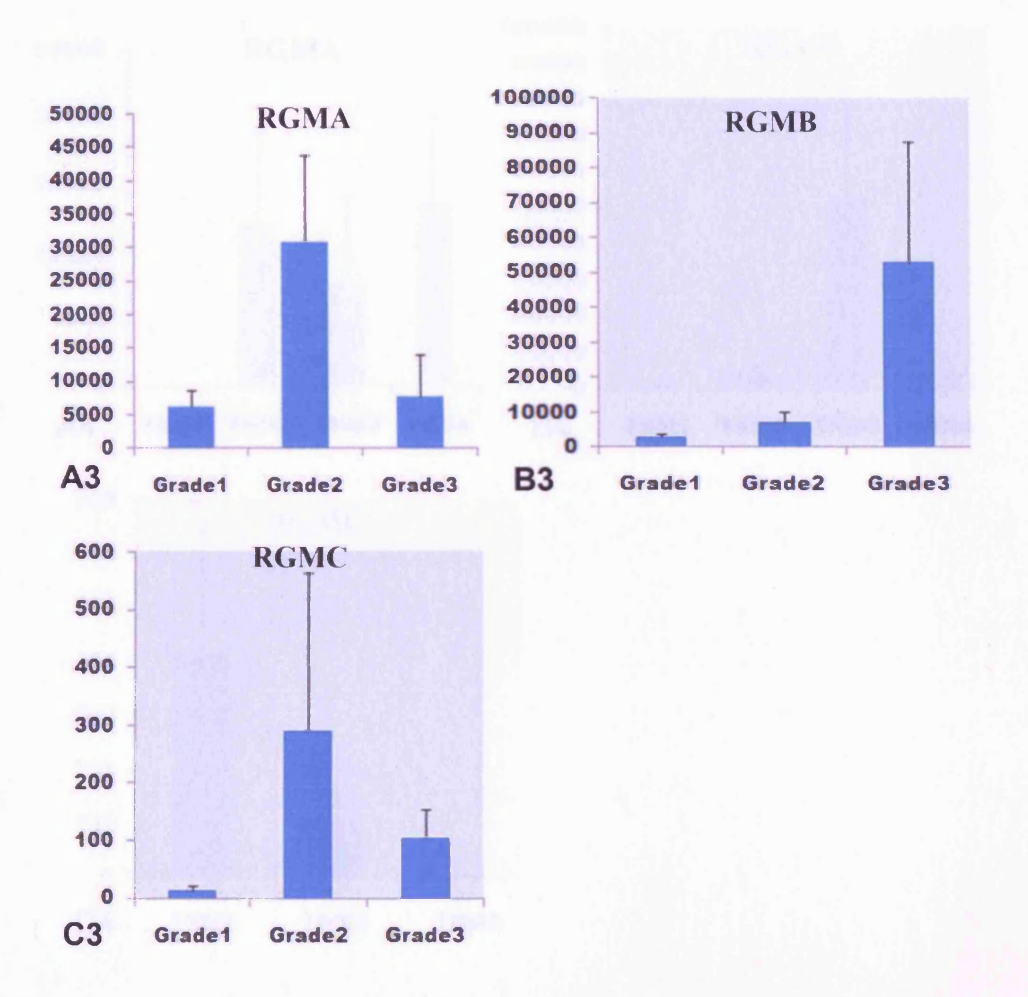


Figure 4.3.2.3 The transcript level of RGMs in breast cohort analyzed against tumour grade

The graphs showed the mean copy number of the genes and the error bars represented the SE Mean of individual experiments. Data was calculated based on three experiments performed independently and a two sample T-test was used to identify significance levels.

A3: There was no trend in expression pattern of RGMA related to tumour grade.

B3: The transcript level of RGMB was higher in patients of tumour grade 3 (52647 ± 34745), compared to tumour grade 1 (2831 ± 1090) and tumour grade 2 (7050 ± 3298), although p value is not significant (p=0.21 and 0.25).

C3: There was no specific pattern shown in the tumour grade data.

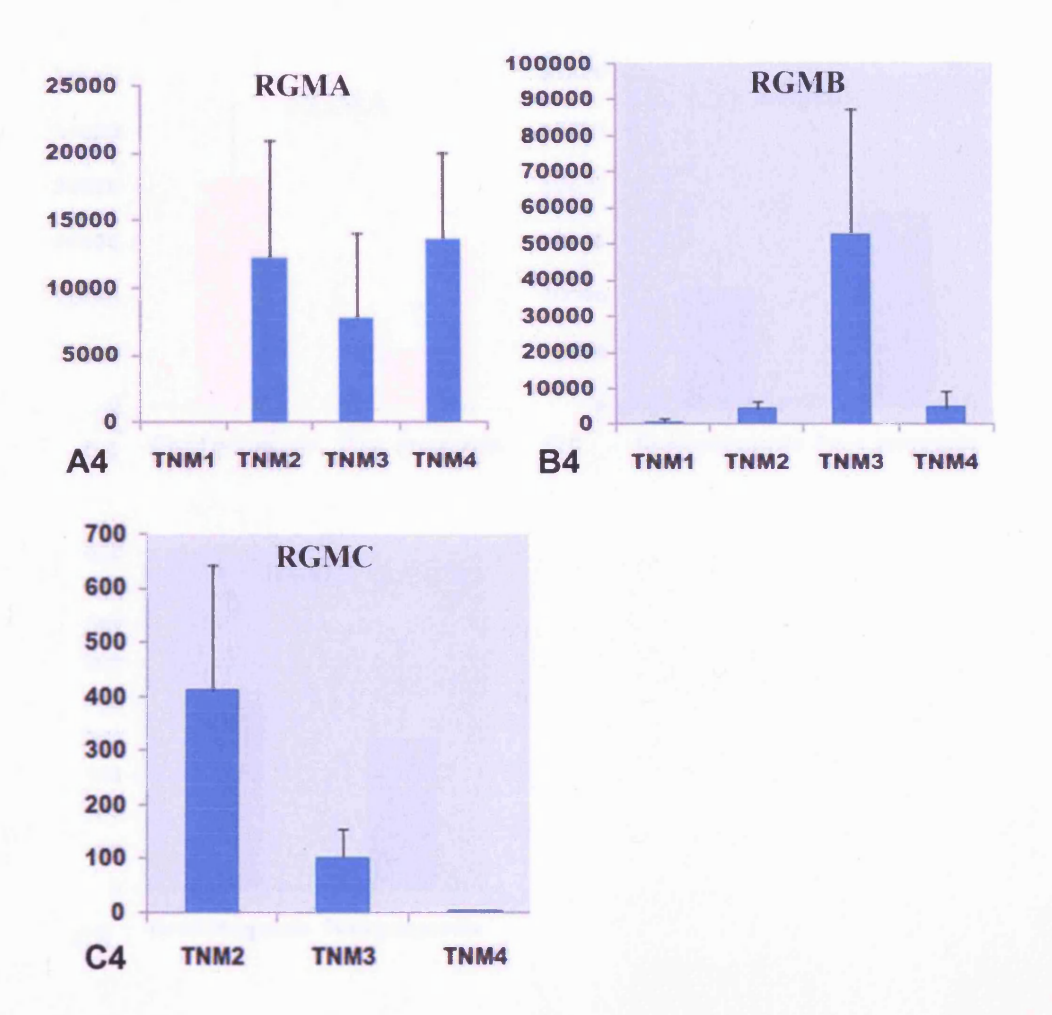


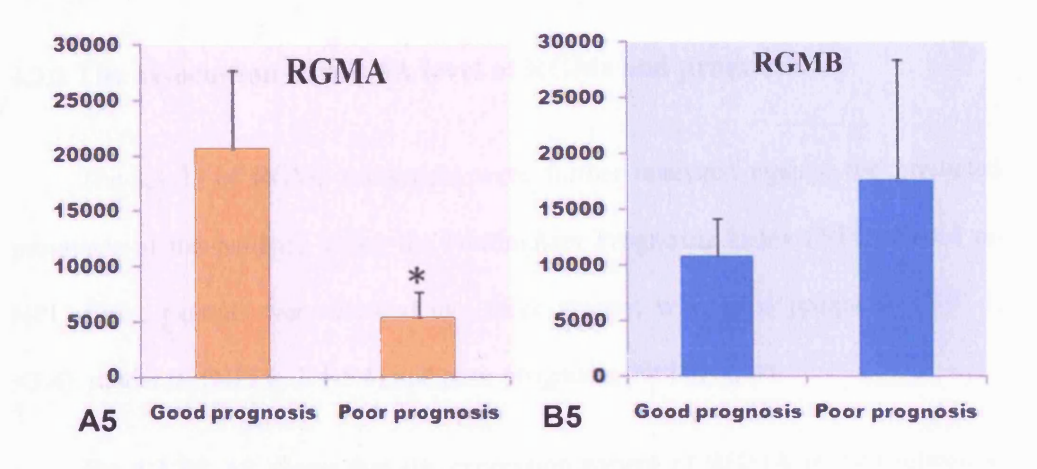
Figure 4.3.2.4 The transcript level of RGMs in breast cohort analyzed against TNM stages

The graphs showed the mean copy number of the genes and the error bars represented the SE Mean of individual experiments.

A4: The RGMA transcript level in the TNM stage 1 was (Mean \pm SE 0.508 \pm 0.292), the stage 2 was (12253 \pm 8626), stage 3 was (7750 \pm 6263) and stage 4 was (13635 \pm 6384).

B4: Even though the transcript level of RGMB was highest in the patients with TNM stage 3, it was not significant when compared with any TNM stages. (as p=0.12 when comparing with TNM1)

C4: The RGMC had decreased levels in the increased TNM stages, however, the TNM1 data was absent and all the p values were not significant. (p=0.2 for TNM2 vs TNM3, p=0.084 for TNM2 vs TNM4 and p=0.097 for TNM3 vs TNM4)



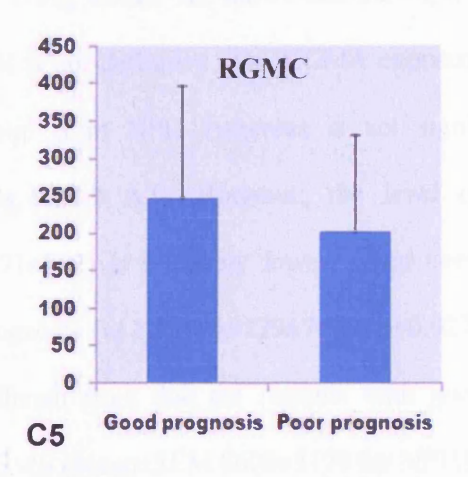


Figure 4.3.2.5 The transcript level of RGMB in breast cohort analyzed against clinical outcome.

A5: The transcript level of RGMA was significantly lower in breast cancer patients with poor prognosis (n=27) (Survival statues 2/3/4), compared to good prognosis (Survival statues 1/2 Disease free) (n=73). (5381±2321 vs 20660±7055, P=0.043)

B5: The transcript level of RGMB showed no significant difference, although it was lower in patients with good clinical prognosis (10857±3364) than poor clinical prognosis (17642±10778)(p=0.55).

C5: There was no obvious trend shown in the data of clinical prognosis (outcome), with similar expression level in patients with good prognosis (245 ± 153) and poor prognosis (201 ± 132).

4.3.2 The association of mRNA level of RGMs and prognosis

The levels of RGMs transcripts were further analyzed against the predicted prognosis of the patients, using the Nottingham Prognostic Index (NPI). Based on NPI scores, patients were divided into three groups; with good prognosis (NPI 1, <3.4), moderate (NPI 2, 3.4-5.4) and poor prognosis (NPI 3, >5.4).

Fig 4.3.2.2 A2 shows that the expression pattern of RGMA in data related to NPI is not definitive. The RGMA expression was increased in the patients of NPI2 group from NPI1 (whereas is not significant, p=0.64) but decreased in NPI3 (Fig.4.3.2.2 A2). However, the level of RGMA with poor prognosis (NPI3: 2071±882) is relatively lower, when compared to those with good and moderate prognosis (vs NPI1: 19129±7439, p=0.027) (vs NPI2: 26324±13149, p=0.075). It is different from that the patients with good prognosis group have lower levels of RGMB (Mean±SEM 8602±3179 for NPI1), compared to that with moderate and poor prognosis: 10325±4678 of NPI2 group and 21245±18926 of NPI3 group (all the P > 0.5) (Fig.4.3.2.2 B2). There was no specific pattern was shown in the data related to NPI scores of RGMC, as the transcript level decreased in NPI2 (55±35) but increased in NPI3 (733±479), comparing with NPI1 (179±168) (Fig.4.3.2.2 C2).

In addition to NPI, the association of RGMs expression to Tumour Nodal Metastasis staging (TNM) and tumour grade were also analysed as further indicators of prognosis.

The RGMA level in the patients with tumour grade 1 was 6340±2391 and increased in tumour grade 2 (30831±13085) and decreased again in the tumour grade 3 (7750±6263) (Fig.4.3.2.3 A3). The same trend was observed in the connection to tumour grade in RGMC (11.7±8.8 for tumour grade 1, 289±275 for tumour grade 2 and 103±52 for tumour grade 3) (Fig.4.3.2.3 C3). There was a different pattern shown in the data when comes to RGMB (2831±1090 for Grade1, 7050±3298 for Grade2 and 52647±34745 for Grade3) (Fig.4.3.2.3 B3), which was distinct from RGMA and RGMC.

The RGMA transcript level was very low in the TNM1 (0.508±0.292) compared to the TNM2 (12253±8626), TNM3 (7750±6263) and TNM4 (13635±6384), however, there is little changes between the three (**Fig.4.3.2.4 A4**). There is no definitive pattern seen in the progressing TNM stages related to RGMB. The RGMB expression appears highest level in TNM3 status with much lower level in TNM2 and TNM4 and lowest in TNM1, p>0.1 in all cases (**Fig.4.3.2.4 B4**). Even though there's no trend shown in the data related to the patients prognosis as NPI and tumour grade (**C2 and C3**), the RGMC expression decreased in the increased TNM stages (**Fig.4.3.2.4 C4**), from TNM2 (412±231) to TNM3 (103±52) (p=0.2) and from TNM3 (103±52) to TNM4 (0.126±0.076) (0.097), as the sample of TNM1 was absent.

These data indicated that there was no obvious trend in RGMA expression associated with tumour progression (the increased NPI score, TNM staging and tumour grade). However, as the higher expression in tumour tissues, RGMB transcript level also gradually increased in the patients with poorer prognosis and

higher NPI index and tumour grade, although these changes did not reach a level of significance (p > 0.2 in all cases). This may be due to the high variances obtained from the data and a relatively small sample in some instance (**Table 4.3.1**). Although statistical significance was not reached, the trend in RNA transcript levels demonstrated that RGMC might have decreased levels in patients with breast cancer, particularly in those with higher TNM staging and poor prognosis.

The transcript level of RGMs in breast cancer and clinical outcome

The association of RGMs transcript expression with clinical outcomes of the patients was also analyzed based on the follow-up data. The patients with poor prognosis, including those with local recurrence (Survival status 2), metastatic disease (Survival status 3) and those who died from breast cancer (Survival states 4) had significant lower transcript levels of RGMA (5381±2321, p=0.043) compared to that of patients who had remained disease free (Survival status 1) (20660±7055) (Fig.4.3.2.5 A5). In fact, the patients of survival status 1 have highest RGMA expression which is significantly higher than those of Survival status 3 (2658±1996, p=0.016) and 4 (2898±897, p=0.015), however not changed much in Survival status 2 (12648±8499, p=0.48).

When look at the survival status related to RGMB, the transcript level of RGMB in patients remained disease free (10857±3364 Surv1) is much higher than those with local recurrence (1714±1082 Surv2) and metastatic disease (71.2±41 Surv3) (p=0.012 and p=0.002 respectively)(Table 4.3.2). However, the RGMB

expression is increased and reached the highest in the patients died from breast cancer (27697±17042). Although the decreased pattern is not consistent within all the four survival status, if combined four together, the RGMB was increased in patients with poor clinical outcome compared to those with good clinical outcome (Surv1 vs Surv2/3/4) (10857±3364 vs 17642±10778), whilst the p-value is 0.55 (Fig.4.3.2.5 B5).

There are no particular pattern shown in the follow-up data of RGMC, however, if taken together, RGMC showed higher expression in patients who remained disease free (245±153), with lower expression in those with metastatic disease or local recurrence or died from breast cancer (201±132) (p=0.83) (Fig.4.3.2.5 C5).

The details of RGMs transcript level in patients with breast cancer was listed below (**Table 4.3.2**). Two sample T-Test was used here.

Table 4.3.1 Clinical and pathologic information

Clinical group	Sample volume (total 139)		
	RGMA	RGMB	RGMC
Tissue sample			
Normal	28	29	28
Tumour	106	94	106
NPI			
1 (NPI score < 3.4)	54	51	54
2 (NPI score 3.4-5.4)	32	29	32
3 (NPI score > 5.4)	15	11	15
Tumour grade			
1	17	17	17
2	33	33	33
3	7	6	7
TNM staging			
I	2	2	2
II	32	24	32
III	7	6	7
IV	4	3	4
Survival status			
Disease free (Surv1)	73	69	73
with metastases (Surv2)	7	, 6	7
with local recurrence (Surv3)	5	2	5
Died of breast cancer (Surv4)	15	13	15

Table 4.3.2 The transcript level of RGMs in breast cancer

Clinical data	Transcripts (Mean±SE)		
	RGMA	RGMB	RGMC
Tissue sample			
Normal	12729±7850	4220±1586	1616±1110
Tumour	18223±5504	12166±3434	220±111
NPI			
1 (NPI score < 3.4)	19129±7439	8602±3179	179±168
2 (NPI score 3.4-5.4)	26324±13149	10325±4678	55±35
3 (NPI score > 5.4)	2071±882	21245±18926	733±479
Tumour grade			
1	6340±2391	2831±1090	11.7±8.8
2	30831±13085	7050±3298	289±275
3	7750±6263	52647±34745	103±52
TNM staging			
I	0.508 ± 0.292	801±801	
II	12253±8626	4401±2033	412±231
III	7750±6263	52647±34745	103±52
IV	13635±6384	4741±4729	0.126±0.076
Survival status			
Disease free (Surv1)	20660±7055	10857±3364	245±153
with metastases (Surv2)	12648±8499	1714±1082	11.2±7.1
with local recurrence (Surv3)	2658±1996	71.2±41	749±689
Died of breast cancer (Surv4)	2898±897	27697±17042	108±64

4.4 Discussion

The mRNA level of RGMB observed from tissue screening was higher in breast cancer tissues, compared to normal/background tissues. Moreover, RGMB mRNA level was higher in the more aggressive breast cancer cell lines. This agrees with the expression analysis of the clinical data, where the transcript levels of RGMB were significantly higher in breast cancer tissues than in normal/background tissues as verified by RT-QPCR. Interestingly, only RGMB was detected in the breast cancer cell lines, whilst RGMA and C had no visible expression at the mRNA level. In addition, the protein levels of RGMA and RGMC showed no significant differences between normal and tumour breast tissues. Therefore, RGMB might be tentatively identified as an important factor contributing to the progression of human breast cancer, a role unique to this member of the RGM family of proteins.

No significant difference was shown from the data analyzed using predicted prognosis of patients, by indicators such as NPI, TNM staging and tumour grade. Trends indicated that increased RGMB expression was associated with higher NPI status and tumour grade, i.e. more aggressive breast tumours. The patients with good survival status (remaining disease free after 120 months) had higher RGMA levels than those with poor prognosis (local recurrence, metastatic disease or patients who had died from breast cancer). Therefore, RGMA might be perceived to have a more protective role against the progression of human breast cancer.

In conclusion, RGMB might function as a key factor in breast cancer related to the disease progression if only inferred from the differences in expression pattern between the normal breast and breast cancer tissues. RGMA and RGMC was not detected in the breast cancer cell lines and appeared to have little correlation with patient prognosis. Although the RGMA showed a putative beneficial correlation with disease progression, its expression was very low in both normal and tumour tissues (as observed from IHC staining) and there were no statistical differences between tissues (Q-PCR analysis). These data offer an intriguing glimpse of how the RGM family might operate in human breast cancer, indicating that a further investigation of the role of RGMB in breast cancer was necessary. The high expression of RGMB in many human breast cancer cell lines, lends itself to a knockdown study.

Although the expression profile of RGMs in breast and prostate cancer cell lines (described in chapter 3) and human tissues is only a preliminary study which is not sufficient to reveal the role of RGMs in cancer, this nonetheless indicates that a comprehensive study should be carried out. For a further study, two cell lines were chosen, PC-3 (prostate cancer) and the MDA-MB-231 (breast cancer), to create the RGMs knockdown variants, due to their strong expression of RGM and highly aggressive phenotype. The role of RGMA, B and C in breast cancer and prostate cancer will be explored in the following chapters.

Chapter 5

Knockdown of RGMs in prostate cancer cells and the influence on cellular functions

5.1Introduction:

As mentioned in chapter 3, RGMs were detected in many prostate cancer cell lines and prostate tissues. Furthermore, RGMB and RGMC showed stronger staining in more aggressive prostate cancer tissues compared to the prostate specimens with less Gleason scores. The aberrant expression of RGMs in prostate cancer indicated an interesting role RGMs might have.

In addition, RGMs were reported as co-receptors of BMPs, while BMPs are key factors that have profound impact on prostate cancer and bone metastasis. BMPs were implicated in prostate cancer through regulation on the BMP signalling pathway activated by BMPs. For example, BMP-7 and BMP9 inhibit the proliferation of PC-3 prostate cancer cells via inducing apoptosis through BMP receptors and Smaddependent pathway (Miyazaki et al., 2004; Ye et al., 2008), while BMP-10 inhibits the growth of prostate cancer cells via Smad independent signalling in which XIAP and ERK1/2 are involved (Ye et al., 2009). These BMPs can also prevent prostate cancer cell migration and invasiveness. Therefore, RGMs might also be involved in the prostate cancer development and metastasis through the participation in BMP signalling pathway.

As described in Chapter 3, all 3 RGMs are expressed in prostate cancer cell lines. To investigate the role of RGMs in prostate cancer, the present study successfully knocked down RGMA, B and C in PC-3 cells, a cell line originally derived from prostate bone metastasis. Using these genetically modified cells, *in vitro*

cellular function assays were conducted to explore the role of RGMs in prostate cancer.

5.2 Materials and methods

5.2.1 Materials

Polyclonal goat anti-RGMA, anti-RGMB and anti-RGMC antibody were obtained from Santa Cruz Biotechnology (Santa Cruz, California, USA). All the primers used are shown in table 2.1.2 and were synthesized and provided by Invitrogen (Paisley, UK). The cell line PC-3 used in this study was routinely maintained in DMEM-F12 medium supplemented with 10% fetal calf serum and antibiotics.

5.2.2 Generation of RGM ribozyme transgenes

RGMA, B and C expression were knocked down in PC-3 using anti-human respective hammerhead ribozyme transgenes which were described in section 2.5.1. The transgenes were generated through touchdown PCR and cloned into pEF6/His TOPO mammalian expression plasmid vectors (Invitrogen Inc., Paisley, UK). Control empty plasmid vectors and the ribozyme transgenes were then transfected into PC-3 cells and the cells underwent selection with $5\mu g/ml$ blasticidin for approximately two weeks, and knockdown of specific RGM were then confirmed before further use.

5.2.3 Real Time Quantitative PCR

The real time quantitative PCR was carried out to determine the levels of RGM transcripts in the control and RGM knockdown cells. The protocol and primers used for RGMs quantitation and housekeeping GAPDH were listed in section 2.1.2 and 2.3.5.

5.2.4 Protein extraction, SDS-PAGE and Western blot analysis

Protein was extracted following cell lysis using lysis buffer listed in section 2.1.4. The protein concentration was then quantified using the DC Protein Assay kit (BIO-RAD, USA) and a spectrophotometer (BIO-TEK, ELx800). Equal amounts of protein from each sample were loaded onto 8% polyacrylamide gel and following SDS-PAGE, the proteins were transferred onto nitrocellulose membranes subjected to blocking, and probing with the specific primary (1:200), and the corresponding peroxidise-conjugated secondary antibodies (1:2000). The protein bands were eventually visualized using the Supersignal_{TM} West Dura system (Pierce Biotechnology, USA). Detail is described in section 2.4.

5.2.5 In vitro cell growth assay

The cells were seeded into a 96 well plate at a concentration of 3,000 cells per well, and incubated for periods of up to 5 days. The cells were then stained with crystal violet, and measured the absorbance. The results were shown as growth rate which was calculated by normalization against the base absorbance measurements at day 0.

5.2.6 In vitro cell-matrix adhesion assay

45,000 cells were seeded onto the 96 well plate coated with Matrigel basement membrane in 200µl of normal medium and incubated for 40 minutes. After wash, adherent cells were fixed and visualized under the microscope under x40 objective magnification and random fields counted.

5.2.7 In vitro cell invasion assay

Transwell inserts (upper chamber) with an 8μm pore size were coated with 50 μg/insert of Matrigel and air-dried, before being rehydrated with normal medium. Then, 2x10⁴ cells were added to each well. After 72 h, cells that had migrated to the other side of the insert through the matrix were fixed and stained with 0.5% (w/v) crystal violet. The invaded cells stained with crystal violet were counted under microscope.

5.2.8 In vitro cell motility assay using Cytodex-2 beads

Cellular motility was assessed using a cytodex-2 bead motility assay. 5×10^5 cells for each cell type were incubated in 10ml of growth medium containing 100 μ l of cytodex-2 microcarrier beads (GE Healthcare, Cardiff, UK) for 3.5 hours to allow the cells to adhere to the beads. After washing the beads were resuspended in growth medium, seeded into a 24 well plate and then incubated overnight at 37°C. Cells that had migrated from the beads and adhered to the base of the well were fixed in 4% formaldehyde (v/v), stained with 0.5% crystal violet (w/v) and counted under x40 objective magnification.

5.2.9 ECIS-based migration assay

We used the electric cell-substrate impedance sensing (ECIS) system (Applied Biophysics, Inc., Troy, NY) to conduct the attachment and wounding assay. PC-3 cells were cultured in 8W1E ECIS arrays (Applied Biophysics). PC-3 cells were seeded at a density of 70,000 cells/well in the arrays. The cells were incubated for 4 hours and the resistance was recorded every 20 seconds. Cell migration was assessed by continuous resistance measurements for 30 hrs after applying an elevated voltage pulse.

Statistical analysis

Normally distributed data was analyzed using the two sample T-test while non-normally distributed data was analyzed using the Mann-Whitney and Kruskal-Wallis tests.

5.3 Results:

5.3.1 Construction of ribozyme transgene targeting at human RGMs and knockdown in PC-3 cell line

To test the potential role of RGMs in prostate cancer cells, the following cell variants from the established cell lines were created: RGM (A/B/C)-knockdown PC-3 prostate cancer cell lines using the ribozyme transgenes specific to human RGMs. The ribozyme transgenes (ribzyme1, 2 and 3) targeting RGMA, RGMB and RGMC respectively were generated through touchdown PCR (Figure 5.3.1.1). The RGM ribozymes were inserted into vector and cloned into bacteria (Figure 5.3.1.1). The colonies positive for the ribozyme were selected to extract the plasmid used for cell line transfection (Figure 5.3.1.1). As shown in Fig.5.3.1.2 and 5.3.1.3, despite the empty plasmid control PC-3 cells being positive for RGMs, RGM ribozyme transgenes successfully reduced up to 98% of the expression of RGMs in the prostate cancer cells at transcript level (Fig.5.3.1.3) or markedly reduced from protein level (Fig.5.3.1.2). (RGMA rib3, RGMB rib1, RGMC rib3 were chosen)

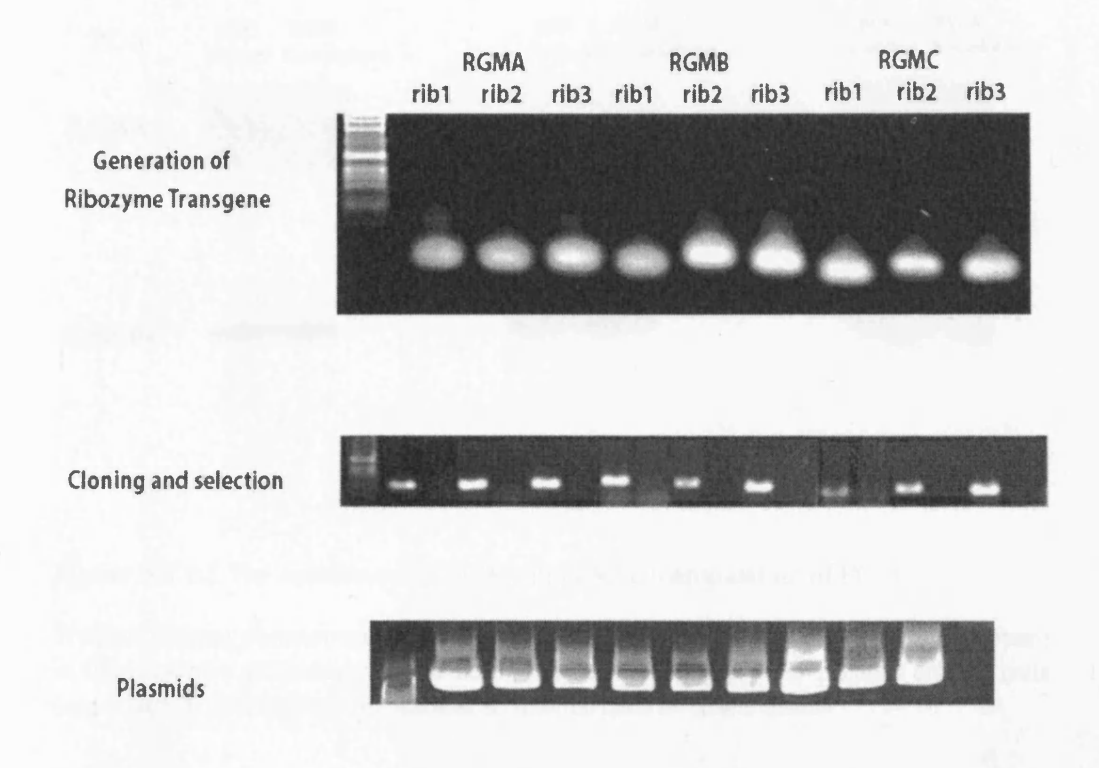


Figure 5.3.1.1 The generation of ribozyme transgenes specific to RGM

The ribozyme transgenes (ribzyme1, 2 and 3) targeting at RGMA, RGMB and RGMC respectively was generated through conventional PCR (first line). The RGM ribozymes were inserted into vector and cloned into bacteria. The colonies positive (positive band followed by one negative band) for the ribozyme were selected (second line) following by the plasmid extraction. The quality of the plasmid extracted was shown in the third line.

RGMs Knockdown in PC-3

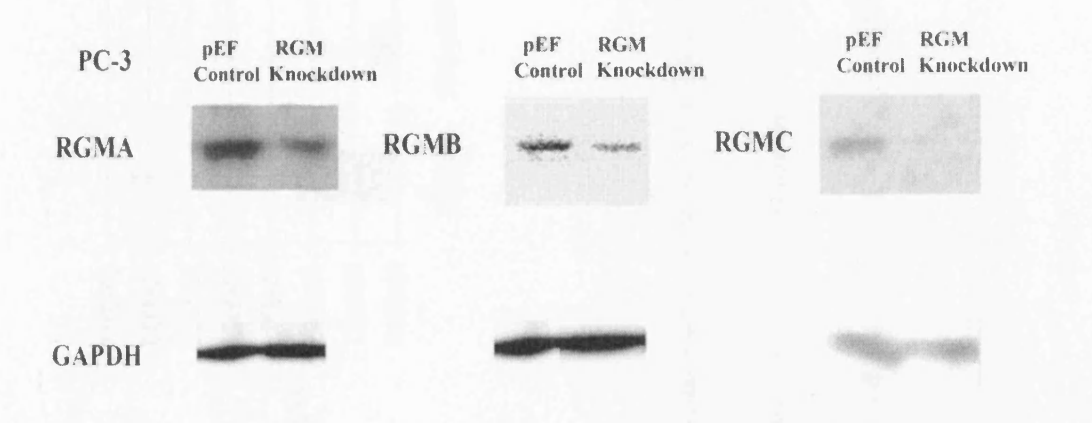


Figure 5.3.1.2 The expression of RGMs in genetic manipulation of PC-3

Western blotting demonstrated reduced expression of RGMA, RGMB and RGMC (protein) in the respective RGM knockdown cells, compared to empty pEF6 plasmid control cells (upper panel). GAPDH was included as an internal control. (lower panel)

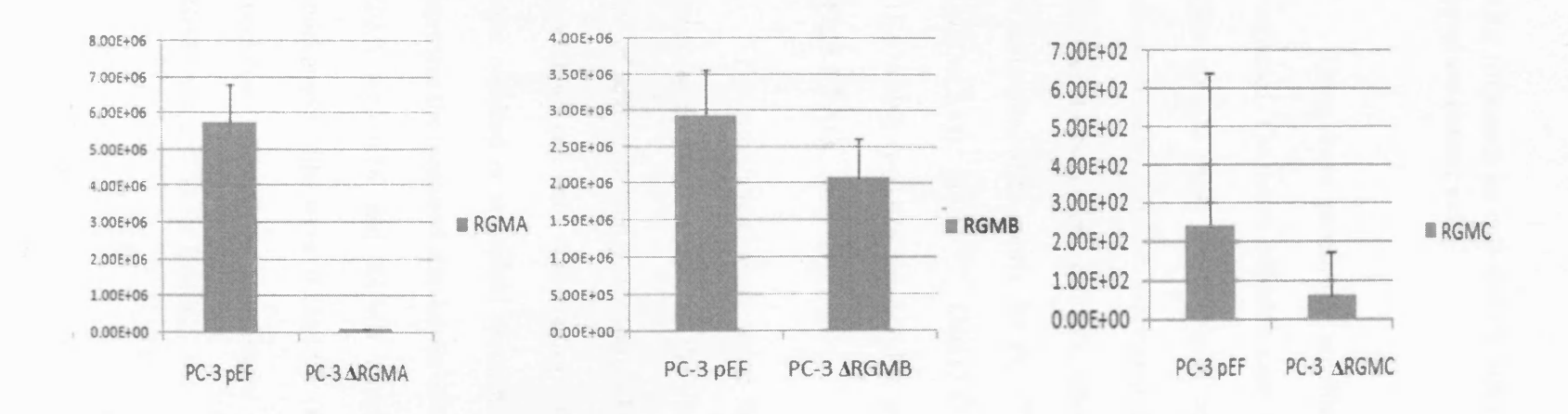


Figure 5.3.1.3 The expression of RGMs in genetic manipulation of PC-3

The knockdown of RGMs was verified by real time quantitative PCR. (Left)The RGMA was knocked down (Mean \pm STD. $1.05E+05\pm1.20E+04$) 98% from control cells ($5.76E+06\pm1.05E+06$). (p=0.007)

(Middle) RGMB expression was reduced 30% from PC-3 control cells (2.92E+06 \pm 0.6E+06) in cells transfected with RGMB ribozyme (2.06E+06 \pm 0.5E+06), though P value is 0.15.

(Right) RGMC was eliminated 73% from PC-3 cells (6.42E+01 \pm 111) compared to control cells (2.39E+02 \pm 404), though P value is not significant (0.51) due to the big variances.

Expression levels shown were normalized using the level of housekeeping gene GAPDH.

5.3.2 Influence on cell-matrix adhesion by knockdown of RGMs in prostate cancer cells

Using these genetically modified cells, *in vitro* cell function analysis was conducted. The matrix adhesion assay (n=6) and the attachment assay of ECIS (n=4) were used to verify the ability of cells adhere to the membrane surface. In the adhesion assay, reduced expression of RGMs (RGMA, B and C) in these cells rendered the cells more readily to adhere, compared to the control cells. The number of cells adhered to matrix for PC-3^{ΔRGMA} (Mean ± Std. 26.93±13.23), PC-3^{ΔRGMB} (30.67±12.43), PC-3^{ΔRGMC} (30±12.43) were increased, compared to PC-3^{pEF/His} (16.67±8.09) (p=0.028 for RGMA, p=0.003 for RGMB and p=0.005 for RGMC) (**Fig.5.3.2 A1**).

The Attachment assay using ECIS displayed the highest speed of RGMB knockdown cells to attach: all the three RGM knockdowns cells showing a higher rate of adherence than pEF control (Fig.5.3.2 A2 left). When comparing the RGMs knockdown cell lines with control cells based on the normalized data at same time point obtained in individual experiments, the average increased impedances which represent the increased attachment of cells in RGMA knockdown cells were (Mean ± SEM) 0.83±0.56 and RGMB knockdown cells were 10.78±4.82 and RGMC knockdown cells were 0.23±4.00 (Fig.5.3.2 A2 right). However, only RGMB knockdown showed the significance at this time point (p=0.01, while p=0.64 for RGMA and p=0.93 for RGMC).

Taken together, the knockdown of RGMs in PC-3 cells enabled the cells to become more adhesive (Figu.5.3.2 A for three respective RGM knockdown cells). Three independent experiments were performed.

5.3.3 Effect on in vitro growth of prostate cancer cells by RGMs

Using the same cells, I further tested the rate of cell growth over a 5-day period (n=6). Three independent experiments were performed. The representative data of Day 3 was shown here (**Fig.5.3.2B**). Compared to control cells (2.03±0.17), RGMA knockdown cells (2.23±0.16) did not showed a significant difference in the rate of cell growth (p=0.07). In contrast, RGMB knockdown (Mean ± Std. 2.70±0.30) and RGMC knockdown (2.89±0.73) cells showed a significant increase in cell growth, compared to the pEF control cells (p<0.01 RGMB vs pEF, p=0.02 RGMC vs pEF). This indicated cells that had lost RGMs by way of ribozyme transgenes displayed a faster rate of growth, compared with cells transfected with control vectors on the Day3 (**Fig.5.3.2 B**).

5.3.4 Effect on *in vitro* motility and mobility of prostate cancer cells by RGMs

Furthermore, the three RGM knockdown cells all displayed an increased motility, when counting the cells moved from beads to matrix in a fixed period (**Fig 5.3.2 C**). Cells with RGM knockdown displayed a higher motility rate after wounding examined by cytodex-2 beads motility assay (n=6). The number of migrated cells in RGMA knockdown was 36±9.2 (Mean ± Std.), in RGMB knockdown was 46.4±7.06,

and RGMC knockdown was 45.54±28.46, compared with 20.2±4.06 in pEF control cells. However, only the increase in the RGMB knockdown cells was statistically significant (p<0.01).

Using the ECIS based cell migration assay (n=4), the migration rate is obviously much higher of PC-3^{ARGMB} cells among these cell lines, while the RGMA and RGMC knockdown has no significant difference compared with pEF control (**Fig.5.3.2 D** left). When comparing the normalized data at the comparable time point, the average impedance in RGMB knockdown cells was significantly higher than the pEF control cells (74.6±7.07 vs 13.37±23.71, RGMB vs pEF, p=0.009). However, the RGMA and RGMC knockdown cells did not show such significance when comparing with pEF control cells (p=0.94 and p=0.22 respectively) (**Fig.5.3.2 D** right). This is thus consistent with the observations made with the carrier beads assays.

5.3.5 Effect on *in vitro* invasion of prostate cancer cells by RGMs knockdown

The *in vitro* invasion assay was also utilized to further investigate the effects on invasion caused by RGM knockdown cells. The number of invaded cells though matrix after RGMA knockdown (Mean ± Std. 29.71±5.53), RGMB knockdown (29.43±6.70) and RGMC knockdown (29±6.45) were almost similar to the pEF control (31.4±5.13) cells (p=0.6 RGMA vs pEF, p=0.59 RGMB vs pEF, p=0.52 RGMC vs pEF) (**Fig.5.3.2** E). Although the profound effect has been shown by RGMs in cell adhesion and mobility, the genetic modification did not seem to alter the PC-3 cells' property of invasiveness (n=7).

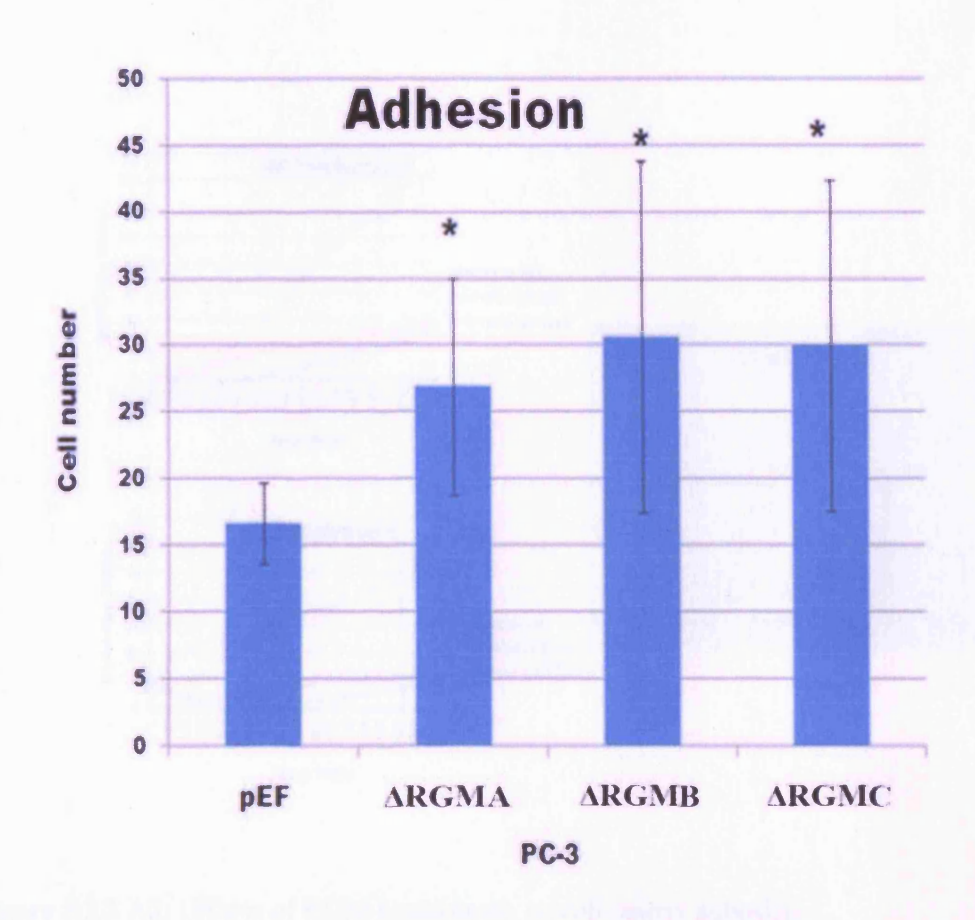


Figure 5.3.2 A1: Impact of RGM knockdown on PC-3 cell-matrix adhesion

Matrix Adhesion in PC-3^{ARGMs} cells (reduced RGMs expression) were increased, as demonstrated by the cell-matrix adhesion assay. Significantly higher number of PC-3^{ARGMA} (26.93±13.23), PC-3^{ARGMB} (30.67±12.43), PC-3^{ARGMC} (30±12.43) cells adhered to cell matrix, compared to PC-3^{PEF/His} (16.67±8.09). * P < 0.05 ν s PC-3^{PEF/His}.

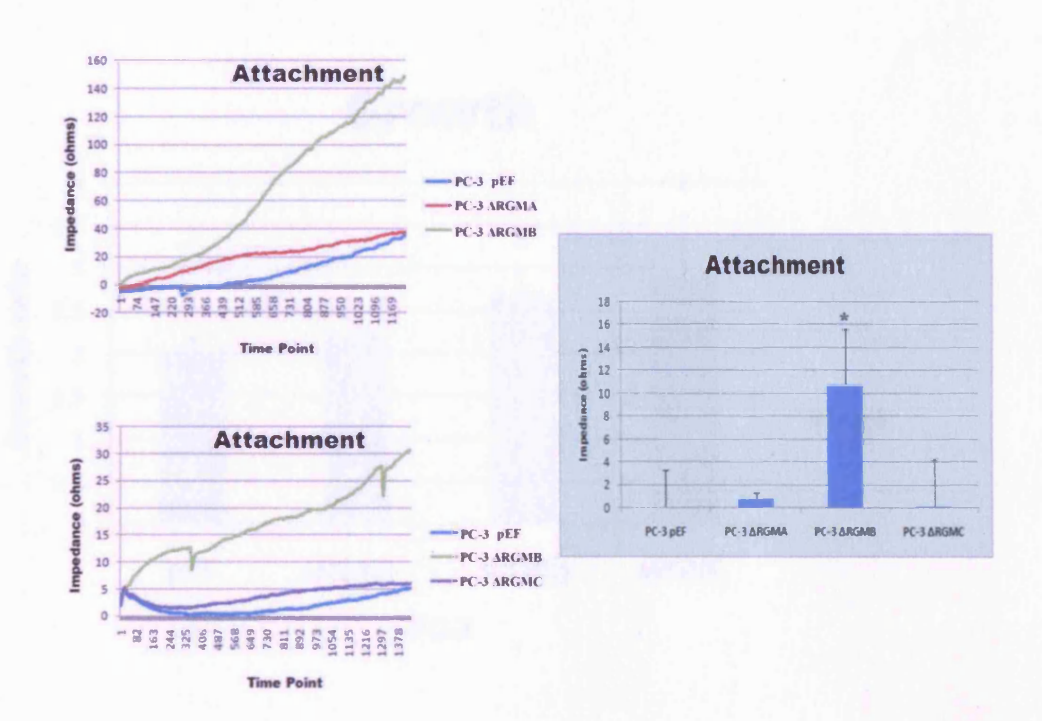


Figure 5.3.2 A2: Effects of RGM knockdown on cell-matrix adhesion.

Attachment of PC-3 control and RGM knockdown cells to the ECIS central electrode over a 4-hour period. PC-3^{ARGMB} cells were the quickest to attach, with subtle increases in RGMA and C knockdown compared to control cells. The time interval was every 20 seconds per time point. More than three independent experiments were conducted and the representative data was displayed (left).

The mean normalized impedance at the comparable time point (1169) was shown in the graph (right side), calculated from the individual experiments. The error bars represented SE Mean of these experiments. The increased impedance in RGMA knockdown was 0.82 ± 0.56 , while RGMB was 10.78 ± 4.82 and RGMC was 0.23 ± 4.0 , based on pEF control cells (p=0.64 for RGMA vs pEF, p=0.01 for RGMB vs pEF, p=0.93 for RGMC vs pEF). * P < 0.05 vs PC- $3^{pEF/His}$

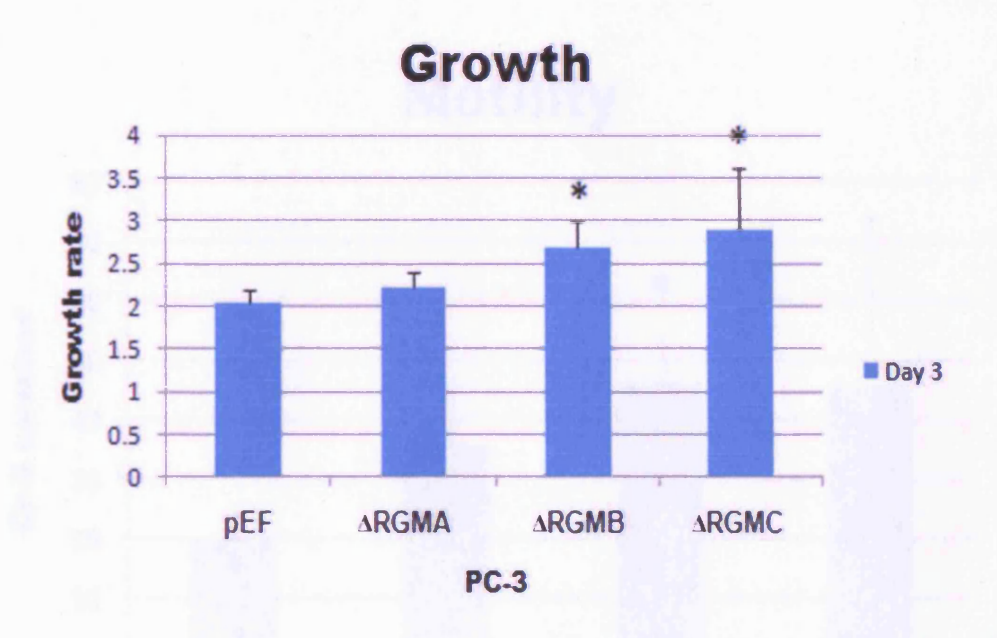


Figure 5.3.2 B. Impact of RGM knockdown on cell growth.

Absorbance of Day 3 is shown, which represented cell density. The reduction of RGMB and C in PC-3 significantly promoted growth rate (2.69 \pm 0.30, 2.89 \pm 0.73 respectively), compared to control cells (2.03 \pm 0.17) (p < 0.05). The growth of PC-3^{ARGMA} was also subtly increased (2.23 \pm 0.17), while p is 0.07. More than three independent experiments were conducted and representative data was displayed. * P < 0.05 vs PC-3^{pEF/His}.

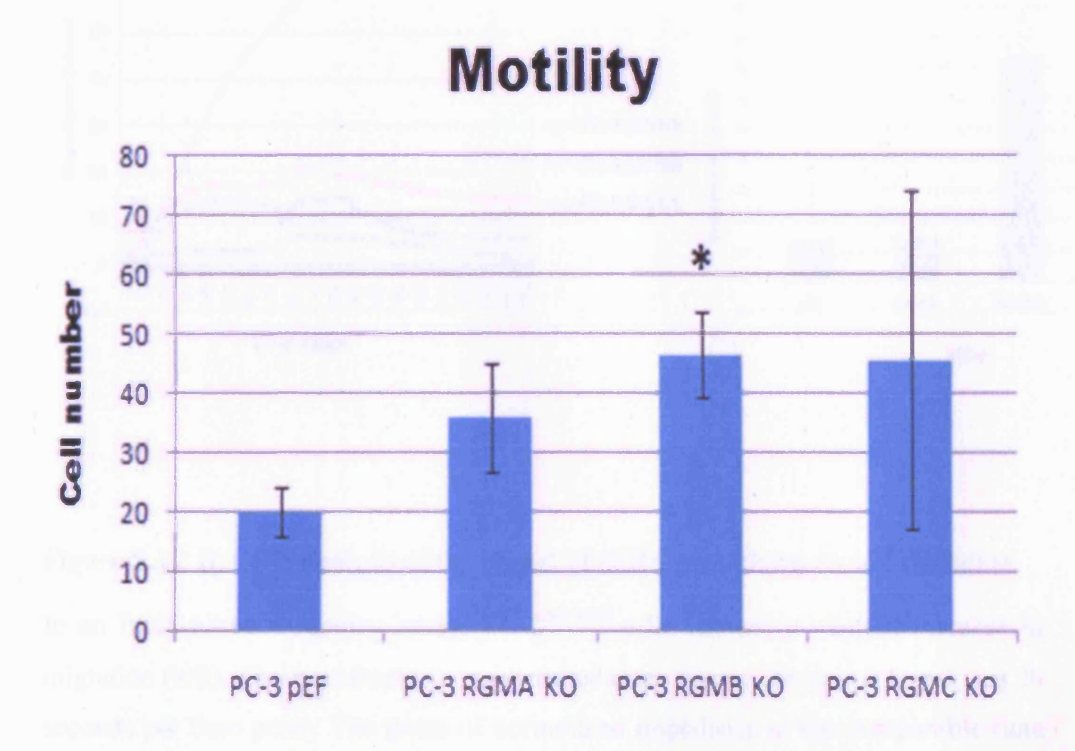


Figure 5.3.2 C. Impact of RGM knockdown on motility

Cell migration following RGM knockdown was assessed using the cytocarrier bead assay. Although the higher average values were seen to be increased compared to the control cells (20.2±4.06) in PC-3^{Δ RGMA} (Mean±SEM 36±9.2) and PC-3^{Δ RGMC} (45.54±28.46), only the motility of PC-3^{Δ RGMB} (46.4±7.06) was found to be significantly higher (p=0.005). The graph shows means values of the repeated experiments and the error bars present the standard error of the mean. * P < 0.05 ν s PC-3^{ρ EF/His}.

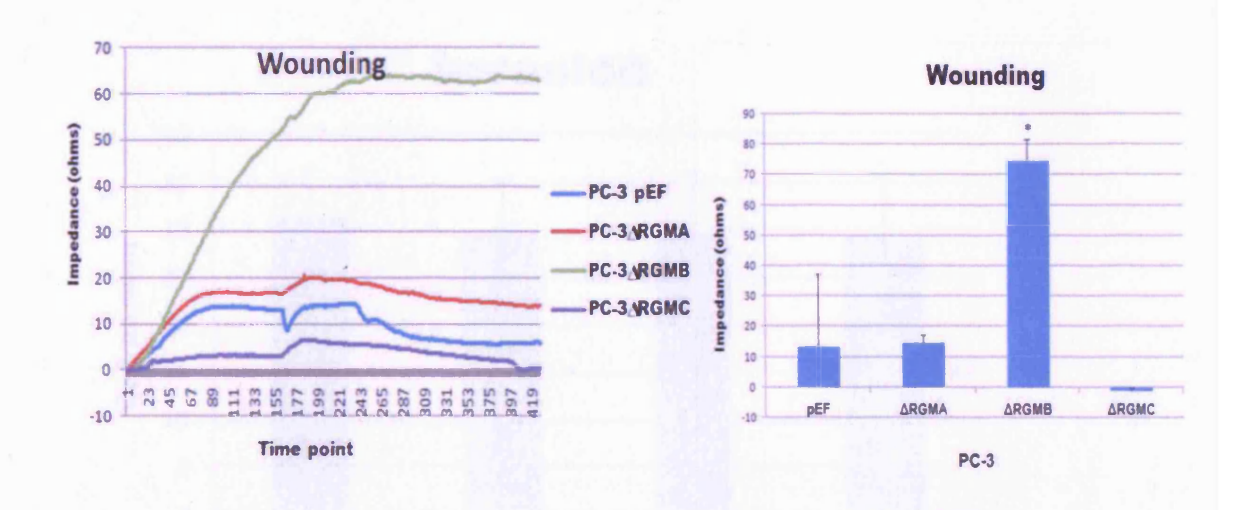
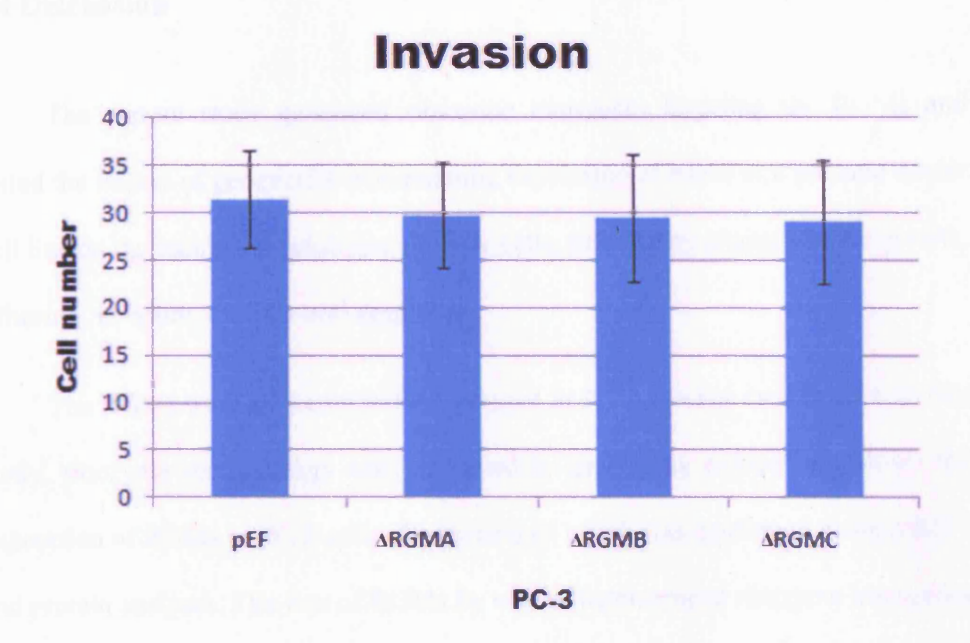


Figure 5.3.2 D. ECIS analysis of the impact of RGM knockdown on cell migration.

In an ECIS-based wounding assay, PC-3^{ARGMB} cells showed a marked increase in migration (left). The experiments were repeated three times. The time interval was 20 seconds per time point. The mean of normalized impedance at the comparable time was calculated based on individual experiments and shown in the graph (right). Two sample T-test was used to identify significance levels. Error bars represent the standard errors of the mean. Only RGMB knockdown cells showed a significant difference compared to control cells.



PC-3	Mean	St.D	P value (vs pEF)
pEF6	31.4	5.13	
RGMA KO	29.71	5.53	0.6
RGMB KO	29.43	6.70	0.59
RGMC KO	29	6.45	0.52

Figure 5.3.2 E RGMs and the *in vitro* invasiveness of cancer cells.

Top: the invasiveness of PC-3 cells had not been altered by the loss of RGMs. At least three independent experiments were conducted and the representative data is displayed. Bottom: statistical information of the analyses. Two sample T-test was used to identify significance levels.

5.4 Discussion

The current study generated ribozyme transgenes targeting the RGMs and tested the impact of genetically manipulating expression of RGM in a prostate cancer cell line on the biological behaviour of these cells, assessed by changes in the growth, adhesion, invasion, motility and migration.

The RGMs were all found to be expressed in PC-3 prostate cancer cells. In this study, ribozyme methodology was employed to genetically reduce/knockdown the expression of RGMs in PC-3 cells, the success of which was confirmed using mRNA and protein analyses. The loss of RGMs by way of hammerhead ribozyme transgenes resulted in accelerated cell growth and enhanced adhesion *in vitro*. Interestingly, the effects on cellular behaviour were most significant in RGMB knockdown cells. The knockdown of RGMB significantly enhanced the prostate cancer cell capacity, namely increased growth, adhesive, motility and mobility. RGMC knockdown did not significantly affect cell motility and mobility, however, had a considerable effect on cell growth.

This indicated that RGMs (especially RGMB) are associated with inhibitory effects on tumour cell growth. The expression of RGMB may also induce a decreased capacity for PC-3 cells to attach to the basement membrane. The present study has also demonstrated that loss of RGMB resulted in more *in vitro* motility and mobility, compared with control cells. An increase in RGMB expression might inhibit prostate cancer cells ability to leave the primary tumour and migrate and attach to the matrix membrane of metastatic site. That indicated the RGMB may play a key role in the

control of the aggressiveness of prostate cancer via mechanism(s) yet to be identified. Hence, RGMB may be a potential anti-metastasis molecule, which is of critical importance in the development of prostate cancer therapies.

The inhibitory role of RGMs might be contrary to the expression postulated from the in prostate cancer specimens (IHC staining in Chapter 3). RGMA showed little difference in staining intensity between the tumour and normal prostate tissues. However, it is interesting to note that RGMB and C had a week protein staining in prostate cancer cells cytoplasm and in the nearby stroma and stromal cells. Thus, it is presently challenging in linking the pattern of tissue expression and the cell fuction tests. Therefore, the mechanism of the RGMs in vitro need be investigated further to confirm their effects on tumour.

Presently, it is not entirely clear by which mechanism RGMs mediated the biological behaviours of prostate cancer cells. We have developed hammerhead ribozyme transgenes targeting the three RGMs. Further studies will utilize the ribozyme constructs to investigate the role of RGMs in human breast cancer cells. Moreover, further investigation of RGMs and the signal transduction of BMPs will be investigated in the following chapters.

Chapter 6

The knockdown of RGMB in breast cancer and influences on cellular behaviours

6.1 Introduction:

As previously described, the RGMB had aberrant expression in breast tissues and the transcript level of RGMA might be associated with good prognosis. However, all the RGMs showed no obvious staining difference of protein in the breast tissues. Due to the interesting expression pattern that the RGMs showed in the tissues from the breast cancer patient cohort and the association of RGMs with clinical prognosis, the present study went on to investigate further the role of RGMB in human breast cancer. To date, there have been no reports on either the expression profile or possible role of this protein in any cancer type.

BMPs as RGM ligands have been implicated in the breast cancer and bone metastasis. However, in some cases, BMP has been shown to play a dual role in these disease processes. For example, the same BMP ligand within the same cancer type seems to act differently depending on the study and the types of analyses and can be both promotion and inhibition of breast cancer progression. BMPs are also critical during epithelial—mesenchymal transition (EMT), via which they may contribute to the metastatic process (Alarmo et al., 2008; Alarmo et al., 2009; Buijs et al., 2007a; Cassar et al., 2009; Takahashi et al., 2008). RGMs which were involved in the BMP signalling might also have impact on breast cancer through regulation on BMP signalling pathway or target genes by themselves. However, there have been no reports concerning their implications in cancer spreading. Therefore, our study aimed to be the first to characterise the role of RGM in human breast cancer.

It was found that only RGMB was expressed in human breast cancer cell lines, whereas little or no expression of RGMA and RGMC at mRNA and protein levels in these cells. However MDA-MB-435s cell was an exception in that all three RGMs were detected. Currently, there is a controversy as to whether the cells is indeed a breast cancer cell line. A few recent studies reported that the cell line may have been a cell line developed from (or mixed with) a metastatic cell line from melanoma (Ellison et al., 2002; Ross et al., 2000). Thus, MDA-MB-435 cells were not used in the present study for this reason. The transcript level of RGMB was higher in breast tumour than in normal breast tissues. However, results did not indicate that the difference in expression were associated with poor prognosis. It appeared from our initial data that RGMB may play an important role in breast cancer, a role which might make it distinct from the other RGM family members. We decided to create RGMB knockdown in the human breast cancer cell line MDA-MB-231, a cell with an extremely aggressive phenotype The impact of loss of RGMB on breast cancer cell behaviour in vitro was subsequently investigated, in order to further reveal the potential role of this protein in human breast cancer.

6.2 Materials and methods

6.2.1 Establishment of MDA-MB-231 RGM knockdown variants

RGMB expression was knocked-down in MDA-MB-231 using anti-human RGM hammerhead ribozyme transgenes which were generated through touchdown PCR

and described in chapter 5. Control empty plasmid vectors and the ribozyme transgenes were then transfected into MDA-MB-231 cells and the cells underwent selection with 5µg/ml blasticidin for approximately two weeks before further use.

6.2.2 RNA isolation and RT-PCR

RNA isolation and RT were carried out as described in previous chapters. This was then used as a template for PCR.

6.2.3 Protein extraction, SDS-PAGE and Western blot analysis

Protein was extracted following cell lysis using lysis buffer listed in section 2.1.4. Equal amounts of protein from each sample were loaded onto 8% polyacrylamide gel and following SDS-PAGE, the proteins probed with the specific primary (1:200), and the corresponding peroxidise-conjugated secondary antibodies (1:1000). Protocol is described in section 2.4.

6.2.4 In vitro cell function assays

The *in vitro* cell growth, adhesion and invasion assay and ECIS-based attachment assay were carried out as described in chapter 5. A wounding/migration assay was

also used to assess the migratory properties of the breast cancer cells. This technique has been modified from a previously described method (Jiang et al., 1999). Cells were grown upon reaching confluence the monolayer of cells was scraped with a 21G needle. The wound was tracked and recorded using a CCD camera attached to a Lecia DM IRB microscope (Lecia GmbH, Bristol, UK) through taking pictures every 15mins over a 90 minute period. The distance cell migrated was measured and converted into µm. The distance that the wound fronts had migrated into the wound at each time point could then be determined based on the start time point.

Statistical analysis

Normally distributed data was analyzed using the two sample T-test while nonnormally distributed data was analyzed using the Mann-Whitney and Kruskal-Wallis tests.

6.3 Results

6.3.1 Knocking down of RGMB in human breast cancer cells.

To investigate the role of RGMB in breast cancer, MDA-MB-231 cells were used which had high levels of expression of RGMB. The wild type MDA-MB-231

cells are highly aggressive cell line derived from metastasis of invasive breast ductal carcinoma. The specific ribozyme transgene targeting at RGMB (as used in the prostate cancer study) were utilized for genetically reducing the expression of RGMB in MDA-MB-231 cells (MDA^{ΔRGMB}). To reiterate our earlier results, it was confirmed that RGMA and RGMC were not expressed in MDA-MB-231 wild typecells (as cell line screening).

As shown in **Fig.6.3.1.1**, the expression of RGMB mRNA was completely eliminated from MDA-MB-231 cells by the ribozyme transgene, in comparison to the level of expression seen in the wild type (MDA^{WT}) cells and MDA-MB-231 empty plasmid control (MDA^{PEF/His}) cells.

It was also determined if there was a reduction of protein levels in the (MDA^{ΔRGMB}) cells following knockdown of RGMB. Western blot analysis was used as shown in **Fig.6.3.1.2.** There was a significant reduction of RGMB protein in MDA^{ΔRGMB} cells, in comparison to the MDA^{pEF/His}.

Immunocytochemical (ICC) staining of RGMB in these transfected cells also confirmed the successful knockdown of RGMB. The staining of RGMB protein in MDA^{pEF/His} cells was markedly stronger than in the cells transfected with RGMB ribozyme. As shown in the **Fig.6.3.1.3**, the staining of the protein in the MDA^{pEF/His} was mainly confined in the cytoplasm, while the staining in the RGMB knockdown cells was obviously reduced.

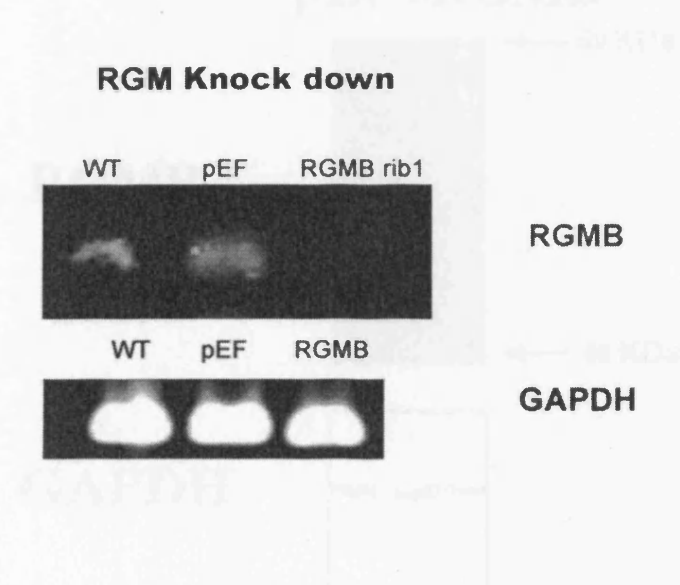


Figure 6.3.1.1 The mRNA level of RGMB in wild type MDA231 and the cells transfected with pEF empty plasmid and RGMB ribozyme.

The RGMB expression was eliminated from mRNA level. The mRNA of RGMB detected in the RT-PCR is 536 bps.

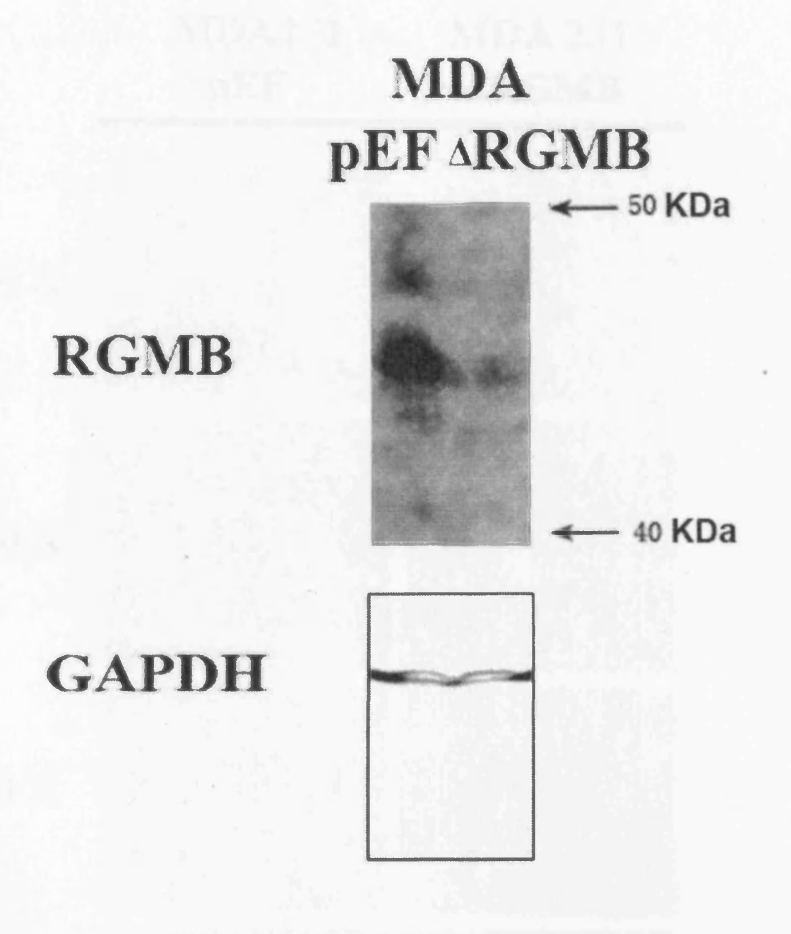


Figure 6.3.1.2 The RGMB expression was reduced in RGMB knockdown cells from protein level compared to the control cells, proved by western blot.

The size of RGMB protein shown in the result is 47.5 kDa. The ladder was indicated on the right.

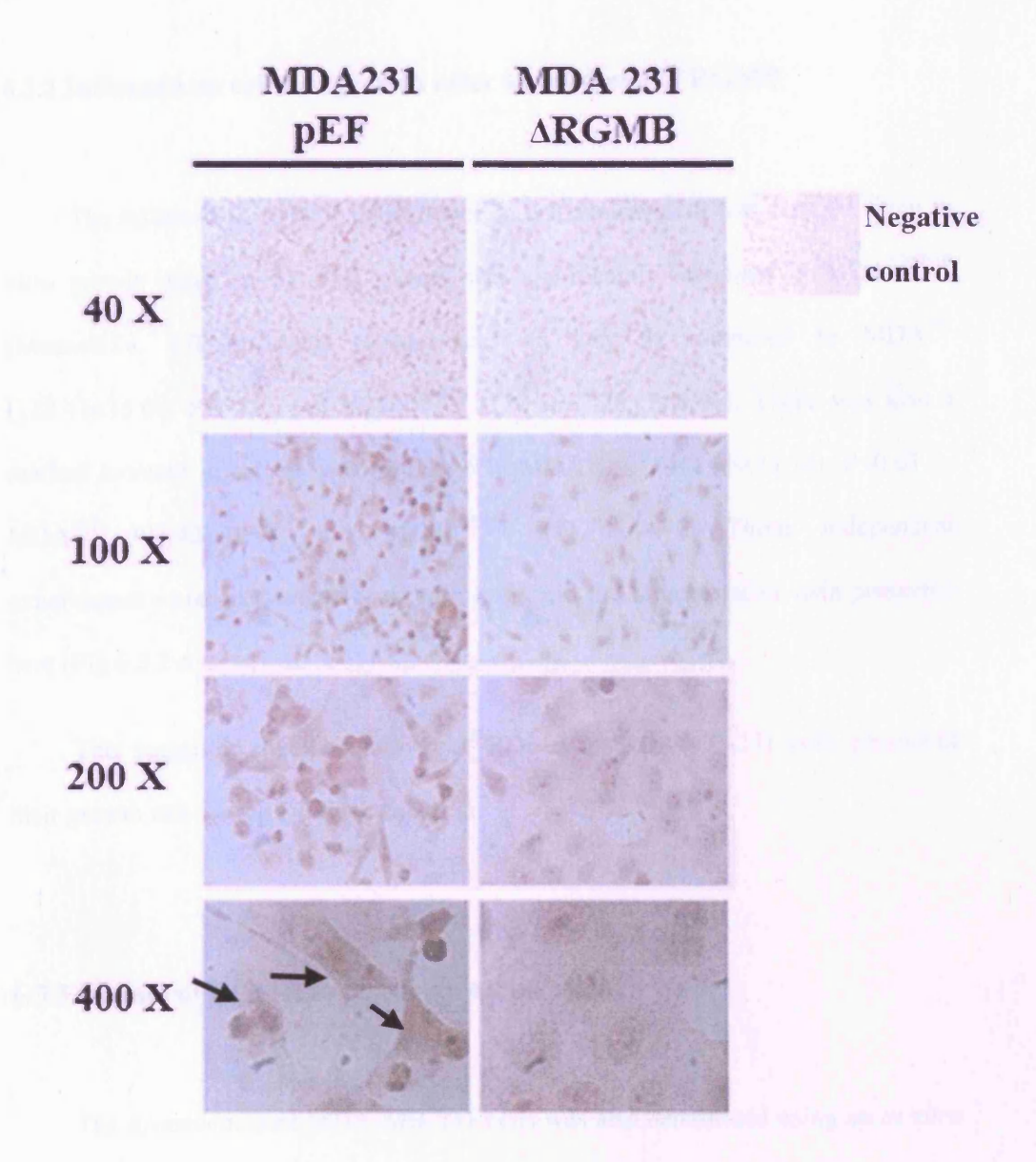


Figure 6.3.1.3 ICC staining of RGMB proteins in RGMB knockdown cells and pEF control cells. The Staining of RGMB was reduced in RGMB knockdown cells, compared to control cells. Arrows indicate the staining of RGMB in the cytoplasm.

6.3.2 Influence on cellular growth after knockdown of RGMB

The influence of RGMB knockdown on cell proliferation was verified using *in vitro* growth assay (n=6). Cell growth was significantly increased in MDA $^{\Delta RGMB}$ (Mean±STd. 170.92±34.90) (absorbance) on Day 3, compared to MDA WT (128.41±15.07, P=0.02) and MDA $^{pEF/His}$ (127.66±7.28, P=0.01). There was also a marked increase in cell growth on Day 5 in MDA $^{\Delta RGMB}$ (461.65±75.16), P<0.01 vs MDA WT 303.43±48.07 and MDA $^{pEF/His}$ 311.74±44.72. Three independent experiments were performed (each with n=6) and the representative data presented here (Fig.6.3.2 A).

This suggested that knockdown of RGMB in MDA-MB-231 cells promoted their growth rate during 5 days incubation.

6.3.3 Impact of RGMB knockdown on invasion in vitro

The invasiveness of MDA-MB-231 cells was also determined using an *in vitro* invasion assay after knockdown of RGMB (n=6). The loss of RGMB had no significant effect on the invasiveness of MDA-MB-231 cells. Although the number of cells invaded for MDA^{ΔRGMB} (Mean±STd. 176.33±33.08) was increased, compared to MDA^{PEF/His} (138.67±94.51), the increase was not reached statistical significance (P=0.54) (Fig.6.3.2 B). The increase of invasion in RGMB knockdown cells was also not significant comparing with the MDA-MB-231 wild type cells.

6.3.4 The influence of RGMB knockdown on adhesion

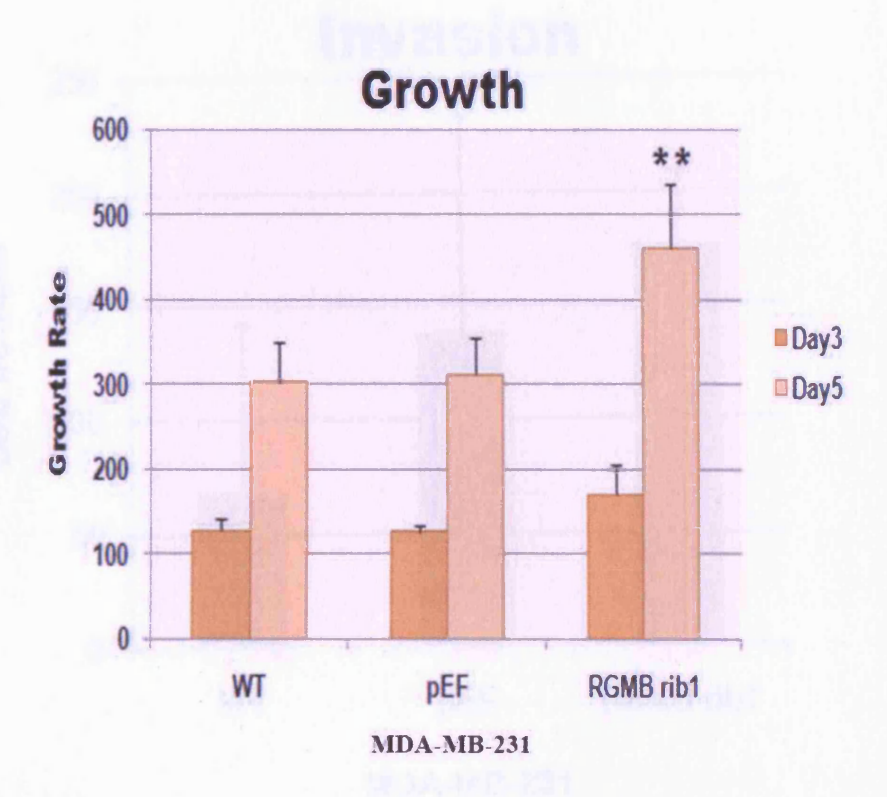
The effect of elimination of RGMB in MDA-MB-231 cells on cell-matrix adhesion, was assessed using an *in vitro* adhesion assay (n=6). (Fig.6.3.2 C). The absorbance of adhered MDA^{ΔRGMB} cell was significantly increased (1.33±0.15), compared to MDA^{pEF/His} (0.85±0.09) (p<0.001). The absorbance of RGMB knockdown cells was higher than it in wild type cells (0.76±0.16), which was also significant.

Moreover, the ability of MDA ARGMB cells to attach to the electrode surface was also faster than control cells, using the EICS-based attachment assay, however, the increase was not as significant as the cell-matrix assay (Fig.6.3.2 D left). When comparing the MDA-MB-231 pEF with RGMB knockdown cells at the final time point, the resistance of RGMB knockdown cells (Mean ± SEM 225.258±42.25) is higher than pEF control cells (168.275±22.62), although the increase did not reach statistical significance, as p=0.055.

6.3.5 The effect of RGMB knockdown on migration assay

The reduced RGMB expression was found to affect the mobility of MDA-MB-231 cells in the wounding assay (Fig.6.3.2 E). The healing and migration speed of MDA^{ΔRGMB} after wounding (the middle of the pictures) was obviously higher compared to the control cells (Fig.6.3.2 E left). More than three points at the front

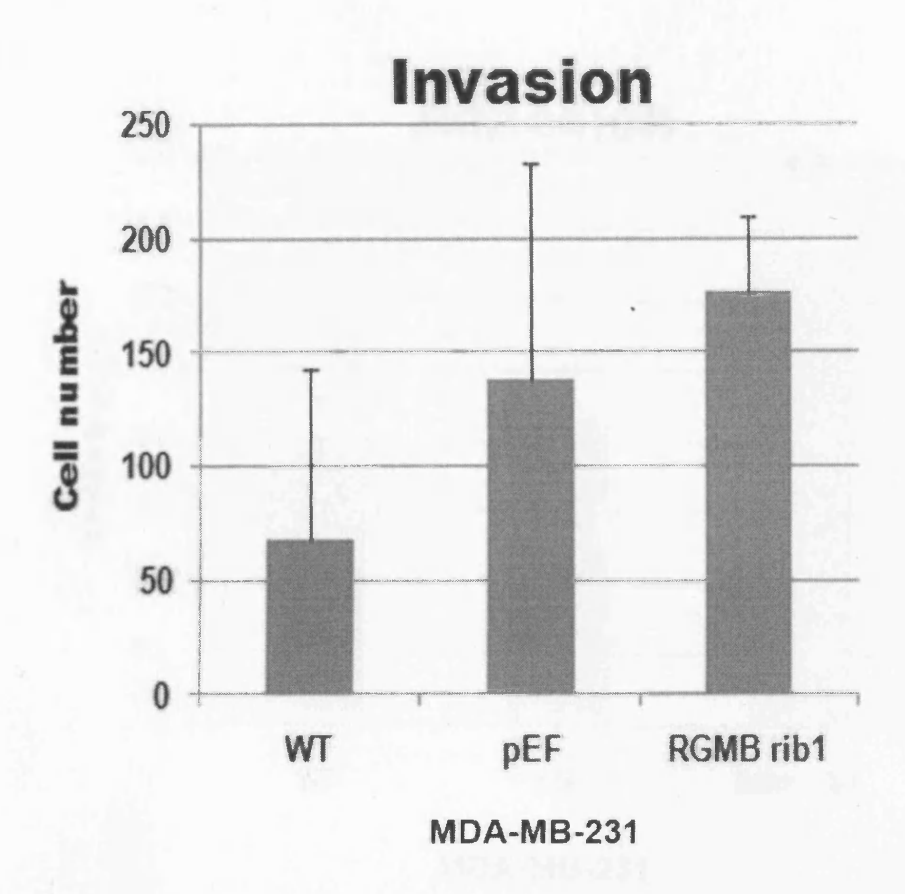
edge were measured under microscope (Fig.6.3.2 E right) and converted to the migrated distance based on the Time 0. The MDA $^{\Delta RGMB}$ cells migrated 83.89 μm at the final time point (120 minutes) while the highest migration distance of pEF control cells was 24.93 (p=0.005). The experiments were repeated three times and the representative data was displayed here.



	Mean (D3/D5)	St.D (D3/D5)	P value (vs RGMB KO, D3/D5)
RGMB rib	170.92/461.64	34.90/75.16	750
pEF	127.65/311.74	7.28/44.72	0.020/0.002
WT	128.41/303.43	15.07/48.07	0.014/0.001

Figure 6.3.2 A RGMB knockdown on cell growth in breast cancer

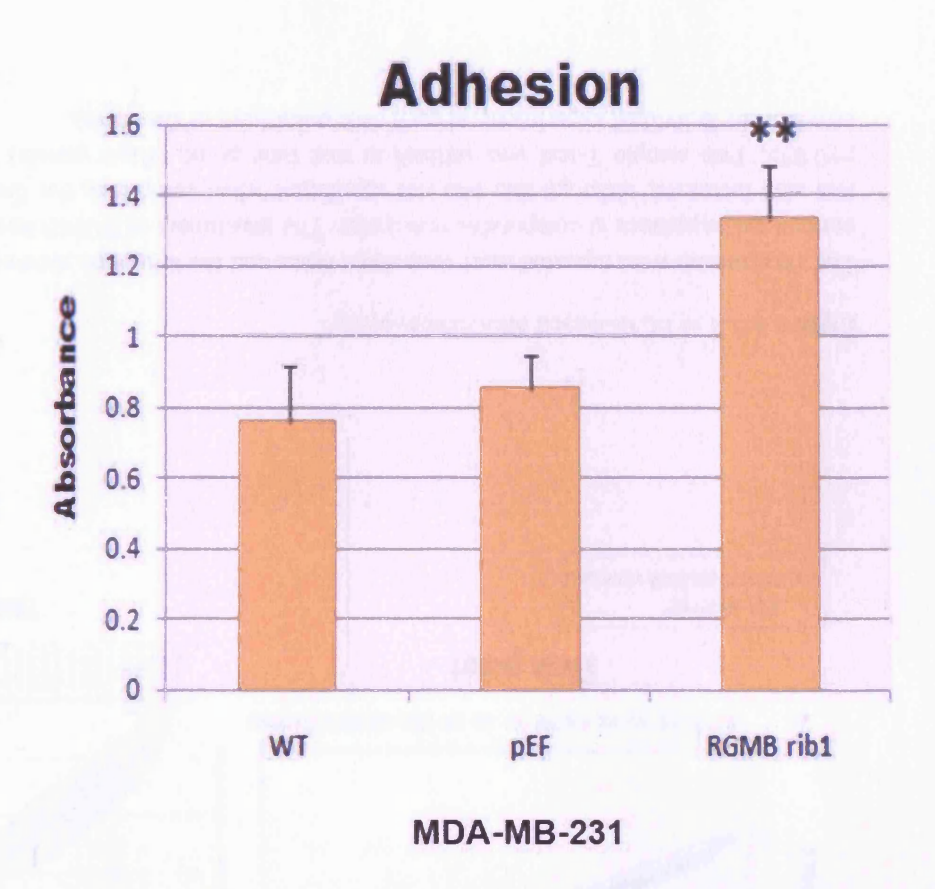
The growth rate of MDA231 cells over 3 and 5days period was increased after the loss of RGMB, compared to wild type and empty plasmid control cells. Table on the bottom displays statistical information of the analyses. The growth rate was calculated based on the data of Day 0. Three experiments were carried out and representive data shown. Two-sample T-test was used to determine significance levels.



	Mean	St.D	P value (vs RGMB rib)
RGMB rib	176.33	33.08	
pEF	138.67	94.50	0.53
WT	67.33	75.44	0.06

Figure 6.3.2 B RGMB knockdown on invation of breast cancer cell.

No significant difference was seen between the invasiveness of the control cells and RGMB knockdown cells. The number of cells invaded through the matrix has no significant differences between the RGMB knockdown and control cells. Table on the bottom displayed statistical information of the analyses. Three experiments were carried out and representive data shown. Two-sample T-test was used to determine significance levels.



	Mean	St.D	P value (vs RGMB rib)
RGMB rib	1.33	0.15	
pEF	0.85	0.09	0.000
WT	0.76	0.16	0.000

Figure 6.3.2 C RGMB knockdown on matrix adhesion of breast cancer cells.

The adhesive capacity was markedly increased in RGMB knockdown cells, compared both to wild type and pEF control cells. Table on the bottom displayed statistical information of the analyses. Three experiments were carried out, and the representive data were shown. Two-sample T-test was used to determine significance levels.

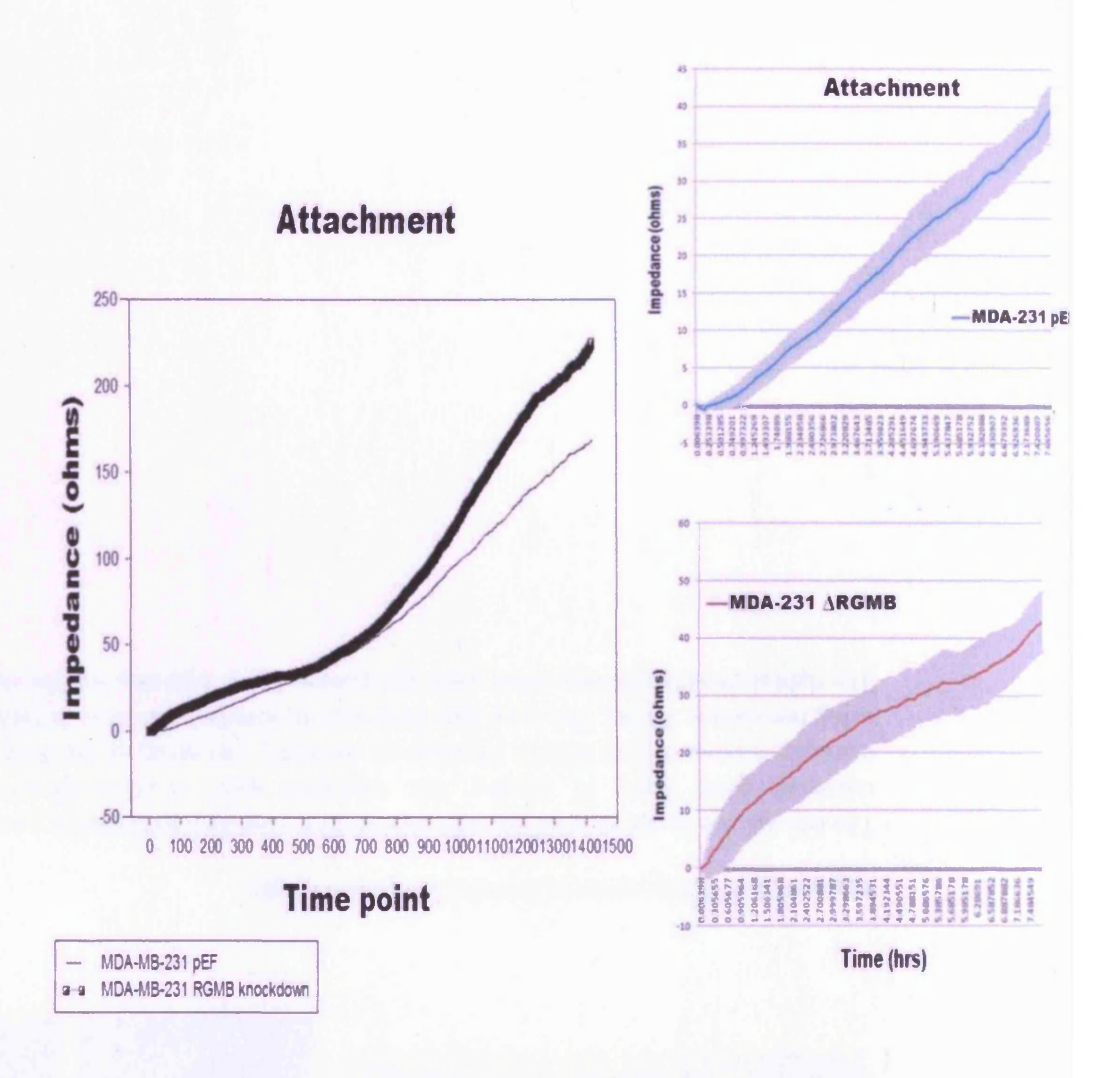


Figure 6.3.2 D ECIS-based attachment assay.

The experiments were repeated more than three times and the left graph showed the mean of normalized impedance at comparable time point. The attachment of RGMB knockdown cells was also increased, although this was not significant when comparing the final time point, p=0.055. Two sample T-test was utilised at that time point. (Right panels) The standard errors of the individual experiments at each time point (part of the curve).

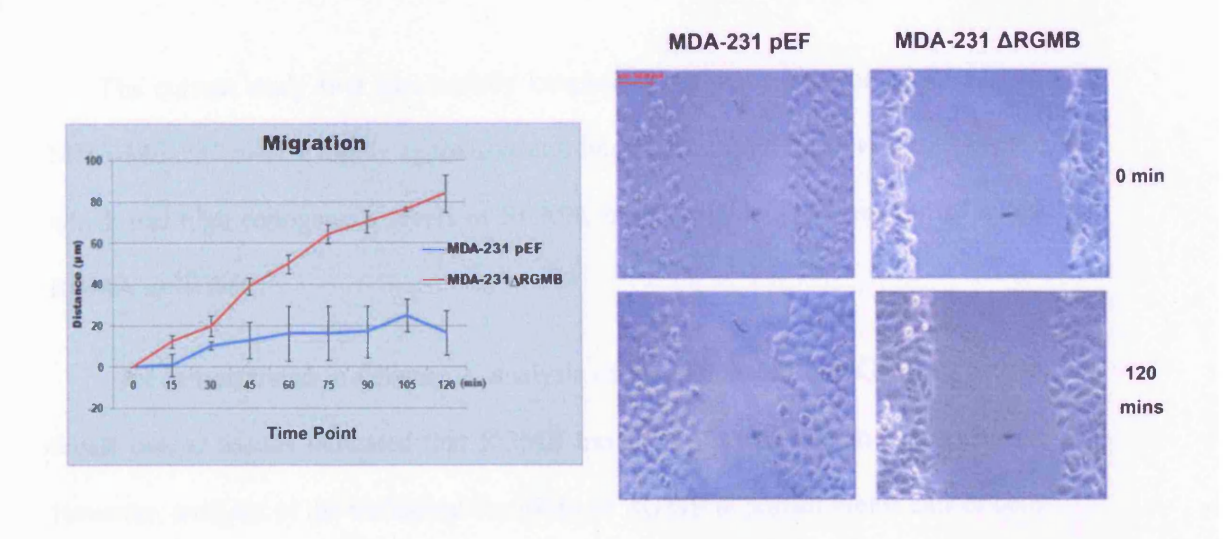


Figure 6.3.2 E Migration of RGMB knockdown cells.

The left showed the distance of the cells moved after wounding measured at more than three consistent points every 15 minutes. The migration speed of MDA-MB-231 cells was markedly increased after RGMB knockdown (p=0.005 comparing at the final time point, using two sample T-test). The error bars displayed the standard deviation at each time point. The right showed the pictures taken under microscope at the beginning and the end.

6.4 Discussion:

The current study first successfully knocked down the expression of RGMB in MDA-MB-231 cells, a highly aggressive cell line derived from invasive breast cancer, which had high endogenous levels of RGMB, but negligible/no expression of either RGMA or RGMC.

As demonstrated in Chapter 3, analysis of the expression of RGMB in human breast cancer tissues indicated that RGMB has a detrimental role in breast cancer. However, analysis of the biological functions of RGMB in human breast cancer cells as presented in this chapter contradicted the initial and clinical observations. It has been shown that the knockdown of RGMB promoted MDA-MB-231 cell proliferation, adhesion and migration capacity in vitro, but have little effect on cellular invasion. These results indicated that RGMB has an inhibitory control on some phenotypic traits cellular of MDA-MB-231 cells. RGMB might inhibit breast cancer cells growth and their ability to attach and migrate. The reasons for these differences remain unclear. It could be possible that there is involvement of an RGM antagonist or any other mechanisms in vivo, that controls the function of RGMB in human breast cancer, despite the higher levels of RGMB expression. Furthermore, RGMs are indicated the co-receptors for BMP proteins. It is quite possible that the impact of RGMs on cancer and cancer cells should be read together with the presence and the status of BMPs and indeed other co-activing proteins. It would be necessary therefore, to confirm the effect of RGMB in human breast cancer via further investigation of the mechanisms that might be involved.

Interestingly, the unique effect of RGMB in breast cancer showed a similar functional trait for RGMB as that observed in prostate cancer (shown in Chapter 5). It was therefore vital that further investigation of the mechanisms by which RGMs execute their functions be undertaken. The role of RGM in cancer might be associated with their participation in the BMP signalling pathways (Kanomata et al., 2009a) which have been shown to be involved in the development of metastatic breast cancer (Alarmo *et al.*, 2008). The mechanisms by which RGMs are regulated/regulate other proteins in the BMP pathways are demonstrated in the following chapter.

Chapter 7

The mechanisms underlying the impact of RGMB on cellular adhesion and motility in breast cancer

7.1 Introduction

As discussed in the previous chapters, knockdown of RGMB played a prominent role in breast cancer promoting the adhesion and motility of breast cancer cells (MDA-MB-231). In order to determine which mechanism may be related to these changes in cellular behaviour, the genes involved in these mediations in MDA ARGMB knockdown cells were further investigated.

Breast cancer and prostate cancer are mainly adenocarcinomas. Normal epithelium shows a strong and well-established network of cell-to-cell contacts that accounts for both the proper development and the functionality of epithelial structures. These cellular contacts greatly limit the ability of epithelial cells to move or migrate. During the last steps of the process of tumour development, epithelial tumour cells lose this restriction, with an associated loss of epithelial characteristics (Guarino et al., 2007). Epithelial-mesenchymal transition or transformation (EMT) is a series of changes in cells characterized by loss of epithelial phenotype such as cell-cell adhesion (E-cadherin), and acquiring mesenchymal phenotype, such as N-cadherin and smooth muscle actin (SMA) which leads to more aggressive behaviour of cancer cells. Several transcription factors such as Snail, slug and twist, and RhoC have been indicated in the procedure of EMT.

In the previous chapters, RGMB was also been shown to increase the adhesive ability of cell-matrix attachment. The loss of cell-cell contacts induced by EMT and the gain of cell-matrix adhesion facilitate the tumour cells to leave original tumour site and attach to matrix surface of metastasis site.

Focal Adhesion Kinase (FAK), also known as protein tyrosine kinase 2 (PTK2), is a focal adhesion-associated protein kinase typically located at structures known as focal adhesions, and is involved in cellular adhesion and the cell spreading process. Focal adhesions are multi-protein structures that link the extracellular matrix (ECM) to the cytoplasm cytoskeleton. Additional components of focal adhesions include paxillin, which is tyrosine-phosphorylated by FAK.

Considering the role of RGMB in cell-matrix adhesion, the present study investigated the regulation of these two candidate molecules (FAK and paxillin) which may be responsible for the increased adhesiveness of human breast cancer cells by RGMB knockdown. Furthermore, the expression of EMT markers and these transcription factors was examined in MDA-MB-231 wild type and transfected cells, to explore the involvement of EMT in the effects on cell mobility induced by RGMB knockdown. As the paramount role of Snai1 is its involvement in EMT and cancer metastasis, it was of great importance to discover that RGMB knockdown significantly increased the expression of Snai1 and to further investigate which signal pathway might be involved in this regulation.

RGMs have been reported to be co-receptors of BMPs (Kanomata et al., 2009a), while BMPs have been involved in cancer progression and bone metastasis. BMP7 has been reported to promote MDA-MB-231 cells migration and invasion (Alarmo *et al.*, 2009) and also associated with bone metastasis (Alarmo *et al.*, 2008). However, BMP7 has also been reported to inhibit EMT via Smad-3 (Buijs et al., 2007a; Cassar et al., 2009). The regulation on the genes (Focal adhesion and EMT transcription factors) by RGMB might be associated with their involvement in BMP signalling

pathways. The present study stimulates the cells with rh-BMP7 to investigate the regulation of RGMB knockdown on the target genes.

FAK has been reportedly regulated by TGF-β via Smad2/3 (Walsh et al., 2008). Snail also has been shown to be upregulated by TGF-β, possibly viaSmad2/3 or a non-Smad signalling pathway or via cooperation with Ras-MAPK signalling in NMuMG cells, although ERK/JNK is not involved (Miyazono, 2009). Therefore, in order to verify if the regulation of FAK and paxillin expression is through the Smad-3 dependent pathway, the smad-3 activation was blocked in the transfected cells by treatment with SIS3 (specific inhibit smad-3) (3μmol/ml, 30 mins) (Jinnin *et al.*, 2006). The expression and activation profile of downstream signalling molecules were examined.

7.2 Materials and Methods:

7.2.1 Materials

Recombinant protein BMP7 (rh-BMP7) was purchased from R&D Systems. Specific Inhibitor of Smad3 (SIS3) was purchased from Merck Chemicals Ltd.

7.2.2 Western blot and SDS-PAGE

Protein samples were loaded onto 8% or 10% polyacrylamide gel following SDS-PAGE, and probed with the specific primary (1:200), and the corresponding peroxidise-conjugated secondary antibodies (1:2000). Detailed procedure is described in section 2.4.

7.2.3 RT-PCR

RNA of the cells subjected to treatments was isolated following a protocol as described in Section 2.3. 0.5µg of the isolated RNA was used for each reverse transcription reaction to synthes cDNA, which was as the template for PCR procedures.

7.3 Results

7.3.1 Focal adhesion kinase (FAK) during ~RGMB mediated cell-matrix adhesion

The expression of FAK and paxillin in RGMB transfected cells (not treated) was examined, to confirm the pro-cell-matrix adhesion effect caused by RGMB knockdown. As seen in Fig.7.3.1.1A, FAK and Paxillin expression were obviously increased by the RGMB knockdown MDA-MB-231 cells, which were further confirmed at mRNA level as shown in Fig.7.3.1.1Bl. This indicates that the loss of RGMB lead to upregulating the expression of FAK and Paxillin, probably at the transcription level.

To further test the role of FAK and RGMB in cell-matrix adhesion, the cells were treated with rh-BMP7 (40ng/ml, 60mins). As shown in **Fig.7.3.1.2**, the total FAK and Paxillin expression were upregulated in the MDA^{ΔRGMB} cells, compared to the control. After treatment with rh-BMP7, the protein levels of these two molecules are to some degree increased, while the upregulation in MDA^{ΔRGMB} cells was enhanced. This suggests the increase of BMP7 might trigger the downstream signalling pathway which played positive role in the regulation on FAK expression.

After Smad-3 was blocked (SIS3 3μ M, 30mins) (**Fig.7.3.1.2**), the upregulation of FAK was not eliminated but was instead increased. The activation of FAK (phosphorylated-FAK) was also tested in the same experimental setting. It was interesting to note that the phosphorylated FAK, p-FAK, showed a similar pattern to

total FAK after treatment. This suggest that regulation of the target genes (FAK and Paxillin) by RGMB in breast cancer is unlikely through Smad-3 activation.

Therefore, I investigated the Smad-1 and Smad-3 phosphorylation in the transfected cells under these conditions. I found that RGMB knockdown slightly promoted Smad-1 and Smad-3 activation and that this effect is more obvious after treatment with rh-BMP-7 (40ng/ml, 30mins) (Fig.7.3.1.2, 7.3.1.3). However, after Smad-3 was blocked by SIS3 (3µM, 30mins), the phosphorylation of Smad-1 in RGMB knockdown cells was markedly increased, compared to control cells (Fig.7.3.1.3), while the Smad-3 pathway was partially maintained by RGMB knockdown (Fig.7.3.1.2). This indicated that BMP-7 might have the ability to activate both Smad-1/5/8 and Smad-3 pathways, by the participation of RGMB knockdown. Altogether, when the Smad-2/3 pathway was blocked, RGMB knockdown facilitated BMP signalling through the Smad-1/5/8 dependent pathway.

The activation of Smad-1 after blocking of Smad-3 was consistent with the pattern of upregulation of FAK and Paxillin in SIS3 treated RGMB knockdown cells. Taken together, the activation of Smad-1 signal pathway by RGMB knockdown might be related to the stimulated FAK and Paxillin expression and activation. Additionally, the Smad-2/3 pathway triggered by BMP might not have significant effect on FAK and Paxillin, as there was no obvious reduction in FAK and Paxillin levels after Smad-3 was blocked (comparison between the MDA-MB-231^{ΔpEF/His} cells).

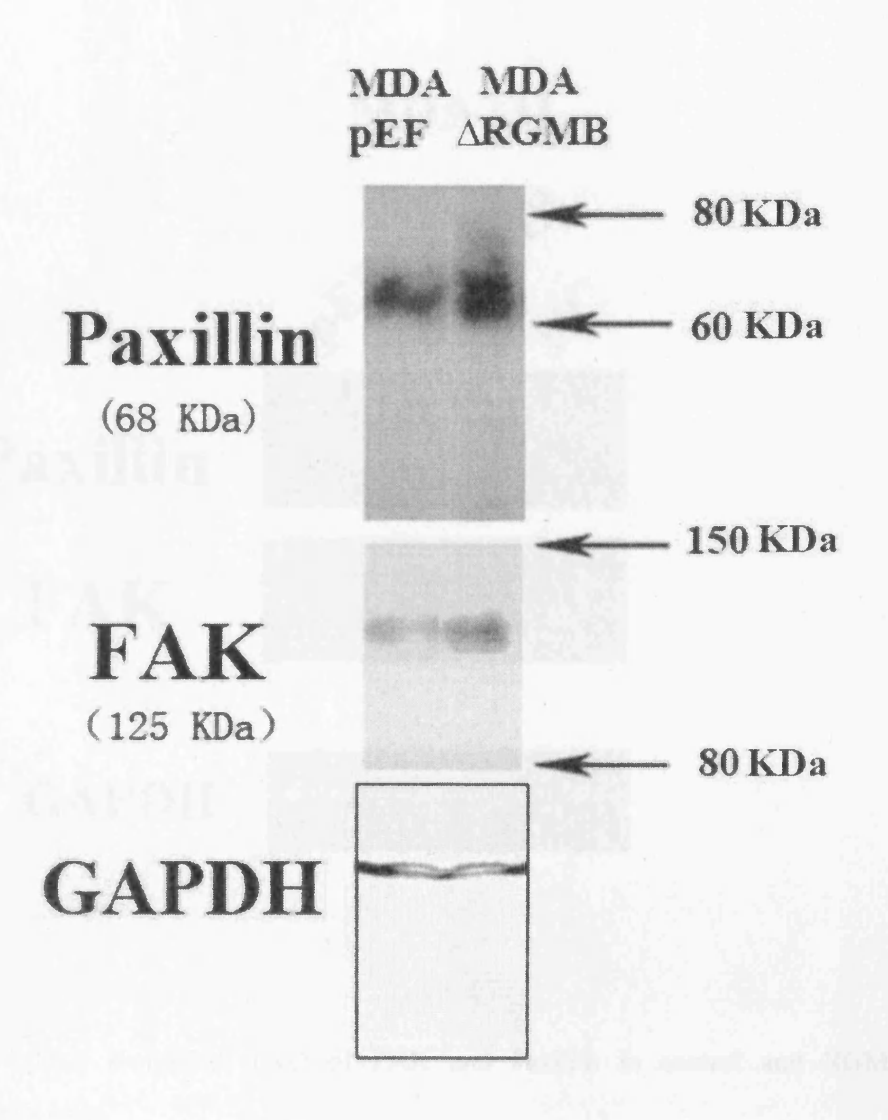


Figure 7.3.1.1A The protein level of FAK and Paxillin in MDA231 cells transfected with empty plasmid and RGMB ribozyme.

The Paxillin and FAK protein levels were upregulated in RGMB knockdown cells. The arrows on the right showed the position of ladders.

Paxillin FAK

GAPDH

MDA231

Figure 7.3.1.1 B mRNA level of FAK and Paxillin in control and RGMB knockdown cells.

The conventional PCR result confirmed the RGMB knockdown induced the expression of FAK and Paxillin from mRNA level. NC: negative control.

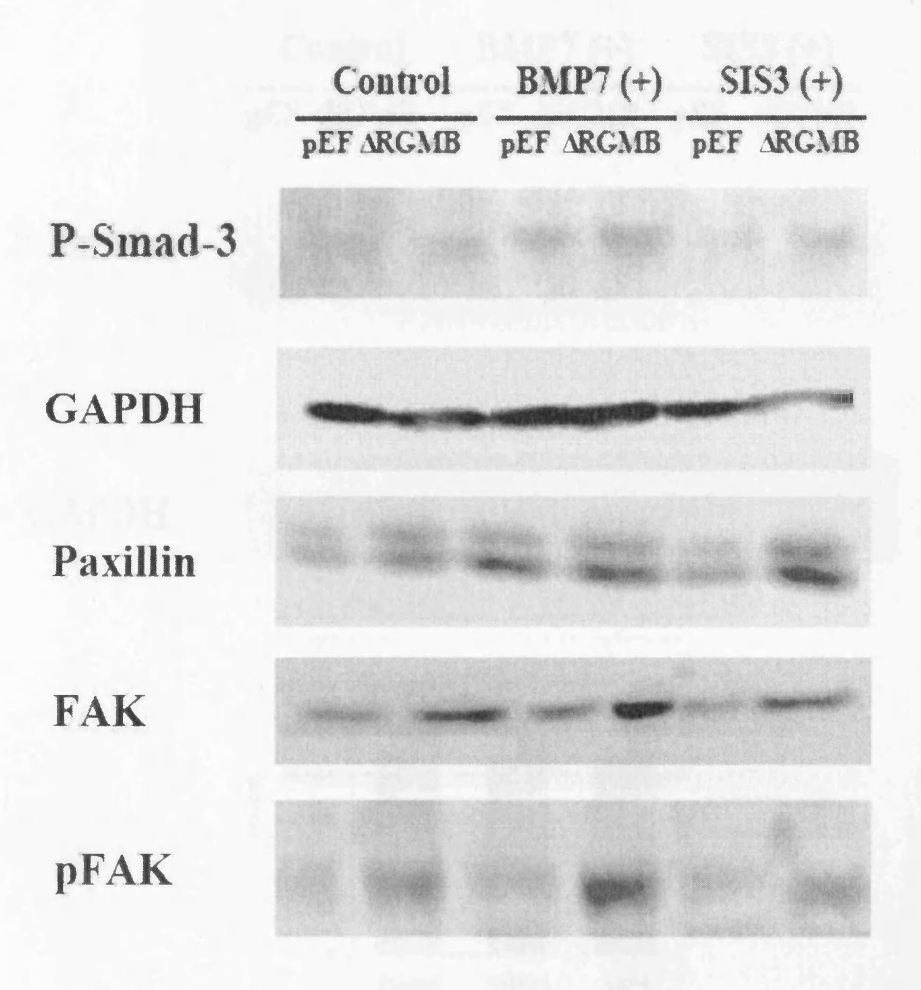


Figure 7.3.1.2 The pattern of activated Smad-dependent pathway molecules in control and RGMB knockdown cells and the association with FAK and Paxillin expression.

The Smad-3-dependent pathway was activated by stimulation of BMP7 (40ng/ml, 30mins), which could be blocked by SIS3 (3 μ M, 30mins). The upregulation of the expression of FAK and Paxillin and phosphorylated FAK (P-FAK) by RGMB knockdown was partially enhanced after BMP7 treatment (40ng/ml, 60mins)

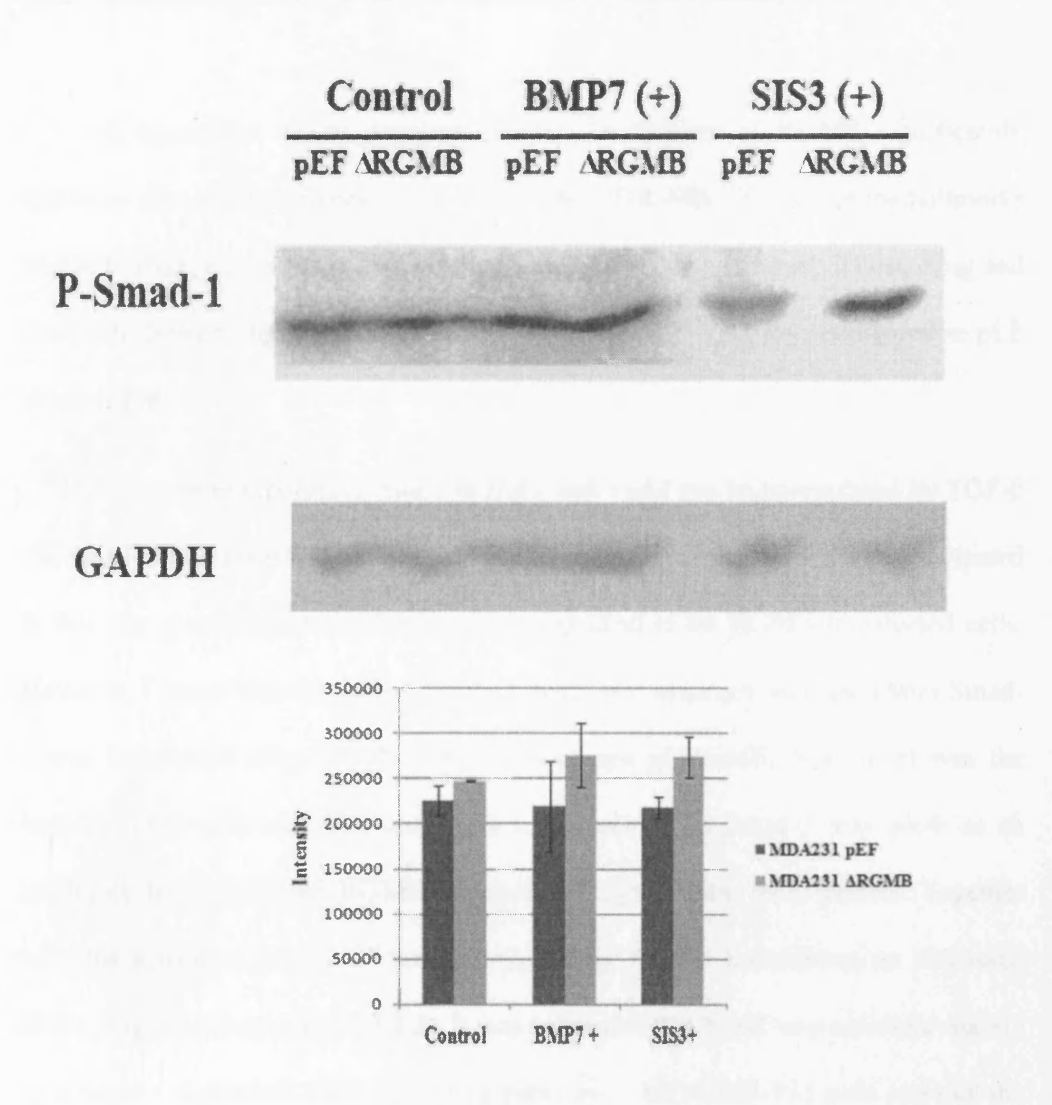


Figure 7.3.1.3 Activated Smad-1 levels in the transfected cells with treatment.

The activated Smad-1 level was upregulated in RGMB knockdown cells and this is enhanced in cells exposed to BMP7 (40ng/ml, 30mins) alone or with Smad-3 inhibitor (SIS3). This indicated the RGMB knockdown resulted in an enhanced Smad-1 dependent pathway. The graph shows the intensity quantification of P-Smad-1 against corresponding GAPDH bands.

7.3.2 Influence of RGMB on the molecular events leading to EMT

As mentioned in the previous chapter, knockdown of RGMB significantly increased the motility of breast cancer cell line MDA-MB-231, one of the hallmarks of EMT. Here, it was further shown that the EMT regulators Snai1, Twist, Slug and RhoC all showed higher mRNA level in MDA-MB-231^{ΔRGMB} cells compared to pEF control (Fig.7.3.2.1).

As the important role of Snail in EMT and Snail can be upregulated by TGF-β via Smad-2/3, to investigate whether Smad-3 signalling pathway of BMP participated in this, the phosphorylation of Smad-3 was blocked in the RGMB transfected cells. However, I found that the mRNA level of Snail was inversely increased after Smad-3 was inactivated (Fig.7.3.2.2). After knockdown of RGMB, Snaillevel was the highest in the cells with blocked Smad-3, indicating that Smad-3 may work as an inhibitory factor here and RGMB knockdown might inhibit these effects. Together with the activation profile of Smads induced by RGMB knockdown as discussed above (Fig.7.3.1.2 and Fig.7.3.1.3), it was suggested that Snail was activated mainly by a Smad-1 dependent BMP signalling pathway in MDA-MB-231 cells and that the activation can be further enhanced by RGMB knockdown after smad-3 was blocked.

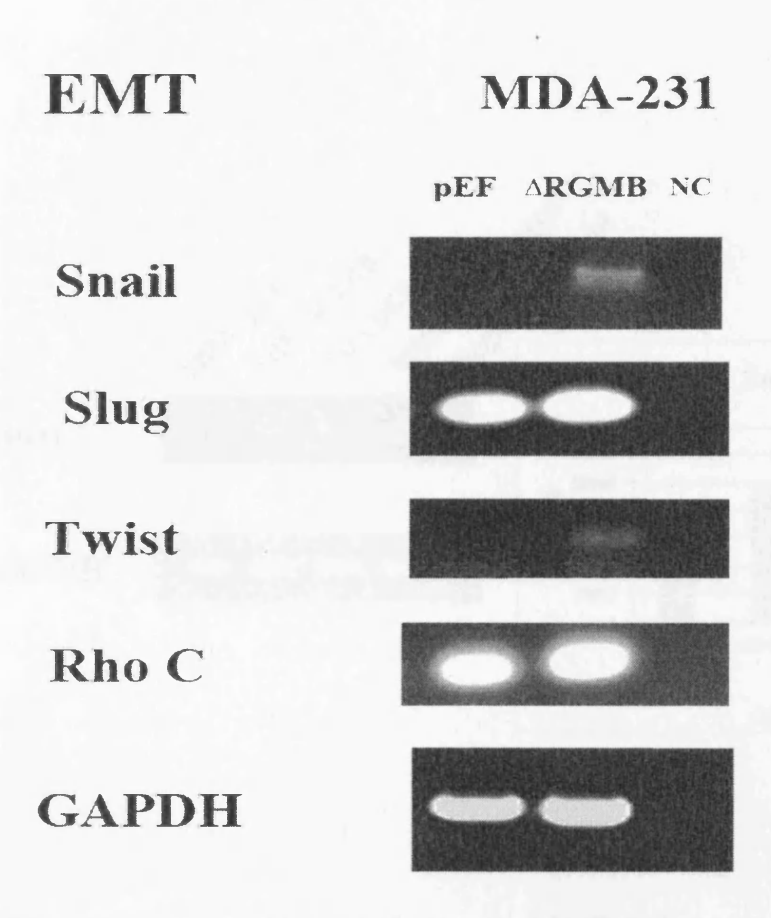


Figure 7.3.2.1 The expression of EMT regulators altered by RGMB knockdown in MDA-MB-231.

The Snail and Twist were significantly upregulated in MDA-MB-231 RGMB knockdown cells compared to the pEF control. NC: negative control.

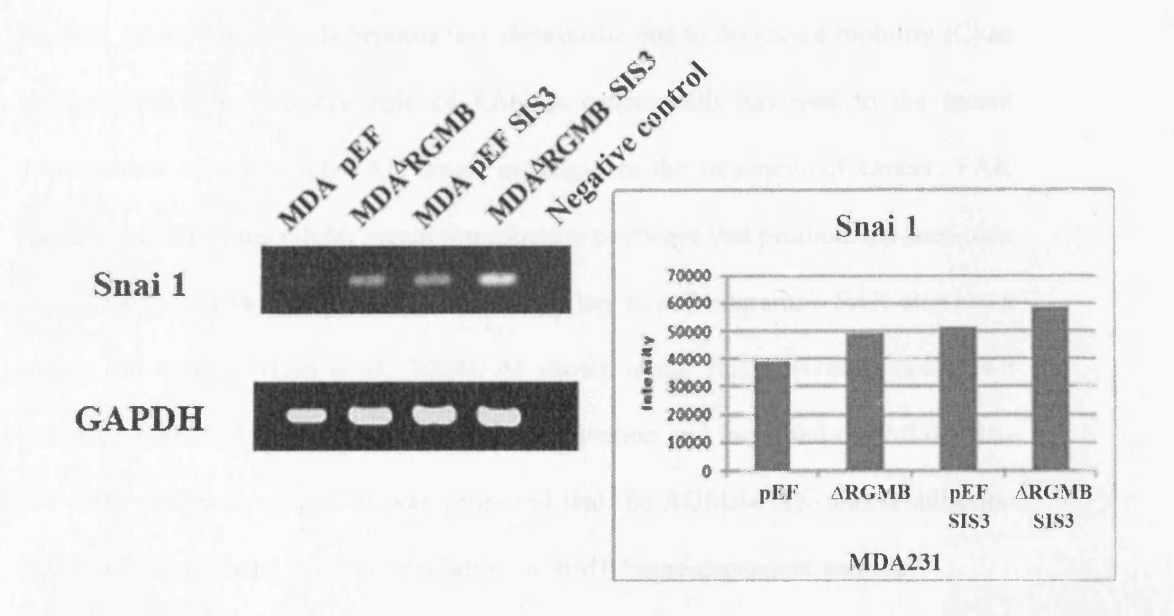


Figure 7.3.2.2 mRNA level of Snail in the transfected cells with treatment.

The RT-PCR (left) shows the Snai1 was upregulated 25% after RGMB was knocked down when calculating the intensity (right), which is enhanced after Smad-3 was blocked by SIS3 (upregulated 50%).

7.4 Discussion:

FAK and paxillin are known as integrin- and growth factor-associated tyrosine kinases promoting cell-matrix adhesion. It also has been shown that when FAK was blocked, breast cancer cells become less metastastic due to decreased mobility (Chan et al., 2009). The potential role of FAK in cancer cells has lead to the recent development of using anti-FAK small molecule in the treatment of cancer. FAK activation elicits intracellular signal transduction pathways that promote the turn-over of cell contacts with the extracellular matrix, a key to cell migration. FAK also has a role in cell survival (Lim et al., 2008). As shown in our study, RGMB knockdown increased FAK and Paxillin expression and activation and increased the MDA-MB-231 cell's ability to adhere. It was proposed that the RGMB-FAK-matrix adhesion link may be associated with the regulation on BMP Smad-dependent pathway.

RGMB knockdown seems to activate Smad-1 and (partially) Smad-3 pathways, which was enhanced by BMP7 stimulation. More interestingly, Smad-1 dependent pathway was switched on after Smad-3 was blocked.

There has been little work to date carried out on the regulation of FAK by BMPs. However, FAK expression has been shown to be induced by TGF-β via Smad-2/3 or P38 in IEC-6 cells (Walsh *et al.*, 2008). The increase of FAK expression in MDA^{ΔRGMB} cells was not blocked by Smad-3 silence in our study, which suggests the regulation on FAK is not due to the activation of Smad-3. However, we found that in the MDA-MB-231 cells, FAK (p-FAK) and Paxillin expression levels were elevated by BMP7. Moreover, RGMB knockdown mainly enhance the Smad-1

dependent pathway and had relatively weaker effect on the Smad-3 signalling. The FAK and paxillin expression might be upregulated by RGMB knockdown in breast cancer cells and enhanced by paracrine BMP7 and these might be linked to the activated Smad-1 by RGMB knockdown (See Fig. 10.1).

Breast cancer progression is associated with aberrant DNA methylation and the expression of genes that control the epithelial-mesenchymal transition (EMT), a critical step in malignant conversion. Snail, the transcriptional repressors of E-Cadherin was upregulated in the MDA-MB-231 ARGMB cells which enabled the cells to lose cell-cell adhesion and increase their motility, possibly contributing to their metastatic phenotype. Through the stimulation of cell migration and invasion, cellsubstrate adhesion, intravasation, and extravasation, as well as cell survival, tumour metastasis is also accelerated through immunosuppression during EMT induced by the transcription factor Snail. The preliminary data presented here indicate that knockdown of RGMB is also associated with a rise in Snail, a transcription factor also known to be key to the EMT process. This interesting observation adds further evidence to the role of RGMB in the regulation of cellular motility, which partly contributed to the EMT process. Although the Snail has been proved to be induced by TGF-β, there is no direct evidence to show that Smad-3 is required for the stimulation of Snail. As it have been shown here, in breast cancer cells MDA-MB-231, the upregulaiton of Snail is not blocked by the inactivation of Smad-3, but inversely increased. The mechanism involved might be similar to that in the regulation of FAK and Paxillin.

Altogether, RGMB knockdown regulated the expression of target genes (FAK, Paxillin, Snai1, c-Myc and Caspase-3 (see next Chapter)) greatly associated with involvement in BMP signalling pathway. The upregulation of FAK, Paxillin and Snai1 by RGMB knockdown, which possibly followed the activation of Smad-1 dependent pathway, not only promote cell adhesion, motility and mobility, but also contribute to the cascade of proteins involved in cell growth. It has been shown that FAK facilitates cell survival through enhanced p53 degradation (Lim et al., 2008) and involvement in regulation of Bcl-2 (Bouchard et al., 2008). Snai1 also regulates on cell survival in cancer cells (Emadi Baygi et al., 2010; Ulianich et al., 2008). The mechanisms underlying the cell growth regulated by RGMB knockdown and the signalling pathway RGMB involved in will be continually discovered in the following chapter.

Chapter 8

Mechanisms underlying the functions of RGMs in breast cancer proliferation

8.1 Introduction:

As discussed in the previous chapters, the knockdown of RGMB was found to significantly promote the proliferation of breast cancer cells (MDA-MB-231). Because of the prominent role played by RGMB especially in breast cancer, the MDA-MB-231^{ARGMB} knockdown cells were further investigated in order to determine what mechanism may be responsible for the changes in cellular behaviour observed.

RGMs were reported to be co-receptors of BMPs (Kanomata et al., 2009a). However, in my present study, the knockdown of RGMB has been shown to switch on Smad-1 dependent pathway and this was enhanced by stimulation with exogenous BMP7. BMP7 has been reported to protect MDA-MB-231 cells from apoptosis (Alarmo *et al.*, 2009) and also associated with bone metastasis in breast cancer (Alarmo *et al.*, 2008). However, it has also been reported to induce MDA-MB-231 cells death via Smad-3 (Buijs et al., 2007a; Cassar et al., 2009). Additionally, it has also been shown that BMP7 and oestrogen together can inhibit MCF-7 proliferation through suppressing p38 mitogen-activated protein kinase activation, but BMP7 alone does not alter cell growth (Takahashi *et al.*, 2008). Although the exact role/function of BMP7 in breast cancer remains controversial, the available evidence still indicates that BMP7 is implicated in the tumour cell proliferation and cell death. The mechanism of RGMs regulation on tumour cell proliferation by the participation in BMP signalling remains unclear as the dual role of BMPs played in cancer.

Apoptosis, a key event in regulation of cell population, may be involved in the effect of RGMB knockdown on cell growth was first investigated in current study. It has been proved that the marked effect was due to an anti-apoptotic effect with subtle regulation on cell cycle. As Caspase-3 is an executioner caspase indicative of end-stage apoptosis, the level of caspase-3 was examined in these transfected MDA-MB-231 cells. The gene (c-Myc) which might have effects on cell apoptosis and cell cycle was further investigated.

RGMB knockdown has been found to be involved in the BMP Smad-dependent signalling pathways, as described in the previous chapters. Additionally, the impact of RGMB on Smad-independent pathways was also investigated in this study, while the Smad-independent pathway has been shown to be associated with the regulation of apoptosis, where the ERK, p38 and JNK pathways amongst the key regulation events (Cocolakis *et al.*, 2001; Hassan *et al.*, 2005; Iyengar *et al.*, 2006; Kumar *et al.*, 2004; Yang *et al.*). The BMP Smad-independent pathway (MAPK pathway) is a chain activation, in which MAPK (as JNK, ERK1/2, P38) is activated by MAP2K, which is activated by MAP3K (as TAK1), which is regulated by MAP4K (mitogens, as ILP).

8.2 Materials and Methods:

8.2.1 Apoptosis analysis using Flow cytometry

In order to detect cells undergoing apoptosis, this current study used the Vybrant® Apoptosis Assay Kit (Invitrogen, Inc., Paisley, UK) which contains recombinant fluorescent conjugated annexin V (FITC annexin V) and Propidium Iodide (PI) solution. This was repeated three times and the number of apoptotic cells including both early (Q4) (FITC-annexin V stained) and late apoptotic cells (Q2) (both FITC-Annexin V and PI stained) in each sample was determined by using a flow cytometer and FlowMax software package. Detailed method is provided in Chapter 2, section 2.7.7.

8.2.2 Cell cycle analysis using Flow cytometry

For the cell cycle analysis, MDA-MB-231 cells transfected with control plasmid and RGMB ribozyme were collected, fixed, permeabilized with 75% ice-cold ethanol, and stored at 20 °C. The cells were resuspended in 1 ml lysis buffer (0.1% Triton X-100, 0.05 mg/ml propidium iodide, and 1 mg/ml RNase A) and after incubation for 30 min at 37 °C, the cells were analyzed in the flow cytometer. The count of cells in each sample was determined according to the staining of PI. This was repeated and the mean percentages of cells in G0/G1, S and G2/M phases were calculated.

8.2.3 Hoechst staining for apoptosis

The cells were incubated either with DMEM media containing 10% FCS or without serum for a period of 48 hours, before both the adherent cells and those floating in the culture medium were harvested and washed in PBS. The cell pellet was then resuspended in 20ng/ml Hoechst solution and incubated in darkness for 15 minutes. The cells were centrifuged and re-suspended with BSS before being counted and documented under a fluorescent microscope. The nucleolus was stained and a percentage for apoptotic cells was then calculated based on the cellular morphology changes happened during apoptosis including blebbing, loss of cell membrane asymmetry and attachment, cell shrinkage, nuclear fragmentation, chromatin condensation.

8.2.4 Immunoprecipitation of phosphorylated proteins

Duplicate sets of 3×10⁶ cells were grown in large 75cm³ flasks overnight. Serum starvation was then induced at 37°C for 2 days. Each of the duplicate flasks was then subjected to a separate treatment or maintain as control. 100µl of cell lysate solution lysed in 300µl SDS-free lysis buffer was taken to run GAPDH or probe total protein. 200µl was left for immunoprecipitation. The phosphorylated protein was immunoprecipitated by pho-S/T antibody and conjugated A/G protein agarose beads,

and then use for SDS-PAGE as western blot mentioned in previous chapters (Chapter4).

8.2.5 ICC

Cells were seeded at a density of 20,000 cells per well in 200µl of normal medium, in a 16 well chamber slide. The immunocytochemical staining was then performed following a protocol in Section 2.4.3. Dilution of primary antibody against c-Myc was 1:100.

8.3 Results:

8.3.1 RGM knockdown and its impact on cell growth and apoptosis

8.3.1.1 RGMB knockdown resulted in inhibition of apoptosis in cancer cells

The proportion of apoptotic cells was analyzed by using flow cytometry (**Fig. 8.3.1.1A**). Apoptotic index refers to total apoptotic population including both early apoptotic cells (Q4) and late apoptotic cells (Q2). There was only a small proportion of apoptotic cells seen in both MDA^{ΔRGMB} cells (6.47%) and MDA^{PEF/His} (8.39%) control cells under normal culture condition, i.e. in DMEM supplemented with 10% FCS. However, a remarked difference in apoptosis between these cells was seen after 48 hours serum starvation. MDA-MB-231^{ΔRGMB} cells had a far smaller proportion of

apoptotic cells (8.22%) compared to that of control cells (27.84%) which had more apoptotic cells induced by serum starvation (**Fig.8.3.1.1A**). This was further confirmed by counting apoptotic cells after Hoechst staining, in which MDA-MB-231^{ARGMB} cells under serum starvation demonstrated a significant decrease in apoptotic population, p<0.05 compared to the control (**Fig. 8.3.1.1B**).

8.3.1.2 The effect of RGMB knockdown on cell cycle

To further understand the mechanism(s) of RGMB knockdown stimulated tumour cell growth, Flow cytometry was also used to investigate the cell cycle of these cells.

The **Fig.8.3.1.2** displayed the cell distribution of MDA-MB-231 pEF and RGMB knockdown cells in G0/G1 (peak1) and G2+M (peak2) phases. The S, G2 and M phases represent the cell ability to propagate. There is a trend of reduction of G0/G1 phase in RGMB knockdown cells (63.77%), compared to pEF control cells (64.62%). However, this was not significant (p=0.39). The Flow cytometry study indicated a non-significant effect on cell cycle progression by RGMB knockdown (G0/G1 -64.62%, S – 9.92%, G2+M – 25.46% in control, and 63.77%, 10.15%, and 26.08%, respectively, in RGMB knockdown cells) (n=3).

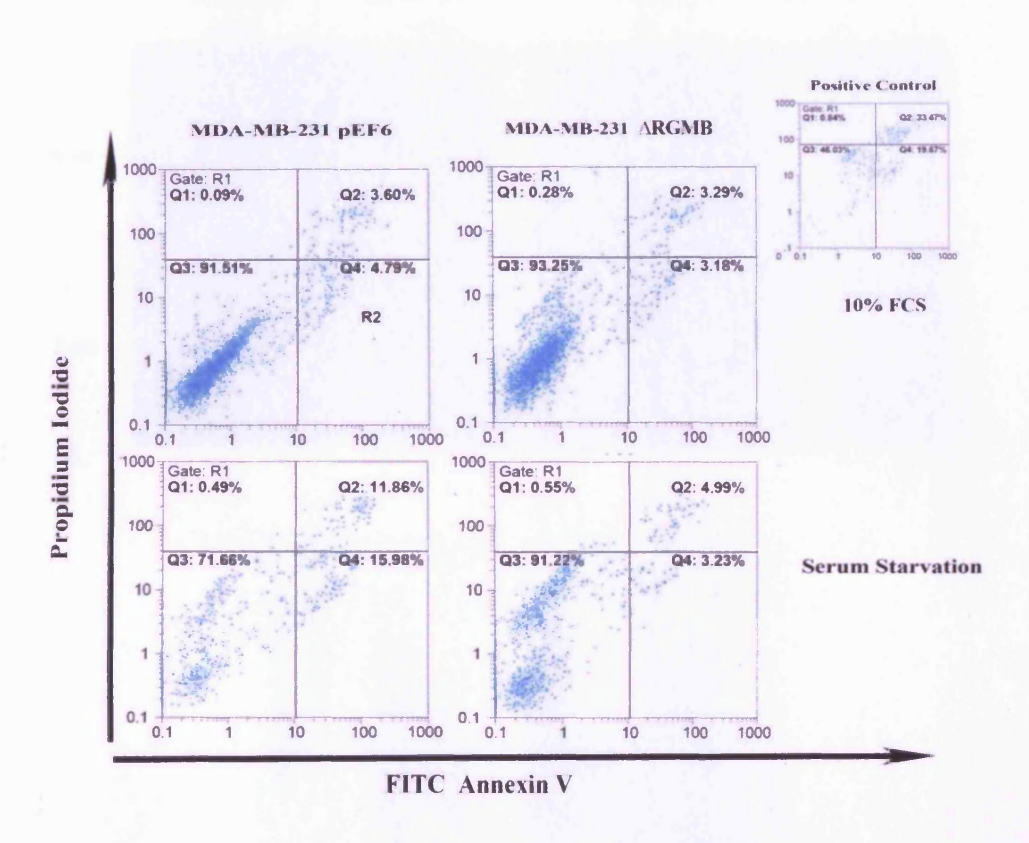
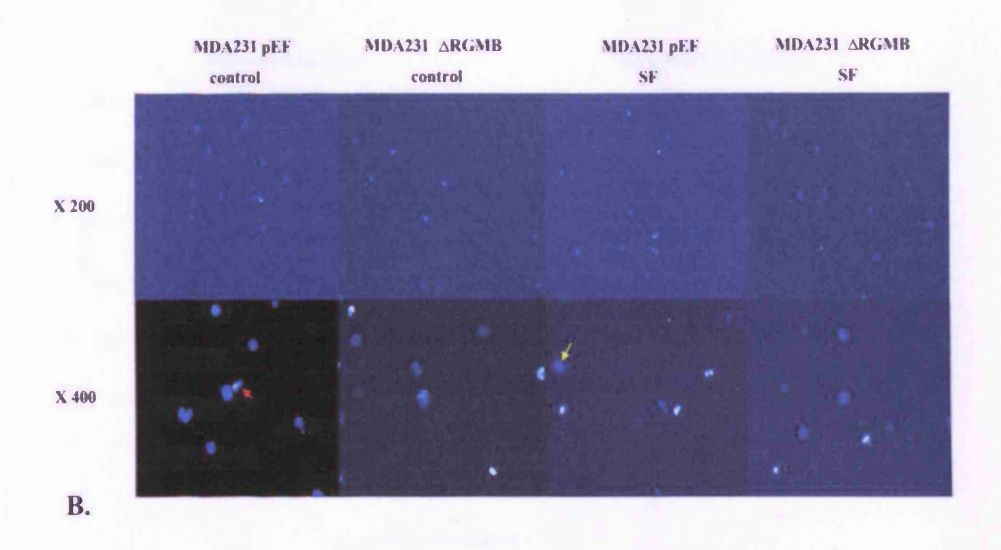


Figure 8.3.1.1A RGMB knockdown protected MDA-MB-231 cells survival from apoptosis.

The apoptotic population in MDA-MB-231 cells was analyzed using flowcytometry. The Q4 shows early apoptotic cells and Q2 shows cells with late phase apoptosis or death. The cells were incubated in media containing 10% FCS as controls. The positive control (top right) shows hydrogen peroxide induced apoptosis. There was a markedly smaller population of cells undergoing apoptosis in the RGMB knockdown cells (8.22%) (Q2+Q4) after 48 hours serum starvation, compared to the control cells (27.84%).



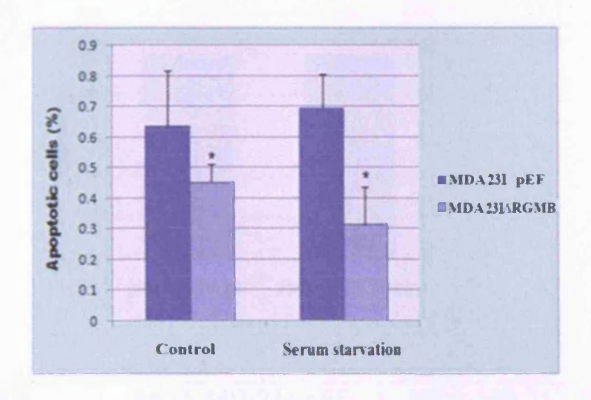
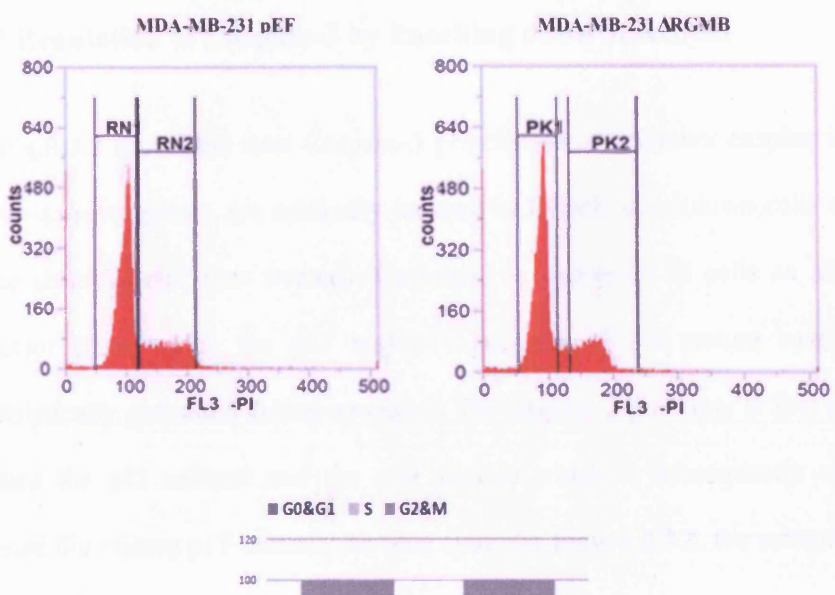
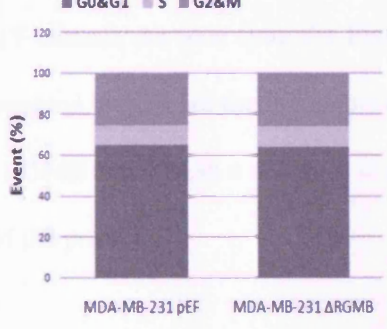


Figure 8.3.1.1B Analysis of apoptotic cells in MDA-MB-231 cells using Hoechst staining.

Yellow arrow heads pointed to the normal cells; red arrow heads pointed to the cells undergoing apoptosis characterized as the chromatin condensation, unsmooth nuclear surface, breaking into small apoptotic bodies. Apoptotic cells were counted and the bar graph presents the percentage of the apoptotic cells. There is a significant reduction of apoptotic cells in MDA $^{\Delta RGMB}$ (0.45±0.06) compared to the control cells (0.63±0.18), under normal condition (p=0.04). This reduction is more obvious in the serum free induced apoptosis (0.31±0.13 vs 0.69±0.11, p=0.000). Representative data were shown of three independent repeats. Error bars represent standard error of mean. SF: Serum Starvation





G0/G1	MDA-MB-231 pEF	MDA-MB-231 ΔRGMB
Ave	64.62%	63.77%
P value		0.39

Fig.8.3.1.2 Cell cycle analysis of RGMB knockdown cells.

Flow cytometry study indicated a non-significant effect on cell cycle progression by RGMB knockdown. The upper shows the two peaks representing G0/G1 and S/G2+M phase. The graph on the bottom shows the cell cycle distribution of MDA231 pEF and RGMB knockdown cells (G0/G1 -64.62%, S – 9.92%, G2+M – 25.46% in control, and 63.77%, 10.15%, and 26.08%, respectively, in RGMB knockdown cells) (n=3). (p=0.39)

8.3.2 Regulation of Caspase-3 by knocking down of RGMB

Fig.8.3.2 shows the total Caspase-3 proteins, an executioner caspase indicative of end-stage apoptosis, are markedly reduced in RGMB knockdown cells compared to the control cells, (not treated). Caspase-3 is expressed in cells as an inactive precursor from which the p17 and p11 subunits of the mature caspase-3 are proteolytically generated during apoptosis. The caspase-3 precursor is first cleaved to produce the p11 subunit and the p20 peptide which is subsequently cleaved to generate the mature p17 subunit. As seen from the Figure 8.3.2, the subunit P11 and P17 have almost disappeared, which are the indicators of activated caspase-3 enzyme. Therefore, the loss of RGMB resulted in a decrease in protein expression of caspase-3 and also activation of the protein.

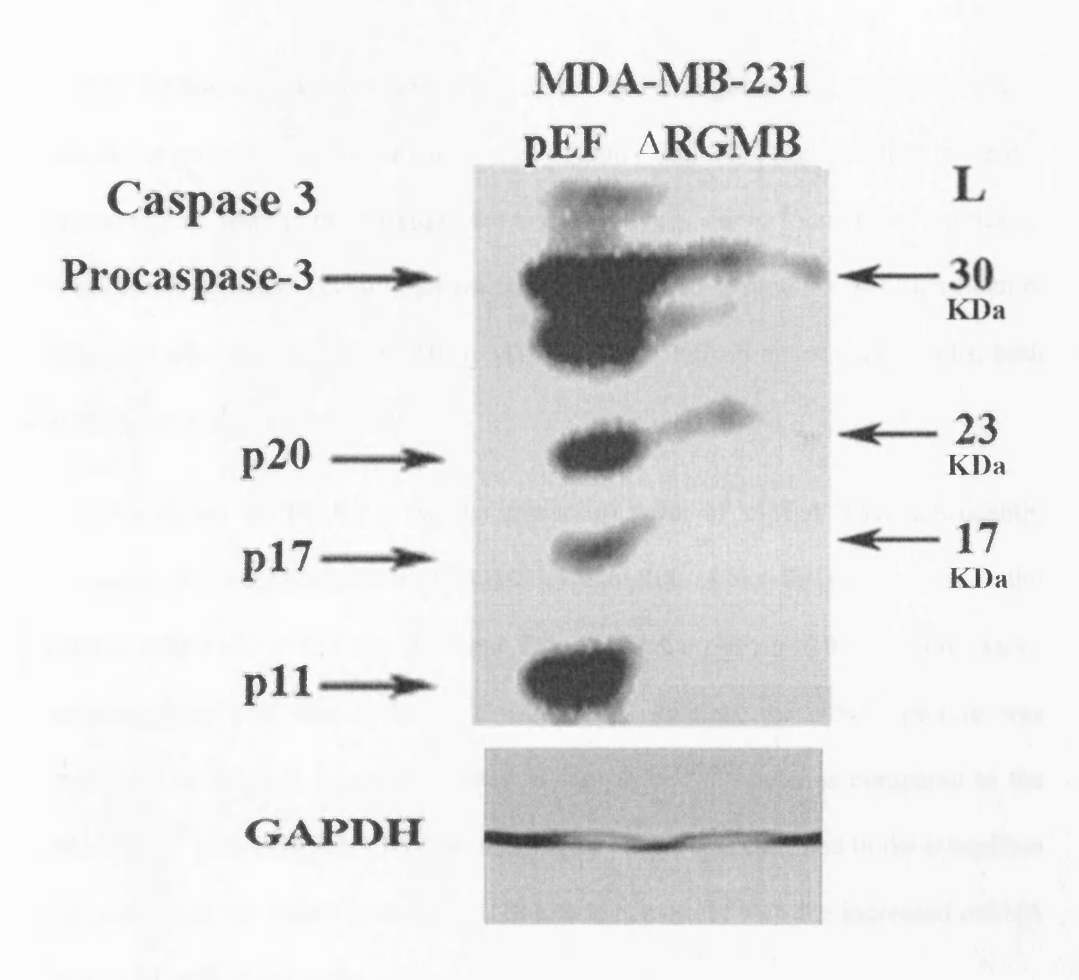


Figure 8.3.2 The protein level of caspase-3 in MDA-MB-231 pEF and RGMB knockdown cells.

The caspase-3 proteins which exists in the forms of procaspase-3 and subunits: p20, p17, p11 are all eliminated by knockdown of RGMB. The left arrows show the procaspase-3 and subunits. The right arrows displayed the ladder.

8.3.3 The gene correlated with cell growth regulated by RGMB knockdown

As RGMB knockdown was found to be able to regulate cell growth in breast cancer via protecting cells from apoptosis, I further examined expression of the genes related to cell death in these transfected cells. C-Myc is a gene found to be implicated in apoptosis and cell cycle to regulate cell growth and its expression was significantly increased after the loss of RGMB in MDA-MB-231 human breast cancer cells, both at the mRNA and protein levels.

As shown in **Fig.8.3.3 A**, the transcript level of c-Myc was significantly increased after the knockdown of RGMB (Mean±Std. 1670 ± 831), compared to the control cells (140 ± 112 for WT and 230 ± 129 for pEF, p<0.05 in both cases), determined by real time Q-PCR. Through ICC staining, the c-Myc protein was confirmed to be more intensely stained in the MDA^{Δ RGMB} cells as compared to the MDA^{Δ PEF/His} cells (**Fig.8.3.3 B**). The staining of c-Myc was confined in the cytoplasm and nucleus of the breast cancer cells. This was consistent with the increased mRNA level in RGMB knockdown cells.

Q-PCR

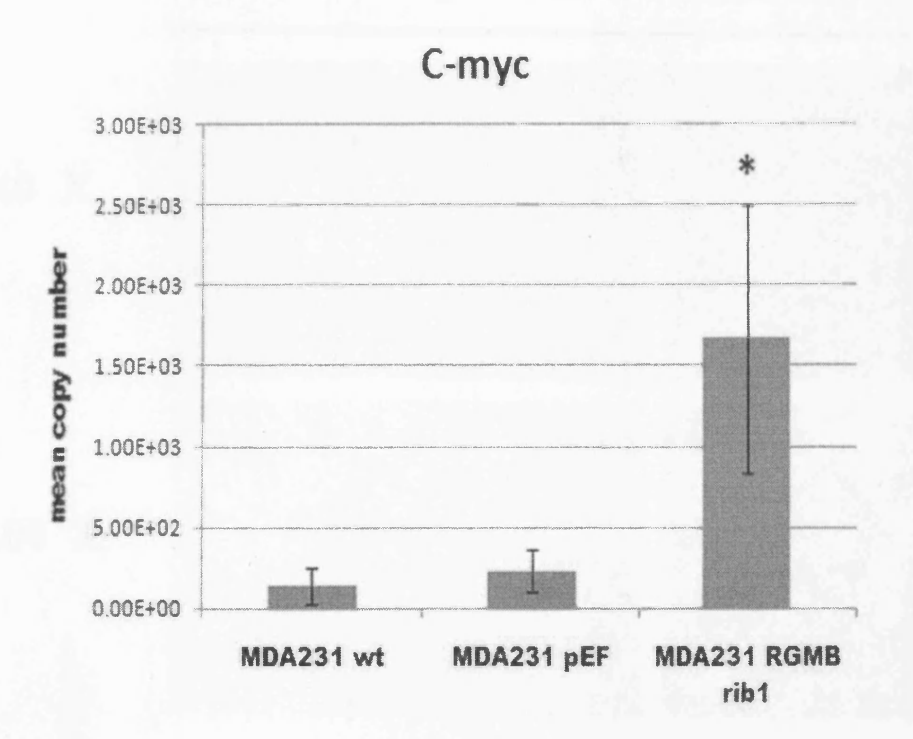


Figure. 8.3.3 A The expression of c-Myc is promoted in RGMB knockdown cells.

The result showed the mRNA level of c-Myc was significantly increased by the loss of RGMB (Mean±Std. 1670 \pm 831), compared to the wild type (140 \pm 112) (p=0.03) and pEF (230 \pm 129) (p=0.04). Two sample T-test was utilised here.

ICC staining

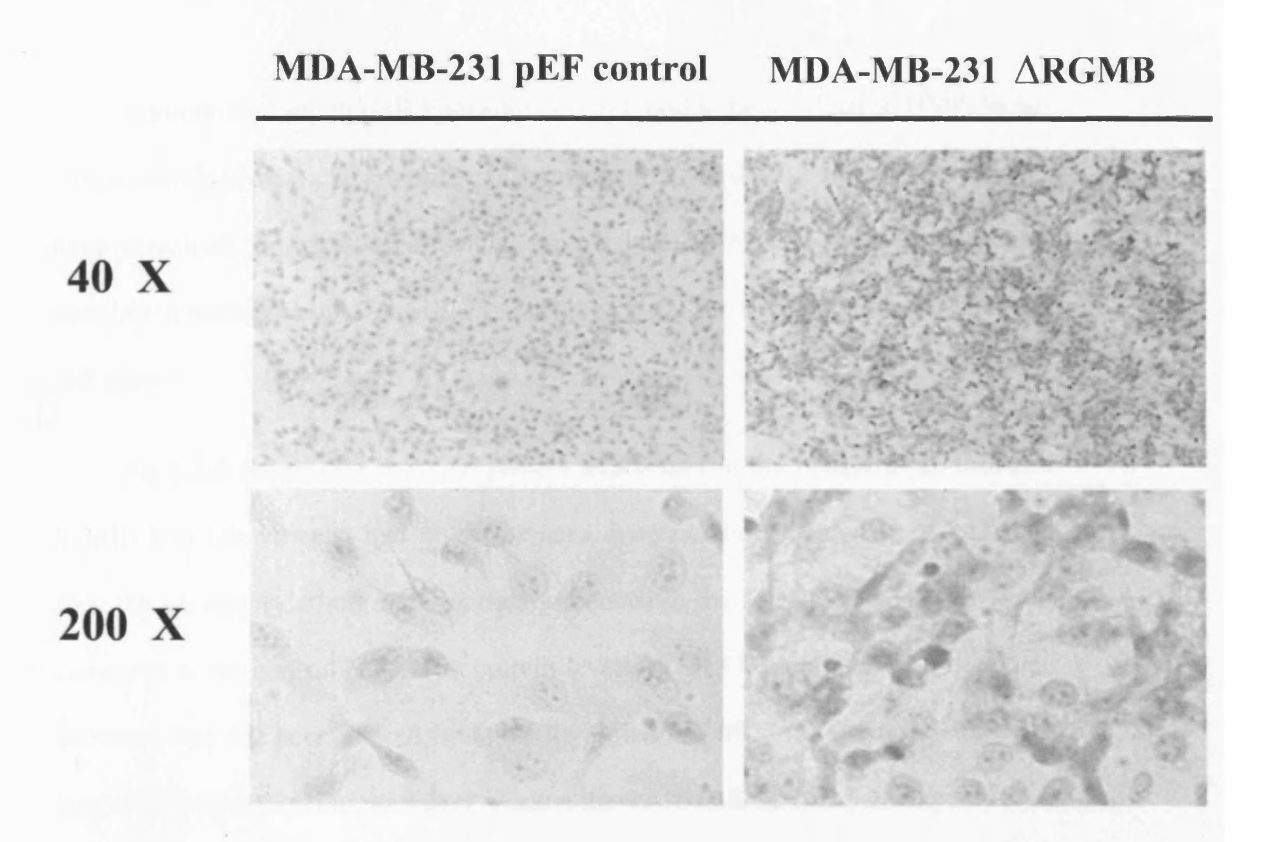


Figure 8.3.3 B ICC staining of c-Myc in RGMB knockdown cells.

ICC staining confirmed the c-Myc proteins were increased in MDA-MB-231 RGMB knockdown cells (right) compared to the control cells (left). The staining of c-Myc was mianly confined to the cytoplasma of the RGMB knockdown cells.

8.3.4 Influences on MAPK pathway

Additionally, the RGMB knockdown was found to be involved in BMP Smad-independent pathways, which has been implicated in cell death by previous studies. I have examined the total and activated protein level of MAPK pathway molecules here in the transfected MDA-MB-231 cells, to reveal the associations with effect on cell growth.

Fig.8.3.4 shows that the total protein expression in the lysates of control and RGMB knockdown cells had no differences, whereas the activated ILP, TAK and JNK (by phosphorylation) were markedly reduced in the MDA-MB-231 ΔRGMB cells, compared to the control cells. The protein levels of ERK1/2 and P38, both total and activated, had not been altered by knocking down RGMB. In the current study, the loss of RGMB appears to markedly weaken the TAK-JNK MAPK pathway and JNK is well known as its important role in cell apoptosis.

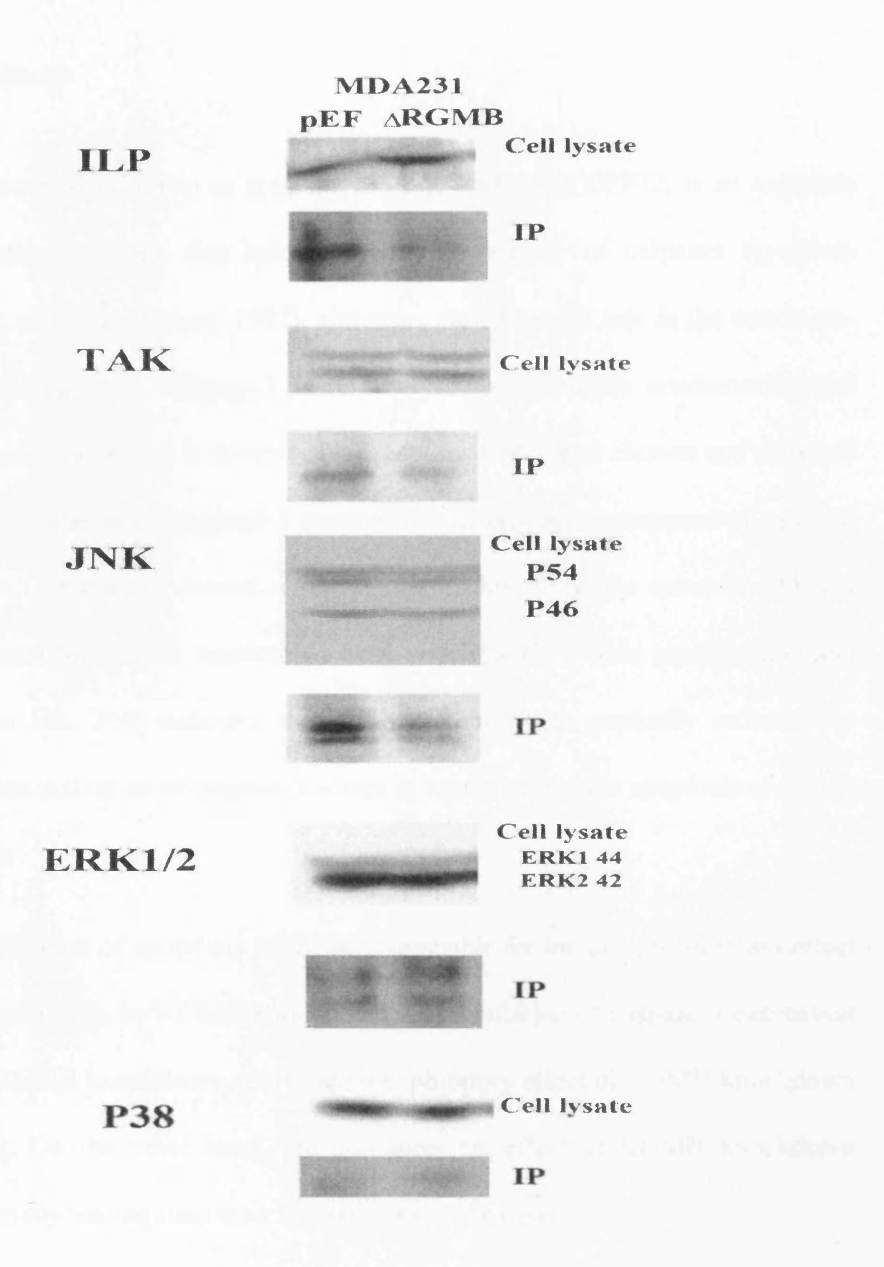


Figure 8.3.4 The MAPK pathway regulated by RGMB.

Each protein had been examined in both cell lysate and immnunoprecipatiant for identification of sering/thereionine phosphrylation. The results showed total proteins of these MAPK signaling molecules are not affected by RGMB knockdown. The phosphorylated protein of ILP, TAK and JNK was reduced after the loss of RGMB which indicated the activation of JNK pathway was inhibited without the effects on expression, while no significant alteration happened on ERK1/2 or P38 pathway.

8.4 Discussion:

Caspase-3, also known as apopain, SCA-1, Yama and CPP32, is an aspartate specific cysteine protease that belongs to the subfamily of caspases (cysteine-aspartic acid protease) (Cohen, 1997). Caspases play a central role in the execution-phase of cell apoptosis. Caspase-3 is responsible for chromatin condensation and DNA fragmentation, which is processed by caspases 8/9/10 and cleaves and activates caspases 6/7/9. The active caspase-3 enzyme is a heterodimer composed of p17 and p11 subunits (Fernandes-Alnemri *et al.*, 1994). In this study, the subunits P11 and P17 disappeared in RGMB knockdown cells with slightly visible procaspase-3 and P20 residues left. This indicated that RGMB knockdown markedly reduced the expression and activation of caspase-3 which in turn inhibited the apoptosis of MDA-MB-231 cells.

The inhibition of apoptosis might be responsible for the pro-proliferation effect on breast cancer cells by RGMB knockdown. The inhibition of caspase-3 expression induced by RGMB knockdown confirmed the inhibitory effect of RGMB knockdown on apoptosis. On the other hand, the anti-apoptotic effect of RGMB knockdown might be partially via regulation on the expression of caspase-3.

It has been recently shown that there is another type of cell death, known as paraptosis (Bredesen *et al.*, 2004). In paraptosis, the absence of ligand (as RGMA) induces self-activation of its receptor (as neogenin), by a mechanism still unknown, and the subsequent proteolytic processing of the receptor triggers apoptosis, which can be blocked by ligand binding. The RGM receptor--Neogenin is one of such

'dependence receptor's, which expose a pro-apoptotic region in the cytoplasmic domains and activate caspase-3, when their ligands being loss-of-function. This is contrary to the phenomena we observed in the transfected cells. Furthermore, I investigated neogenin mRNA levels in the transfected cells, however, there was no changes after RGM was knocked down. (Data not shown) Therefore, the pro-apoptosis effect might be caused by RGMB itself.

C-Myc is a strong proto-oncogene and works as a transcription factor in activating the expression of a great number of genes. For many years, c-Myc function has been linked to the control of cell-cycle progression (Steiner *et al.*, 1995) and to the inducement of apoptosis. However, increasing evidence now shows that c-Myc also stimulates cell growth (Schuhmacher *et al.*, 1999), and these two processes being regulated independently. It is very often found to be upregulated in many types of cancers and this upregulation was enhanced by RGMB knockdown in breast cancer cells, although there was no significant effect shown in cell-cycle analysis. The expression of c-Myc might still contribute to the promotion on cell growth caused by RGMB knockdown, as the effect of c-Myc is diverse and the mechanism is as yet unclear.

In response to both the extrinsic and intrinsic apoptotic stimuli, JNK plays an essential role through its ability to interact and modulate the activities of diverse proand anti-apoptotic proteins (induce BAX, inhibit Bcl2 and so on) (Dhanasekaran and Reddy, 2008). Through the coordinated regulation of the nuclear and mitochondrial events, JNK ensures the efficient execution of apoptosis. The activation of TAK1MKK4-JNK pathway was proved to result in apoptotic cell death (Yang *et al.*, 2004).

In the MAPK pathway, P38, ERK1/2 and JNK pathways all have effect in the regulation of apoptosis. Loss of RGMB mainly induced JNK pathway inhibition with little effect on other MAPK pathways. The repressed JNK pathway might also contribute to the negative regulation on cell apoptosis by RGMB knockdown, which might promote cell growth (see figure 10.1).

Furthermore, although c-Myc has been reported that it could be repressed by TGF-β via Smad-3 (Yagi *et al.*, 2002), there are also evidences to show c-Myc mediated apoptosis can be inhibited by the inactive form of JNK (APF) (Noguchi *et al.*, 2000). Which was consistent with this in this study, considering the less effect on Smad-3 induced by RGMB, c-Myc might be regulated through Smad-independent pathway by RGMB.

Additionally, there are also studies reported TGF-β and BMP signalling pathways have been involved in the regulation of cell growth in breast cancer via Smad-4, a common Smad required by both pathways (Forootan *et al.*, 2007; Ketolainen *et al.*; Leeper *et al.*; Wu *et al.*, 2003). Almost all these studies indicated the breast cancer cell proliferation is mediated by TGF-β via Smad-2/3 pathway, as a dual role in apoptosis (Ehata et al., 2007; Li et al., 2009a; Tan et al., 2009). Further investigation may elucidate coordinating role played by RGMB in Smad-1 and Smad-3 signal transduction

Chapter 9

Effect on BMP signalling transduction by RGMs knockdown in prostate cancer and consequent regulation on BMP responsive genes

9.1 Introduction:

As discussed in the previous chapters, the knockdown of RGMs was found to promote the proliferation, adhesion, motility and mobility of prostate cancer cells (PC-3). RGMB and RGMC knockdown significantly induced PC-3 cells' proliferation. RGMB knockdown further promoted cell mobility, and all the three RGMs showed significant impact on cell-matrix adhesion ability, which might contribute to prostate cancer metastasis. The impact of RGMA in prostate cancer was relatively weaker than RGMB and RGMC.

To reveal what mechanism(s) involved in the regulation of prostate cancer by RGMs, the level of one of the BMP target genes ID-1(DNA-binding protein inhibitor) was investigated in PC-3 cells transfected with RGM ribozymes, as the involvement of RGMs in BMP signalling and BMPs are key factors in prostate cancer and bone metastasis (Ye et al., 2007; Ying et al., 2003). ID-1 proteins belong to the helix-loophelix (HLH) transcriptional regulator family, and functions as an antagonists of basic HLH transcription factors by inhibiting their ability to bind specific DNA sequences within target gene promoters, thereby to negatively regulate cell differentiation (Norton, 2000). Additionally, they have been revealed to participate in tumour cell growth and promote cell survival in breast cancer and prostate cancer (Forootan et al., 2007). Including the effects on cancer cell proliferation, ID-1 was also reported to promote tumour cell invasion (Gautschi et al., 2008) activated by BMP2 and promote migration and invasion of prostate cancer cells activated by BMP6 (Darby et al., 2008).

BMPs were shown to be involved in prostate cancer and bone metastasis greatly through BMP-Smad dependent pathway (Brubaker *et al.*, 2004; Dai *et al.*, 2005; Ye *et al.*, 2008; Ye *et al.*, 2009). Secondly, ID-1 expression was proved to be regulated by BMPs through BMP-Smad-Id pathway in cancer (Gautschi *et al.*, 2008; Ohtani *et al.*, 2001; Ying *et al.*, 2003). To investigate whether the mediation of prostate cancer by RGMs was via BMP Smad-dependent signal pathway, I verified the expression and activation profile of BMP signalling molecules in RGMs knockdown cells.

9.2 Materials and Methods:

9.2.1 Western blot and SDS-PAGE

Duplicate sets of 3×10^6 cells were grown in large 75cm^3 flasks overnight and subjected to serum hunger for 2 hours and then treatment with rh-BMP7 (40ng/ml) for 30 minutes or no treatment. Cell lysates was collected and protein samples were subjected to SDS-PAGE and probed with the specific primary (1:200), and the corresponding peroxidise-conjugated secondary antibodies (1:2000). This is described in detail in section 2.4.

9.2.2 RT-PCR

Cells treated with medium containing rh-BMP7 (40ng/ml, 30mins) or normal growth medium were collected. RNA isolation was carried out as described before. (Section 2.3) 0.5µg of the isolated RNA was converted into cDNA which was then used as a template for PCR.

9.2.3 Q-PCR

The real time quantitative PCR (Q-PCR) was carried out to determine the levels of ID-1 transcripts in the control and RGM knockdown cells. The protocol and primers used for ID-1 quantitation and housekeeping GAPDH were listed in section 2.1.2 and 2.3.5.

9.2.4 Immunofluorescent staining

Cells were seeded in normal medium and subjected to treatment, in a 16 well chamber slide (Lab-Tek, Nagle Nunc Int., Illinois, USA). Specific staining was then undertaken through the addition of a specific primary antibody against ID-1 (1:200) and appropriate FITC conjugated secondary antibody (1:150). After this protocol had been completed, the cells were covered with Fluoro-save (Merck Chemicals Ltd., Nottingham, UK) before visualizing any staining under a fluorescent microscope (Olympus, Japan) using a GFP filter. The experiment was repeated three times and representative data is presented.

Statistical analysis

Normally distributed data was analyzed using the two sample T-test while nonnormally distributed data was analyzed using the Mann-Whitney and Kruskal-Wallis tests.

9.3Results:

9.3.1 The regulation on BMP target gene (ID-1) of RGMs knockdown in PC-3

The knockdown of RGMs had diverse effects on ID1 in PC-3 prostate cancer cells. The RGMB (Mean±Std. $4.4\times10^8 \pm 3.24\times10^8$) and RGMC knockdown $(6.49\times10^8\pm3.77\times10^8)$ significantly promoted the expression of ID-1 (compared to pEF $3.76\times10^7\pm0.28\times10^7$, p<0.1 and p< 0.05 respectively) (Fig.9.3.1). The increase in ID-1 expression was enhanced by BMP-7 stimulation $(2.94\times10^9 \pm 2.6\times10^8 \text{ for RGMB}, 1.03\times10^{10} \pm 3.7\times10^9 \text{ for RGMC})$ (Fig.9.3.2), compared to control cells $(4.49\times10^8 \pm 3.22\times10^7, \text{ p<0.01})$. There was also an increased ID-1 level in RGMA knockdown cells $(4.93\times10^7 \pm 2.83\times10^7)$, compared to pEF control cells, although the p-value was not significant (0.52). The effect was also enhanced by BMP7 treatment, however, RGMA knockdown has not shown such marked increase as RGMB and RGMC $(1.35\times10^8 \pm 1.42\times10^8 \text{ after treatment})$ (Fig.9.3.1 and Fig.9.3.2). The ID-1 levels increased 5.68 times in RGMB knockdown cells and 14.80 times in RGMC knockdown cells after BMP7 stimulation, compared to the levels under no treatment, whilst RGMA knockdown have 1.74 times increases.

Notably, BMP7 itself could stimulate the expression of ID-1. Therefore, ID-1 was confirmed to be one of the target genes for BMP signalling, as ID-1 expression has been reported to be directly regulated by BMP-Smad pathway.

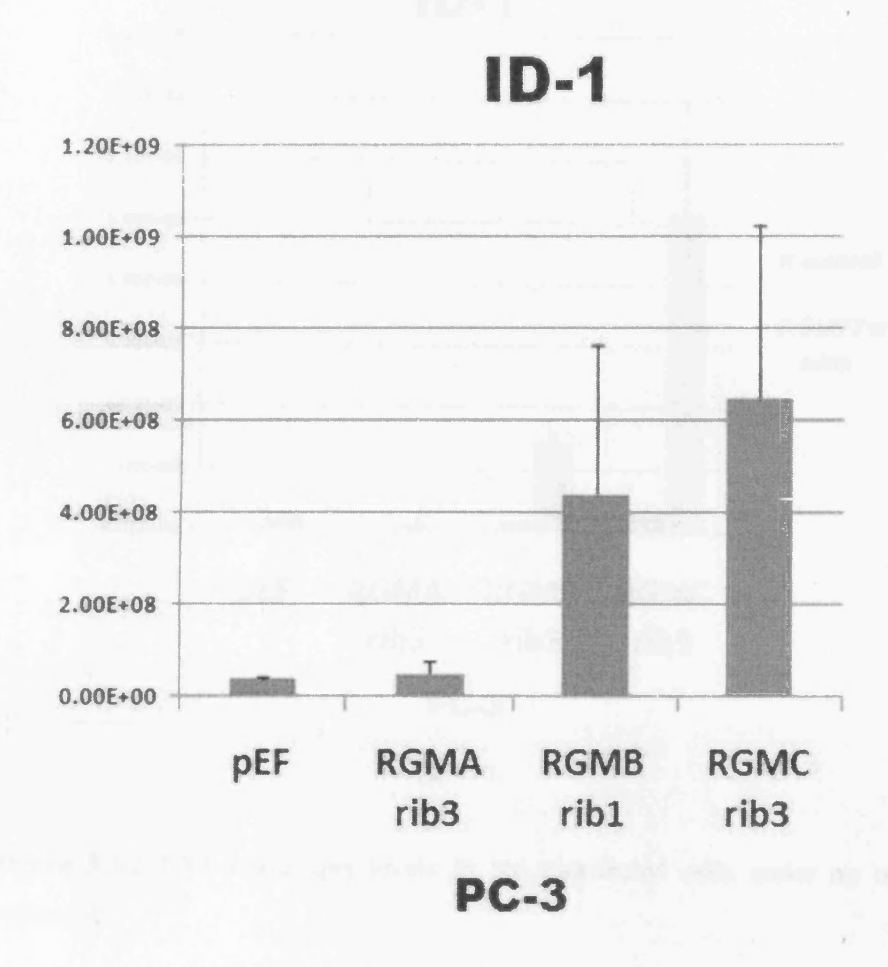


Figure 9.3.1 ID-1transcripts level in the transfected cells.

The QPCR result shows ID-1 level in RGMA, RGMB and RGMC knockdown cells were upregulated (Mean±STd. $4.93\times10^7\pm2.83\times10^7$ for RGMA, $4.4\times10^8\pm3.24\times10^8$ for RGMB and $6.49\times10^8\pm3.77\times10^8$ for RGMC), compared to pEF control cells ($3.76\times10^7\pm0.28\times10^7$). (p=0.52, 0.09 and 0.05 respectively) Data were normalised against GAPDH. Two sample T-test was utilised here.

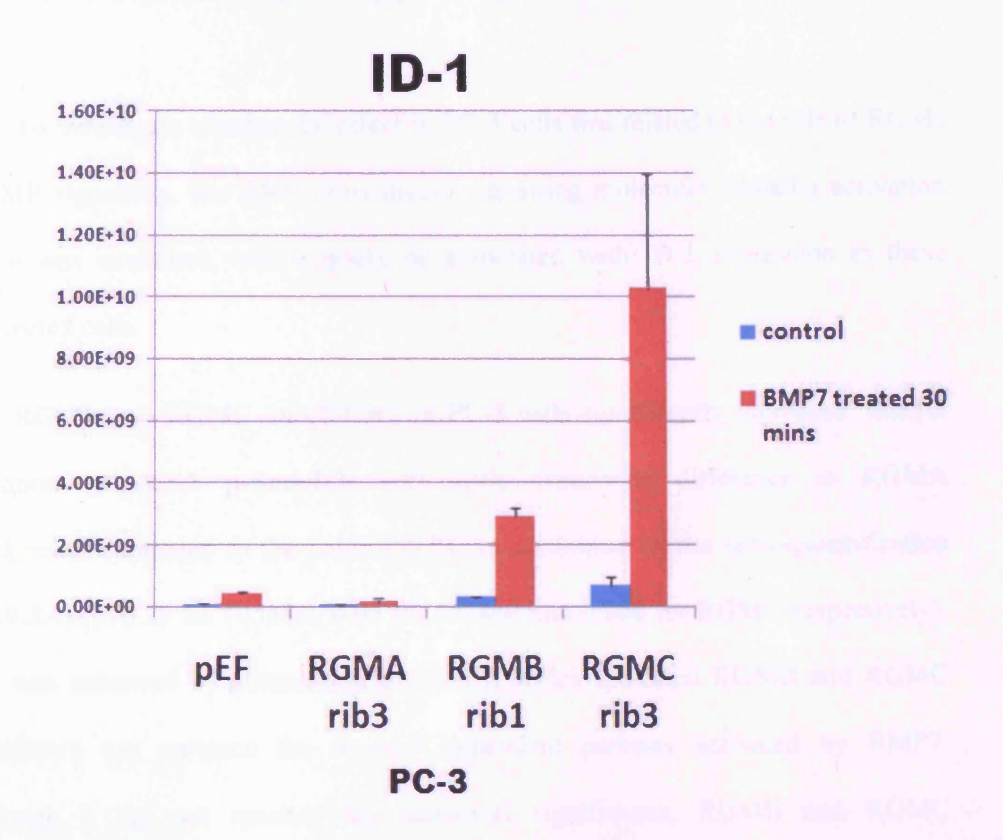


Figure 9.3.2 ID-1 transcripts levels in the transfected cells under no or BMP7 treatment.

The ID-1 level was elevated in RGMs knockdown cells which was amplified after BMP7 treatment (40ng/ml, 30mins) and this effect was markedly in RGMB and RGMC. Data were normalised against GAPDH. Two sample T-test was utilised.

9.3.2 The association of ID-1 expression and involvement of RGMs in BMP Smad-dependent signalling pathway

To investigate whether the effect in PC-3 cells was related to the role of RGMs in BMP signalling, the BMP downstream signalling molecules (Smads) activation profile was examined, which might be associated with ID-1 expression in these transfected cells.

RGMB and RGMC knockdown in PC-3 cells significantly increased Smad-3 activation (Fig.9.3.3 p-Smad-3) with little observable difference in RGMA knockdown, compared to the control cells, as confirmed by the semi-quantification (Fig.9.3.4) (p=0.29 for RGMA, 0.05 for RGMB and 0.008 for RGMC respectively). This was enhanced by stimulation of BMP7, which indicated RGMB and RGMC knockdown can enhance the Smad-3 dependent pathway activated by BMP7. Although it has not reached the statistical significance, RGMB and RGMC knockdown cells further elevated P-Smad-3 level after BMP7 treatment (107653±730 for RGMB and 143872±25556 for RGMC), compared to the level before treatment (93734±24708 for RGMB and 120426±22938 for RGMC, p=0.38 and 0.3 respectively).

Additionally, the recombinant protein BMP7 was able to stimulate Smad-3 activation, with the control cells and RGMs knockdown cells all had increased level of P-Smad-3 after BMP7 treatment (p values were especially significant in pEF and RGMA knockdown cells, p<0.05).

The pattern of Smad-3 activation was consistent with the increased ID-1 level in the transfected cells. Treatment of BMP7 and RGM knockdown in prostate cancer cell line PC-3 did not show stimulation on Smad-1 activation (**Fig.9.3.3** p-Smad-1). Altogether, RGM (B and C) knockdown possibly regulate the downstream gene expression through the enhancement on BMP-Smad-3 signalling pathway while not by Smad-1/5/8.

Additionally, the association of activation of Smad-3 and ID-1 expression was further supported by the Immunofluorescent staining in RGMB and RGMC knockdown cells (Fig.9.3.5 and 9.3.6). RGMB and RGMC knockdown cells showed Smad-3 activated in the nucleus or focused on the nuclear membranes with slightly staining in the cytoplasma. BMP7 treatment enhanced the activation of Smad-3 in RGMB and RGMC knockdown cells and the effect was also existed in control cells but not as obvious as in the RGMs knockdown cells. Fig.9.3.6 showed the expression and activation of ID-1. As a transcriptional factor, ID-1 was mainly stained in the nucleus. ID-1 levels were markedly increased in the nucleus of RGMB and RGMC knockdown cells after BMP7 treatment, compared to the control cells.

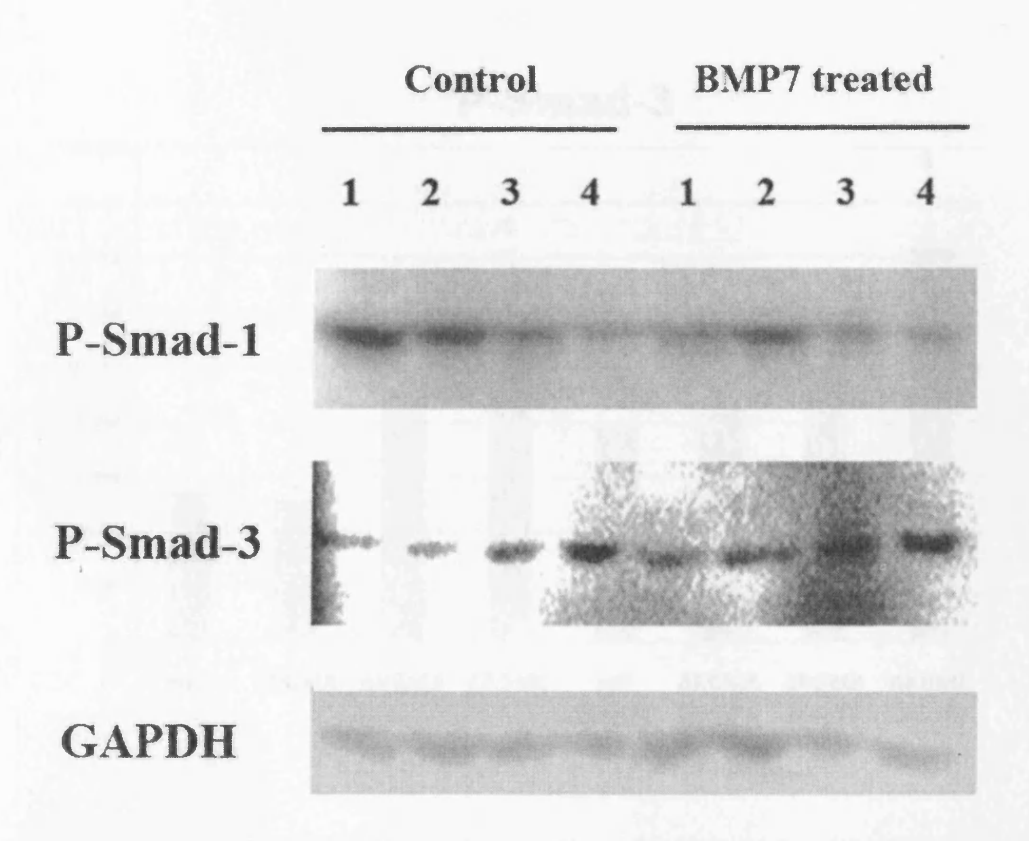


Figure 9.3.3 Smad1 and Smad3 activation in the transfected cells under no or BMP7 treatement.

Activated Smad-3 expression were upregulated after RGMB and RGMC were knocked down and this is enhanced by stimulation of BMP7 (40ng/ml, 30mins), while there is no significant change in phosphoryated Smad-1 levels.

- 1: PC-3 pEF
- 2: PC-3 ΔRGMA
- 3: PC-3 ΔRGMB
- 4: PC-3 ΔRGMC

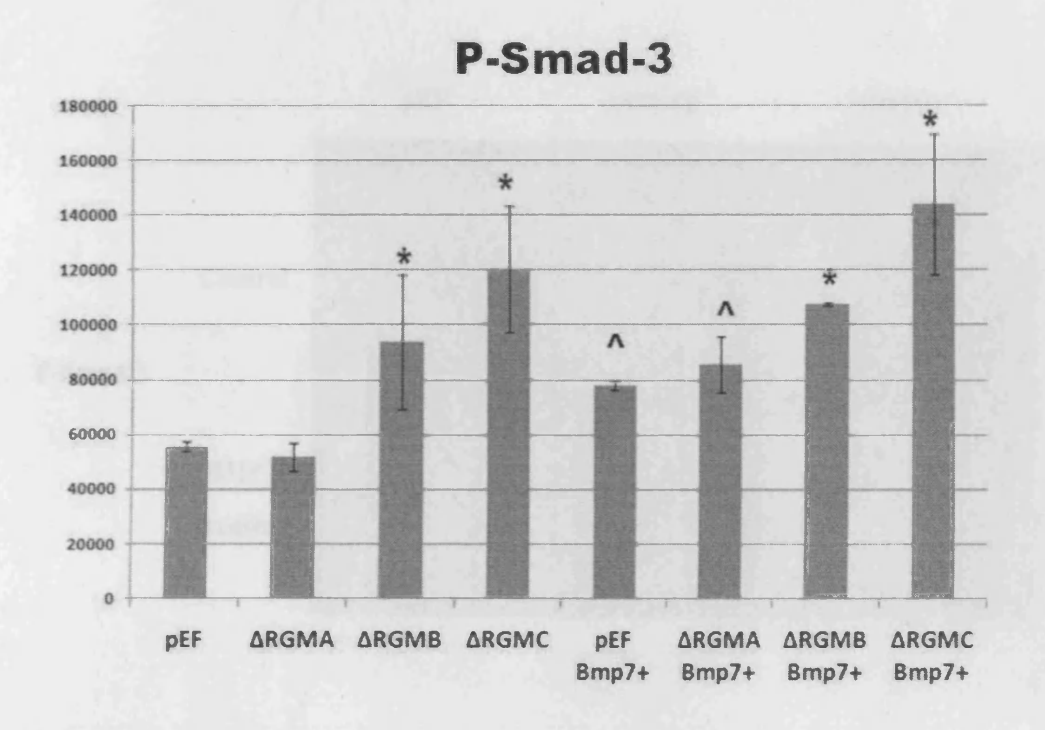


Figure 9.3.4 Quantification of P-Smad-3 level showed in the western.

RGMB and RGMC knockdown cells showed significantly higher level of activated Smad-3 compared to the pEF control cells (*), which was enhanced by BMP7. The RGMA and control cells were also stimulated activation of Smad-3 by BMP7, compared to the level under no treatment (p<0.05) (^).

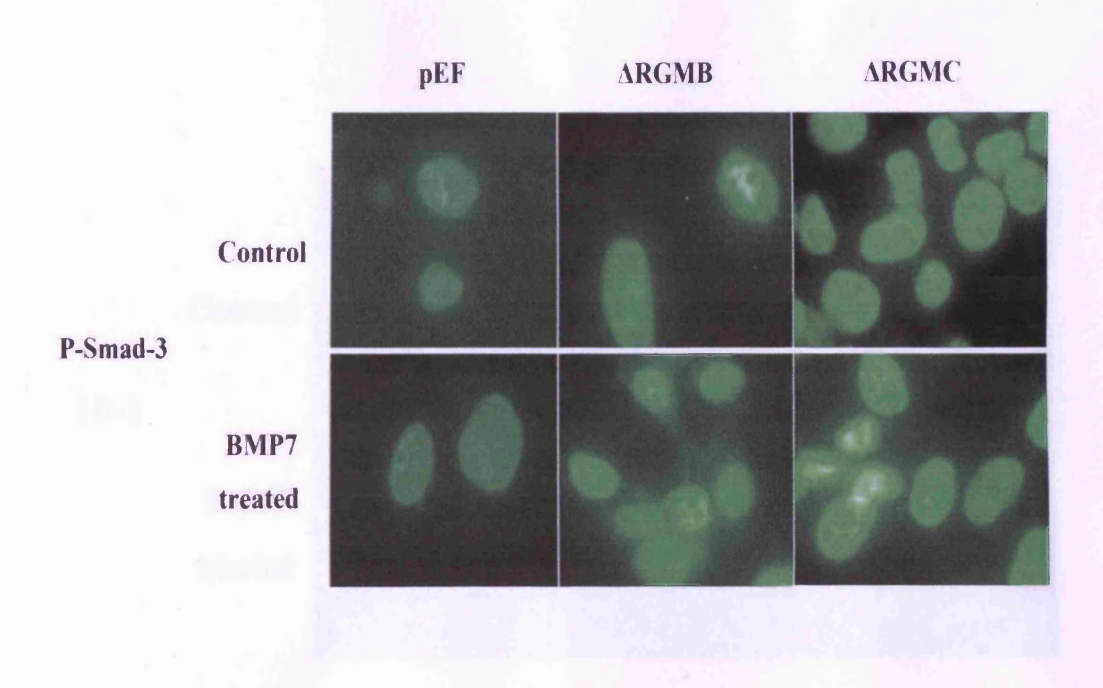


Figure 9.3.5 IFC staining of activated Smad-3.

IFC staining showed the staining of phosphorylated Smad-3 in the nucleus of control and RGMB, C knockdown cells, which was elevated by RGMB and RGMC knockdown and enhanced by BMP7 treatment.

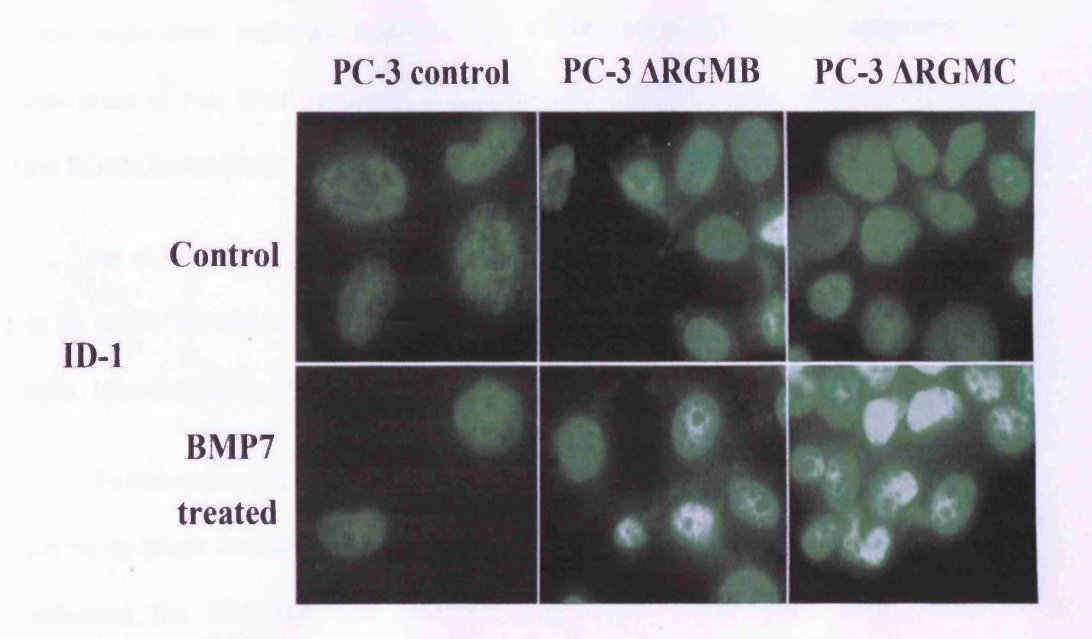


Figure 9.3.6 IFC staining of ID-1

IFC staining showed the ID-1 level was markedly increased in the nucleus (or nucleolus membrane) in the RGMB and RGMC knockdown cells under BMP7 stimulation.

9.3.3 The interaction of RGMs and BMP receptors

To further reveal which BMP receptor might be involved in the activation of Smad-dependent pathway regulated by RGMs knockdown, the expression and activation of two BMP receptors (BMPRIA and BMPRII) were also investigated in the RGMs knockdown cells and their response to the BMP7 treatment.

As shown in Fig.9.3.7, RGMC (and RGMB) knockdown in PC-3 cell resulted in an subtle increase in BMPRIA and BMPRII expression compared to the control cells. However, this effect was not promoted by BMP7 treatment.

Furthermore, the activated forms of these two BMP receptors were difficult to detect in these transfected cells using immunoprecipitation. Taken together, this indicated the BMPRIA and BMPRII might not be the main BMP receptors responsible for RGMs regulation on BMP signalling.

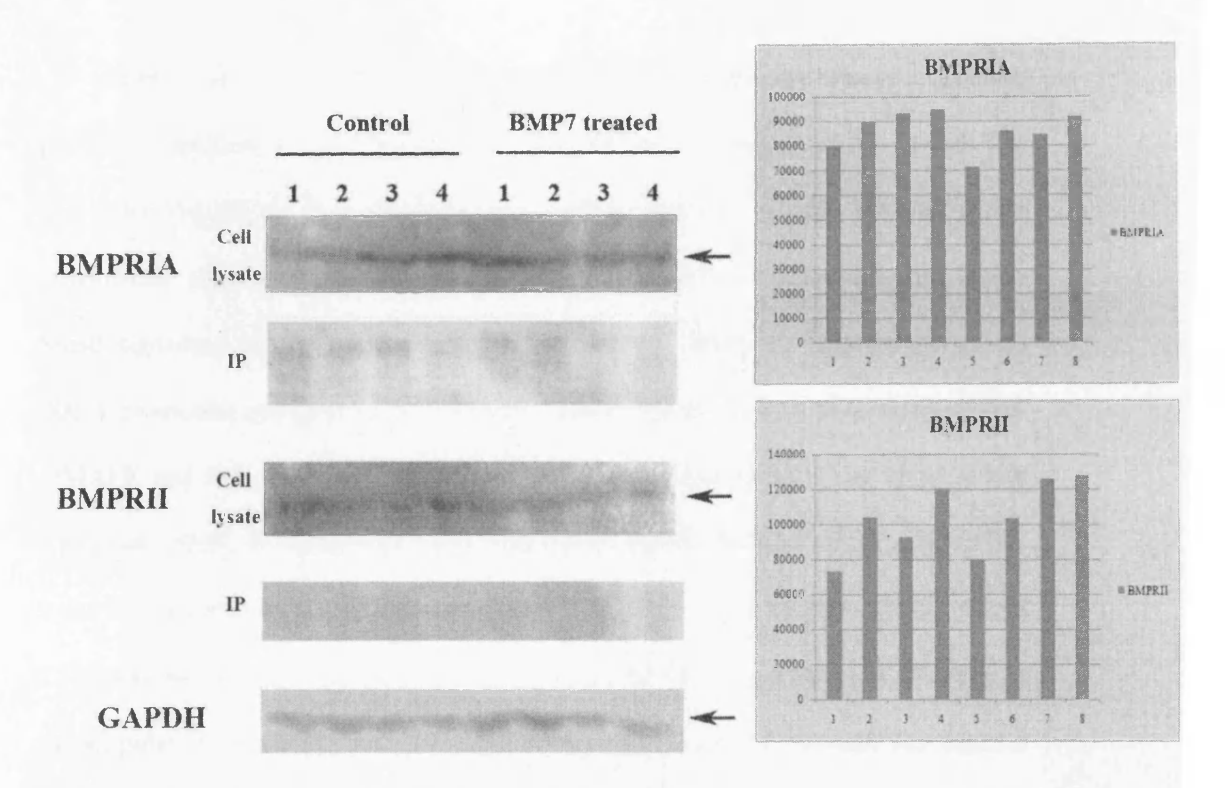


Figure 9.3.7 BMPRI A and BMPRII levels in transfected PC-3 cells.

The phosphorylated BMPRIA and BMPRII were barely detected in these cells using immunoprecipitation (IP). The right panel shows the quantification of intensity of BMPRIA and BMPRII in the western blot (cell lysate).

- 1: PC-3 pEF
- 2: PC-3 ARGMA
- 3: PC-3 ΔRGMB
- 4: PC-3 ΔRGMC

9.4 Discussion:

In PC-3 cells, RGMB and RGMC knockdown stimulated the Smad-3 signalling pathway which has been enhanced by BMP7, followed by increased ID-1 level. The loss of RGMA did not cause such significant effect on the PC-3 cells. ID-1 is a direct downstream effector of BMPs which has been reported to be induced by the BMP-Smad signalling pathway (Miyazono and Miyazawa, 2002; Valdimarsdottir et al., 2002), promoting cell growth and inhibiting cell differentiation via regulation of Raf-1/MAPK and JNK pathways in breast cancer and prostate cancer (Yap et al., 2008; Yap et al., 2010). In the current study, it has been shown that ID-1 expression in PC-3 can be regulated by BMP7 signalling pathway which is enhanced by RGM (B and C) knockdown (compared to RGMA, RGMB and RGMC might be more sensitive to the stimulation of BMP). However, this effect may be largely through the Smad-3 pathway, rather than the BMP-Smad-1/5/8 pathway as previously reported (Belletti et al., 2001; Lasorella et al., 2000; Ohtani et al., 2001; Ying et al., 2003). The main evidence to support this was the observation that the effect of BMP7 and RGMs on Smad-1 was minimal. Although there are other studies to claim that BMP7 has little direct effect on prostate cancer cell growth (Dai et al., 2005), the increase in ID-1 expression in RGM knockdown cells was consistent with the promotion of cell growth as mentioned in previous chapter, which was further support a positive role of RGMs knockdown and ID1 in cancer. In fact, the function of ID-1 also includes the promotion of tumour cell invasion, angiogenesis which may also contribute to the metastasis of prostate cancer. It is recognised that data presented here only decipher part of the signalling events in RGM-BMP medicated cell functions, the study

indicated the interesting role of RGMs played in prostate cancer and a potential therapy target in the future.

Chapter 10 General discussion

RGMs have been shown to play role in axonal guidance during embryo development, neuronal cell adhesion, regulation of systemic iron metabolism (Doya et al., 2006; Hata et al., 2006). However, the role of RGMs in cancer has not been elucidated, although they have been reported as co-receptor of BMPs, a group of protein implicated in the development of prostate cancer, particularly in bony metastasis.

Main findings

Firstly, I screened the expression of RGMs. The expression of RGMs was detected in a panel of cell lines from a variety of tumour types and tissues using RT-PCR. The current study also has examined the staining pattern of RGMs in human prostate tissues and breast tissues. The transcript expression level of RGMs was determined in a panel of breast cohort through Q-PCR, which is from the patients followed up to 120 months. All the three RGM isoforms were found expressed in the prostate cell lines including PC-3, while only RGMB was found in breast cancer cell line MDA-MB-231. However, during the tissue screening, almost all the RGMs were detected in the breast tissues with only RGMB absent in normal breast. Although there was no obvious difference of RGMB protein staining between normal and tumour, the transcript level determined by Q-PCR showed RGMB had significantly higher expression in breast tumour tissues. All the RGMs except RGMA were detected in prostate tissues, while RGMB and RGMC expression were slightly higher in tumour according to the staining in tissues.

The higher transcript level of RGMA was associated with breast cancer patients with good prognosis, while RGMC has no obvious trend in the patients with progression of breast cancer. The initial study of RGMs expression and their association with clinical data suggests an intriguing role of RGMs in cancer. In the present study, to further investigate what the effect RGMs may have on cancer cells, the ribozyme method was employed to genetically reduce the expression of RGMs in PC-3 and RGMB in MDA-MB-231, because of their strong and consistent expression and aggressiveness. The RGMA, RGMB and RGMC expression were reduced in the PC-3 both from mRNA and protein level. RGMB was also eliminated from MDA-MB-231 cells.

The loss of RGMB in MDA-MB-231 resulted in a phenotype with faster rate of cell growth and aggressiveness compared with control cells: with an increase in proliferation, cell-matrix adhesion, motility and mobility *in vitro*. This indicates that RGMB may play an inhibitory role in breast cancer, through inhibition on cancer cell growth and ability to migrate and attach to cell matrix. However, the *in vitro* inhibitory effect did not match with the increased expression of RGMB in tumour tissues. The mechanism(s) of the regulation on RGMB expression remain unknown.

Knock-down of RGMs in PC-3 also promoted the cells ability to grow, adhere and migrate. The effect in RGMB knockdown cells was most significant, compared to the two RGMs. All the RGM knockdown cells increased the cell-matrix adhesion. RGMB and RGMC knockdown cells have a significant effect on cell growth. Only RGMB knockdown cells showed its significant effect on motility after wounding. All the evidence suggests that RGMs (especially RGMB) also inhibited prostate cancer

cell growth, cell-matrix adhesion, motility and mobility. Consistent with that observed in the breast cancer cells and tissues, the inhibitory role of RGMs in PC-3 cells was in contrast to the increased expression pattern in tumour tissues staining.

Potential mechansims underlying the action of RGM proteins

To investigate the mechanism(s) and cascade downstream of RGM, I proposed that the involvement of RGMB in BMP signalling could be at three distinct but related steps, namely targeting BMP binding or the activation of BMP downstream signalling, the interaction of phosphorylated Smads and BMP regulated genes.

RGMB knockdown facilitated the Smad-1 dependent pathway. This effect was linked to upregulated EMT regulators including Snai1 and adhesion molecules such as FAK and Paxillin. As a consequence of these changes of intracellular regulator, cells lost their cell-cell contacts, acquired migration and cell-matrix adhesion ability (Fig.10.1).

It was also strongly suggested that the RGMB knock-down inhibits apoptosis via reducing caspase-3 expression and activation. This suggestion was further supported by the weakening of MAPK / JNK pathway, a known regulatory pathway of apoptosis. C-Myc is a proto-oncogene with profound influence on cell cycle but inducing apoptosis. However, this effect of c-Myc on apoptosis can be inhibited by inactivation of the JNK pathway (Noguchi *et al.*, 2000). Additionally, the other reported role for c-Myc is to stimulate cell growth independently (Schuhmacher *et al.*,

1999; Steiner *et al.*, 1995). It was interesting to find expression of c-Myc was significantly increased in RGMB knockdown cells.

Therefore, it is anticipated that the biological effect of RGMB on MDA-MB-231 is likely to be associated with reducing the BMP Smad dependent pathway (mainly Smad-1) and enhancing BMP non-Smad pathway (JNK pathway).

In PC-3 cells, RGMB and RGMC knock-down also promoted BMP/Smad-3 dependent pathway. This is clearly correlated with the upregulation on ID-1, a transcription factor for cell growth and differentiation regulatory proteins. This was well reflected in the *in vitro* data here that RGMB and RGMC knockdown cells had an increased rate of cellular growth. BMP7 has been shown in the past to be able to induce Smad-3 phosphorylation (Cassar *et al.*, 2009). Here and for the first time, we presented evidence that BMP7 induced upregulation of ID-1 was enhanced by RGMs knockdown and that this might be via the Smad-3 pathway.

RGMs were reported as co-receptors of BMPs and can enhance the BMP signalling pathways. However, the present study has shown that the co-receptor and co-regulation by RGM are probably more complicated. Here, we clearly demonstated that RGMs inhibit the BMP Smad-dependent pathway. This was seen for RGMB and RGMC in PC-3 cells and for RGMB in MDA-MB-231cells. It is more interesting to note that RGMs not only inhibit the Smad-dependent pathway, they appear to skillfully switch the signal to Smad-independent MAPK pathway in MDA-MB-231 (RGMB).

It is concluded that RGM proteins influence the biological function of breast and prostate cancer cells. Collectively and as shown in **Fig. 10.1**, these effects are more likely to be mediated by the change of the BMP receptor downstream signalling. The study has further shown that the change/switch of the pathways by RGM might be via the interference of the interaction between BMP and the BMP receptors, thus at the upstream of Smads.

Future work

In the current study of RGMB knockdown, increased Paxillin, FAK and Snail have been correlated with adhesion and motility of MDA-MB-231. Furthermore, this effect seems associated with the promotion on Smad-1 dependent pathway. However, the direct relationship of the Smad-1 activation and these target genes expression has not been established due to the absence of specific Smad-1 inhibitor. Smad-1 or Smad-4 could be double knocked down in RGMB knockdown cells to investigate whether this effect on these molecules or integrins will be reversed.

There might be a link between the JNK inhibition and apoptosis reduction. However, in order to confirm whether the inhibited JNK pathway was sufficient to cause anti-apoptotic effect of RGMB knockdown, the JNK inhibitor could be used. The expression of c-Myc and caspase-3 could also be determined again to reveal the correlation with JNK.

It's also very interesting to further reveal the nature of RGMs binding to BMPs and BMP receptors, and the insight of the Smad pathway switch, namely from Smad-dependent to Smad-independent.

Furthermore, the structure of RGMs gene promoter or the regulation of RGMs expression remains unknown. The RGMB induced inhibitory effect on breast cancer whereas its expression was increased in the tumour tissues compared to the normal tissues, a pattern also seen in prostate cancer. The presence of a possible feedback loop to upregualte the expression of RGMB *in vivo* would be worthwhile to explore.

Above all, as potential tumour suppressor genes, further studies using in vivo tumour model are helpful to elucidate the implication of RGMs in prostate cancer and breast cancer and their metastasis. The role of RGMs *in vivo* may indicate us a therapeutic target for prevention and treatment of prostate cancer and breast cancer.

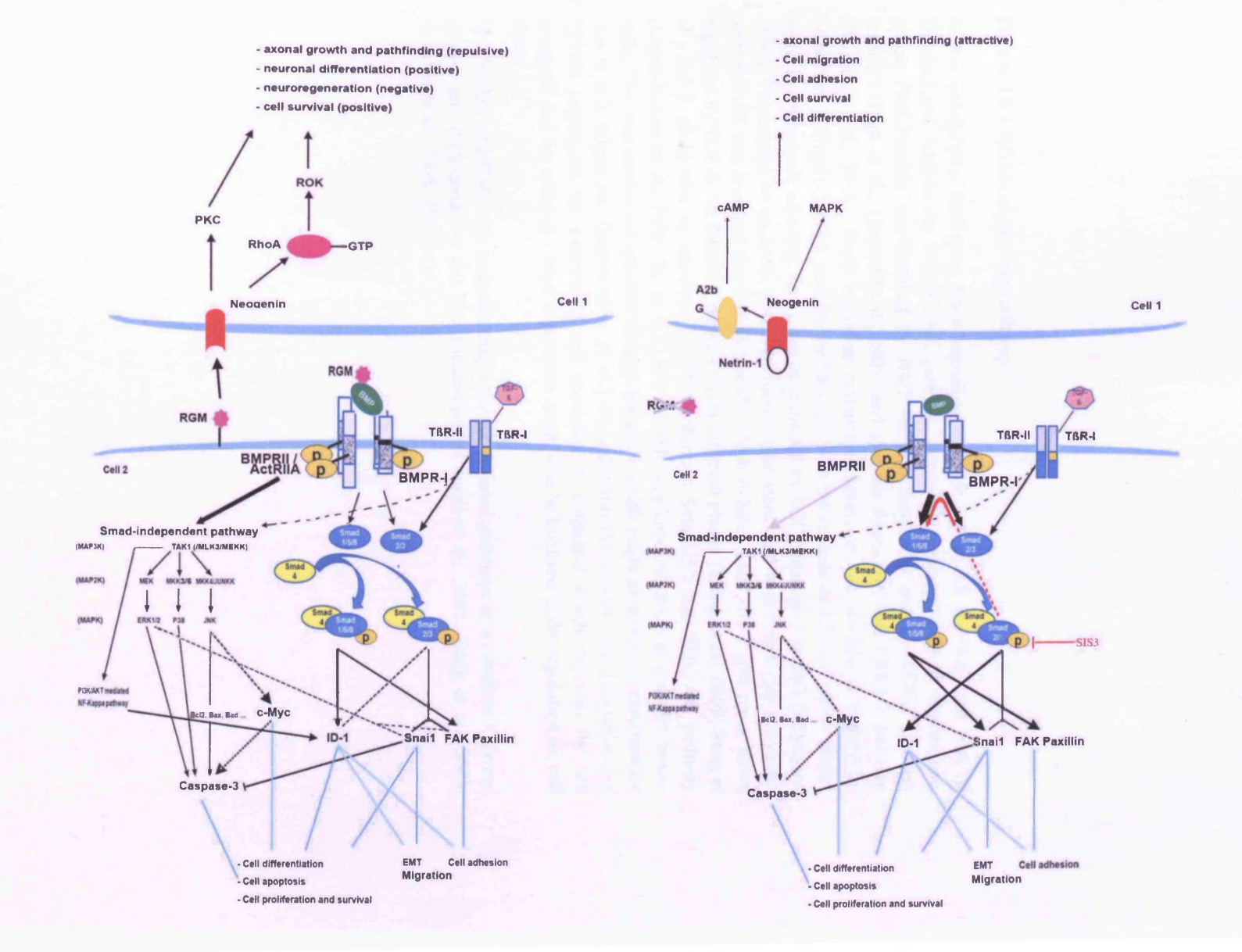


Figure 10.1 RGMs signalling pathway

RGMs knockdown facilitates BMP signalling through Smad1/5/8 pathway and part of Smad2/3 and inhibits the MAPK JNK pathway thereby to mediate the BMP downstream genes. FAK/Paxillin was induced by BMP through Smad1/5/8 and by TGF-ß through Smad2/3 (Park et al.; Tamura et al., 2001) and also has interaction with ERK1/2 pathway (Bechara et al., 2008). Focal adhesion molecules expression was stimulated mainly by activation of Smad1/5/8 and partially by Smad2/3 with the absence of RGMB, which leaded to the increased cell adhesion. Snail can be regulated by TGF-ß through Smad2/3 (Miyazono, 2009). The regulation on Snail was also found to be associated with Smad1/5/8 activation after RGMB was knocked down in this study which induced EMT. ID-1 was up or down regulated by TGF-ß via Smad2/3 depending on different phases (Liang et al., 2009; Song et al.) and it could also be activated by BMPs through Smad1/5/8 and PI3K/Akt pathway (Lopez-Rovira et al., 2002; Su et al.). After RGMs was knocked down in prostate cancer cells, ID-1 was mainly upregulated through Smad2/3 which might promote cell proliferation (Lo et al.), migration (Bhattacharya et al.) and adhesion (Su et al.). The knockdown of RGMB suppressed the expression and activation of caspsae-3 which executes the cell apoptosis and the reduced c-Myc expression might also be involved in the regulation on cell death.

The binding of RGMs with neogenin might trigger different pathways on to mediate neuronal growth and differentiation and iron metabolism (Conrad et al., 2007; Jiang et al., 2003; Schaffar et al., 2008; Zhou et al.).

Bibliography

- Achbarou, A., Kaiser, S., Tremblay, G., Ste-Marie, L. G., Brodt, P., Goltzman, D., and Rabbani, S. A. (1994). Urokinase overproduction results in increased skeletal metastasis by prostate cancer cells in vivo. Cancer Res 54, 2372-2377.
- Alarmo, E. L., and Kallioniemi, A. Bone morphogenetic proteins in breast cancer: dual role in tumourigenesis? Endocr Relat Cancer 17, R123-139.
- Alarmo, E. L., Korhonen, T., Kuukasjarvi, T., Huhtala, H., Holli, K., and Kallioniemi, A. (2008). Bone morphogenetic protein 7 expression associates with bone metastasis in breast carcinomas. Ann Oncol 19, 308-314.
- Alarmo, E. L., Parssinen, J., Ketolainen, J. M., Savinainen, K., Karhu, R., and Kallioniemi, A. (2009). BMP7 influences proliferation, migration, and invasion of breast cancer cells. Cancer letters 275, 35-43.
- Albini, A., Iwamoto, Y., Kleinman, H. K., Martin, G. R., Aaronson, S. A., Kozlowski, J. M., and McEwan, R. N. (1987). A rapid *in vitro* assay for quantitating the invasive potential of tumor cells. Cancer Research 47, 3239 3245.
- Andriopoulos, B., Jr., Corradini, E., Xia, Y., Faasse, S. A., Chen, S., Grgurevic, L., Knutson, M. D., Pietrangelo, A., Vukicevic, S., Lin, H. Y., and Babitt, J. L. (2009). BMP6 is a key endogenous regulator of hepcidin expression and iron metabolism. Nature genetics 41, 482-487.
- Aoki, H., Fujii, M., Imamura, T., Yagi, K., Takehara, K., Kato, M., and Miyazono, K. (2001). Synergistic effects of different bone morphogenetic protein type I receptors on alkaline phosphatase induction. J Cell Sci 114, 1483-1489.
- Aono, A., Hazama, M., Notoya, K., Taketomi, S., Yamasaki, H., Tsukuda, R., Sasaki, S., and Fujisawa, Y. (1995). Potent ectopic bone-inducing activity of bone morphogenetic protein-4/7 heterodimer. Biochemical and biophysical research communications *210*, 670-677.
- Arens, N., Gandhari, M., Bleyl, U., and Hildenbrand, R. (2005). In vitro suppression of urokinase plasminogen activator in breast cancer cells--a comparison of two antisense strategies. Int J Oncol 26, 113-119.
- Astrom, A. K., Jin, D., Imamura, T., Roijer, E., Rosenzweig, B., Miyazono, K., ten Dijke, P., and Stenman, G. (1999). Chromosomal localization of three human genes encoding bone morphogenetic protein receptors. Mamm Genome 10, 299-302.
- Babitt, J. L., Huang, F. W., Wrighting, D. M., Xia, Y., Sidis, Y., Samad, T. A., Campagna, J. A., Chung, R. T., Schneyer, A. L., Woolf, C. J., *et al.* (2006). Bone morphogenetic protein signaling by hemojuvelin regulates hepcidin expression. Nat Genet *38*, 531-539.
- Babitt, J. L., Huang, F. W., Xia, Y., Sidis, Y., Andrews, N. C., and Lin, H. Y. (2007). Modulation of bone morphogenetic protein signaling in vivo regulates systemic iron balance. J Clin Invest 117, 1933-1939.
- Babitt, J. L., Zhang, Y., Samad, T. A., Xia, Y., Tang, J., Campagna, J. A., Schneyer, A. L., Woolf, C. J., and Lin, H. Y. (2005). Repulsive guidance molecule (RGMa), a DRAGON homologue, is a bone morphogenetic protein co-receptor. J Biol Chem 280, 29820-29827.
- Balemans, W., and Van Hul, W. (2002). Extracellular regulation of BMP signaling in vertebrates: a cocktail of modulators. Dev Biol 250, 231-250.
- Barallobre, M. J., Pascual, M., Del Rio, J. A., and Soriano, E. (2005). The Netrin family of guidance factors: emphasis on Netrin-1 signalling. Brain Res Brain Res Rev 49, 22-47.

- Barton, J. C., Acton, R. T., Leiendecker-Foster, C., Lovato, L., Adams, P. C., Eckfeldt, J. H., McLaren, C. E., Reiss, J. A., McLaren, G. D., Reboussin, D. M., et al. (2008). Characteristics of participants with self-reported hemochromatosis or iron overload at HEIRS study initial screening. Am J Hematol 83, 126-132.
- Barton, J. C., Acton, R. T., Leiendecker-Foster, C., Lovato, L., Adams, P. C., McLaren, G.
 D., Eckfeldt, J. H., McLaren, C. E., Reboussin, D. M., Gordeuk, V. R., et al. (2007).
 HFE C282Y homozygotes aged 25-29 years at HEIRS Study initial screening. Genet Test 11, 269-275.
- Bechara, A., Nawabi, H., Moret, F., Yaron, A., Weaver, E., Bozon, M., Abouzid, K., Guan, J. L., Tessier-Lavigne, M., Lemmon, V., and Castellani, V. (2008). FAK-MAPK-dependent adhesion disassembly downstream of L1 contributes to semaphorin3A-induced collapse. EMBO J 27, 1549-1562.
- Belletti, B., Prisco, M., Morrione, A., Valentinis, B., Navarro, M., and Baserga, R. (2001). Regulation of Id2 gene expression by the insulin-like growth factor I receptor requires signaling by phosphatidylinositol 3-kinase. J Biol Chem 276, 13867-13874.
- Benshushan, A., and Brzezinski, A. (2002). Hormonal manipulations and breast cancer. Obstet Gynecol Surv 57, 314-323.
- Beppu, H., Minowa, O., Miyazono, K., and Kawabata, M. (1997). cDNA cloning and genomic organization of the mouse BMP type II receptor. Biochemical and biophysical research communications 235, 499-504.
- Bewick, M., Conlon, M., Parissenti, A. M., Lee, H., Zhang, L., Gluck, S., and Lafrenie, R. M. (2001). Soluble Fas (CD95) is a prognostic factor in patients with metastatic breast cancer undergoing high-dose chemotherapy and autologous stem cell transplantation. J Hematother Stem Cell Res 10, 759-768.
- Bhattacharya, R., Kowalski, J., Larson, A. R., Brock, M., and Alani, R. M. Idl promotes tumor cell migration in nonsmall cell lung cancers. J Oncol 2010, 856105.
- Biglia, N., Cozzarella, M., Cacciari, F., Ponzone, R., Roagna, R., Maggiorotto, F., and Sismondi, P. (2003). Menopause after breast cancer: a survey on breast cancer survivors. Maturitas 45, 29-38.
- Bill-Axelson, A., Holmberg, L., Ruutu, M., Haggman, M., Andersson, S. O., Bratell, S., Spangberg, A., Busch, C., Nordling, S., Garmo, H., *et al.* (2005). Radical prostatectomy versus watchful waiting in early prostate cancer. N Engl J Med *352*, 1977-1984.
- Bokobza, S. M., Ye, L., Kynaston, H. E., Mansel, R. E., and Jiang, W. G. (2009). Reduced expression of BMPR-IB correlates with poor prognosis and increased proliferation of breast cancer cells. Cancer Genomics Proteomics 6, 101-108.
- Bouchard, V., Harnois, C., Demers, M. J., Thibodeau, S., Laquerre, V., Gauthier, R., Vezina, A., Noel, D., Fujita, N., Tsuruo, T., *et al.* (2008). B1 integrin/Fak/Src signaling in intestinal epithelial crypt cell survival: integration of complex regulatory mechanisms. Apoptosis 13, 531-542.
- Boyde, A., Ali, N. N., and Jones, S. J. (1985). Optical and scanning electron microscopy in the single osteoclast resorption assay. Scan Electron Microsc, 1259-1271.
- Bredesen, D. E., Mehlen, P., and Rabizadeh, S. (2004). Apoptosis and dependence receptors: a molecular basis for cellular addiction. Physiol Rev 84, 411-430.
- Bright, M. D., Garner, A. P., and Ridley, A. J. (2009). PAK1 and PAK2 have different roles in HGF-induced morphological responses. Cell Signal 21, 1738-1747.
- Brinks, H., Conrad, S., Vogt, J., Oldekamp, J., Sierra, A., Deitinghoff, L., Bechmann, I., Alvarez-Bolado, G., Heimrich, B., Monnier, P. P., et al. (2004). The repulsive guidance molecule RGMa is involved in the formation of afferent connections in the dentate gyrus. J Neurosci 24, 3862-3869.
- Brubaker, K. D., Corey, E., Brown, L. G., and Vessella, R. L. (2004). Bone morphogenetic protein signaling in prostate cancer cell lines. J Cell Biochem 91, 151-160.

- Bryden, A. A., Hoyland, J. A., Freemont, A. J., Clarke, N. W., and George, N. J. (2002). Parathyroid hormone related peptide and receptor expression in paired primary prostate cancer and bone metastases. Br J Cancer 86, 322-325.
- Buchholz, S., Horn, F., and Ortmann, O. (2008). [Hormone replacement therapy in peri- and postmenopausal women and breast cancer risk]. Ther Umsch 65, 231-234.
- Buijs, J. T., Henriquez, N. V., van Overveld, P. G., van der Horst, G., Que, I., Schwaninger, R., Rentsch, C., Ten Dijke, P., Cleton-Jansen, A. M., Driouch, K., et al. (2007a). Bone morphogenetic protein 7 in the development and treatment of bone metastases from breast cancer. Cancer Res 67, 8742-8751.
- Buijs, J. T., Rentsch, C. A., van der Horst, G., van Overveld, P. G., Wetterwald, A., Schwaninger, R., Henriquez, N. V., Ten Dijke, P., Borovecki, F., Markwalder, R., et al. (2007b). BMP7, a putative regulator of epithelial homeostasis in the human prostate, is a potent inhibitor of prostate cancer bone metastasis in vivo. The American journal of pathology 171, 1047-1057.
- Butler, S. J., and Dodd, J. (2003). A role for BMP heterodimers in roof plate-mediated repulsion of commissural axons. Neuron 38, 389-401.
- Canalis, E., Economides, A. N., and Gazzerro, E. (2003). Bone morphogenetic proteins, their antagonists, and the skeleton. Endocr Rev 24, 218-235.
- Carter, B. S., Beaty, T. H., Steinberg, G. D., Childs, B., and Walsh, P. C. (1992). Mendelian inheritance of familial prostate cancer. Proc Natl Acad Sci U S A 89, 3367-3371.
- Carter, H. B., Walsh, P. C., Landis, P., and Epstein, J. I. (2002). Expectant management of nonpalpable prostate cancer with curative intent: preliminary results. J Urol 167, 1231-1234.
- Cassar, L., Nicholls, C., Pinto, A. R., Li, H., and Liu, J. P. (2009). Bone morphogenetic protein-7 induces telomerase inhibition, telomere shortening, breast cancer cell senescence, and death via Smad3. FASEB J 23, 1880-1892.
- Chambers, A. F., and Matrisian, L. M. (1997). Changing views of the role of matrix metalloproteinases in metastasis. J Natl Cancer Inst 89, 1260-1270.
- Chan, D. W., Beveridge, R. A., Muss, H., Fritsche, H. A., Hortobagyi, G., Theriault, R., Kiang, D., Kennedy, B. J., and Evelegh, M. (1997). Use of Truquant BR radioimmunoassay for early detection of breast cancer recurrence in patients with stage II and stage III disease. J Clin Oncol 15, 2322-2328.
- Chan, K. T., Cortesio, C. L., and Huttenlocher, A. (2009). FAK alters invadopodia and focal adhesion composition and dynamics to regulate breast cancer invasion. J Cell Biol 185, 357-370.
- Chang, S. C., Hoang, B., Thomas, J. T., Vukicevic, S., Luyten, F. P., Ryba, N. J., Kozak, C. A., Reddi, A. H., and Moos, M., Jr. (1994). Cartilage-derived morphogenetic proteins. New members of the transforming growth factor-beta superfamily predominantly expressed in long bones during human embryonic development. The Journal of biological chemistry 269, 28227-28234.
- Chikumi, H., Fukuhara, S., and Gutkind, J. S. (2002). Regulation of G protein-linked guanine nucleotide exchange factors for Rho, PDZ-RhoGEF, and LARG by tyrosine phosphorylation: evidence of a role for focal adhesion kinase. The Journal of biological chemistry 277, 12463-12473.
- Choo, R., Hruby, G., Hong, J., Bahk, E., Hong, E., Danjoux, C., Morton, G., and DeBoer, G. (2002). (IN)-efficacy of salvage radiotherapy for rising PSA or clinically isolated local recurrence after radical prostatectomy. Int J Radiat Oncol Biol Phys 53, 269-276.
- Cirulli, V., and Yebra, M. (2007). Netrins: beyond the brain. Nat Rev Mol Cell Biol 8, 296-306.

- Cocolakis, E., Lemay, S., Ali, S., and Lebrun, J. J. (2001). The p38 MAPK pathway is required for cell growth inhibition of human breast cancer cells in response to activin. J Biol Chem 276, 18430-18436.
- Cohen, G. M. (1997). Caspases: the executioners of apoptosis. Biochem J 326 (Pt 1), 1-16. Conrad, S., Genth, H., Hofmann, F., Just, I., and Skutella, T. (2007). Neogenin-RGMa signaling at the growth cone is bone morphogenetic protein-independent and involves RhoA, ROCK, and PKC. J Biol Chem 282, 16423-16433.
- Conrad, S., Stimpfle, F., Montazeri, S., Oldekamp, J., Seid, K., Alvarez-Bolado, G., and Skutella, T. RGMb controls aggregation and migration of Neogenin-positive cells in vitro and in vivo. Mol Cell Neurosci 43, 222-231.
- Constante, M., Wang, D., Raymond, V. A., Bilodeau, M., and Santos, M. M. (2007). Repression of repulsive guidance molecule C during inflammation is independent of Hfe and involves tumor necrosis factor-alpha. Am J Pathol 170, 497-504.
- Cooney, K. A., McCarthy, J. D., Lange, E., Huang, L., Miesfeldt, S., Montie, J. E., Oesterling, J. E., Sandler, H. M., and Lange, K. (1997). Prostate cancer susceptibility locus on chromosome 1q: a confirmatory study. J Natl Cancer Inst 89, 955-959.
- Coussens, L. M., and Werb, Z. (2002). Inflammation and cancer. Nature 420, 860-867.
- Dai, J., Keller, J., Zhang, J., Lu, Y., Yao, Z., and Keller, E. T. (2005). Bone morphogenetic protein-6 promotes osteoblastic prostate cancer bone metastases through a dual mechanism. Cancer Res 65, 8274-8285.
- Darby, S., Cross, S. S., Brown, N. J., Hamdy, F. C., and Robson, C. N. (2008). BMP-6 over-expression in prostate cancer is associated with increased Id-1 protein and a more invasive phenotype. J Pathol 214, 394-404.
- De Marzo, A. M., DeWeese, T. L., Platz, E. A., Meeker, A. K., Nakayama, M., Epstein, J. I., Isaacs, W. B., and Nelson, W. G. (2004). Pathological and molecular mechanisms of prostate carcinogenesis: implications for diagnosis, detection, prevention, and treatment. J Cell Biochem 91, 459-477.
- Demou, Z. N., and Hendrix, M. J. (2008). Microgenomics profile the endogenous angiogenic phenotype in subpopulations of aggressive melanoma. J Cell Biochem 105, 562-573.
- Dennler, S., Goumans, M. J., and ten Dijke, P. (2002). Transforming growth factor beta signal transduction. J Leukoc Biol 71, 731-740.
- Dennler, S., Huet, S., and Gauthier, J. M. (1999). A short amino-acid sequence in MH1 domain is responsible for functional differences between Smad2 and Smad3. Oncogene 18, 1643-1648.
- Dhanasekaran, D. N., and Reddy, E. P. (2008). JNK signaling in apoptosis. Oncogene 27, 6245-6251.
- Dong, J., Albertini, D. F., Nishimori, K., Kumar, T. R., Lu, N., and Matzuk, M. M. (1996). Growth differentiation factor-9 is required during early ovarian folliculogenesis. Nature 383, 531-535.
- Doya, H., Ito, T., Hata, K., Fujitani, M., Ohtori, S., Saito-Watanabe, T., Moriya, H., Takahashi, K., Kubo, T., and Yamashita, T. (2006). Induction of repulsive guidance molecule in neurons following sciatic nerve injury. J Chem Neuroanat 32, 74-77.
- Dudley, A. T., Lyons, K. M., and Robertson, E. J. (1995). A requirement for bone morphogenetic protein-7 during development of the mammalian kidney and eye. Genes Dev 9, 2795-2807.
- Duffy, M. J., Maguire, T. M., Hill, A., McDermott, E., and O'Higgins, N. (2000). Metalloproteinases: role in breast carcinogenesis, invasion and metastasis. Breast Cancer Res 2, 252-257.
- Duffy, M. J., and McCarthy, K. (1998). Matrix metalloproteinases in cancer: prognostic markers and targets for therapy (review). Int J Oncol 12, 1343-1348.

- Ebara, S., and Nakayama, K. (2002). Mechanism for the action of bone morphogenetic proteins and regulation of their activity. Spine (Phila Pa 1976) 27, S10-15.
- Eeles, R. A., Durocher, F., Edwards, S., Teare, D., Badzioch, M., Hamoudi, R., Gill, S., Biggs, P., Dearnaley, D., Ardern-Jones, A., *et al.* (1998). Linkage analysis of chromosome 1q markers in 136 prostate cancer families. The Cancer Research Campaign/British Prostate Group U.K. Familial Prostate Cancer Study Collaborators. Am J Hum Genet *62*, 653-658.
- Ehata, S., Hanyu, A., Hayashi, M., Aburatani, H., Kato, Y., Fujime, M., Saitoh, M., Miyazawa, K., Imamura, T., and Miyazono, K. (2007). Transforming growth factor-beta promotes survival of mammary carcinoma cells through induction of antiapoptotic transcription factor DEC1. Cancer Res 67, 9694-9703.
- el-Geneidy, M., Garzotto, M., Panagiotou, I., Hsieh, Y. C., Mori, M., Peters, L., Klein, T., and Beer, T. M. (2004). Delayed therapy with curative intent in a contemporary prostate cancer watchful-waiting cohort. BJU Int *93*, 510-515.
- Ellison, G., Klinowska, T., Westwood, R. F., Docter, E., French, T., and Fox, J. C. (2002). Further evidence to support the melanocytic origin of MDA-MB-435. Mol Pathol 55, 294-299.
- Emadi Baygi, M., Soheili, Z. S., Schmitz, I., Sameie, S., and Schulz, W. A. (2010). Snail regulates cell survival and inhibits cellular senescence in human metastatic prostate cancer cell lines. Cell Biol Toxicol.
- Epstein, R. J. (2003). Adhesion molecules and the extracellular matrix Cambridge University Press).
- Fernandes-Alnemri, T., Litwack, G., and Alnemri, E. S. (1994). CPP32, a novel human apoptotic protein with homology to Caenorhabditis elegans cell death protein Ced-3 and mammalian interleukin-1 beta-converting enzyme. J Biol Chem 269, 30761-30764.
- Finberg, K. E., Whittlesey, R. L., Fleming, M. D., and Andrews, N. C. Down-regulation of Bmp/Smad signaling by Tmprss6 is required for maintenance of systemic iron homeostasis. Blood 115, 3817-3826.
- Finberg, K. E., Whittlesey, R. L., Fleming, M. D., and Andrews, N. C. (2010). Down-regulation of Bmp/Smad signaling by Tmprss6 is required for maintenance of systemic iron homeostasis. Blood 115, 3817-3826.
- Forootan, S. S., Wong, Y. C., Dodson, A., Wang, X., Lin, K., Smith, P. H., Foster, C. S., and Ke, Y. (2007). Increased Id-1 expression is significantly associated with poor survival of patients with prostate cancer. Hum Pathol 38, 1321-1329.
- Fowler, C. (2008). Hereditary hemochromatosis: pathophysiology, diagnosis, and management. Crit Care Nurs Clin North Am 20, 191-201, vi.
- Francis-West, P. H., Robertson, K. E., Ede, D. A., Rodriguez, C., Izpisua-Belmonte, J. C., Houston, B., Burt, D. W., Gribbin, C., Brickell, P. M., and Tickle, C. (1995). Expression of genes encoding bone morphogenetic proteins and sonic hedgehog in talpid (ta3) limb buds: their relationships in the signalling cascade involved in limb patterning. Dev Dyn 203, 187-197.
- Francis, P. H., Richardson, M. K., Brickell, P. M., and Tickle, C. (1994). Bone morphogenetic proteins and a signalling pathway that controls patterning in the developing chick limb. Development 120, 209-218.
- Fujii, M., Takeda, K., Imamura, T., Aoki, H., Sampath, T. K., Enomoto, S., Kawabata, M., Kato, M., Ichijo, H., and Miyazono, K. (1999). Roles of bone morphogenetic protein type I receptors and Smad proteins in osteoblast and chondroblast differentiation. Mol Biol Cell 10, 3801-3813.
- Fujita, E., Soyama, A., Kawabata, M., and Momoi, T. (1999). BMP-4 and retinoic acid synergistically induce activation of caspase-9 and cause apoptosis of P19 embryonal carcinoma cells cultured as a monolayer. Cell Death Differ 6, 1109-1116.

- Gautschi, O., Tepper, C. G., Purnell, P. R., Izumiya, Y., Evans, C. P., Green, T. P., Desprez, P. Y., Lara, P. N., Gandara, D. R., Mack, P. C., and Kung, H. J. (2008). Regulation of Id1 expression by SRC: implications for targeting of the bone morphogenetic protein pathway in cancer. Cancer Res 68, 2250-2258.
- Gazzerro, E., and Canalis, E. (2006). Bone morphogenetic proteins and their antagonists. Rev Endocr Metab Disord 7, 51-65.
- Geisbrecht, B. V., Dowd, K. A., Barfield, R. W., Longo, P. A., and Leahy, D. J. (2003). Netrin binds discrete subdomains of DCC and UNC5 and mediates interactions between DCC and heparin. The Journal of biological chemistry 278, 32561-32568.
- Gion, M., Mione, R., Leon, A. E., and Dittadi, R. (1999). Comparison of the diagnostic accuracy of CA27.29 and CA15.3 in primary breast cancer. Clin Chem 45, 630-637.
- Guarino, M., Rubino, B., and Ballabio, G. (2007). The role of epithelial-mesenchymal transition in cancer pathology. Pathology *39*, 305-318.
- Guise, T. A., and Mundy, G. R. (1996). Physiological and pathological roles of parathyroid hormone-related peptide. Curr Opin Nephrol Hypertens 5, 307-315.
- Guise, T. A., Yin, J. J., Taylor, S. D., Kumagai, Y., Dallas, M., Boyce, B. F., Yoneda, T., and Mundy, G. R. (1996). Evidence for a causal role of parathyroid hormone-related protein in the pathogenesis of human breast cancer-mediated osteolysis. J Clin Invest 98, 1544-1549.
- Gulubova, M., Manolova, I., Ananiev, J., Julianov, A., Yovchev, Y., and Peeva, K. (2010). Role of TGF-beta1, its receptor TGFbetaRII, and Smad proteins in the progression of colorectal cancer. Int J Colorectal Dis 25, 591-599.
- Gutierrez, L. S., Eliza, M., Niven-Fairchild, T., Naftolin, F., and Mor, G. (1999). The Fas/Fas-ligand system: a mechanism for immune evasion in human breast carcinomas. Breast cancer research and treatment *54*, 245-253.
- Halbrooks, P. J., Ding, R., Wozney, J. M., and Bain, G. (2007). Role of RGM coreceptors in bone morphogenetic protein signaling. Journal of molecular signaling 2, 4.
- Hanahan, D., and Weinberg, R. A. (2000). The hallmarks of cancer. Cell 100, 57-70.
- Hardwick, J. C., Van Den Brink, G. R., Bleuming, S. A., Ballester, I., Van Den Brande, J. M., Keller, J. J., Offerhaus, G. J., Van Deventer, S. J., and Peppelenbosch, M. P. (2004). Bone morphogenetic protein 2 is expressed by, and acts upon, mature epithelial cells in the colon. Gastroenterology *126*, 111-121.
- Hassan, M., Ghozlan, H., and Abdel-Kader, O. (2005). Activation of c-Jun NH2-terminal kinase (JNK) signaling pathway is essential for the stimulation of hepatitis C virus (HCV) non-structural protein 3 (NS3)-mediated cell growth. Virology 333, 324-336.
- Hata, K., Fujitani, M., Yasuda, Y., Doya, H., Saito, T., Yamagishi, S., Mueller, B. K., and Yamashita, T. (2006). RGMa inhibition promotes axonal growth and recovery after spinal cord injury. J Cell Biol 173, 47-58.
- Hata, K., Kaibuchi, K., Inagaki, S., and Yamashita, T. (2009). Unc5B associates with LARG to mediate the action of repulsive guidance molecule. J Cell Biol 184, 737-750.
- Heldin, C. H., Miyazono, K., and ten Dijke, P. (1997). TGF-beta signalling from cell membrane to nucleus through SMAD proteins. Nature 390, 465-471.
- Helms, M. W., Packeisen, J., August, C., Schittek, B., Boecker, W., Brandt, B. H., and Buerger, H. (2005). First evidence supporting a potential role for the BMP/SMAD pathway in the progression of oestrogen receptor-positive breast cancer. J Pathol 206, 366-376.
- Herrera, B., van Dinther, M., Ten Dijke, P., and Inman, G. J. (2009). Autocrine bone morphogenetic protein-9 signals through activin receptor-like kinase-2/Smad1/Smad4 to promote ovarian cancer cell proliferation. Cancer Res 69, 9254-9262.

- Hiscox, S., Parr, C., Nakamura, T., Matsumoto, K., Mansel, R. E., and Jiang, W. G. (2000). Inhibition of HGF/SF-induced breast cancer cell motility and invasion by the HGF/SF variant, NK4. Breast Cancer Res Treat *59*, 245-254.
- Hong, J. H., Lee, G. T., Lee, J. H., Kwon, S. J., Park, S. H., Kim, S. J., and Kim, I. Y. (2009). Effect of bone morphogenetic protein-6 on macrophages. Immunology 128, e442-450.
- Hoodless, P. A., Haerry, T., Abdollah, S., Stapleton, M., O'Connor, M. B., Attisano, L., and Wrana, J. L. (1996). MADR1, a MAD-related protein that functions in BMP2 signaling pathways. Cell 85, 489-500.
- Hotten, G. C., Matsumoto, T., Kimura, M., Bechtold, R. F., Kron, R., Ohara, T., Tanaka, H., Satoh, Y., Okazaki, M., Shirai, T., et al. (1996). Recombinant human growth/differentiation factor 5 stimulates mesenchyme aggregation and chondrogenesis responsible for the skeletal development of limbs. Growth Factors 13, 65-74.
- Huang, F. W., Pinkus, J. L., Pinkus, G. S., Fleming, M. D., and Andrews, N. C. (2005). A mouse model of juvenile hemochromatosis. J Clin Invest 115, 2187-2191.
- Ishida, W., Hamamoto, T., Kusanagi, K., Yagi, K., Kawabata, M., Takehara, K., Sampath, T. K., Kato, M., and Miyazono, K. (2000). Smad6 is a Smad1/5-induced smad inhibitor. Characterization of bone morphogenetic protein-responsive element in the mouse Smad6 promoter. J Biol Chem 275, 6075-6079.
- Ishikawa, T., Yoshioka, H., Ohuchi, H., Noji, S., and Nohno, T. (1995). Truncated type II receptor for BMP-4 induces secondary axial structures in Xenopus embryos. Biochemical and biophysical research communications *216*, 26-33.
- Ishitani, T., Ninomiya-Tsuji, J., Nagai, S., Nishita, M., Meneghini, M., Barker, N., Waterman, M., Bowerman, B., Clevers, H., Shibuya, H., and Matsumoto, K. (1999). The TAK1-NLK-MAPK-related pathway antagonizes signalling between beta-catenin and transcription factor TCF. Nature 399, 798-802.
- Israel, D. I., Nove, J., Kerns, K. M., Kaufman, R. J., Rosen, V., Cox, K. A., and Wozney, J. M. (1996). Heterodimeric bone morphogenetic proteins show enhanced activity in vitro and in vivo. Growth Factors 13, 291-300.
- Itoh, F., Asao, H., Sugamura, K., Heldin, C. H., ten Dijke, P., and Itoh, S. (2001). Promoting bone morphogenetic protein signaling through negative regulation of inhibitory Smads. EMBO J 20, 4132-4142.
- Itoh, S., Itoh, F., Goumans, M. J., and Ten Dijke, P. (2000). Signaling of transforming growth factor-beta family members through Smad proteins. Eur J Biochem 267, 6954-6967.
- Iyengar, L., Patkunanathan, B., Lynch, O. T., McAvoy, J. W., Rasko, J. E., and Lovicu, F. J. (2006). Aqueous humour- and growth factor-induced lens cell proliferation is dependent on MAPK/ERK1/2 and Akt/PI3-K signalling. Exp Eye Res 83, 667-678.
- Izumi, N., Mizuguchi, S., Inagaki, Y., Saika, S., Kawada, N., Nakajima, Y., Inoue, K., Suehiro, S., Friedman, S. L., and Ikeda, K. (2006). BMP-7 opposes TGF-beta1-mediated collagen induction in mouse pulmonary myofibroblasts through Id2. Am J Physiol Lung Cell Mol Physiol 290, L120-126.
- Jemal, A., Siegel, R., Ward, E., Hao, Y., Xu, J., and Thun, M. J. (2009). Cancer statistics, 2009. CA Cancer J Clin 59, 225-249.
- Jeon, H. S., and Jen, J. (2010). TGF-beta signaling and the role of inhibitory Smads in non-small cell lung cancer. J Thorac Oncol 5, 417-419.
- Jiang, W. G., Davies, G., Martin, T. A., Parr, C., Watkins, G., Mason, M. D., Mokbel, K., and Mansel, R. E. (2005a). Targeting matrilysin and its impact on tumor growth in vivo: the potential implications in breast cancer therapy. Clin Cancer Res 11, 6012-6019.
- Jiang, W. G., Davies, G., Martin, T. A., Parr, C., Watkins, G., Mason, M. D., Mokbel, K., and Mansel, R. E. (2005b). targeting Matrilysin and Its Impact on Tumour Growth *In*

- vivo: The Potential Implications in Breast Cancer Theray. Clinical Cancer Research 11, 6012 6019.
- Jiang, W. G., Grimshaw, D., Lane, J., Martin, T. A., Abounader, R., Laterra, J., and Mansel, R. E. (2001). A hammerhead ribozyme suppresses expression of hepatocyte growth factor/scatter factor receptor c-MET and reduces migration and invasiveness of breast cancer cells. Clin Cancer Res 7, 2555-2562.
- Jiang, W. G., Hiscox, S., Hallett, M. B., Horrobin, D. F., Scott, C., and Puntis, M. C. A. (1995a). Inhibition of invasion and motility of human colon cancer cells by gamma linolenic acid. British Journal of Cancer 71, 744 752.
- Jiang, W. G., Hiscox, S., Singhrao, S. K., Nakamura, T., Puntis, M. C. A., and Hallet, M. B. (1995b). Inhibition of HGF/SF-Induced Membrane Ruffling and Cell Motility by Transient Elevation of Cytosolic Free Ca2+. Experimental Cell Research 220, 424 - 433.
- Jiang, W. G., HIscox, S. E., Parr, C., Martin, T. A., Matsumoto, K., Nakamura, T., and Mansel, R. E. (1999). Antagonistic effect of NK4, a novel hepatocyte growth factor variant, on *in vitro* angiogenesis of human vascular endothelial cells. Cacner Research 5, 3695 - 3703.
- Jiang, Y., Liu, M. T., and Gershon, M. D. (2003). Netrins and DCC in the guidance of migrating neural crest-derived cells in the developing bowel and pancreas. Dev Biol 258, 364-384.
- Jikko, A., Harris, S. E., Chen, D., Mendrick, D. L., and Damsky, C. H. (1999). Collagen integrin receptors regulate early osteoblast differentiation induced by BMP-2. J Bone Miner Res 14, 1075-1083.
- Jin, X., Yagi, M., Akiyama, N., Hirosaki, T., Higashi, S., Lin, C. Y., Dickson, R. B., Kitamura, H., and Miyazaki, K. (2006). Matriptase activates stromelysin (MMP-3) and promotes tumor growth and angiogenesis. Cancer Sci 97, 1327-1334.
- Jinnin, M., Ihn, H., and Tamaki, K. (2006). Characterization of SIS3, a novel specific inhibitor of Smad3, and its effect on transforming growth factor-beta1-induced extracellular matrix expression. Mol Pharmacol 69, 597-607.
- Jones, C. M., Lyons, K. M., and Hogan, B. L. (1991). Involvement of Bone Morphogenetic Protein-4 (BMP-4) and Vgr-1 in morphogenesis and neurogenesis in the mouse. Development 111, 531-542.
- Jonk, L. J., Itoh, S., Heldin, C. H., ten Dijke, P., and Kruijer, W. (1998). Identification and functional characterization of a Smad binding element (SBE) in the JunB promoter that acts as a transforming growth factor-beta, activin, and bone morphogenetic protein-inducible enhancer. The Journal of biological chemistry 273, 21145-21152.
- Jorieux, S., Fressinaud, E., Goudemand, J., Gaucher, C., Meyer, D., and Mazurier, C. (2000). Conformational changes in the D' domain of von Willebrand factor induced by CYS 25 and CYS 95 mutations lead to factor VIII binding defect and multimeric impairment. Blood 95, 3139-3145.
- Kanomata, K., Kokabu, S., Nojima, J., Fukuda, T., and Katagiri, T. (2009a). DRAGON, a GPI-anchored membrane protein, inhibits BMP signaling in C2C12 myoblasts. Genes Cells 14, 695-702.
- Kanomata, K., Kokabu, S., Nojima, J., Fukuda, T., and Katagiri, T. (2009b). DRAGON, a GPI-anchored membrane protein, inhibits BMP signaling in C2C12 myoblasts. Genes Cells.
- Ketolainen, J. M., Alarmo, E. L., Tuominen, V. J., and Kallioniemi, A. Parallel inhibition of cell growth and induction of cell migration and invasion in breast cancer cells by bone morphogenetic protein 4. Breast Cancer Res Treat.
- Kimura, N., Matsuo, R., Shibuya, H., Nakashima, K., and Taga, T. (2000). BMP2-induced apoptosis is mediated by activation of the TAK1-p38 kinase pathway that is negatively regulated by Smad6. J Biol Chem *275*, 17647-17652.

- Klotz, L., Schellhammer, P., and Carroll, K. (2004). A re-assessment of the role of combined androgen blockade for advanced prostate cancer. BJU Int 93, 1177-1182.
- Kobayashi, H. (2001). Suppression of urokinase expression and tumor metastasis by bikunin overexpression [mini-review]. Hum Cell 14, 233-236.
- Kodach, L. L., Bleuming, S. A., Musler, A. R., Peppelenbosch, M. P., Hommes, D. W., van den Brink, G. R., van Noesel, C. J., Offerhaus, G. J., and Hardwick, J. C. (2008). The bone morphogenetic protein pathway is active in human colon adenomas and inactivated in colorectal cancer. Cancer 112, 300-306.
- Kong, X. T., Choi, S. H., Bessho, F., Kobayashi, M., Hanada, R., Yamamoto, K., and Hayashi, Y. (2001). Codon 201(Gly) polymorphic type of the DCC gene is related to disseminated neuroblastoma. Neoplasia 3, 267-272.
- Kumano, M., Miyake, H., Muramaki, M., Furukawa, J., Takenaka, A., and Fujisawa, M. (2009). Expression of urokinase-type plasminogen activator system in prostate cancer: correlation with clinicopathological outcomes in patients undergoing radical prostatectomy. Urol Oncol 27, 180-186.
- Kumar, P., Miller, A. I., and Polverini, P. J. (2004). p38 MAPK mediates gamma-irradiation-induced endothelial cell apoptosis, and vascular endothelial growth factor protects endothelial cells through the phosphoinositide 3-kinase-Akt-Bcl-2 pathway. J Biol Chem 279, 43352-43360.
- Kuninger, D., Kuns-Hashimoto, R., Nili, M., and Rotwein, P. (2008). Pro-protein convertases control the maturation and processing of the iron-regulatory protein, RGMc/hemojuvelin. BMC Biochem 9, 9.
- Kuninger, D., Kuzmickas, R., Peng, B., Pintar, J. E., and Rotwein, P. (2004). Gene discovery by microarray: identification of novel genes induced during growth factor-mediated muscle cell survival and differentiation. Genomics 84, 876-889.
- Kuns-Hashimoto, R., Kuninger, D., Nili, M., and Rotwein, P. (2008). Selective binding of RGMc/hemojuvelin, a key protein in systemic iron metabolism, to BMP-2 and neogenin. Am J Physiol Cell Physiol *294*, C994-C1003.
- Kwon, H., Kim, H. J., Rice, W. L., Subramanian, B., Park, S. H., Georgakoudi, I., and Kaplan, D. L. Development of an in vitro model to study the impact of BMP-2 on metastasis to bone. J Tissue Eng Regen Med.
- Lagna, G., Hata, A., Hemmati-Brivanlou, A., and Massague, J. (1996). Partnership between DPC4 and SMAD proteins in TGF-beta signalling pathways. Nature 383, 832-836.
- Lamszus, K., Joseph, A., Jin, L., Yao, Y., Chowdhury, S., Fuchs, A., Polverini, P. J., Goldberg, I. D., and Rosen, E. M. (1996). Scatter factor binds to thrombospondin and other extracellular matrix components. Am J Pathol *149*, 805-819.
- Lasorella, A., Noseda, M., Beyna, M., Yokota, Y., and Iavarone, A. (2000). Id2 is a retinoblastoma protein target and mediates signalling by Myc oncoproteins. Nature 407, 592-598.
- Lee, D. H., Zhou, L. J., Zhou, Z., Xie, J. X., Jung, J. U., Liu, Y., Xi, C. X., Mei, L., and Xiong, W. C. (2010). Neogenin inhibits HJV secretion and regulates BMP-induced hepcidin expression and iron homeostasis. Blood *115*, 3136-3145.
- Lee, S. W., Han, S. I., Kim, H. H., and Lee, Z. H. (2002). TAK1-dependent activation of AP-1 and c-Jun N-terminal kinase by receptor activator of NF-kappaB. J Biochem Mol Biol 35, 371-376.
- Leeper, N. J., Raiesdana, A., Kojima, Y., Chun, H. J., Azuma, J., Maegdefessel, L., Kundu, R. K., Quertermous, T., Tsao, P. S., and Spin, J. M. MicroRNA-26a is a novel regulator of vascular smooth muscle cell function. J Cell Physiol.
- Lejmi, E., Leconte, L., Pedron-Mazoyer, S., Ropert, S., Raoul, W., Lavalette, S., Bouras, I., Feron, J. G., Maitre-Boube, M., Assayag, F., et al. (2008). Netrin-4 inhibits

- angiogenesis via binding to neogenin and recruitment of Unc5B. Proc Natl Acad Sci U S A 105, 12491-12496.
- Li, H., Sekine, M., Seng, S., Avraham, S., and Avraham, H. K. (2009a). BRCA1 interacts with Smad3 and regulates Smad3-mediated TGF-beta signaling during oxidative stress responses. PLoS One 4, e7091.
- Li, I. W., Cheifetz, S., McCulloch, C. A., Sampath, K. T., and Sodek, J. (1996). Effects of osteogenic protein-1 (OP-1, BMP-7) on bone matrix protein expression by fetal rat calvarial cells are differentiation stage specific. J Cell Physiol 169, 115-125.
- Li, V. S., Yuen, S. T., Chan, T. L., Yan, H. H., Law, W. L., Yeung, B. H., Chan, A. S., Tsui, W. Y., So, S., Chen, X., and Leung, S. Y. (2009b). Frequent inactivation of axon guidance molecule RGMA in human colon cancer through genetic and epigenetic mechanisms. Gastroenterology 137, 176-187.
- Liang, Y. Y., Brunicardi, F. C., and Lin, X. (2009). Smad3 mediates immediate early induction of Id1 by TGF-beta. Cell Res 19, 140-148.
- Lim, S. T., Chen, X. L., Lim, Y., Hanson, D. A., Vo, T. T., Howerton, K., Larocque, N., Fisher, S. J., Schlaepfer, D. D., and Ilic, D. (2008). Nuclear FAK promotes cell proliferation and survival through FERM-enhanced p53 degradation. Mol Cell 29, 9-22.
- Lin, L., Goldberg, Y. P., and Ganz, T. (2005). Competitive regulation of hepcidin mRNA by soluble and cell-associated hemojuvelin. Blood 106, 2884-2889.
- Lin, L., Nemeth, E., Goodnough, J. B., Thapa, D. R., Gabayan, V., and Ganz, T. (2008). Soluble hemojuvelin is released by proprotein convertase-mediated cleavage at a conserved polybasic RNRR site. Blood Cells Mol Dis 40, 122-131.
- Ling, M. T., Wang, X., Zhang, X., and Wong, Y. C. (2006). The multiple roles of Id-1 in cancer progression. Differentiation 74, 481-487.
- Liu, F., Hata, A., Baker, J. C., Doody, J., Carcamo, J., Harland, R. M., and Massague, J. (1996). A human Mad protein acting as a BMP-regulated transcriptional activator. Nature 381, 620-623.
- Liu, F., Ventura, F., Doody, J., and Massague, J. (1995). Human type II receptor for bone morphogenic proteins (BMPs): extension of the two-kinase receptor model to the BMPs. Mol Cell Biol 15, 3479-3486.
- Liu, G., Beggs, H., Jurgensen, C., Park, H. T., Tang, H., Gorski, J., Jones, K. R., Reichardt, L. F., Wu, J., and Rao, Y. (2004). Netrin requires focal adhesion kinase and Src family kinases for axon outgrowth and attraction. Nat Neurosci 7, 1222-1232.
- Liu, X., Hashimoto, M., Horii, H., Yamaguchi, A., Naito, K., and Yamashita, T. (2009). Repulsive guidance molecule b inhibits neurite growth and is increased after spinal cord injury. Biochemical and biophysical research communications *382*, 795-800.
- Lo, A. K., Dawson, C. W., Lo, K. W., Yu, Y., and Young, L. S. Upregulation of Id1 by Epstein-Barr virus-encoded LMP1 confers resistance to TGFbeta-mediated growth inhibition. Mol Cancer 9, 155.
- Lopez-Rovira, T., Chalaux, E., Massague, J., Rosa, J. L., and Ventura, F. (2002). Direct binding of Smad1 and Smad4 to two distinct motifs mediates bone morphogenetic protein-specific transcriptional activation of Id1 gene. J Biol Chem 277, 3176-3185.
- Luo, G., Hofmann, C., Bronckers, A. L., Sohocki, M., Bradley, A., and Karsenty, G. (1995). BMP-7 is an inducer of nephrogenesis, and is also required for eye development and skeletal patterning. Genes Dev 9, 2808-2820.
- Lyons, K. M., Pelton, R. W., and Hogan, B. L. (1990). Organogenesis and pattern formation in the mouse: RNA distribution patterns suggest a role for bone morphogenetic protein-2A (BMP-2A). Development 109, 833-844.
- Macias-Silva, M., Hoodless, P. A., Tang, S. J., Buchwald, M., and Wrana, J. L. (1998). Specific activation of Smad1 signaling pathways by the BMP7 type I receptor, ALK2. The Journal of biological chemistry 273, 25628-25636.

- Macias, D., Ganan, Y., Sampath, T. K., Piedra, M. E., Ros, M. A., and Hurle, J. M. (1997). Role of BMP-2 and OP-1 (BMP-7) in programmed cell death and skeletogenesis during chick limb development. Development *124*, 1109-1117.
- Manitt, C., Thompson, K. M., and Kennedy, T. E. (2004). Developmental shift in expression of netrin receptors in the rat spinal cord: predominance of UNC-5 homologues in adulthood. J Neurosci Res 77, 690-700.
- Marquardt, H., Lioubin, M. N., and Ikeda, T. (1987). Complete amino acid sequence of human transforming growth factor type beta 2. J Biol Chem 262, 12127-12131.
- Martin, T. A., Mansel, R. E., and Jiang, W. G. (2002). Antagonistic effect of NK4 on HGF/SF induced changes in the transendothelial resistance (TER) and paracellular permeability of human vascular endothelial cells. J Cell Physiol 192, 268-275.
- Martin, T. A., Parr, C., Davies, G., Watkins, G., Lane, J., Matsumoto, K., Nakamura, T., Mansel, R. E., and Jiang, W. G. (2003a). Growth and angiogenesis of human breast cancer in a nude mouse tumour model is reduced by NK4, a HGF/SF antagonist. Carcinogenesis 24, 1317 1323.
- Martin, T. A., Parr, C., Davies, G., Watkins, G., Lane, J., Matsumoto, K., Nakamura, T., Mansel, R. E., and Jiang, W. G. (2003b). Growth and angiogenesis of human breast cancer in a nude mouse tumour model is reduced by NK4, a HGF/SF antagonist. Carcinogenesis 24, 1317-1323.
- Martin, T. A., Watkins, G., Mansel, R. E., and Jiang, W. G. (2004). Hepatocyte growth factor disrupts tight junctions in human breast cancer cells. Cell Biol Int 28, 361-371.
- Massague, J., Attisano, L., and Wrana, J. L. (1994). The TGF-beta family and its composite receptors. Trends Cell Biol 4, 172-178.
- Matsunaga, E., and Chedotal, A. (2004). Repulsive guidance molecule/neogenin: a novel ligand-receptor system playing multiple roles in neural development. Development, growth & differentiation 46, 481-486.
- Matsunaga, E., Nakamura, H., and Chedotal, A. (2006). Repulsive guidance molecule plays multiple roles in neuronal differentiation and axon guidance. J Neurosci 26, 6082-6088.
- Matsunaga, E., Tauszig-Delamasure, S., Monnier, P. P., Mueller, B. K., Strittmatter, S. M., Mehlen, P., and Chedotal, A. (2004). RGM and its receptor neogenin regulate neuronal survival. Nat Cell Biol 6, 749-755.
- Matteucci, E., Locati, M., and Desiderio, M. A. (2005). Hepatocyte growth factor enhances CXCR4 expression favoring breast cancer cell invasiveness. Exp Cell Res *310*, 176-185.
- McPherron, A. C., Lawler, A. M., and Lee, S. J. (1997). Regulation of skeletal muscle mass in mice by a new TGF-beta superfamily member. Nature 387, 83-90.
- Meiners, S., Brinkmann, V., Naundorf, H., and Birchmeier, W. (1998). Role of morphogenetic factors in metastasis of mammary carcinoma cells. Oncogene 16, 9-20.
- Metzger, M., Conrad, S., Alvarez-Bolado, G., Skutella, T., and Just, L. (2005). Gene expression of the repulsive guidance molecules during development of the mouse intestine. Dev Dyn 234, 169-175.
- Miki, T., Yano, S., Hanibuchi, M., and Sone, S. (2000). Bone metastasis model with multiorgan dissemination of human small-cell lung cancer (SBC-5) cells in natural killer cell-depleted SCID mice. Oncol Res *12*, 209-217.
- Mine, S., Fujisaki, T., Kawahara, C., Tabata, T., Iida, T., Yasuda, M., Yoneda, T., and Tanaka, Y. (2003). Hepatocyte growth factor enhances adhesion of breast cancer cells to endothelial cells in vitro through up-regulation of CD44. Exp Cell Res 288, 189-197.
- Miyazaki, H., Watabe, T., Kitamura, T., and Miyazono, K. (2004). BMP signals inhibit proliferation and in vivo tumor growth of androgen-insensitive prostate carcinoma cells. Oncogene 23, 9326-9335.
- Miyazawa, K., Shinozaki, M., Hara, T., Furuya, T., and Miyazono, K. (2002). Two major Smad pathways in TGF-beta superfamily signalling. Genes Cells 7, 1191-1204.

- Miyazono, K. (2009). Transforming growth factor-beta signaling in epithelial-mesenchymal transition and progression of cancer. Proc Jpn Acad Ser B Phys Biol Sci 85, 314-323.
- Miyazono, K., and Miyazawa, K. (2002). Id: a target of BMP signaling. Sci STKE 2002, pe40.
- Monnier, P. P., Sierra, A., Macchi, P., Deitinghoff, L., Andersen, J. S., Mann, M., Flad, M., Hornberger, M. R., Stahl, B., Bonhoeffer, F., and Mueller, B. K. (2002). RGM is a repulsive guidance molecule for retinal axons. Nature 419, 392-395.
- Mor, G., Kohen, F., Garcia-Velasco, J., Nilsen, J., Brown, W., Song, J., and Naftolin, F. (2000). Regulation of fas ligand expression in breast cancer cells by estrogen: functional differences between estradiol and tamoxifen. J Steroid Biochem Mol Biol 73, 185-194.
- Moriguchi, T., Gotoh, Y., and Nishida, E. (1996a). Roles of the MAP kinase cascade in vertebrates. Adv Pharmacol 36, 121-137.
- Moriguchi, T., Kuroyanagi, N., Yamaguchi, K., Gotoh, Y., Irie, K., Kano, T., Shirakabe, K., Muro, Y., Shibuya, H., Matsumoto, K., *et al.* (1996b). A novel kinase cascade mediated by mitogen-activated protein kinase kinase 6 and MKK3. J Biol Chem *271*, 13675-13679.
- Moustakas, A., and Heldin, C. H. (2002). From mono- to oligo-Smads: the heart of the matter in TGF-beta signal transduction. Genes Dev 16, 1867-1871.
- Mundy, G. R. (2002). Metastasis to bone: causes, consequences and therapeutic opportunities. Nat Rev Cancer 2, 584-593.
- Murugan, R. C., Lee, P. L., Kalavar, M. R., and Barton, J. C. (2008). Early age-of-onset iron overload and homozygosity for the novel hemojuvelin mutation HJV R54X (exon 3; c.160A-->T) in an African American male of West Indies descent. Clin Genet 74, 88-92.
- Nagarajan, R. P., Zhang, J., Li, W., and Chen, Y. (1999). Regulation of Smad7 promoter by direct association with Smad3 and Smad4. J Biol Chem 274, 33412-33418.
- Naslund, M. J., Strandberg, J. D., and Coffey, D. S. (1988). The role of androgens and estrogens in the pathogenesis of experimental nonbacterial prostatitis. J Urol 140, 1049-1053.
- Newman, L. A., Kuerer, H. M., Hunt, K. K., Singh, G., Ames, F. C., Feig, B. W., Ross, M. I., Taylor, S., and Singletary, S. E. (1999). Local recurrence and survival among black women with early-stage breast cancer treated with breast-conservation therapy or mastectomy. Ann Surg Oncol 6, 241-248.
- Niederkofler, V., Salie, R., and Arber, S. (2005). Hemojuvelin is essential for dietary iron sensing, and its mutation leads to severe iron overload. J Clin Invest 115, 2180-2186.
- Niederkofler, V., Salie, R., Sigrist, M., and Arber, S. (2004). Repulsive guidance molecule (RGM) gene function is required for neural tube closure but not retinal topography in the mouse visual system. J Neurosci 24, 808-818.
- Noguchi, K., Yamana, H., Kitanaka, C., Mochizuki, T., Kokubu, A., and Kuchino, Y. (2000). Differential role of the JNK and p38 MAPK pathway in c-Myc- and s-Myc-mediated apoptosis. Biochem Biophys Res Commun 267, 221-227.
- Nohe, A., Hassel, S., Ehrlich, M., Neubauer, F., Sebald, W., Henis, Y. I., and Knaus, P. (2002). The mode of bone morphogenetic protein (BMP) receptor oligomerization determines different BMP-2 signaling pathways. The Journal of biological chemistry 277, 5330-5338.
- Nohe, A., Keating, E., Knaus, P., and Petersen, N. O. (2004). Signal transduction of bone morphogenetic protein receptors. Cell Signal 16, 291-299.
- Noldus, J., Graefen, M., Huland, E., Busch, C., Hammerer, P., and Huland, H. (1998). The value of the ratio of free-to-total prostate specific antigen for staging purposes in previously untreated prostate cancer. J Urol 159, 2004-2007; discussion 2007-2008.
- Norton, J. D. (2000). ID helix-loop-helix proteins in cell growth, differentiation and tumorigenesis. J Cell Sci 113 (Pt 22), 3897-3905.

- Ohtani, N., Zebedee, Z., Huot, T. J., Stinson, J. A., Sugimoto, M., Ohashi, Y., Sharrocks, A. D., Peters, G., and Hara, E. (2001). Opposing effects of Ets and Id proteins on p16INK4a expression during cellular senescence. Nature 409, 1067-1070.
- Oldekamp, J., Kramer, N., Alvarez-Bolado, G., and Skutella, T. (2004). Expression pattern of the repulsive guidance molecules RGM A, B and C during mouse development. Gene Expr Patterns 4, 283-288.
- Omi, M., Sato-Maeda, M., and Ide, H. (2000). Role of chondrogenic tissue in programmed cell death and BMP expression in chick limb buds. Int J Dev Biol 44, 381-388.
- Onichtchouk, D., Chen, Y. G., Dosch, R., Gawantka, V., Delius, H., Massague, J., and Niehrs, C. (1999). Silencing of TGF-beta signalling by the pseudoreceptor BAMBI. Nature 401, 480-485.
- Ozkaynak, E., Rueger, D. C., Drier, E. A., Corbett, C., Ridge, R. J., Sampath, T. K., and Oppermann, H. (1990). OP-1 cDNA encodes an osteogenic protein in the TGF-beta family. Embo J 9, 2085-2093.
- Papageorgis, P., Lambert, A. W., Ozturk, S., Gao, F., Pan, H., Manne, U., Alekseyev, Y. O., Thiagalingam, A., Abdolmaleky, H. M., Lenburg, M., and Thiagalingam, S. Smad signaling is required to maintain epigenetic silencing during breast cancer progression. Cancer Res 70, 968-978.
- Papanikolaou, G., Samuels, M. E., Ludwig, E. H., MacDonald, M. L., Franchini, P. L., Dube, M. P., Andres, L., MacFarlane, J., Sakellaropoulos, N., Politou, M., et al. (2004). Mutations in HFE2 cause iron overload in chromosome 1q-linked juvenile hemochromatosis. Nature genetics 36, 77-82.
- Parish, C. R., Jakobsen, K. B., and Coombe, D. R. (1992). A basement membrane permeability assay which correlates with the metastatic potential of tumor cells. International Journal of Cancer *52*, 378 383.
- Park, K. W., Crouse, D., Lee, M., Karnik, S. K., Sorensen, L. K., Murphy, K. J., Kuo, C. J., and Li, D. Y. (2004). The axonal attractant Netrin-1 is an angiogenic factor. Proc Natl Acad Sci U S A 101, 16210-16215.
- Park, M. S., Kim, Y. H., and Lee, J. W. FAK mediates signal crosstalk between type II collagen and TGF-beta 1 cascades in chondrocytic cells. Matrix Biol 29, 135-142.
- Parr, C., and Jiang, W. G. (2006). Hepatocyte growth factor activation inhibitors (HAI-1 and HAI-2) regulate HGF-induced invasion of human breast cancer cells. Int J Cancer 119, 1176-1183.
- Parr, C., Sanders, A. J., Davies, G., Martin, T., Lane, J., Mason, M. D., Mansel, R. E., and Jiang, W. G. (2007). Matriptase-2 inhibits breast tumor growth and invasion and correlates with favorable prognosis for breast cancer patients. Clin Cancer Res 13, 3568-3576.
- Parr, C., Watkins, G., and Jiang, W. G. (2004). The possible correlation of Notch-1 and Notch-2 with clinical outcome and tumour clinicopathological parameters in human breast cancer. Int J Mol Med 14, 779-786.
- Partin, A. W., Carter, H. B., Chan, D. W., Epstein, J. I., Oesterling, J. E., Rock, R. C., Weber, J. P., and Walsh, P. C. (1990). Prostate specific antigen in the staging of localized prostate cancer: influence of tumor differentiation, tumor volume and benign hyperplasia. J Urol 143, 747-752.
- Patel, M. I., DeConcini, D. T., Lopez-Corona, E., Ohori, M., Wheeler, T., and Scardino, P. T. (2004). An analysis of men with clinically localized prostate cancer who deferred definitive therapy. J Urol 171, 1520-1524.
- Piscione, T. D., Phan, T., and Rosenblum, N. D. (2001). BMP7 controls collecting tubule cell proliferation and apoptosis via Smad1-dependent and -independent pathways. Am J Physiol Renal Physiol 280, F19-33.

- Polascik, T. J., Oesterling, J. E., and Partin, A. W. (1999). Prostate specific antigen: a decade of discovery--what we have learned and where we are going. J Urol 162, 293-306.
- Porter, A. G., and Dhakshinamoorthy, S. (2004). Apoptosis initiated by dependence receptors: a new paradigm for cell death? Bioessays 26, 656-664.
- Powell, G. J., Southby, J., Danks, J. A., Stillwell, R. G., Hayman, J. A., Henderson, M. A., Bennett, R. C., and Martin, T. J. (1991). Localization of parathyroid hormone-related protein in breast cancer metastases: increased incidence in bone compared with other sites. Cancer research *51*, 3059-3061.
- Pulukuri, S. M., and Rao, J. S. (2007). Small interfering RNA directed reversal of urokinase plasminogen activator demethylation inhibits prostate tumor growth and metastasis. Cancer Res 67, 6637-6646.
- Rabbani, S. A., Mazar, A. P., Bernier, S. M., Haq, M., Bolivar, I., Henkin, J., and Goltzman, D. (1992). Structural requirements for the growth factor activity of the amino-terminal domain of urokinase. J Biol Chem 267, 14151-14156.
- Rajagopalan, S., Deitinghoff, L., Davis, D., Conrad, S., Skutella, T., Chedotal, A., Mueller, B. K., and Strittmatter, S. M. (2004). Neogenin mediates the action of repulsive guidance molecule. Nat Cell Biol 6, 756-762.
- Rasmussen, A. A., and Cullen, K. J. (1998). Paracrine/autocrine regulation of breast cancer by the insulin-like growth factors. Breast cancer research and treatment 47, 219-233.
- Reddi, A. H. (2001). Interplay between bone morphogenetic proteins and cognate binding proteins in bone and cartilage development: noggin, chordin and DAN. Arthritis Res 3, 1-5.
- Ren, X. R., Ming, G. L., Xie, Y., Hong, Y., Sun, D. M., Zhao, Z. Q., Feng, Z., Wang, Q., Shim, S., Chen, Z. F., et al. (2004). Focal adhesion kinase in netrin-1 signaling. Nat Neurosci 7, 1204-1212.
- Ross, D. T., Scherf, U., Eisen, M. B., Perou, C. M., Rees, C., Spellman, P., Iyer, V., Jeffrey, S. S., Van de Rijn, M., Waltham, M., *et al.* (2000). Systematic variation in gene expression patterns in human cancer cell lines. Nat Genet *24*, 227-235.
- Ruoslahti, E., and Obrink, B. (1996). Common principles in cell adhesion. Exp Cell Res 227, 1-11
- Sadler, J. E. (1998). Biochemistry and genetics of von Willebrand factor. Annu Rev Biochem 67, 395-424.
- Samad, T. A., Rebbapragada, A., Bell, E., Zhang, Y., Sidis, Y., Jeong, S. J., Campagna, J. A., Perusini, S., Fabrizio, D. A., Schneyer, A. L., et al. (2005). DRAGON, a bone morphogenetic protein co-receptor. The Journal of biological chemistry 280, 14122-14129.
- Samad, T. A., Srinivasan, A., Karchewski, L. A., Jeong, S. J., Campagna, J. A., Ji, R. R., Fabrizio, D. A., Zhang, Y., Lin, H. Y., Bell, E., and Woolf, C. J. (2004). DRAGON: a member of the repulsive guidance molecule-related family of neuronal- and muscle-expressed membrane proteins is regulated by DRG11 and has neuronal adhesive properties. J Neurosci 24, 2027-2036.
- Sampath, T. K., Maliakal, J. C., Hauschka, P. V., Jones, W. K., Sasak, H., Tucker, R. F., White, K. H., Coughlin, J. E., Tucker, M. M., Pang, R. H., and et al. (1992).
 Recombinant human osteogenic protein-1 (hOP-1) induces new bone formation in vivo with a specific activity comparable with natural bovine osteogenic protein and stimulates osteoblast proliferation and differentiation in vitro. J Biol Chem 267, 20352-20362.
- Sanders, A. J., Parr, C., Martin, T. A., Lane, J., Mason, M. D., and Jiang, W. G. (2008). Genetic upregulation of matriptase-2 reduces the aggressiveness of prostate cancer cells in vitro and in vivo and affects FAK and paxillin localisation. J Cell Physiol 216, 780-789.

- Schaffar, G., Taniguchi, J., Brodbeck, T., Meyer, A. H., Schmidt, M., Yamashita, T., and Mueller, B. K. (2008). LIM-only protein 4 interacts directly with the repulsive guidance molecule A receptor Neogenin. J Neurochem 107, 418-431.
- Schmidtmer, J., and Engelkamp, D. (2004). Isolation and expression pattern of three mouse homologues of chick Rgm. Gene Expr Patterns 4, 105-110.
- Schnichels, S., Conrad, S., Warstat, K., Henke-Fahle, S., Skutella, T., Schraermeyer, U., and Julien, S. (2007). Gene expression of the repulsive guidance molecules/neogenin in the developing and mature mouse visual system: C57BL/6J vs. the glaucoma model DBA/2J. Gene Expr Patterns 8, 1-11.
- Schuhmacher, M., Staege, M. S., Pajic, A., Polack, A., Weidle, U. H., Bornkamm, G. W., Eick, D., and Kohlhuber, F. (1999). Control of cell growth by c-Myc in the absence of cell division. Curr Biol 9, 1255-1258.
- Schwab, J. M., Conrad, S., Monnier, P. P., Julien, S., Mueller, B. K., and Schluesener, H. J. (2005a). Spinal cord injury-induced lesional expression of the repulsive guidance molecule (RGM). Eur J Neurosci 21, 1569-1576.
- Schwab, J. M., Monnier, P. P., Schluesener, H. J., Conrad, S., Beschorner, R., Chen, L., Meyermann, R., and Mueller, B. K. (2005b). Central nervous system injury-induced repulsive guidance molecule expression in the adult human brain. Arch Neurol 62, 1561-1568.
- Sheen-Chen, S. M., Liu, Y. W., Eng, H. L., and Chou, F. F. (2005). Serum levels of hepatocyte growth factor in patients with breast cancer. Cancer Epidemiol Biomarkers Prev 14, 715-717.
- Shi, Y., and Massague, J. (2003). Mechanisms of TGF-beta signaling from cell membrane to the nucleus. Cell 113, 685-700.
- Shi, Y., Wang, Y. F., Jayaraman, L., Yang, H., Massague, J., and Pavletich, N. P. (1998). Crystal structure of a Smad MH1 domain bound to DNA: insights on DNA binding in TGF-beta signaling. Cell 94, 585-594.
- Shibuya, H., Iwata, H., Masuyama, N., Gotoh, Y., Yamaguchi, K., Irie, K., Matsumoto, K., Nishida, E., and Ueno, N. (1998). Role of TAK1 and TAB1 in BMP signaling in early Xenopus development. EMBO J 17, 1019-1028.
- Shibuya, H., Yamaguchi, K., Shirakabe, K., Tonegawa, A., Gotoh, Y., Ueno, N., Irie, K., Nishida, E., and Matsumoto, K. (1996). TAB1: an activator of the TAK1 MAPKKK in TGF-beta signal transduction. Science 272, 1179-1182.
- Shin, G. J., and Wilson, N. H. (2008). Overexpression of repulsive guidance molecule (RGM) a induces cell death through Neogenin in early vertebrate development. J Mol Histol 39, 105-113.
- Shirakabe, K., Yamaguchi, K., Shibuya, H., Irie, K., Matsuda, S., Moriguchi, T., Gotoh, Y., Matsumoto, K., and Nishida, E. (1997). TAK1 mediates the ceramide signaling to stress-activated protein kinase/c-Jun N-terminal kinase. The Journal of biological chemistry 272, 8141-8144.
- Silvestri, L., Pagani, A., and Camaschella, C. (2008a). Furin-mediated release of soluble hemojuvelin: a new link between hypoxia and iron homeostasis. Blood 111, 924-931.
- Silvestri, L., Pagani, A., Fazi, C., Gerardi, G., Levi, S., Arosio, P., and Camaschella, C. (2007). Defective targeting of hemojuvelin to plasma membrane is a common pathogenetic mechanism in juvenile hemochromatosis. Blood *109*, 4503-4510.
- Silvestri, L., Pagani, A., Nai, A., De Domenico, I., Kaplan, J., and Camaschella, C. (2008b). The serine protease matriptase-2 (TMPRSS6) inhibits hepcidin activation by cleaving membrane hemojuvelin. Cell Metab 8, 502-511.
- Smith, H. S., Lu, Y., Deng, G., Martinez, O., Krams, S., Ljung, B. M., Thor, A., and Lagios, M. (1993). Molecular aspects of early stages of breast cancer progression. J Cell Biochem Suppl 17G, 144-152.

- Smith, J. R., Freije, D., Carpten, J. D., Gronberg, H., Xu, J., Isaacs, S. D., Brownstein, M. J., Bova, G. S., Guo, H., Bujnovszky, P., et al. (1996). Major susceptibility locus for prostate cancer on chromosome 1 suggested by a genome-wide search. Science 274, 1371-1374.
- Song, H., Guo, B., Zhang, J., and Song, C. Transforming growth factor-beta suppressed Id-1 Expression in a smad3-dependent manner in LoVo cells. Anat Rec (Hoboken) 293, 42-47.
- Southby, J., Kissin, M. W., Danks, J. A., Hayman, J. A., Moseley, J. M., Henderson, M. A., Bennett, R. C., and Martin, T. J. (1990). Immunohistochemical localization of parathyroid hormone-related protein in human breast cancer. Cancer research 50, 7710-7716.
- Sprague, J., Bayraktaroglu, L., Clements, D., Conlin, T., Fashena, D., Frazer, K., Haendel, M., Howe, D. G., Mani, P., Ramachandran, S., et al. (2006). The Zebrafish Information Network: the zebrafish model organism database. Nucleic Acids Res 34, D581-585.
- Stahl, B., Muller, B., von Boxberg, Y., Cox, E. C., and Bonhoeffer, F. (1990). Biochemical characterization of a putative axonal guidance molecule of the chick visual system. Neuron 5, 735-743.
- Stamey, T. A., and Kabalin, J. N. (1989). Prostate specific antigen in the diagnosis and treatment of adenocarcinoma of the prostate. I. Untreated patients. J Urol 141, 1070-1075
- Stamey, T. A., Kabalin, J. N., and Ferrari, M. (1989a). Prostate specific antigen in the diagnosis and treatment of adenocarcinoma of the prostate. III. Radiation treated patients. J Urol 141, 1084-1087.
- Stamey, T. A., Kabalin, J. N., Ferrari, M., and Yang, N. (1989b). Prostate specific antigen in the diagnosis and treatment of adenocarcinoma of the prostate. IV. Anti-androgen treated patients. J Urol 141, 1088-1090.
- Stamey, T. A., Kabalin, J. N., McNeal, J. E., Johnstone, I. M., Freiha, F., Redwine, E. A., and Yang, N. (1989c). Prostate specific antigen in the diagnosis and treatment of adenocarcinoma of the prostate. II. Radical prostatectomy treated patients. J Urol 141, 1076-1083.
- Steiner, P., Philipp, A., Lukas, J., Godden-Kent, D., Pagano, M., Mittnacht, S., Bartek, J., and Eilers, M. (1995). Identification of a Myc-dependent step during the formation of active G1 cyclin-cdk complexes. EMBO J 14, 4814-4826.
- Stewart, A. F., Vignery, A., Silverglate, A., Ravin, N. D., LiVolsi, V., Broadus, A. E., and Baron, R. (1982). Quantitative bone histomorphometry in humoral hypercalcemia of malignancy: uncoupling of bone cell activity. J Clin Endocrinol Metab 55, 219-227.
- Storm, E. E., Huynh, T. V., Copeland, N. G., Jenkins, N. A., Kingsley, D. M., and Lee, S. J. (1994). Limb alterations in brachypodism mice due to mutations in a new member of the TGF beta-superfamily. Nature 368, 639-643.
- Su, Y., Zheng, L., Wang, Q., Bao, J., Cai, Z., and Liu, A. The PI3K/Akt pathway upregulates Id1 and integrin alpha4 to enhance recruitment of human ovarian cancer endothelial progenitor cells. BMC Cancer 10, 459.
- Suzuki, A., Kaneko, E., Maeda, J., and Ueno, N. (1997). Mesoderm induction by BMP-4 and -7 heterodimers. Biochemical and biophysical research communications 232, 153-156.
- Swiercz, J. M., Kuner, R., Behrens, J., and Offermanns, S. (2002). Plexin-B1 directly interacts with PDZ-RhoGEF/LARG to regulate RhoA and growth cone morphology. Neuron 35, 51-63.
- Tabas, J. A., Hahn, G. V., Cohen, R. B., Seaunez, H. N., Modi, W. S., Wozney, J. M., Zasloff, M., and Kaplan, F. S. (1993). Chromosomal assignment of the human gene for bone morphogenetic protein 4. Clin Orthop Relat Res, 310-316.

- Takahashi, M., Otsuka, F., Miyoshi, T., Otani, H., Goto, J., Yamashita, M., Ogura, T., Makino, H., and Doihara, H. (2008). Bone morphogenetic protein 6 (BMP6) and BMP7 inhibit estrogen-induced proliferation of breast cancer cells by suppressing p38 mitogenactivated protein kinase activation. J Endocrinol 199, 445-455.
- Tamaki, K., Souchelnytskyi, S., Itoh, S., Nakao, A., Sampath, K., Heldin, C. H., and ten Dijke, P. (1998). Intracellular signaling of osteogenic protein-1 through Smad5 activation. J Cell Physiol 177, 355-363.
- Tamura, Y., Takeuchi, Y., Suzawa, M., Fukumoto, S., Kato, M., Miyazono, K., and Fujita, T. (2001). Focal adhesion kinase activity is required for bone morphogenetic protein-Smad1 signaling and osteoblastic differentiation in murine MC3T3-E1 cells. J Bone Miner Res 16, 1772-1779.
- Tan, A. R., Alexe, G., and Reiss, M. (2009). Transforming growth factor-beta signaling: emerging stem cell target in metastatic breast cancer? Breast Cancer Res Treat 115, 453-495.
- Taniguchi, T., Toi, M., Inada, K., Imazawa, T., Yamamoto, Y., and Tominaga, T. (1995). Serum concentrations of hepatocyte growth factor in breast cancer patients. Clin Cancer Res 1, 1031-1034.
- Ueno, T., Toi, M., and Tominaga, T. (1999). Circulating soluble Fas concentration in breast cancer patients. Clin Cancer Res 5, 3529-3533.
- Ulianich, L., Garbi, C., Treglia, A. S., Punzi, D., Miele, C., Raciti, G. A., Beguinot, F., Consiglio, E., and Di Jeso, B. (2008). ER stress is associated with dedifferentiation and an epithelial-to-mesenchymal transition-like phenotype in PC Cl3 thyroid cells. J Cell Sci 121, 477-486.
- Valdimarsdottir, G., Goumans, M. J., Rosendahl, A., Brugman, M., Itoh, S., Lebrin, F., Sideras, P., and ten Dijke, P. (2002). Stimulation of Id1 expression by bone morphogenetic protein is sufficient and necessary for bone morphogenetic protein-induced activation of endothelial cells. Circulation 106, 2263-2270.
- Vielmetter, J., Kayyem, J. F., Roman, J. M., and Dreyer, W. J. (1994). Neogenin, an avian cell surface protein expressed during terminal neuronal differentiation, is closely related to the human tumor suppressor molecule deleted in colorectal cancer. J Cell Biol 127, 2009-2020
- Wallace, D. M., Chisholm, G. D., and Hendry, W. F. (1975). T.N.M. classification for urological tumours (U.I.C.C.) 1974. Br J Urol 47, 1-12.
- Walsh, M. F., Ampasala, D. R., Hatfield, J., Vander Heide, R., Suer, S., Rishi, A. K., and Basson, M. D. (2008). Transforming growth factor-beta stimulates intestinal epithelial focal adhesion kinase synthesis via Smad- and p38-dependent mechanisms. Am J Pathol 173, 385-399.
- Wilkinson, L., Kolle, G., Wen, D., Piper, M., Scott, J., and Little, M. (2003). CRIM1 regulates the rate of processing and delivery of bone morphogenetic proteins to the cell surface. J Biol Chem 278, 34181-34188.
- Wilson, N. H., and Key, B. (2006). Neogenin interacts with RGMa and netrin-1 to guide axons within the embryonic vertebrate forebrain. Dev Biol 296, 485-498.
- Wilson, N. H., and Key, B. (2007). Neogenin: one receptor, many functions. Int J Biochem Cell Biol 39, 874-878.
- Winnier, G., Blessing, M., Labosky, P. A., and Hogan, B. L. (1995). Bone morphogenetic protein-4 is required for mesoderm formation and patterning in the mouse. Genes Dev 9, 2105-2116.
- Wolfman, N. M., Hattersley, G., Cox, K., Celeste, A. J., Nelson, R., Yamaji, N., Dube, J. L., DiBlasio-Smith, E., Nove, J., Song, J. J., et al. (1997). Ectopic induction of tendon and ligament in rats by growth and differentiation factors 5, 6, and 7, members of the TGF-beta gene family. J Clin Invest 100, 321-330.

- Wozney, J. M., Rosen, V., Byrne, M., Celeste, A. J., Moutsatsos, I., and Wang, E. A. (1990). Growth factors influencing bone development. J Cell Sci Suppl 13, 149-156.
- Wozney, J. M., Rosen, V., Celeste, A. J., Mitsock, L. M., Whitters, M. J., Kriz, R. W., Hewick, R. M., and Wang, E. A. (1988). Novel regulators of bone formation: molecular clones and activities. Science (New York, NY 242, 1528-1534.
- Wu, K., Yang, Y., Wang, C., Davoli, M. A., D'Amico, M., Li, A., Cveklova, K., Kozmik, Z., Lisanti, M. P., Russell, R. G., et al. (2003). DACH1 inhibits transforming growth factor-beta signaling through binding Smad4. J Biol Chem 278, 51673-51684.
- Wu, R. Y., Zhang, Y., Feng, X. H., and Derynck, R. (1997). Heteromeric and homomeric interactions correlate with signaling activity and functional cooperativity of Smad3 and Smad4/DPC4. Mol Cell Biol 17, 2521-2528.
- Xia, Y., Babitt, J. L., Sidis, Y., Chung, R. T., and Lin, H. Y. (2008). Hemojuvelin regulates hepcidin expression via a selective subset of BMP ligands and receptors independently of neogenin. Blood 111, 5195-5204.
- Xia, Y., Sidis, Y., Mukherjee, A., Samad, T. A., Brenner, G., Woolf, C. J., Lin, H. Y., and Schneyer, A. (2005). Localization and action of Dragon (repulsive guidance molecule b), a novel bone morphogenetic protein coreceptor, throughout the reproductive axis. Endocrinology 146, 3614-3621.
- Xia, Y., Yu, P. B., Sidis, Y., Beppu, H., Bloch, K. D., Schneyer, A. L., and Lin, H. Y. (2007). Repulsive guidance molecule RGMa alters utilization of bone morphogenetic protein (BMP) type II receptors by BMP2 and BMP4. The Journal of biological chemistry 282, 18129-18140.
- Yager, J. D. (2000). Endogenous estrogens as carcinogens through metabolic activation. J Natl Cancer Inst Monogr, 67-73.
- Yagi, K., Furuhashi, M., Aoki, H., Goto, D., Kuwano, H., Sugamura, K., Miyazono, K., and Kato, M. (2002). c-myc is a downstream target of the Smad pathway. J Biol Chem 277, 854-861.
- Yamaguchi, A. (1995). Regulation of differentiation pathway of skeletal mesenchymal cells in cell lines by transforming growth factor-beta superfamily. Semin Cell Biol 6, 165-173.
- Yamaguchi, K., Nagai, S., Ninomiya-Tsuji, J., Nishita, M., Tamai, K., Irie, K., Ueno, N., Nishida, E., Shibuya, H., and Matsumoto, K. (1999). XIAP, a cellular member of the inhibitor of apoptosis protein family, links the receptors to TAB1-TAK1 in the BMP signaling pathway. EMBO J 18, 179-187.
- Yang, F., West, A. P., Jr., Allendorph, G. P., Choe, S., and Bjorkman, P. J. (2008). Neogenin interacts with hemojuvelin through its two membrane-proximal fibronectin type III domains. Biochemistry 47, 4237-4245.
- Yang, J. J., Lee, Y. J., Hung, H. H., Tseng, W. P., Tu, C. C., Lee, H., and Wu, W. J. ZAK inhibits human lung cancer cell growth via ERK and JNK activation in an AP-1-dependent manner. Cancer Sci 101, 1374-1381.
- Yang, X., Kovalenko, D., Nadeau, R. J., Harkins, L. K., Mitchell, J., Zubanova, O., Chen, P. Y., and Friesel, R. (2004). Sef interacts with TAK1 and mediates JNK activation and apoptosis. J Biol Chem 279, 38099-38102.
- Yap, W. N., Chang, P. N., Han, H. Y., Lee, D. T., Ling, M. T., Wong, Y. C., and Yap, Y. L. (2008). Gamma-tocotrienol suppresses prostate cancer cell proliferation and invasion through multiple-signalling pathways. Br J Cancer 99, 1832-1841.
- Yap, W. N., Zaiden, N., Tan, Y. L., Ngoh, C. P., Zhang, X. W., Wong, Y. C., Ling, M. T., and Yap, Y. L. (2010). Id1, inhibitor of differentiation, is a key protein mediating antitumor responses of gamma-tocotrienol in breast cancer cells. Cancer Lett 291, 187-199.
- Ye, L., Bokobza, S., Li, J., Moazzam, M., Chen, J., Mansel, R. E., and Jiang, W. G. Bone morphogenetic protein-10 (BMP-10) inhibits aggressiveness of breast cancer cells and correlates with poor prognosis in breast cancer. Cancer Sci 101, 2137-2144.

- Ye, L., Kynaston, H., and Jiang, W. G. (2008). Bone morphogenetic protein-9 induces apoptosis in prostate cancer cells, the role of prostate apoptosis response-4. Mol Cancer Res 6, 1594-1606.
- Ye, L., Kynaston, H., and Jiang, W. G. (2009). Bone morphogenetic protein-10 suppresses the growth and aggressiveness of prostate cancer cells through a Smad independent pathway. J Urol 181, 2749-2759.
- Ye, L., Lewis-Russell, J. M., Kyanaston, H. G., and Jiang, W. G. (2007). Bone morphogenetic proteins and their receptor signaling in prostate cancer. Histol Histopathol 22, 1129-1147.
- Yin, J. J., Selander, K., Chirgwin, J. M., Dallas, M., Grubbs, B. G., Wieser, R., Massague, J., Mundy, G. R., and Guise, T. A. (1999). TGF-beta signaling blockade inhibits PTHrP secretion by breast cancer cells and bone metastases development. J Clin Invest 103, 197-206.
- Ying, Q. L., Nichols, J., Chambers, I., and Smith, A. (2003). BMP induction of Id proteins suppresses differentiation and sustains embryonic stem cell self-renewal in collaboration with STAT3. Cell 115, 281-292.
- Yingling, J. M., Datto, M. B., Wong, C., Frederick, J. P., Liberati, N. T., and Wang, X. F. (1997). Tumor suppressor Smad4 is a transforming growth factor beta-inducible DNA binding protein. Mol Cell Biol 17, 7019-7028.
- Yu, H., and Rohan, T. (2000). Role of the insulin-like growth factor family in cancer development and progression. J Natl Cancer Inst 92, 1472-1489.
- Yu, J., Bian, D., Mahanivong, C., Cheng, R. K., Zhou, W., and Huang, S. (2004). p38 Mitogen-activated protein kinase regulation of endothelial cell migration depends on urokinase plasminogen activator expression. J Biol Chem 279, 50446-50454.
- Zawel, L., Dai, J. L., Buckhaults, P., Zhou, S., Kinzler, K. W., Vogelstein, B., and Kern, S. E. (1998). Human Smad3 and Smad4 are sequence-specific transcription activators. Mol Cell 1, 611-617.
- Zhang, A. S., Anderson, S. A., Meyers, K. R., Hernandez, C., Eisenstein, R. S., and Enns, C. A. (2007). Evidence that inhibition of hemojuvelin shedding in response to iron is mediated through neogenin. J Biol Chem 282, 12547-12556.
- Zhang, A. S., West, A. P., Jr., Wyman, A. E., Bjorkman, P. J., and Enns, C. A. (2005). Interaction of hemojuvelin with neogenin results in iron accumulation in human embryonic kidney 293 cells. J Biol Chem 280, 33885-33894.
- Zhang, A. S., Yang, F., Wang, J., Tsukamoto, H., and Enns, C. A. (2009). Hemojuvelin-neogenin interaction is required for bone morphogenic protein-4-induced hepcidin expression. J Biol Chem 284, 22580-22589.
- Zhang, H., and Bradley, A. (1996). Mice deficient for BMP2 are nonviable and have defects in amnion/chorion and cardiac development. Development 122, 2977-2986.
- Zhang, Y., Feng, X., We, R., and Derynck, R. (1996). Receptor-associated Mad homologues synergize as effectors of the TGF-beta response. Nature 383, 168-172.
- Zhao, G. Q., Deng, K., Labosky, P. A., Liaw, L., and Hogan, B. L. (1996). The gene encoding bone morphogenetic protein 8B is required for the initiation and maintenance of spermatogenesis in the mouse. Genes Dev 10, 1657-1669.
- Zhao, Y., Lyons, C. E., Jr., Xiao, A., Templeton, D. J., Sang, Q. A., Brew, K., and Hussaini, I. M. (2008). Urokinase directly activates matrix metalloproteinases-9: a potential role in glioblastoma invasion. Biochemical and biophysical research communications 369, 1215-1220.
- Zhou, Z., Xie, J., Lee, D., Liu, Y., Jung, J., Zhou, L., Xiong, S., Mei, L., and Xiong, W. C. Neogenin regulation of BMP-induced canonical Smad signaling and endochondral bone formation. Dev Cell 19, 90-102.

- Zietman, A. L., Thakral, H., Wilson, L., and Schellhammer, P. (2001). Conservative management of prostate cancer in the prostate specific antigen era: the incidence and time course of subsequent therapy. J Urol 166, 1702-1706.
- Zou, H., Wieser, R., Massague, J., and Niswander, L. (1997). Distinct roles of type I bone morphogenetic protein receptors in the formation and differentiation of cartilage. Genes Dev 11, 2191-2203.
- Zuker, M. (2003). Mfold web server for nucleic acid folding and hybridization prediction. Nucleic Acids Research *31*, 3406 3415.